PHD

A Comparative study of the antiproliferative activity of iron chelators PIH, SIH and their light-activated caged derivatives in skin cells

Aroun, Asma

Award date:
2010

Awarding institution:
University of Bath

A Comparative study of the antiproliferative activity of iron chelators PIH, SIH and their light-activated caged derivatives in skin cells

Asma Aroun

A thesis submitted for the degree of Doctor of Philosophy

University of Bath

Department of Pharmacy and Pharmacology

November 2010

To my family…

TABLE OF CONTENTS

ACKNOWLEDGEMENTS

I am extremely grateful to Dr Charareh Pourzand for giving me the opportunity to work under her supervision. I would like to thank her for the endless support, encouragement, and guidance. I am also very grateful to Dr Olivier Reelfs for his training, supervision and constant advice.

I am very thankful and appreciative to Professor Rex Tyrrell for giving me access to his laboratory facilities as well as his highly valued support and advice. I am particularly grateful to Dr Abdullah Al-Qenaei for his advice and training input.

I am very grateful to Dr James Dowden from the department of Chemistry (University of Nottingham) and all his laboratory members especially Dr Sara Rossi for their help to prepare the chemical compounds.

I would like to thank Dr Ian Egglestion and Dr Amit Nathubhai for their advice and practical help.

I am also very thankful to Professor Irene Leigh (University of Dundee) for providing cancer and psoriatic cell lines and her advice on organo-typic cultures.

I am also very thankful to Dr Nick Hall and Dr Michael Rowan for their highly valued support and advice during my PhD work.

I would like to thank Professor Susan Wannacott from the Department of Biology and Biochemistry (University of Bath) for giving me access to her laboratory facilities.

I would also like to thank Dr. Adrian Rogers from the Bioimaging suite for his help and advice as well as Mr Kevin Smith for practical help.

Many thanks to all members of laboratories 5W 2.20 and 5W 2.14, both past and present, particularly to Tina Radka for their support and friendly chats. I am also very thankful to Benjamin Young for his help during *viva* preparation.

I am also very grateful and appreciative to my dear parents: Ghania and Taïb and my lovely sister Nassima, and brothers Redha, Hakim and Abderrahmane for their constant prayers, love and support. I am also thankful to my dear friends Dr Nassima Abdelouahab-Ouitas and Nour Alhusein.

I am extremely grateful to the Algerian Government for sponsoring me during my studies.

ABSTRACT

In the present study, we investigated the long term antiproliferative potential of iron chelators Salicylaldehyde Isonicotinoyl Hydrazone (SIH), Pyridoxal Isonicotinoyl Hydrazone (PIH) and their caged-derivatives 2-Nitrophenyl Ethyl-SIH and –PIH (2NPE-SIH and 2NPE-PIH) using human primary fibroblast cell line FEK4 and the spontaneously immortalised human keratinocyte cell line, HaCaT as models.

We then extended the study to additional hyperproliferative skin keratinocyte cell lines notably MKPS (immortalised psoriatic cell line) as well as PM1 and MET2 that represent two cancerous skin cell lines isolated at different stages of malignant transformation of squameous cell carcinoma (SCC) from a single adult individual. Iron depletion with SIH and its UVA-activated caged-derivative (i.e. 2NPE-SIH) led to significant cell death in all cell models presumably as a result of inhibition of G1/S progression in cell cycle. PIH and 2NPE-PIH on the other hand only caused transient growth retardation in cells due to delayed S Phase but with no apparent toxicity. The growth inhibitory/retardation effects of SIH/PIH or UVA-activated caged-SIH/PIH were related to their iron-chelating properties, as their saturation with iron could reverse their antiproliferative activity in the analysed skin cells. Taken together the results suggested that 2NPE-PIH which possesses very high iron chelating potential, but low antiproliferative activity (i.e. upon uncaging by UVA) is more suitable for skin photoprotection. In contrast, 2NPE-SIH which remains inactive inside the cells until its strong iron binding activity and high antiproliferative properties are activated by UVA, may offer a highly selective and dose-controlled alternative for treatment of hyperproliferative skin disorders such as skin cancer.

ABBREVIATIONS

311	2-hydroxy-1-naphthylaldehyde isonicotinoyl hydrazone
BNIP3	BCL2/adenovirus E1B 19 kDa protein-interacting protein 3
BrdU	5-Bromo-2'-deoxy-uridine
2-NPE-PIH	2-Nitrophenyl Ethyl Pyridoxal Isonicotinoyl Hydrazone
2-NPE-SIH	2-Nitrophenyl Ethyl Salicylaldehyde Isonicotinoyl Hydrazone
3-AP	3-aminopyridine-2-carboxyaldehyde thiosemicarbazone
4Fe–4S	Iron-sulphur centre
8-OHdG	8-hydroxydeoxyguanosine
AK	Actinic Keratoses
5-ALA	5-aminolevulinic acid
ALA S	Aminolevulinate synthase
APC	Antigen presenting cells
apoTf	Apo Transferrin
ARE	Antioxidant-responsive element
ATM	Ataxia telangiectasia mutated protein
ATP	Adenosine 5'-triphosphate
ATR	Ataxia telangiectasia-related phosphokinase
BIH	Isonicotinic acid benzylidene-hydrazide
CA	Calcein
CA-AM	Calcein-acetoxymethyl ester
CA-assay	Fluorescence calcein assay
CFA	Colony forming ability
CA-Fe	Calcein-bound iron
CIC	Caged iron chelator
CICs	Caged iron chelators
CAKs	cyclin-activating kinases
CHK2	check-point kinase 2
CKI	Cdk inhibitors
CM	Condition media

CO	Carbon monoxide
DMF	Dimethylformamide
Cs_2CO_3	Caesium carbonate
Cu^{2+}	Cupric Copper
D_2O	Deuterium oxide
DCM	Dichloromethane
DISC	Death-inducing signaling complex
DED	De-epidermalized dermis
dNTP	Deoxyribonucleotide
DFO	Desferrioxamine or desferrioxamine mesylate or Desferal
PK3BBH	Di-2-pyridylketone 3-bromobenzoyl hydrazone
PKIH	Di-2-pyridylketone isonicotinoyl hydrazone
DMEM	Dulbecco's Modified Eagle's Medium
DMSO	Dimethyl sulphoxide
DMT1	Divalent metal transporter 1
DNA	Deoxyribonucleic acid
DpT	Di-2-pyridylketone thiosemicarbazone
DTPA	Diethylenetriamine pentaacetic acid
Dcytb	Duodenal cytochrome b
EDTA	Ethylenediaminetetracetic acid
EMEM	Earle’s modified minimal essential medium
ER	Endoplasmic reticulum
EtOH	Ethanol
Et_2O	Diethyl ether
EtOAc	Ethyl acetate
ERK	Extracellular signal regulated kinase
JNK	c Jun N terminal protein kinase
SAPK	Stress activated protein kinase
FAS	Ferrous ammonium sulphate
FCS	Foetal calf serum
Fe	Iron
Fe^{2+}	Ferrous iron
Fe^{3+}	Ferric iron

FP1	Ferroportin (1)
FITC	Fluorescein Isothiocyanate
Ft	Ferritin
M phase	Mitotic phase
G1	Gap1
S	Synthesis
G2	Gap2
GADD45	Growth arrest and DNA damage 45α
GSH	Glutathione (L-gamma-glutamyl-L-cysteinyl glycine)
GAG	Glycosaminoglycans
GPx	Glutathione peroxidase
GR	Glutathione reductase
GSH	Glutathione (reduced)
GSSG	Glutathione disulphide (oxidised glutathione)
min	Minutes
h	hour / hours
H_2O_2	Hydrogen peroxide
HCP-1	Heme carrier protein-1
HEPES	N-[2-hydroxyethyl]piperazine-N'-[2-ethanesulfonic acid]
H-Ft	H-chain of Ferritin
HO-1	Haem oxygenase 1
HO-2	Haem oxygenase 2
HO-3	Haem oxygenase 3
Hp	Hephaestin
HPLC	High-performance liquid chromatography
HU	Hydroxyurea
IC	Iron Chelator
ICAM-1	Intercellular adhesion molecule –1
ICT	Iron chelation therapy
IL	Interleukin
IRE	Iron response element
IRP	Iron-regulatory protein
K_2CO_3	Potassium carbonate

kDa	Kilo Dalton
KC	Keratinocyte
KCs	Keratinocytes
kJ/m^2	KiloJoules per metre square
$L^{\bullet}$	Fatty acid radical
L-Ft	L-chain of Ferritin
LI	Labile iron
LIP	Labile iron pool
LMW	Low molecular weight
MW	Molecular weight
$LO^{\bullet}$	(Lipid) alkoxyl radical
$LOO^{\bullet}$	Fatty acid peroxyl radical
LOOH	Lipid hydroperoxide
MAPK	Mitogen-activated protein kinases
BCC	Basal cell carcinoma
mBCC	Morphoeiform basal cell carcinoma
MeOH	Methanol
MT	Metallothionein
mALA	Methyl ester of ALA
MAPK	Mitogen-activated protein kinases
MMP1	Matrix metalloprotenase-1
Mn-SOD	Manganese–superoxide dismutase
mRNA	Messenger RNA
Mt-Ft	Mitochondrial ferritin
MTT	3-(4,5-dimethylthiazol-2-ye)-2,5-diphenyltertrazolium bromide
mdm-2	Murine double minute-2
Tachpyridine	N,N′,N″-tris(2-pyridylmethyl)-cis,cis-1,3,5-triaminocyclohexane
NAC	N-acetyl cysteine
NADH	Nicotine adenine dinucleotide
NADP	Nicotine adeninedinucleotide phosphate
nBCC	Nodular basal cell carcinoma
NBTI	Non-transferrin bound iron
Ndrg1	N-myc downstream regulated gene-1

TNFR1	Necrosis factor receptor-1
NB	Neuroblastoma
NF-kappaB	Nuclear Factor kappa B
NMR	Nuclear magnetic resonance
NMSC	Non-melanoma skin cancer
NP-40	(octylphenoxy)-polyethoxiethanol or Nonidet P-40
MTT	(3-[4,5-dimethylthiazol-2-yl]-2,5-diphenyl tetrazolium bromide)
$O_2^{\bullet-}$	Superoxide anion
OES	17β-oestradiol
$OH^{\bullet}$	Hydroxyl radical
O_3	Ozone
PBS	Phosphate buffered saline
PPIX	Protoporphyrin IX
P/S	Penicillin/ streptomycin.
PDT	Photodynamic therapy
PI	Propidium Iodide
PIH	Pyridoxal Isonicotinoyl Hydrazone
PLAGL2	Pleomorphic adenoma gene like 2
AIF	Apoptosis inducing factor
PPIX	Protoporphyrin IX
pRb	Retinoblastoma protein
PUFA	Polyunsaturated fatty acid
PUVA	Psolaren UVA
RME	Receptor-mediated endocytosis
RNA	Ribonucleic acid
ROS	Reactive oxygen species
RP-HPLC	Reversed phase High-performance liquid chromatography
RR	Ribonucleotide reductase
RT	Room temperature
sBCC	Superficial basal cell carcinoma
SC	Stratum Corneum
Se	Selenium
SFM	Serum-free medium

SIH	Salicylaldehyde Isonicotinoyl Hydrazone
SOD	Superoxide dismutase
Tf	Transferrin
TFA	Trifluoroacetic acid
TfR	Transferrin receptor
TGF	Transforming growth fators
TNFa	Tumor necrosis factor alpha
Triapine®	3-aminopyridine-2-carboxyaldehyde thiosemicarbazone
Tris	Tris[hydroxymethyl]-aminomethane
TRx	Thioredoxin
UTR	Untranslated region
UV	Ultraviolet
UVA(B, C)	Ultraviolet A(B, C)
UVR	Ultraviolet radiation
V	Volts
VHL	Von Hippel Lindau
W/V	Weight per volume
XLSA	X-linked sideroblastic anemia
Zn^{2+}	Zinc
CuZnSOD	Copper-zinc-containing superoxide dismutase
MnSOD	Manganese-containing superoxide dismutase
Cu/Zn SOD	Copper-zinc superoxide dismutase

CHAPTER ONE

INTRODUCTION

1.1 Human Skin

Skin is the largest organ in the body weighing approximately six pounds and providing around 10% of the body mass of an average person (Williams, 2003).

Because it interfaces with the environment, skin plays a key role in protecting the body against pathogens (Proksch *et al.*, 2008) and excessive water loss (Madison, 2003). Skin also provides other functions such as insulation, temperature regulation, sensation and synthesis of vitamin D.

The skin is composed of multiple layers, epidermis, dermis and hypodermis (**Fig. 1.1**).

1.1.1 Epidermis

Epidermis is the outermost layer of the skin. It forms the waterproof, protective wrap over the body's surface and is made up of stratified squamous epithelium with an underlying basal lamina. In humans, epidermis is thinnest on the eyelids at 0.1 mm and thickest on the palms and soles at 1.5 mm (Madison, 2003).

Keratinocytes are the major epidermal cell types, constituting 95% of the epidermis (McGrath *et al.*, 2004). The epidermis is continuously renewed by the mitotic activity of the stem cells in the basal layer, which provides new keratinocytes. Upon withdrawal from the cell cycle, basal keratinocytes detach from the basement membrane and undergo a terminal differentiation program to become corneocytes in the outer layers of the epidermis. At the final stage of differentiation, the keratinocytes lose their nuclei, die, dehydrate and flatten out to form a cornified external layer i.e. *Stratum corneum* (SC) (Lippens *et al.*, 2009). Dead cells are constantly being shed, while new cells are continuously being produced in the basal layer. Turnover of the epidermis allows the organ to maintain its barrier function, repair injured skin in wound healing, and receive the signals that stimulate or inhibit cell proliferation (Lippens *et al.*, 2009). However hyperproliferation may represent a risk factor for skin cancer and occurs in some physiologic conditions such as wound healing and altered permeability

barrier function as well as pathologic conditions such as psoriasis (Lippens *et al.*, 2009). Thus, cell cycle and keratinocyte turnover have significant roles in pathogenesis of skin diseases and response to therapy (Lippens *et al.*, 2009). It has been estimated that a cell from the basal layer takes at least 14 days to reach the SC whereas in the rapidly proliferating epidermis of psoriasis, it only takes 2 days. Similarly, the turnover time in the SC is some 13 or 14 days in normal skin with the residence time in psoriatic SC shortening to 2 days (Barry, 1983). In addition to the keratinocytes, other specialized cells are present in the basal layer are melanocytes, Langerhans cells and Merkel cells. Melanocytes secrete melanosomes containing melanin (the black eumelanin or the reddish phaeomelanin) that protects the skin from ultraviolet radiations and free radicals (Benjamin *et al.*, 2008). The melanogenesis activity of these cell lines defines the skin color (Biro *et al.*, 2009). Langerhans cells are derived from bone-marrow and as part of the immune system function as antigen presenting cells (APC) of the skin (Benjamin *et al.*, 2008). Merkel cells function as mechanoreceptors for the sensation of touch and pressure (Biro *et al.*, 2009). Additionally, sensory nerve endings which are responsible for cutaneous sensation such as touch, pressure, temperature as well as pain and itch, might also reach the lower layers of the epidermis (Biro *et al.*, 2009).

The epidermis can be further subdivided into the following *strata* (beginning with the innermost layer): *basale, spinosum, granulosum, corneum.*

Stratum basale (or basal layer) is often described as one cell thick, though it may in fact be two to three cells thick in glabrous (hairless) skin and hyperproliferative epidermis (from a skin disease) (McGrath *et al.*, 2004).

The basal cells of the *stratum basale* can be considered the stem cells of the epidermis and is the only layer that is capable of cell division (Benjamin *et al.*, 2008). The keratinocytes in this layer are connected with the basement membrane (or dermo-epidermal membrane) by proteinaceous structures called hemidesmosomes and with cells of *stratum spinosum* layer by desmosomes (Benjamin *et al.*, 2008).

Stratum spinosum (or spinous layer) is the next viable epidermal layer; it consists of 2 – 6 layers of columnar keratinocytes that modify themselves into polygonal shapes. The keratin in this layer aggregates to form filaments called tonofi laments that on further condensation produce cell membrane-connecting structures called desmosomes (Benjamin *et al.*, 2008). Keratinization begins in the *stratum spinosum* (Marks and Miller, 2006).

Stratum granulosum (or granular layer) is 1–3 cell layers thick, and contains enzymes that have the potential to degrade vital cell organelles such as nuclei (Benjamin *et al.*, 2008).

By synthesizing keratin and degrading cell organelles, the keratinocytes **(**which are known as granular cells**)** gradually differentiate into the corneocytes of SC. The granular cells also synthesize membrane coating granules that carry the precursors for intercellular lipid lamellae of the stratum corneum (Benjamin *et al.*, 2008).

Stratum corneum (SC., horny layer) is a nonviable epidermal layer of 10 – 15 cell layers thick, with anucleated keratinocytes (corneocytes) oriented like bricks in the surrounding lipid (that serve as a mortar) and forms the prime barrier to the transdermal delivery of drugs. The SC has a thickness of ~ 10 μm. Corneocytes which have migrated up from the *stratum granulosum* (Marks *et al.,* 2006) slough off on the surface in the thin air-filled *stratum disjunctum*, they are continuously replaced by new cells from the *stratum basale*. Corneocytes contain keratin, a protein that helps keep the skin hydrated by preventing waterevaporation.

1.1.2 Dermis

The dermis (or corium) is a connective tissue matrix that is between the epidermis and the hypodermis. The dermis is 3 – 5 mm thick and consists essentially of a matrix of connective tissue woven by fibrous proteins (collagen, 75%; elastin, 4%; and reticulin, 0.4%) (Barry, 1983). It is supplied with a reticulate network of blood vessels, lymphatic vessels, nerve endings and numerous appendages (Benjamin *et al.*, 2008).

Fibroblasts are the major cells in the dermis. They synthesise collagen, elastin and glycosaminoglycans (GAG). Collagen fibres provide strength and resilience while elastin fibres provide elasticity to the skin. GAG provides viscosity, hydration and allows the dermis limited movement. Other cells embedded in the reticular layer include fat cells and dermal dendrocytes, mast cells, macrophages and lymphocytes.

1.1.3 Hypodermis

The hypodermis (or subcutaneous layer) spreads all over the body as a fibro-fatty layer, with the exception of the eyelids and the male genital region (Barry, 1983). It connects the dermis with the underlying organs. Hypodermis is made of adipocytes, fibroblasts and macrophages and is well supplied by vessels and nerve fibres (Biro *et al.*, 2009). Hypodermis provides a thermal barrier and a mechanical cushion; it is a site of synthesis and a depot of readily available high-energy chemicals (Barry, 1983).

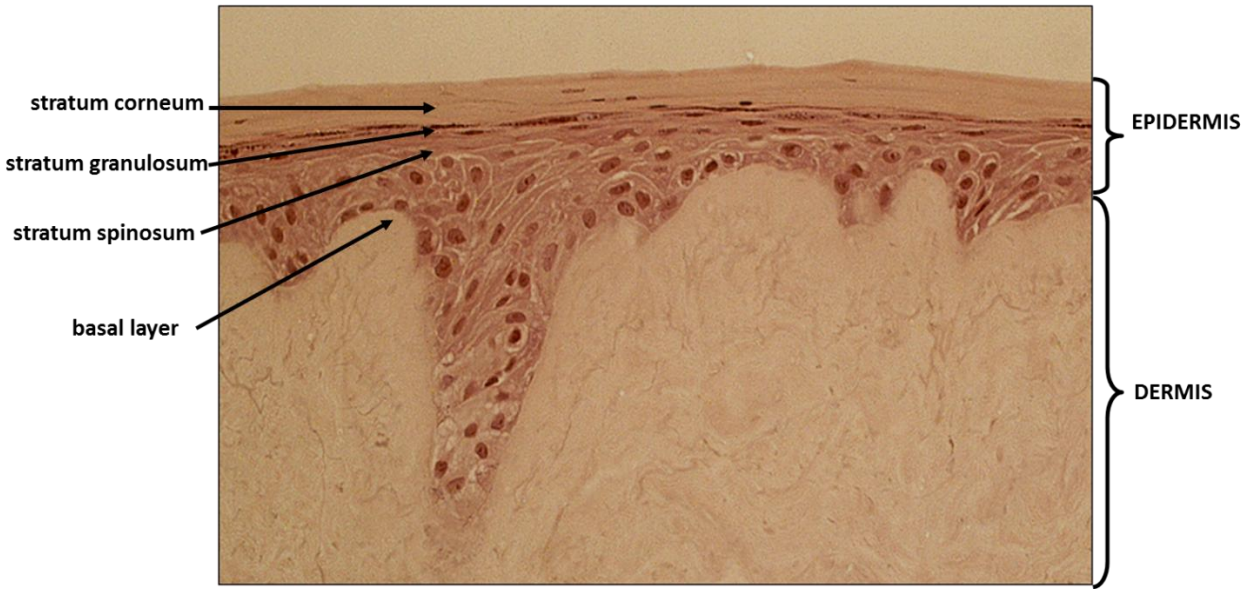

Figure 1.1: Representative section of skin epidermal and dermal layers
(Source: 3 dimensional de-epidermalised dermis (DED)-raft culture performed in Pourzand's laboratory by Dr Reelfs, with permission)

1.2 Ultraviolet (UV) Radiation

1.2.1 General information

Ultraviolet (UV) is part of the non-ionising electromagnetic radiation and it spans between 100 nm and 400 nm. Exposure to UV occurs from both natural and artificial sources. The sun is the major source of natural radiation, and it emits radiation with wavelengths ranging from infrared (760-3000 nm) and visible (400-760 nm) to UV (190-400nm) (**Fig. 1.2)** (Pastila, 2006).

Ultraviolet radiation (UVR) is located in the electromagnetic spectrum between the ionizing x-rays and the non-ionizing visible light. The UV component of sunlight is subdivided to long-wave UVA (320-400 nm), mid-wave UVB (290-320 nm) and shortwave UVC (190-290 nm) wavelengths.

The quality (spectrum) and quantity (intensity) of sunlight are modified during its passage through the atmosphere where ozone, clouds, and pollutants scatter and absorb UV rays (**Fig. 1.3**) (Diffey, 2002).

Solar UV radiation at ground level represents about 5% of the total solar energy; the radiation spectrum is between 290 and 400 nm, and comprises approximately 95% UVA and 5% UVB; UVC is completely filtered out by the stratospheric ozone (Frederick and Alberts, 1992). The spectrum of solar UV radiation to which an individual may be exposed varies with latitude, altitude, ground reflectance, season, time of day, weather, stratospheric ozone and other atmospheric components such as air pollution (Secretan, 2009). For most individuals, solar radiation is the major source of exposure to UV radiation (Secretan, 2009). However, several UV lamps have been developed for use in tanning devices, for germicidal purposes and for the therapeutic use (phototherapy). Depending on the lamp type and filters used, UV sources can provide very different UV spectra from the broadband solar simulated radiation spectrum to specific narrow-band applications (Pastila, 2006).

The effects of solar UV radiation on biological systems concern only UVA and UVB wavelengths, since UVC does not reach the earth's surface.

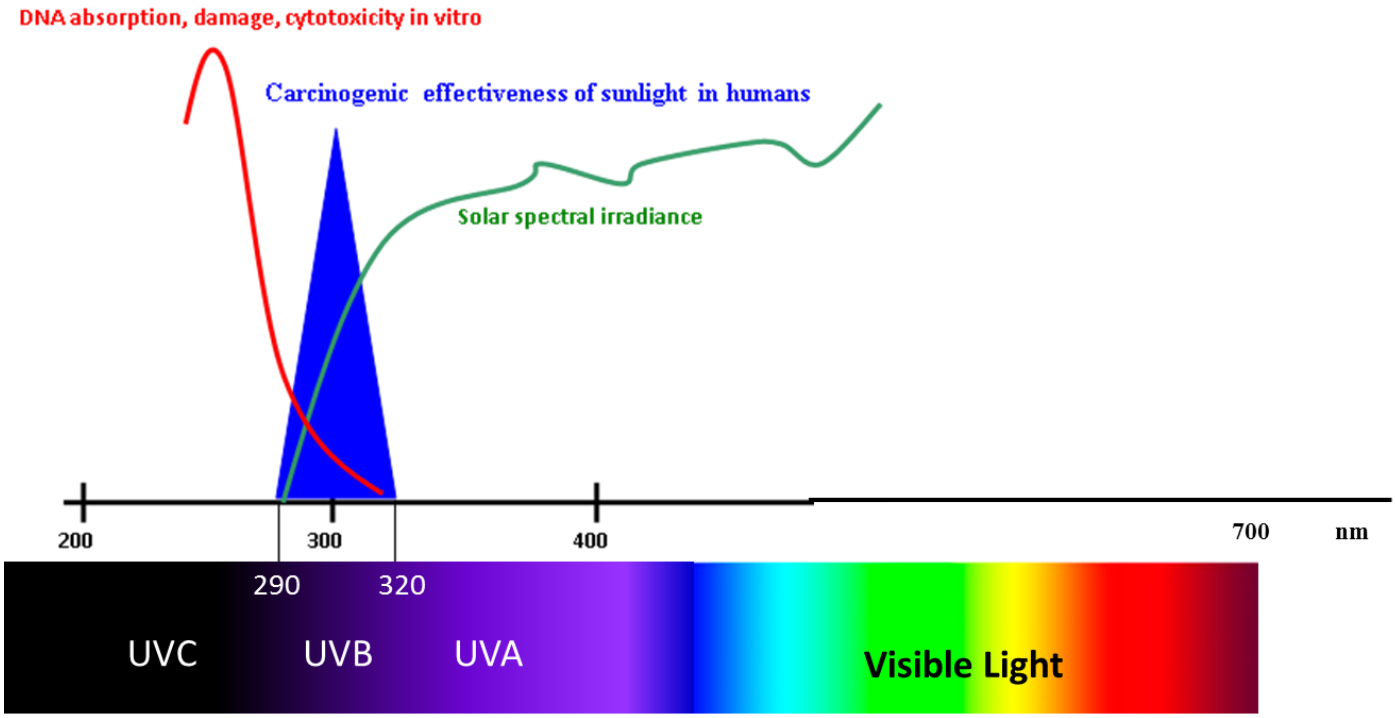

Figure 1.2: Diagrammatic representation of the ranges of UV and visible radiation on the surface of the earth (modified from Tyrrell, 1994).

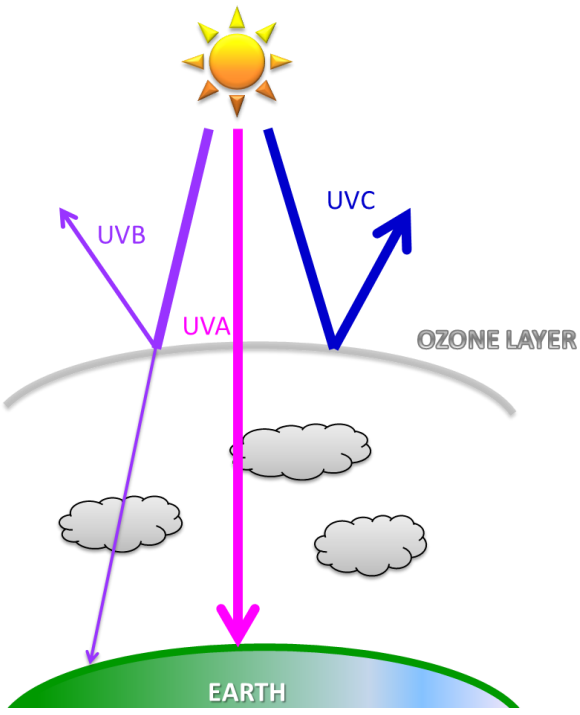

Figure 1.3: Representation of solar UV components and stratospheric ozone layer.

UVC component of sunlight is completely absorbed by Oxygen and stratospheric Ozone, and can not reach the surface of the earth. UVB is partially absorbed by the ozone layer, whereas UVA is not absorbed by the ozone layer. The solar UV components reaching the earth's surface are composed of UVA and UVB only.

1.2.2 Biological effects of solar UV radiation

The major targets for UV in humans are the skin and the eyes. The transmission of UV through these tissues and cells increases with increase in wavelength (see **Fig. 1.4**). Thus the longer wavelengths can penetrate deeper causing effects on targets that differ sharply from those of short wavelengths. While UVA readily reaches the dermis, including its deeper portions, most of the UVB is absorbed in the epidermis, and only a small proportion reaches the upper dermis. UVC, if it reached the earth's surface, would be absorbed or reflected predominantly in the SC and in upper layers of the epidermis (Secretan, 2009). It has been shown that 35-50% of the overall UVA component of sunlight can reach the dermis of Caucasian skin (Bruls *et al.*, 1984). However only a small amount of UVA can reach below the surface of the skin and penetrate blood vessels (see **Fig. 1.4**).

Therefore the amount of radiation received by the two major skin cells, the epidermal keratinocytes and dermal fibroblast are different. The epidermal keratinocytes are exposed to both UVA and UVB radiation while the dermal fibroblasts are protected from UV radiation to a considerable extent by the overlying epidermis and will mostly receive UVA radiation (see **Fig. 1.4**).

Both acute and chronic exposures to sunlight are associated with various physiological and pathological states. The acute response involves immediate effects including erythema, heat, swelling, sunburn, pigmentation, hyperplasia, immune suppression and vitamin D synthesis (Gasparro *et al.*, 1998). The chronic response involves delayed effects such as cataract and skin ageing (also called photo-ageing), which is the result of morphological changes such as wrinkling, elasticity loss, uneven pigmentation due to general alteration of all the epidermal and dermal components of skin. Chronic exposures of skin to UV radiation may lead to skin cancer (reviewed by Tyrrell, 1994; Reelfs *et al.*, 2010). An individual's tendency to develop sunburn and tanning after sun exposure correlates with the individual's susceptibility to long-term effects as well. Therefore, those individuals with higher acute sun sensitivity are generally also more at risk for developing skin cancers after chronic UV exposure (Rünger, 2009). In the recent decades, there has been a substantial decrease in the ozone layer and as a consequence the earth is exposed to more UV radiation. This phenomenon has had an impact on human health in the form of increased incidence of sun-related skin disorders notably actinic keratoses (AK) and skin cancer. Nevertheless sunlight has several beneficial effects. The sun rays provide heat, light and the general feeling of wellbeing. The sunlight also

stimulates blood circulation and the production of Vitamin D that is required for maintaining blood calcium levels in individuals.

At the cellular level, the interaction of UV with biological material changes as a function of wavelength and requires the absorption of the radiation by biomolecules. The UVB region overlaps with the DNA absorption spectrum and as a result the direct absorption of UVB by cellular DNA causes DNA photodamage and mutagenesis (Freeman, 1975; Tyrrell, 1994). In contrast, UVA is weakly absorbed by most biomolecules but is oxidative in nature, generating reactive oxygen species (ROS) such as singlet oxygen ($^1O_2$) via photochemical interactions with intracellular chromophores (Tyrrell, 1991; Tyrrell, 1996a, b).

1.2.3 Biological effects of solar UVA radiation

UVA is about 10^3-10^4 fold less efficient than UVB to initiate the short and long term responses of UVR, as underlined by their action spectra (Parrish *et al.*, 1982). These ratios of efficiency also apply to other responses like mutagenicity or lethality in cell cultures (Keyse *et al.*, 1983; Tyrrell and Pidoux, 1987). Most of the biological effects of UVA are oxygen-dependent, either in cultured cells (Danpure and Tyrrell, 1976) or in skin (Auletta *et al.*, 1986). The UVA component of sunlight contributes up to 80% of the cytotoxic action of sunlight at the basal layer of epidermis (Tyrrell and Pidoux, 1987). Indeed the greater histological effect of UVA is relatively observed on the dermis than on the epidermis. Human skin showed decreased permeability on the barrier of the SC when exposed to UVA (McAuliffe and Blank, 1991). UVA also depletes epidermal Langerhans cells, and recruits neutrophils into irradiated skin (Gilchrest *et al.*, 1983).

At the cellular level, at biologically relevant doses, UVA has been shown to cause lipid peroxidation in the membrane of human cultured fibroblasts (Vile and Tyrrell, 1995). UVA-induced lipid peroxidation was found to be dependent on the "chemical" composition of membranes, as polyunsaturated fatty acid enrichment of human keratinocytes increases the peroxidation process (Quiec *et al.*, 1995). Keratinocytes' peroxidised membranes tend to lose their fluidity following UVA irradiation. This suggested that loss of membrane integrity and selective permeability might result in alteration of transport systems, as well as the leakage of essential components or influx of extracellular molecules such as calcium and toxins. This was confirmed by the findings that UVA radiation inhibited both receptor-mediated and non-specific uptake of exogenous molecules in a dose-dependent manner (Djavaheri-Mergny *et al.*, 1993).

Internal lipid membranes of eukaryotic cells (e.g. lysosomal, mitochondrial and nuclear) have also been shown to be damaged following UVA irradiation. UVA-induced damage to lysosomes is an early event that leads to temporary intracellular leakage of lysosomal proteases into the cytosol which in turn causes the degradation of cytosolic proteins notably the iron storage protein, ferritin (Ft) (Pourzand *et al.*, 1999b). The UVA-induced proteolytic degradation of Ft leads to an immediate measurable increase in the level of the potentially harmful redox active free transit iron pool, known as labile iron pool (LIP). The UVA-mediated increase in LIP has been shown to further exacerbate the peroxidative damage in cultured skin fibroblasts (Zhong *et al.*, 2004) that may lead to the loss of cell membrane integrity.

UVA also damages the mitochondrial membrane leading to immediate depletion of intracellular Adenosine triphosphate (ATP). The depletion of cellular ATP, along with loss of membrane integrity, leads to necrotic cell death in irradiated skin cells (Zhong *et al.*, 2004).

Furthermore it was found that the slow kinetics of the induction of the nuclear transcription factor kappa B (NF-kappaB) by UVA relative to other oxidants is due to a transient increase in the permeability of the nuclear membrane to proteins and occurs as a result of iron-mediated damage to the nuclear membrane (Reelfs *et al.*, 2004). The apparent slow response of NF-kappaB to UVA radiation is likely to have consequences on the kinetics of activation of NF-kappaB target genes in the nucleus notably pro-inflammatory cytokines and proto-oncogenes (Tyrrell, 1996a; Soriani *et al.*, 1998; Reelfs *et al.*, 2010).

Lipid peroxidation products may also induce damage to DNA (Vaca *et al.*, 1988) as illustrated by the finding that lipid hydroperoxide decomposition products induced DNA adducts *in vivo* in liver and kidney (Wang and Liehr, 1995a, b). Therefore, mutations may arise and alter gene expression (Wang and Liehr, 1995a, b).

Photodermatological studies have shown that the morphology of “sunburn” keratinocytes is associated with characteristic features such as pyknotic nucleus and eosinophilic cytoplasm.

The “sunburn” cells were first discovered in the epidermis of mammalian cells exposed to UVB radiation and later on regarded as an example of programmed cell death pathway now referred to as “apoptosis” (Weedon *et al.*, 1979; Ley and Applegate, 1985; Young, 1987; Vaca *et al.*, 1988). This self-destructive programme can eliminate pre-cancerous cells (Ziegler *et al.*, 1994), and it was necessary to understand the phenomenon in order to develop therapeutic strategies for control of the carcinogenesis process (Barber *et al.*, 1998). Interest in the link between UV and apoptosis has increased since Godar *et al.* (1994) investigated cell death mechanisms in different waveband regions of UV (UVC, UVB and UVA) on

murine lymphoma cells (Godar *et al.*, 1994). They found that UVA induced immediate (0-4h) and delayed apoptosis, whereas UVB or UVC induced delayed apoptosis (>20h). In contrast, studies from this laboratory have shown that unlike murine cultured cells, human skin fibroblasts and keratinocytes are quite resistant to UVA-induced apoptosis and upon severe UVA insult, they die mainly by necrotic cell death (Pourzand *et al.*, 1997; Pourzand and Tyrrell, 1999; Zhong *et al.*, 2004; Reelfs *et al.*, 2010).

DNA may be a target to UVA radiation, since it absorbs, although very weakly, in the UVA region up to 360 nm (Sutherland and Griffin, 1981). However, in contrast to UVB, UVA genotoxicity is most likely induced by indirect mechanisms involving absorption of photons by unidentified endogenous photosensitisers and generation of ROS. This is suggested by (i) the oxygen-dependence of induction of most DNA lesions by UVA (Peak *et al.*, 1987) and (ii) the fact that the frequency of lesions induced by UVA does not follow the absorption spectrum of DNA, either *in vivo* (Freeman *et al.*, 1989) or *in vitro* (Peak and Peak, 1995). Lesions include mainly DNA strand breaks and protein cross-links (covalent links between a protein and DNA). However, the formation of 8-hydroxydeoxyguanosine (8-OHdG), seems to be the most important type of lesion occurring in the UVA range, as has been shown in different mammalian cell types (Kielbassa *et al.*, 1997; Zhang *et al.*, 1997). Most importantly the damage has been shown to depend on $^1O_2$ generation (Kvam and Tyrrell, 1997). This is the major interest since UVA radiation of sunlight produces biologically relevant levels of $^1O_2$ and also other ROS (Tyrrell, 1991) and the effects of UVA, including cell inactivation, are completely dependent on the presence of molecular oxygen (Danpure and Tyrrell, 1976). Another type of damage, pyrimidine dimerisation, has been shown to occur in human skin following UVA irradiation (Burren *et al.*, 1998).

Direct damage to proteins can happen at much longer wavelengths than direct damage to DNA. Although proteins absorb most strongly in the UVC range, as the wavelength is increased through the environmentally relevant UVB and UVA regions, damage to proteins becomes increasingly important relative to DNA damage because of the absorption properties of the aromatic amino acids (Tyrosine, tryptophan) which exhibit absorption that tail into the UVA range (Vile and Tyrrell, 1995). Protein and amino acid hydroperoxides then produce various radicals via Fenton-like reactions catalysed by metal ions, particularly ferrous iron (Fe^{2+}) (Dean *et al.*, 1993; Neuzil *et al.*, 1993). Heme-containing proteins, including cytochromes, the antioxidant enzymes catalase and peroxidases are potential targets for damage by UVA.

Repair enzymes have also been shown to be sensitive to UVA radiation and there is evidence that UV-induced repair disruption plays a role in cell death and mutagenesis (Webb, 1977; Menezes and Tyrrell, 1982).

Oxidative modifications of, for example collagen and transcription factors, appear to mark them for degradation in some systems (Helm and Gunn, 1986; Vince and Dean, 1987; Pacifici and Davies, 1990), but in others inefficient catabolism of oxidised proteins contributes to their accumulation (Davies, 1986; Wolff and Dean, 1986; Grant *et al.*, 1992; Jessup *et al.*, 1992; Stadtman, 1992).

Artificial sources of UV, including UVA radiation, has been used for treatment of a number of diseases notably rickets, psoriasis, eczema and jaundice. In view of the potentially harmful effects of UV radiation, the treatments take place only when their benefits outweigh the risks.

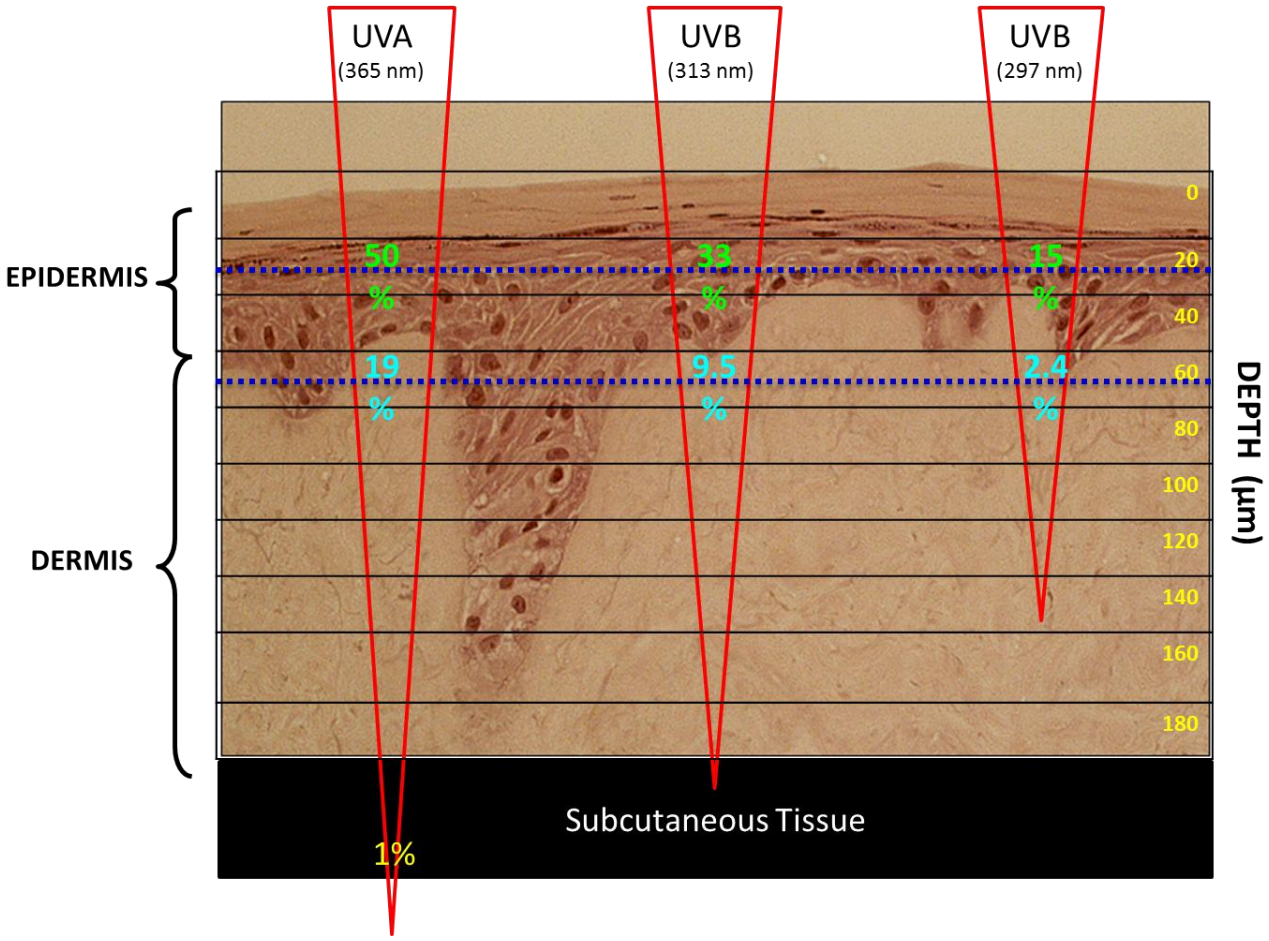

Figure 1.4: Penetration of solar UV radiation into the skin.
UVA (320-400nm) has a deeper penetration potential through the skin layers than UVB (290-320 nm). (Source: 3 dimensional DED-raft culture performed in Pourzand's laboratory by Dr Reelfs, with permission. (%) of UV penetration obtained from Tyrrell, 1994).

1.3 Oxidative Stress and Reactive Oxygen Species (ROS)

1.3.1 Oxidative Stress

Oxygen is a diatomic molecule, O_2, which is referred to as dioxygen. It exists in the atmosphere at the percentage of 21%, and except from certain anaerobic and aero-tolerant unicellular organisms, O_2 plays a pivotal role in all animals, plants, and bacteria, since it is essential for the production of energy by the use of O_2-dependent electron transport chains. However, when O_2 is supplied at concentrations higher than normal, it can be toxic to all living organisms (Martinez-Cayuela, 1995).

"Oxidative stress" is a term introduced to illustrate the imbalance within cells between the mechanisms triggering oxidative conditions (pro-oxidants) and the cellular antioxidant defences in favour of the former (Halliwell and Gutteridge, 1999; Morel and Barouki, 1999).

Free Radicals

A free radical is defined as "atom or molecule with one or more unpaired electron(s) in an orbital in the outermost electron shell" (Cadogan, 1973). Free radicals are capable of independent existence and are able to donate or take an electron from an unpaired electron to another molecule, generating another radical by a chain reaction, which enhances the initial damage. The primary target of free radicals is the lipid bilayer of the membrane. However, free radicals can also oxidize protein, lipid and carbohydrate.

Free radicals can be formed by three independent methods:

(a) Addition of a single electron: $A + e^- \longrightarrow A^{\bullet -}$

(b) Loss of a single electron: $A \longrightarrow A^{\bullet +} + e^-$

(c) Homolytic fission of a covalent bond where each component possesses one of the unpaired electron: $A{:}\,B \longrightarrow A^{\bullet} + B^{\bullet}$

The primary source of the production of free radicals within the cells is the leakage of electrons, in the mitochondria and the endoplasmic reticulum (ER), from the electron transport chain. Free radicals are also produced by activated phagocytes (i.e. macrophages, monocytes, and lymphocytes) during inflammation (Cheeseman and Slater, 1993). In addition to these endogenous sources, there are also exogenous sources such as ultraviolet light, ionizing radiation, tobacco smoking, ozone and pollutants (Martinez-Cayuela, 1995).

Reactive oxygen species (ROS)

Reactive oxygen species (ROS) is a term used to include not only the oxygen radicals (i.e. superoxide ($O_2^{\bullet-}$) and hydroxyl ($OH^{\bullet}$)) but also some non-radical derivatives such as singlet oxygen ($^1O_2$), hydrogen peroxide (H_2O_2) and ozone (O_3), which are capable of forming radicals.

Molecular O_2 has two unpaired electrons in a parallel spin and it can easily absorb electrons from surrounding molecules, therefore it can be a powerful oxidizing agent. Reduction of O_2 to water (H_2O) requires a series of four one-electron-uptake steps, which involves a series of ROS, as shown in equation below. This process makes O_2 reaction with biomolecules poor, unless a transition metal such as iron is present as a catalyst.

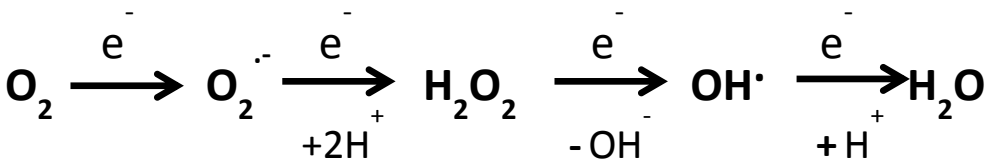

The first product of an electron reduction of O_2 molecule yields the $O_2^{\bullet-}$ via the NADPH oxidase enzymatic system. This reaction seems to occur in the ER within all aerobic cells during respiration (by electron transfer in the mitochondrial electron transfer chain).

At physiological O_2 levels, it has been suggested that about 1-3% of the O_2 reduced in mitochondria may form $O_2^{\bullet-}$, depending on intra-mitochondrial O_2 concentrations. $O_2^{\bullet-}$ has a very short life (milliseconds) and is relatively unreactive towards most biomolecules, including lipids and nucleic acids (Fridovich, 1978). However, it may react with certain proteins and inactivate those, especially proteins in the presence of transition metals prosthetic groups such as heme moieties or iron-sulphur (4Fe–4S) clusters (Gardner *et al.*, 1995). As a consequence, $O_2^{\bullet-}$ toxicity is highly dependent on the availability of iron in the system.

The most important reaction of $O_2^{\bullet-}$ is the dismutation reaction which produces H_2O_2 which is an oxidant without an unpaired electron that has a longer life (minutes) than $^{\bullet}O_2^-$.

This reaction can occur either spontaneously or via the catalysis by a group of enzymes, the superoxide dismutases (SOD). H_2O_2 on its own is a weak oxidizing and reducing agent and is generally poorly reactive. Only in the presence of transition metals, is it capable of inactivating proteins via oxidation of essential thiol (-SH) groups or proteins containing (4Fe–4S) clusters, reduced heme moieties or copper prosthetic groups. Most of the damaging effects of H_2O_2 are thought to be the result of the formation of the highly toxic $OH^{\bullet}$. The

biological importance of H_2O_2 also arises from its ability to readily permeate across membranes and therefore migrate within the cell and extend cellular damage. H_2O_2 has also been found to be generated after UVA radiation (**see section 1.3.2**).

$OH^{\bullet}$ is the most reactive of all oxygen radicals possessing a short half-life, and will readily oxidize lipids, proteins, carbohydrates and nucleic acids (Martinez-Cayuela, 1995). The importance of $OH^{\bullet}$ as oxidant in biological systems was first suggested during generation by X-ray irradiation. The $OH^{\bullet}$ is the product of Fenton reaction involving H_2O_2 and reduced iron **(see also section 1.5.2)**.

ROS form as natural by-products of the normal metabolism of oxygen and have important roles in the normal cellular signalling, including the delivery of electrons across membranes, heme oxidation and oxidative modification of proteins and DNA. ROS also play a role in the defence against infectious pathogens. However, under environmental stress or certain pathological conditions such as hypoxia, intracellular ROS levels can increase dramatically, leading to the formation of oxidative stress (Wang *et al.*, 2008). Oxidative stress exerts significant harmful effects on cell structures by inducing structural changes in lipids, membranes, proteins or nucleic acids (Wang *et al.*, 2008). Potentially dangerous oxygen-linked damaging processes are thought to form the basis of a number of physiological and patho-physiological events such as inflammation, ageing, carcinogenesis, drug action, drug toxicity and more recently programmed cell death.

Nowadays, it is known that both beneficial and damaging effects of O_2 are caused by the same types of ROS. $OH^{\bullet}$ generated *via* Fenton chemistry is able to initiate lipid peroxidation.

The cell membrane and the membrane of cell organelles (e.g. mitochondria, lysosomes, and peroxisomes) are rich in polyunsaturated fatty acids (PUFAs). Polyunsaturated fatty acids contain two or more carbon-carbon double bonds. The oxidative damage of PUFAs will result in lipid peroxidation; a free radical chain reaction that will generate a fatty acid radical ($L^{\bullet}$) and consequently a fatty acid peroxyl radical (LOO•), and aldehydes (Cheeseman and Slater, 1993). In addition to rupturing the membrane and causing cell death, lipid peroxidation products can inhibit protein synthesis and block macrophage action (Winrow *et al*, 1993). This deleterious process of the peroxidation of lipids is apparent in cancer, inflammation and arteriosclerosis (Wang *et al.*, 2008). Furthermore ROS can cause disturbances in proteins since they could react with amino acids such as histidine and cysteine. ROS can also cause a cellular ion imbalance by attacking the proteins responsible for the maintenance of such balance (Halliwell and Gutteridge, 1999).

Additionally, DNA strand breakage has been demonstrated in the nucleus and mitochondria when cells were exposed to ROS, since $OH^{\bullet}$ can damage sugars, purines, and pyrimidines. DNA damage may result in the arrest of transcription, replication errors and genomic instability, all of which are linked with carcinogenesis (Wang *et al*., 2008).

Carbohydrate damage has also been noticed in view of the fact that $OH^{\bullet}$ in the presence of iron is responsible for the depolymerization of hyaluronic acid in *in vitro* studies (Wong *et al.*, 1981).

Moreover, oxidative stress plays an important role in the regulation of cell growth because the cell cycle is regulated by intracellular concentrations of GSH. ROS can activate cell growth transcription factors, including MAP-kinase/AP-1, NF-kappaB and p53 pathways, that have a direct effect on cell proliferation and apoptosis. ROS also regulate protein kinase or tyrosine kinase activities (Wang *et al*., 2008).

1.3.2 UVA and ROS

The biological effects of UVA radiation on cells are dependent on the presence of oxygen (Danpure and Tyrrell, 1976; Tyrrell and Pidoux, 1989), implying the involvement of ROS in UVA-mediated cytotoxicity. UVA is the oxidizing component of sunlight as it triggers the generation of ROS in exposed cells/tissues via interactions with a variety of photosensitisers known as 'chromophores'. UVA must be absorbed in order to produce a chemical change. Absorption of UVA radiation by a biomolecule leads to an excited state in which one electron of the absorbing molecule is raised to a higher energy level. UVA absorption by the biomolecule may either lead to the generation of reactive species in a metastable excited state, or to free radical production. Both outcomes are formed extremely fast, since chemical reactions often occur within microseconds, but may last for hours.

These relatively fast processes are eventually translated into photobiological responses which could occur in seconds but can take years to become apparent (e.g. cancer). *In vitro,* UVA irradiation of macromolecules has been shown to generate H_2O_2, $O_2^{\bullet-}$ and $OH^{\bullet}$ (see Tyrrell, 1991). The highly reactive $OH^{\bullet}$ can be generated via iron-catalyzed reduction of H_2O_2 by $O_2^{\bullet-}$ (Beauchamp and Fridovich, 1970). *In vivo,* UVA irradiation may also generate ROS (Tyrrell, 1991; Beauchamp and Fridovich, 1970) via interaction with intracellular chromophores notably quinones, flavins, steroids and porphyrins, although the exact species remain to be defined (Tyrrell, 1994). UVA effects also involve H_2O_2 formation and iron-catalysed generation of $OH^{\bullet}$ (Tyrrell, 1991; Pourzand *et al.*, 1999b; Zhong *et al.*, 2004; Reelfs *et al.*, 2010). Based on these findings the UVA irradiation is now considered as a generator of intracellular oxidative stress.Anderson and Parrish in 1981 confirmed that melanin (a complex polymeric protein produced by melanocytes and confined to the epidermis and the SC) is another important UVA absorbing chromophore in human skin (Anderson and Parrish, 1981). Melanocytes are stimulated upon UVA irradiation and divide and synthesize melanin. Both forms of melanin, phaeomelanin and eumelanin, take part in the screening effect of the whole epidermis. Human melanoma cells with high melanin content have been shown to accumulate twice as much oxidative damage upon UVA radiation than cells with low melanin content (Kvam and Tyrrell, 1997). Additionally, *in vitro* studies have suggested that the epidermal urocanic acid (a deamination product of histidine), is another important chromophore that may initiate chemical processes that could lead to the photoaging of the skin (Hanson and Simon, 1998). Furthermore, the amino acids tyrosine and tryptophan as well as NADH and NADPH, also exhibit absorption within the UVA range (Tyrrell, 1991).

$^1O_2$ and H_2O_2 are thought to be the most important ROS generated intracellularly by UVA, promoting biological damage in exposed tissues via iron-catalysed oxidative reactions (Vile and Tyrrell, 1995). It has been shown that physiologically relevant doses of UVA induce lipid peroxidation leading to production of alkoxyl radical ($LO^{\bullet}$), peroxyl radical ($LOO^{\bullet}$) and lipid peroxide (LOOH) in membranes of human primary fibroblasts and keratinocytes, via pathways involving iron and $^1O_2$ (Morliere *et al.*, 1991; Punnonen *et al.*, 1991; Vile and Tyrrell, 1995). Indeed, iron 'at' or 'near' strategic targets such as cell membranes, can undergo redox cycling by reacting sequentially with one electron reductants and oxidants, thereby generating toxic oxidants such as $OH^{\bullet}$ and lipid-derived alkoxyl and peroxyl radicals and can elicit biological damage (Aust *et al.*, 1985; Halliwell and Gutteridge, 1999). However, in relation to UVA, current data from the literature suggest that $O_2^{\bullet-}$ is not involved in any of the cellular effects mediated by UVA observed so far, including lipid peroxidation and protein oxidation (Vile and Tyrrell, 1995; Giordani *et al.*, 1997). It is now well known that UVA is a strong membrane-damaging agent. UVA-induced lipid peroxidation was also found to be dependent on the chemical composition of membranes, as polyunsaturated fatty acid enrichment of human keratinocytes increased the peroxidation process (Quiec *et al.*, 1995). UVA-induced membrane damage has also been directly correlated with cell death in human skin fibroblasts (Applegate *et al.*, 1994). Internal lipid membranes in eukaryotic cells, such as those of lysosomes, mitochondria and the nucleus, have also been shown to be damaged following UVA radiation.

Immediate cellular effects of physiologically relevant doses of UVA include depletion of cellular glutathione (GSH) content, membrane lipid peroxidation and alteration in nuclear transcription factor activity and gene expression (Vile and Tyrrell, 1995; Djavaheri-Mergny *et al.*, 1996; Tyrrell, 1996a; Klotz *et al.*, 1997; Wlaschek *et al.*, 1997). The potentiation of UVA photokilling by GSH depletion provides further evidence for ROS involvement in UVA effects (Tyrrell and Pidoux, 1988).

The UVA-induced generation of $^1O_2$ has been shown to play a crucial role in UVA-induced peroxidation of membrane lipids of cultured human skin fibroblasts as well as activation of nuclear transcription factors such as NF-kappaB (Gaboriau *et al.*, 1995; Reelfs *et al.*, 2004). Studies with iron chelators have demonstrated that iron-catalyzed ROS are also certainly involved in UVA-induced NF-kappaB activation, membrane damage and cell death (Reelfs *et al.*, 2004; Zhong *et al.*, 2004; Yiakouvaki *et al.*, 2006; Reelfs *et al.*, 2010).

The gene whose expression is most enhanced by UVA, encodes the mammalian stress protein and heme degrading enzyme, heme-oxygenase-1 (HO-1) (Keyse and Tyrrell, 1989). The transcriptional activation of HO-1 is now used as a marker of oxidative stress in mammalian cells (Keyse and Tyrrell, 1989; Tyrrell, 1994). Studies with deuterium oxide (D_2O, that enhances the lifetime of $^1O_2$) and sodium azide and L-histidine (two quenchers of $^1O_2$) have shown that $^1O_2$ may be the primary effector in the transcriptional activation of HO-1 by UVA in cultured skin fibroblasts (Basu-Modak and Tyrrell, 1993).

A major consequence of UVA irradiation of human skin cells is the immediate release of chelatable 'labile' iron (LI) in the cytosol that appears to exacerbate the oxidative damage exerted by ROS generated by UVA. The UVA-mediated increase in LI in human skin fibroblasts plays a key role in activation of NF-kappa B and UVA-induced necrotic cell death (Pourzand and Tyrrell, 1999; Pourzand *et al.*, 1999b; Reelfs *et al.*, 2004; Zhong *et al.*, 2004; Reelfs *et al.*, 2010).

1.4 Skin Antioxidant Defence against UVA

As mentioned above, skin is the first interface with the external environment. As such it is extremely exposed to oxidative stress which generates ROS directly or indirectly derived from the presence of oxygen. Due to the susceptibility of cellular components to potentially harmful oxidation, cell survival could only happen by the existence of a large range of antioxidants defences, which are composed of free radical scavengers, either enzymatic or non-enzymatic, which sometimes act in synergy. *In vivo* measurements in mouse and human skin have demonstrated that both enzymatic (catalase, glutathione peroxidase, glutathione reductase, and hemeoxygenase-2) and non-enzymatic (GSH, urate, ascorbate) antioxidant capacities of the epidermis is higher than that of the dermis (Shindo *et al.*, 1993; Applegate *et al.*, 1995; Applegate *et al.*, 1996). However, UV radiation (UVB and UVA) reduces both enzymatic and non-enzymatic antioxidant defences in cultured skin cells. Possible mechanisms involved in defence against UVA-mediated oxidative stress in the skin are presented in this section.

1.4.1 Non-enzymatic antioxidants

1.4.1.1 Glutathione

Glutathione (L-gamma-glutamyl-L-cysteinyl glycine, GSH) is a tripeptide antioxidant that is present in most mammalian cells in high concentrations (i.e. 3-5 mM) and it is the major cellular antioxidant (Meister and Anderson, 1983). It is synthesised by two steps (Halliwell and Gutteridge, 1999) as detailed below:

First, the dipeptide formation is catalysed by γ- glutamylcysteine synthetase:

L-glutamate + L-cysteine + ATP → L-γ-glutamyl-L-cysteine + ADP + Pi

Then GSH is produced by glutathione synthetase:

L-γ-glutamyl-L-cysteine + glycine + ATP → GSH + ADP + Pi

Glutathione is present in two forms, the reduced form (GSH) and the oxidized form (GSSG) where it redox-cycles between them, but the vast majority (95-99%) is in the reduced form (Dethmers and Meister, 1981; Meister and Anderson, 1983)

In human skin cells in culture, there is a direct correlation between the levels of endogenous GSH and sensitivity for cell killing by UVA (Tyrrell and Pidoux, 1986, 1988)

GSH levels modulate the levels of pre-mutagenic damage arising as a result of normal metabolism in cultured human cells and following UVA radiation (Applegate *et al.*, 1992). It has been shown that in murine skin, GSH in both dermis and epidermis is depleted by UVA treatment (Connor and Wheeler, 1987).

The protection mechanism of GSH is unknown. However, as the most important intracellular thiol, it may act directly by scavenging radicals by hydrogen donation, competing with protein thiols for oxidising species, or indirectly as a cofactor for a number of protective enzymes including glutathione peroxidases (GPxs involved in detoxification of H_2O_2 or organic peroxides) (Ursini *et al.*, 1982; Tyrrell and Pidoux, 1988; Lautier *et al.*, 1992; Jornot and Junod, 1993). Many of the radical or non-radical reactions in cells involving GSH may lead to thiol oxidation to the disulphide, i.e., the oxidation of GSH to form GSSG. Therefore the regeneration of GSH (catalysed by GSSG reductase), as well as the provision of essential reducing equivalents (NADPH) to this enzyme, are important in antioxidant defense.

1.4.1.2 Vitamins

Antioxidant protection can also be achieved by vitamins that are available in our diet. Vitamin E, that is found mainly in green vegetables and cereal grains, is a major lipophilic antioxidant, that comprises at least eight isomers of tocopherol, from which α- tocopherol is the best characterized. As well as inhibiting lipid peroxidation, α-tocopherol also acts as a scavenger of lipid peroxyl radicals (Cheeseman and Slater, 1993). It has also been demonstrated that α-tocopherol can inhibit the UVA-mediated lipid membrane damage (Morliere *et al.,* 1991; Vile and Tyrrell, 1995). *In vitro* studies have demonstrated that α-tocopherol is capable of reacting and quenching $^1O_2$ (Grams and Eskins, 1972; Foote *et al.*, 1974), however the importance of this phenomenon in biological membranes remains to be established. In addition to the role of α-tocopherol in preventing lipid peroxidation *in vivo,* there is also weak evidence for the photoprotective effects of vitamin E in animal cells and tissues (Bissett *et al.*, 1990; Record *et al.*, 1991; Fryer, 1993). Some protective effects have been reported in rodent cells in culture against UVB-induced cytotoxicity (Sugiyama *et al.*, 1992), but not against DNA damage. Topical application of α-tocopherol acetate on the skin of mice prevented UVB-induced erythema and sunburn (Trevithick *et al.*, 1992). UVA-induced cytotoxicity could be inhibited only in the case of a photosensitivity disease i.e solar dermatitis (sun burn) by a water soluble vitamin E analog, Trolox C (Kralli and Moss, 1987). Nevertheless, in Pourzand's laboratory, it has been demonstrated that pre-treatment of cultured human primary fibroblasts with α-tocopherol-acetate could partially protect the cells against UVA-induced lysosomal damage and necrotic cell death (Zhong *et al.*, 2004). Additionally, there is evidence that vitamin E, at least when applied topically to the skin, is able to protect partially against ozone-mediated lipid peroxidation (Thiele *et al.*, 1997). α-tocopherol is closely coupled to both vitamin C and thiol cycle for the generation and maintenance of sufficient levels of cellular reducing power.

Vitamin C (ascorbic acid) is a hydrophilic antioxidant that exerts its effect by scavenging ROS i.e. $O_2^{\bullet-}$ and $OH^{\bullet}$. Furthermore, vitamin C may have a role in preventing oxidative damage by acting synergistically with vitamin E. The GSH-dependent free radical reductase may also generate oxidised vitamin E. A dietary antioxidant mixture (vitamin E, vitamin C and GSH) clearly reduced the UVB-induced tumour multiplicity and increased the tumour latent period in mouse studies (Black *et al.*, 1985), demonstrating the importance of the concept of interaction between different antioxidants. Ascorbate is able to react with a variety

of active oxygen species (Halliwell and Gutteridge, 1999). It is for example able to quench $^1O_2$ (Chou and Khan, 1983), which is potentially an important way of protection in biological systems where $^1O_2$ is produced in aqueous phase. However, *in vitro* studies have shown that ascorbate has prooxidant properties as it acts as an iron reductant to produce $OH^{\bullet}$. For example, ascorbate stimulates iron-dependent peroxidation of membrane lipids in certain circumstances (Muakkassah-Kelly *et al.*, 1982; Basu-Modak *et al.*, 1996). However, this has no major physiological relevance as any excess is excreted from the body (Halliwell and Gutteridge, 1999). The levels of vitamin C in human plasma were found to be around 10-100 μM (Halliwell and Gutteridge, 1999). Good sources of vitamin C in our diet are vegetables and fresh fruits, especially tomatoes.

Carotenoid pigments such as vitamin A (β-carotene) are lipid-soluble compounds which can protect cells against photosensitised reactions in different ways (Krinsky and Deneke, 1982), including quenching of triplet sensitisers, quenching of $^1O_2$. This property is particularly important in the skin, since $^1O_2$ is probably the primary species generated by the interaction of UV/visible radiation with the photosensitizer PPIX present close to the skin surface. Studies have also shown that β-carotene inhibits UV-induced epidermal damage and tumour formation in mouse models (Epstein, 1977; Mathews-Roth and Krinsky, 1987). The role of the antioxidant in protecting cells against UV-induced oxidative stress requires further clarification.

1.4.2 Enzymatic antioxidants

The enzymatic system of the skin acts by catalysing the decomposition of oxidants and free radicals into less reactive species. Mammalian detoxifying enzymes include glutathione peroxidases/reductases, superoxide dismutase, catalase and thioredoxin reductase.

1.4.2.1 Glutathione peroxidase (GPx) / Glutathione reductase (GR)

Glutathione peroxidases (GPxs) and associated enzymes form a family of selenium-dependent hemoproteins which not only detoxify H_2O_2, but also reduce harmful hydroperoxides such as those resulting from lipid peroxidation (Ursini *et al.*, 1995). Glutathione peroxidase (GPx) and Glutathione reductase (GR) are present at high concentrations in some parts of the human body i.e. liver, kidney, and whole blood. GPx, first

discovered in 1957, can be found in the cytoplasm and the mitochondria. It has four selenium atoms (Se), on its four protein subunits, which are responsible for its activity.

GPx catalyses the reduction of H_2O_2 yielding oxidised glutathione (GSSG):

$$H_2O_2 + 2GSH \xrightarrow{GPx} GSSG + 2H_2O$$

It also catalyses the reduction of lipid hydroperoxides (Martinez-Cayuela, 1995):

$$LOOH + 2GSH \xrightarrow{GPx} GSSG + H_2O + LOH$$

On the other hand GR, which is a cytosolic protein, contains flavin adenine dinucleotide (FAD), as its active site, on its two protein subunits. Whilst the conversion of GSH to GSSG is high in normal cells (Halliwell and Gutteridge, 1999), GR acts by reducing oxidised glutathione to GSH.

$$GSSG + NADPH + H^+ \xrightarrow{GR} 2GSH + NADP^+$$

GPx, according to studies by Leccia *et al.* (1993), can also significantly decrease the level of UVA-induced oxidative membrane damage (Leccia *et al.*, 1993). Recently it has been shown that low doses of UVA radiation lead to an up-regulation of GPx activity, protecting cells against a subsequent challenge of higher doses of UVA (Meewes *et al.*, 2001). In cultured human cells, GPx and SOD are not affected by UVA radiation; however catalase is very sensitive to UVA and could be inactivated as a result of the radiation insult (Tyrrell and Pidoux, 1989; Moysan *et al.*, 1993). Enhancing GPx activity of cultured human cells by supplementing them with selenium provided protection against UVA-mediated damage (Leccia *et al.*, 1993). Conversely, selenium deprivation of cells sensitized them to UVA- and H_2O_2 -mediated cytotoxicity and lipid peroxidation (Bertling *et al.*, 1996).

1.4.2.2 Superoxide dismutase (SOD)

SOD exerts its activity by catalysing the reduction of $O_2^{\bullet-}$ to less reactive H_2O_2 (Martinez-Cayuela, 1995).

$$O_2^{\bullet-} + O_2^{\bullet-} + 2H^+ \xrightarrow{SOD} H_2O_2 + O_2$$

In mammalian cells three SODs are present: SOD1, SOD2 and SOD3 (Raha and Robinson, 2000). SOD1 is the cytosolic copper-zinc (CuZn)-containing superoxide dismutase (CuZnSOD), SOD2 is the intramitochondrial manganese (Mn) superoxide dismutase (MnSOD), and SOD3 is the extracellular CuZn superoxide dismutase (Halliwell and Gutteridge, 1999). The activity of SOD varies among the tissues and its activity is regulated through biosynthesis, which is sensitive to tissue oxygenation (Yu, 1994). Since SOD reduces

$O_2^{\bullet-}$ to H_2O_2, the increase in SOD activity has been shown to be accompanied by an increase in catalase and/or GPx to prevent H_2O_2 formation (Amstad *et al.*, 1991; Yohn *et al.*, 1991).

1.4.2.3 Catalase

Catalase is composed of four protein subunits, each of which has a ferric (Fe^{3+}) heme group bound to its active site (Halliwell and Gutteridge, 1999). It is present in all major body organs and at high concentrations in the liver. Catalase is mainly located in the peroxisome, a cellular organelle found in the cytoplasm bound by a single membrane.

As mentioned in the previous section, H_2O_2 is the product of the dismutation of $O_2^{\bullet-}$. Catalase acts by catalysing the direct decomposition of H_2O_2 to ground state oxygen and water reaction (Martinez-Cayuela, 1995):

$$2\ H_2O_2 \xrightarrow{\text{catalase}} 2\ H_2O + O_2$$

Also, there is evidence showing that catalase activity is strongly inhibited after UVA exposure, in cultured human fibroblasts and keratinocytes (Punnonen *et al.*, 1991; Moysan *et al.*, 1993; Shindo and Hashimoto, 1997). However, compared to GSH, catalase is less important for the protection of cells to oxidative damage, since it has been shown that when cells are deficient in catalase there is no decrease in cell survival after UVA radiation (Tyrrell and Pidoux, 1989; Peak and Peak, 1990).

1.4.2.4 Thioredoxin (TRx)

Thioredoxin is a small protein which, in its reduced form, has a general protein disulphide reductase activity via its two reactive thiol groups (Holmgren, 1985). It is generally concentrated in the ER and also can be found on the cell surface. TRx is also a major carrier of redox potential within cells (Kontou *et al.*, 2004). Together with glutathione, they both maintain signaling components in a reduced state and are counter-balanced in signaling by oxidative stress, typically ROS (Jones *et al.*, 2004).

TRx has two reduced –SH groups, and is converted to an oxidised TRx with a disulphide (-S-S-) in the presence of proteins (Halliwell and Gutteridge, 1999):

$$TRx{-}(SH)_2 + protein{-}S_2 \rightleftharpoons TRx{-}S_2 + protein{-}(SH)_2$$

Thioredoxin exerts its antioxidant activity by different pathways; it has been shown to possess a radical-scavenging activity (Schenk *et al.*, 1994). It has been also involved in DNA repair, since it acts as a hydrogen donor for ribonucleotide reductase. It is also implicated in

protein repair since it provides electrons to methionine sulphoxide reductase, which repairs oxidative damage to methionine residues (Halliwell and Gutteridge, 1999). The thioredoxin/thioredoxin reductase (Trx/TR) system may also have a role in the cellular defence of skin against oxidative stress including UV radiation. Thioredoxin reduces free radicals in human keratinocytes *in vivo* (Schallreuter *et al.*, 1986). Thioredoxin expression is induced by oxidative stress, including H_2O_2 and UV (Spector *et al.*, 1988; Nakamura *et al.*, 1994) in a variety of cell types in culture including keratinocytes. Also, a prognostic value for Trx has been described in malignant melanoma (Schallreuter *et al.*, 1991).

Owing to its metal-binding capacity, metallothionein (MT) could contribute to skin protection against phototoxicity injury. In fact, MT has been shown to be induced *in vitro* by UVC and UVB radiation (Stein *et al.*, 1989; Hansen *et al.*, 1997). Rodent cells with elevated levels of MT have been shown to have increased resistance to UVA radiation (Dudek *et al.*, 1993). The induction of expression of this gene also seems to correlate with a resistance to killing by several mutagenic agents. However, basal MT levels may also function to regulate intracellular redox status in mammalian cells, since rodent MT-null cells showed enhanced sensitivity to oxidative stress (i.e. tert-butylhydroperoxide) as compared to normal cells (Lazo *et al.*, 1995).

Finally the copper-containing protein caeruloplasmin may represent an additional and distinct type of antioxidant behaviour, by oxidizing Fe^{2+} to Fe^{3+} (ferroxidase activity), thus preventing the iron from entering into a reversible redox system (Omoto and Tavassoli, 1990). This may facilitate iron incorporation by iron-binding proteins (Boyer and Schori, 1983; Samokyszyn *et al.*, 1989).

1.4.3 The inducible cellular defence

1.4.3.1 Heme oxygenase (HO)

Different forms of oxidative stress, including UVA radiation and H_2O_2, are capable of inducing gene expression in mammalian cells. Among these genes, heme-oxygenase (HO) has been shown to become highly activated under conditions of oxidative stress (Keyse and Tyrrell, 1990).

Heme oxygenase (HO) is a microsomal isozyme that is the rate-limiting enzyme that catalyzes the degradation of heme (prooxidant) to biliverdin and carbon monoxide (CO), and the release of ferrous iron ions (Halliwell and Gutteridge, 1999):

$$\text{Heam} \xrightarrow{\text{HO}} \text{Biliverdin} + \text{CO} + \text{Fe}^{2+}$$

Biliverdin is then reduced, by biliverdin reductase, to bilirubin (an antioxidant) in the cytosol. Bilirubin has been discovered to account for the majority of the antioxidant activity of human serum (Gopinathan *et al.*, 1994). With a decrease in the pH, the potency of bilirubin as a free radical scavenger is increased (Winrow *et al.*, 1993).

The active site of HO is located on the cytoplasmic site of the ER (Hino *et al.*, 1979). To date three isoforms of mammalian HO have been identified: HO-1, an inducible enzyme that is most highly concentrated in tissues that are heavily involved in the catabolism of heme proteins; HO-2, a non-inducible (in general; the constitutive) isoform that is thought to be particularly involved in signalling pathways; and HO-3 which has low catalytic activity and uncertain physiological role (Maines *et al.*, 1986; McCoubrey *et al.*, 1997). While HO-2 is believed to be the constitutive form of HO, HO-1 is a stress-induced enzyme (Keyse and Tyrrell, 1989).

In 1989, Tyrrel and collegues identified HO-1 as the 32kD protein which is highly expressed following UVA and H_2O_2 treatments in human skin fibroblasts (Keyse and Tyrrell, 1989, 1990). Both UVA and H_2O_2 release heme, the substrate of the HO-1 reaction, from microsomal heme-containing proteins and this correlates with UVA-mediated HO-1 activation (Kvam *et al.*, 1999). Further to this, Basu-Modak and Tyrrell (1993) have shown that UVA-mediated generation of $^1O_2$ species plays a central role in activation of the heme oxygenase 'decycling' 1 *hmox-1*, the gene that encodes HO-1. Furthermore, UVA irradiation in presence of D_2O (an $^1O_2$ enhancer), further increases accumulation of HO-1 mRNA, while UVA irradiation in the presence of sodium azide or histidine ($^1O_2$ quenchers) decreases HO-1 expression (Basu-Modak and Tyrrell, 1993). Additionally, UVA treatment with beta carotene, the natural $^1O_2$ quencher, suppresses UVA mediated HO-1 activation in human skin fibroblasts (Trekli *et al.*, 2003). Taken together, these observations are consistent with the concept that both the substrate heme and UVA-mediated release of $^1O_2$ play a major role in UVA mediated HO-1 activation (Raval, 2008). Moreover, studies by Ferris *et al.* (1999) showed that HO-1 absence leads to iron accumulation, whereas HO-1 overexpression decreases cellular iron levels (Ferris *et al.*, 1999). Thus the protective effect of HO-1 following oxidative stress can be mimicked by iron chelation. Interestingly, the enhanced

protective role of HO-1 is central to the development of an adaptive response that involves Ft. The overall effect of HO is to remove the pro-oxidant heme while generating the anti-oxidant, bilirubin, and another pro-oxidant, iron that will be taken up by Ft. Vile *et al.* in 1994 clearly demonstrated that when human skin fibroblasts were treated with HO-1 anti-sense oligonunleotides, the UVA-induced increase in Ft levels was prevented as well as the adaptive response that leads to protection against oxidative damage (Vile *et al.*, 1994). An additional study by Rothfuss *et al.* (2001) in human lymphocytes also demonstrated the functional involvement of HO-1 against the induction of oxidative DNA damage, but the exact mechanism remains to be elucidated (Rothfuss *et al.*, 2001).

In addition to HO-1, the other two constitutive isoforms, HO-2 (36 kDa) and HO-3 (33 kDa) have also been extensively studied although their exact function has yet to be elucidated. So far, studies by Rotenberg and Maines (1991) and McCourbey *et al.* (1992, 1993) have revealed that the amino acid sequences of HO-1 and HO-2 are around 40% similar and both isoforms display the same enzymatic activity and hence the molecular mechanism of the enzyme action should be analogous (Rotenberg and Maines, 1991; McCoubrey *et al.*, 1997). Ishikawa *et al.* (1995), who expressed the human HO-2 protein in a bacterial expression system, suggested that the HO-2 catalytic mechanism of heme degradation is very similar to HO-1 (Ishikawa *et al.*, 1995). Finally, in an HO-2 gene-deletion mouse model, HO-1 induction increased oxidative damage during hyperoxia by mechanisms that appeared to involve a two-fold increase in lung GSH and accumulation of redox active iron (Dennery *et al.*, 1998), suggesting an indirect role for HO-2 in induction of oxidative damage. The function of the third isoform of heme oxygenase (HO-3) still remains unknown. The only proposed mechanism regarding its function is that since it contains a heme regulatory motif, it might be a heme sensing/binding protein (reviewed by McCoubrey *et al.*, 1997).

1.4.3.2 Ferritin (Ft)

Cairo *et al.* (1995) have suggested that liver Ft can act as a pro- or an anti-oxidant in a time-dependent manner. Treating Wistar rats with phorone, a glutathione-depleting drug that amplifies the effects of ROS, led to an early decrease in Ft. Interestingly, a 6-fold increase of Ft synthesis was shown as a late response (Cairo *et al.*, 1995). Treatment of skin fibroblasts with UVA led to a total degradation of Ft (Pourzand *et al.*, 1999b). However, Ft levels returned to normal six hours following UVA treatment. Then Ft levels increased up to 3-fold 24-48h following UVA treatment (Vile and Tyrrell, 1993). Furthermore, it seems from

studies with different cell types: in the early stages of oxidative challenge including H_2O_2 treatment, Ft might act as a pro-oxidant molecule since its degradation could be a potential source of iron involved in exacerbating the oxidative damage occurred in cells as a result of oxidative insult (Balla *et al.*, 1992; Balla *et al.*, 1993; Lin and Girotti, 1997; Garner *et al.*, 1998). The evidence for Ft acting as an antioxidant molecule is also overwhelming (reviewed in Arosio and Levi, 2002). Various studies have reported that different forms of oxidative challenge have demonstrated an increase in Ft levels, conferring resistance to the subsequent insult. It was demonstrated that the ferroxidase sites in H-Ft significantly reduces the production of $OH^{\bullet}$ from the Fenton reaction (Zhao *et al.*, 2006).UV radiation has also been shown to increase Ft levels in both the epidermal and dermal tissue allowing increased protection against oxidative stress (Applegate *et al.*, 1998). Further *in vivo* and *in vitro* studies demonstrated that acute UVA exposure increased in the long term the Ft levels in basal epidermal cells (Seite *et al.*, 2004). Also, an increase in H- and L-Ft synthesis was observed after exposing Hela cells to H_2O_2 treatment and this overexpression in turn reduced the accumulation of ROS (Orino *et al.*, 2001). It was suggested that Ft has an active role in regulating LIP levels and reducing ROS generation in human erythroleukemia cells (Kakhlon *et al.*, 2001). Interestingly, L-Ft has been suggested to have an important role in the protection against oxidative damage due to the presence of an antioxidant-responsive element (ARE) in the human L-Ft gene, which was positively regulated by hemin (Hintze and Theil, 2005). The ARE increases the expression of a diverse set of proteins involved in redox homeostasis such as TRx, HO and glutathione.

Levi *et al*, (2001) have described a gene that encodes a mitochondrial ferritin (MtF) located inside the matrix of human mitochondria. MtF has been suggested to be responsible for the detoxification and the trafficking of iron in the mitochondria (reviewed in Arosio and Levi, 2002).

Since iron has an important role as a catalyst in oxidative reactions, iron transport- and storage-proteins may play an important part as constitutive and/or inducible antioxidant defense by keeping "circulating iron" low and in a non-toxic form. The intracellular storage protein Ft appears to play a critical role in this respect (**see section 1.4.3.2**).

1.5 Iron

1.5.1 General aspects

Iron is a transition metal that can exist in two stable configurations: electron donor ferrous (Fe^{2+}) and electron acceptor ferric (Fe^{3+}). The easy access to two oxidation states allows iron to act as a catalyst in mammalian cellular pathways that involve redox mechanisms (Richardson and Ponka, 1997; Hentze *et al.*, 2004).

Iron plays a key role in cell growth, respiration and replication. Many iron-containing proteins catalyze key reactions involved in energy metabolism (cytochromes, mitochondrial aconitase, iron-sulfur proteins of the electron transport chain), respiration (hemoglobin and myoglobin), and DNA synthesis (ribonucleotide reductase). And it is well known that iron depletion leads to G1/S cell cycle arrest and apoptosis (Le and Richardson, 2002). Additionally, iron-containing proteins are required for the metabolism of collagen, tyrosine and catecholamines (Richardson and Ponka, 1997).

The total amount of iron in an average human body is about 4-5g (Trenam *et al.*, 1992), the majority of which is incorporated into the heme complex which is present in proteins such as haemoglobin, myoglobin and cytochromes (**Fig. 1.5**). The other type of iron is non-heme iron that is found in (4Fe–4S) cluster proteins such as iron regulatory proteins (IRPs), transferrin (Tf), ferritin (Ft) and hemosiderin (Cairo *et al.*, 2006).

In addition, there is now a strong evidence for the existence of a pool of "free" transit ionic iron known as the labile iron pool "LIP". The cellular LIP in quiescent conditions comprises only minor fractions of the total cellular iron (i.e. less than 5%) (Kakhlon and Cabantchik, 2002; Kruszewski, 2003).

Labile iron pool (LIP):

The intracellular LIP which exists at concentrations of 0.1-1µM , is defined as a pool of redox-active iron complexes and it was first suggested by Jacobs (1977) as an intermediate or transitory pool between extracellular iron and cellular iron associated with proteins (Jacobs, 1977). Iron belonging to this intracellular pool is considered to be in steady-state equilibrium, loosely bound to low-molecular-weight compounds, accessible to permeant chelators and metabolically and catalytically reactive (Breuer *et al.*, 1996; Epsztejn *et al.*, 1997; Cairo and Pietrangelo, 2000; Petrat *et al.*, 2001). Cabantchik and coworkers have

defined LIP operationally as a cell chelatable pool that comprises both ionic forms of iron (Fe^{2+} and Fe^{3+}) associated with a diverse population of ligands such as organic anions (phosphates and carboxylates), polypeptides, and surface components of membranes (e.g. phospholipid head groups) (see Kakhlon and Cabantchik, 2002; Kruszewski, 2003). This definition implies that LIP can not only potentially participate in redox cycling but also be scavenged by permeant chelators. The latter properties form the basis for the quantification of the cellular LIP (Kakhlon and Cabantchik, 2002; Kruszewski, 2003).

Labile iron pool is associated with important functions: (a) physiologically, as readily available sources of iron for incorporation into proteins; (b) pharmacologically, as targets for chelators or metal scavengers; and (c) toxicologically, as vehicles for promoting the formation of free radicals.

However, labile iron in excess can be highly toxic due to its ability to react with ROS such as $O_2^{\bullet-}$ and H_2O_2 giving rise to $OH^{\bullet}$ via Haber-Weiss and Fenton reactions (Halliwell and Gutteridge, 1999). Such highly ROS are capable of interacting with most biomolecules that results in damage in cells, tissues and organs (Shinar and Rachmilewitz, 1990; Wong *et al.*, 1999). In contrast to the intracellular LIP, there is also the presence of the extracellular LIP, which is often associated with pathological conditions. This form of LIP has been originally observed in iron-over-load β-thalassemia patients whose plasma Tf iron-binding capacity was surpassed (Hershko *et al.*, 1978). Further to β-thalassemia, other conditions of iron imbalance have been defined (i.e. hemochromatosis), in which the LIP has been found to be bound to ligands other than Tf as non-Tf bound iron. Finally there is evidence for age-related accumulation of LIP associated with rheumatoid arthritis (Guillen *et al.*, 1998).

Therefore, the pool of reactive iron in cells is strictly regulated by specialised proteins which transport and store iron in a soluble and non-toxic form (Richardson and Ponka, 1997).

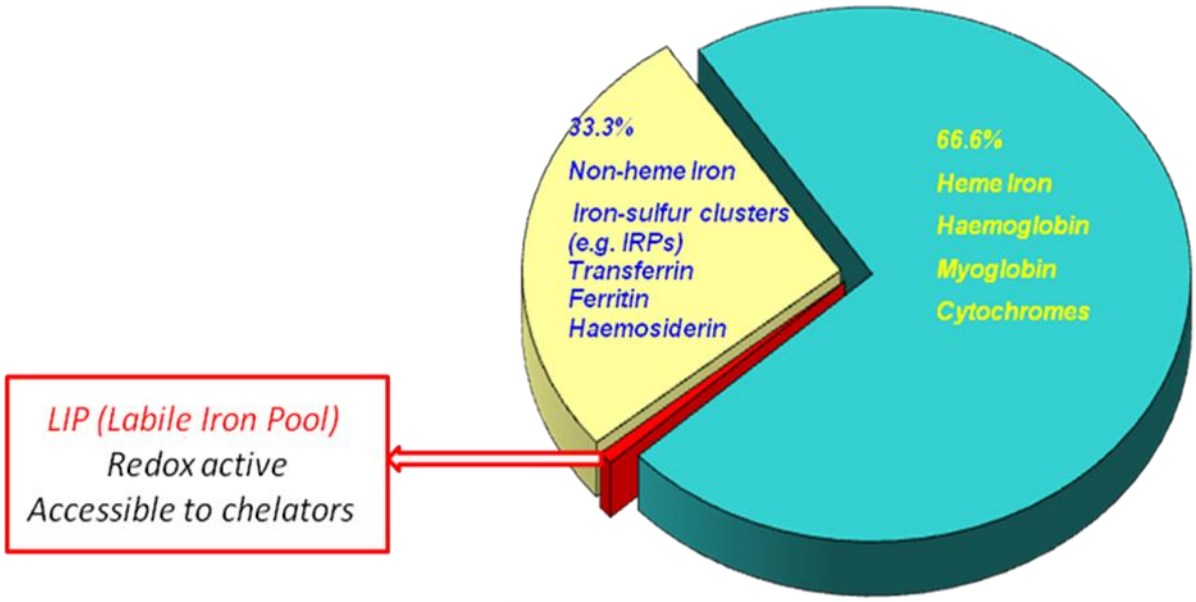

Figure 1.5: Diagrammatic representation of iron distribution in the body**.** Reproduced with the permission of Dr Pourzand.

1.5.2 Iron and oxidative stress

The LIP is able to induce oxidative stress through its ability to increase the rate of reactions to produce ROS, giving rise to a highly reactive $OH^{\bullet}$ via the Fenton reaction (2) or the Haber-Weiss reaction (3)

$$O_2^{\bullet -} + Fe^{3+} \longrightarrow Fe^{2+} + O_2 \qquad (1)$$

$$H_2O_2 + Fe^{2+} \longrightarrow OH^{\bullet} + OH^{-} + Fe^{3+} \qquad (2) \qquad \textbf{(Fenton reaction)}$$

Net: $$O_2^{\bullet -} + H_2O_2 \xrightarrow{Iron} OH^{\bullet} + OH^{-} + O_2 \qquad (3) \qquad \textbf{(Haber-Weiss reaction)}$$

(**Halliwell and Gutteridge, 1999**)

And, vice versa, Oxidative stress in the form of UV light has been shown to accumulate iron. UVB radiation was shown to increase the skin level of non-heme iron (Bissett *et al.*, 1991) and UVA radiation caused an immediate increase in 'free' iron in fibroblast (Pourzand *et al.*, 1999b). Such highly ROS are capable of interacting with most biomolecules, depending on the site of bound iron, including sugars, lipids, proteins, and nucleic acids. These interactions that promote various harmful processes in cells such as lipid peroxidation, protein oxidation, DNA/RNA oxidation and DNA lesions, ultimately overwhelm the cellular antioxidant defense mechanisms and lead to cell damage and death. As a consequence of these reactions, high levels of iron have been identified as a risk factor for the development of cancer (Toyokuni, 1996). Numerous studies across a variety of populations have found a positive correlation between iron stores in the body and risk of the development of a range of cancers including colorectal, liver, kidney, lung and stomach cancers (Richardson *et al.*, 2009).

Furthermore, the pathological consequences of iron-catalyzed oxidative damage are recognised in diseases such as hepatitis, hemochromatosis, liver cirrhosis, cancer and neurodegenerative disease (Bacon and Britton, 1990; Kowdley, 2004; Gaeta and Hider, 2005; Kalinowski and Richardson, 2005; Valko *et al.*, 2006; Valko *et al.*, 2007; Molina-Holgado *et al.*, 2008). Excess iron may also aggravate diabetes, cancer, cardiovascular disease and alcoholic and non-alcoholic steatohepatitis (Swanson, 2003; Kohgo *et al.*, 2005; Petersen, 2005; Brewer, 2007; Imeryuz *et al.*, 2007). The presence of excess iron has also been demonstrated in a variety of skin disorders such as psoriasis (Molin and Wester, 1973), venous ulceration (Ackerman *et al.*, 1988) and atopic eczema (David *et al.*, 1990), indicating the involvement of iron in the pathology of skin.

To minimise damage caused by labile iron, cellular iron levels are tightly regulated in order to maintain an adequate substrate for vital cell functions, while also minimising the pool of potentially toxic LIP.

1.5.3 Overview of iron homeostasis

1.5.3.1 Systemic iron absorption, recycling and storage

Due to the dual role of iron, there are strict control mechanisms that maintain appropriate iron levels by means of a complex network of transporters, storage molecules and regulators that coordinately govern iron absorption, iron recycling, and the mobilisation of stored iron. Any disruption in these processes causes a variety of disorders associated with iron deficiency or overload (Camaschella, 2005; Piccinelli and Samuelsson, 2007; Andrews, 2008; De Domenico *et al.*, 2008; MacKenzie *et al.*, 2008).

Iron is absorbed by enterocytes in the small intestine (Yu *et al.,* 2007). In the diet iron exists as either heme or non-heme (inorganic) iron (Yu *et al.,* 2007). There are two separate pathways that facilitate the absorption of these two forms of dietary iron (Recalcati *et al.*, 2010) **(Fig. 1.6)**. The majority of the non-heme iron is in the Fe^{3+} form, which needs to be reduced in the duodenal lumen by the postulated ferrireductase, Duodenal cytochrome b (Dcytb) (Recalcati *et al.*, 2010) which catalyses the conversion of Fe^{3+} to Fe^{2+}(Richardson *et al.,* 2009).Although studies in Dcytb-knockout mice have found that the activity of this enzyme is not critical for the uptake of dietary iron (Frazer *et al.*, 2005; Gunshin *et al.*, 2005) suggesting the presence of an alternative ferrireductase (Richardson *et al.,* 2009). Once iron is in the Fe^{+2} form , it is able to be transported into enterocytes via the divalent metal ion transporter (DMT1) that is expressed on the apical pole of enterocytes in the proximal duodenum (Mims and Prchal, 2005). Uptake of iron through DMT1 is regulated at the mRNA level, in part, by the iron-regulatory proteins 1 and 2 (IRP1 and IRP2). On the other hand, heme iron is thought to be transported to the cell by heme carrier protein 1 (HCP1) that was recently identified in the apical membrane of duodenal enterocytes (Shayeghi *et al.,* 2005; Latunde-Dada *et al.,* 2006). However, while this protein appears to transport heme, there is no strong evidence as yet that it is a physiologically-relevant mechanism. In addition, a latter study demonstrated that HCP1 was a folate transporter (Qiu *et al.*, 2006), questioning its role in heme metabolism (Andrews, 2007), or suggesting that it transports both heme and folate (Richardson *et al.,* 2009). Once internalized, heme is metabolized by HO to release iron,

carbon monoxide (CO) and bilirubin (**section 1.4.3.1**) (Yu *et al.*, 2007). After transport into the enterocyte, these forms of iron are consolidated to form the intracellular LIP consisting of Fe^{2+} and Fe^{+3} in redox equilibrium (St Pierre *et al.*, 1992). Iron is either stored in Ft or transported out of the enterocyte into the blood via the basolateral iron export protein, ferroportin-1 (FP1) (Hugman, 2006). The intracellular ferroxidase, hephaestin, also appears to be involved in this process, although its exact contribution remains unclear (Vulpe *et al.*, 1999; Han and Kim, 2007). Once at the surface of the enterocyte, $Fe^{2+}$is converted back to $Fe^{3+}$by means of multicopper oxidases (ceruloplasmin in the circulation and hephaestin on the basolateral membrane of enterocytes) (Recalcati *et al.*, 2010)**.** To keep to a minimum the level of unbound iron, and its consequent redox activity, body iron is either incorporated to Tf or recycled for heme synthesis as found in hemoproteins and myoglobin, haemoglobin being the major protein, or stored in the safe form in Ft in liver.

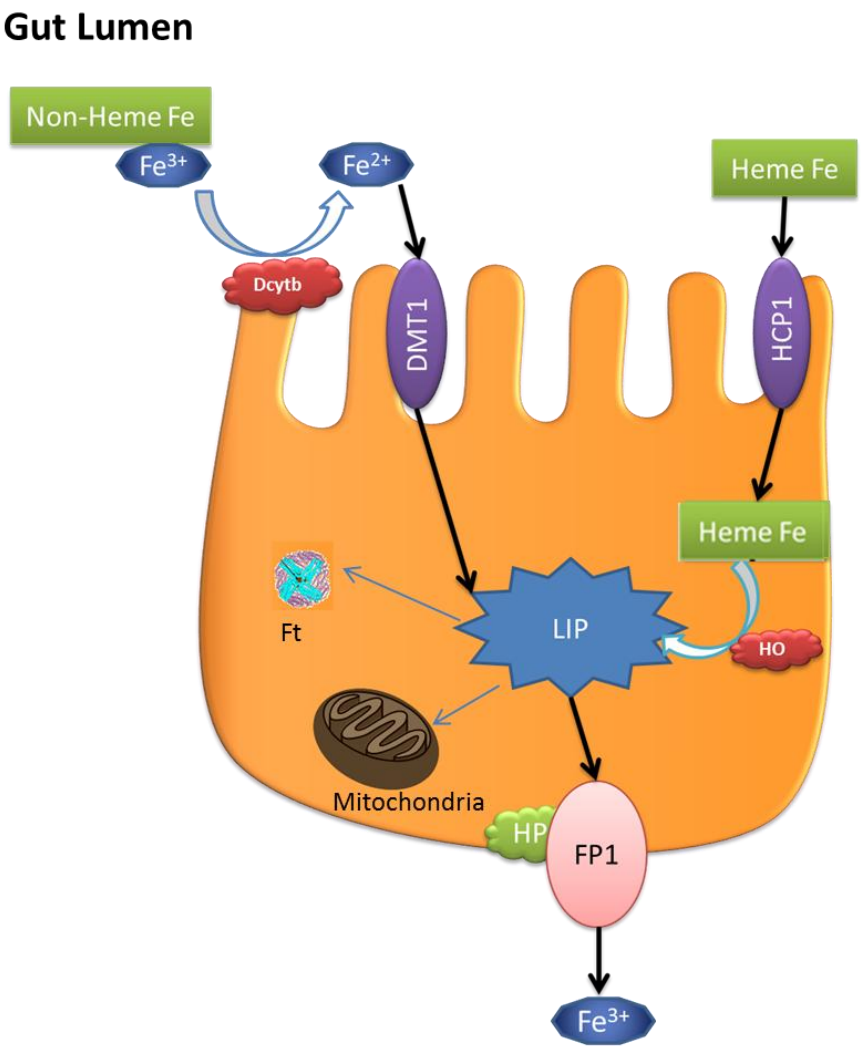

Figure 1.6: Schematic diagram of the pathways of absorption of heme and non-heme iron from the gut lumen to the portal circulation (Adapted from Syed *et al.*, 2006).

Heme enters the cells via the Heme Carrier Protein 1 (HCP1) which is expressed in the apical membrane of duodenal epithelial cells, and is degraded by Heme Oxygenase (HO) to yield ferrous iron inside the cell. Iron enters the LIP where it may be then stored in Ferritin (Ft) or transferred to the plasma and tissues via Ferroportin 1 (FP1) aided by Hephaestin (Hp) which exhibits ferroxidase activity. The enterocytes of the lumenal brush border contain an enzymatic ferric reductase activity, apparently the cytochrome *b*-like protein Dcytb, to ensure that non-heme iron is reduced when it is in the ferric state. Divalent Metal Transporter (DMT1) is the apical major ferrous transporter, which is responsible for transporting iron into cells.

HCP1: heme carrier protein 1; Dcytb: duodenal cytochrome b; FP1: ferroportin 1 (=Ireg1); Hp: hephaestin; Tf: transferrin; Ft: Ferritin; DMT1: divalent metal transporter 1

1.5.3.2 Cellular iron uptake and storage

Cells which require iron express the transferrin receptor-1 (TfR1) on their surface, which binds two molecules of Tf (Yu *et al.*, 2007) . Tf has a high affiniy for Fe^{+3} (Kd= 10^{-23} mol/L) and its primary function is to accept iron from plasma (and become the diferric form) and to transport iron into various cells and tissues, by binding to TfR1 . The Tf-TfR1 complex is then internalized by receptor-mediated endocytosis, where the diferric Tf-TfR1 complex is taken into the cell (Klausner *et al.*, 1983a; Klausner *et al.*, 1983b; Kalinowski and Richardson, 2005). Once in the endosome, the pH decreases via a proton pump present on the endosomal membrane allowing the Fe^{3+} to dissociate from the Tf-TfR1 complex. The endosomal ferrireductase, six-transmembrane epithelial antigen of the prostate-3 (Steap3) (Ohgami *et al.*, 2005), is thought to convert Fe^{3+} to Fe^{2+} in the endosome, allowing Fe^{2+} to be transported out of the endosome by DMT1 (Gunshin *et al.*, 1997). Once in the cell, Fe^{2+}can either be directly stored in iron storage protein Ft or it can first enter the intracellular LIP and then be subsequently stored in Ft (Harrison and Arosio, 1996). Alternatively the newly entered ferrous iron can be used in the synthesis of various proteins and enzymes such as ribonucleotide reductase (RR) (Yu *et al.*, 2006). The endosome containing the Tf–TfR1 complex then undergoes exocytosis to recycle TfR1 and return the apo-Tf to the bloodstream where it is able to bind more iron from the liver (Eisenstein, 2000) **(see Fig. 1.7).**

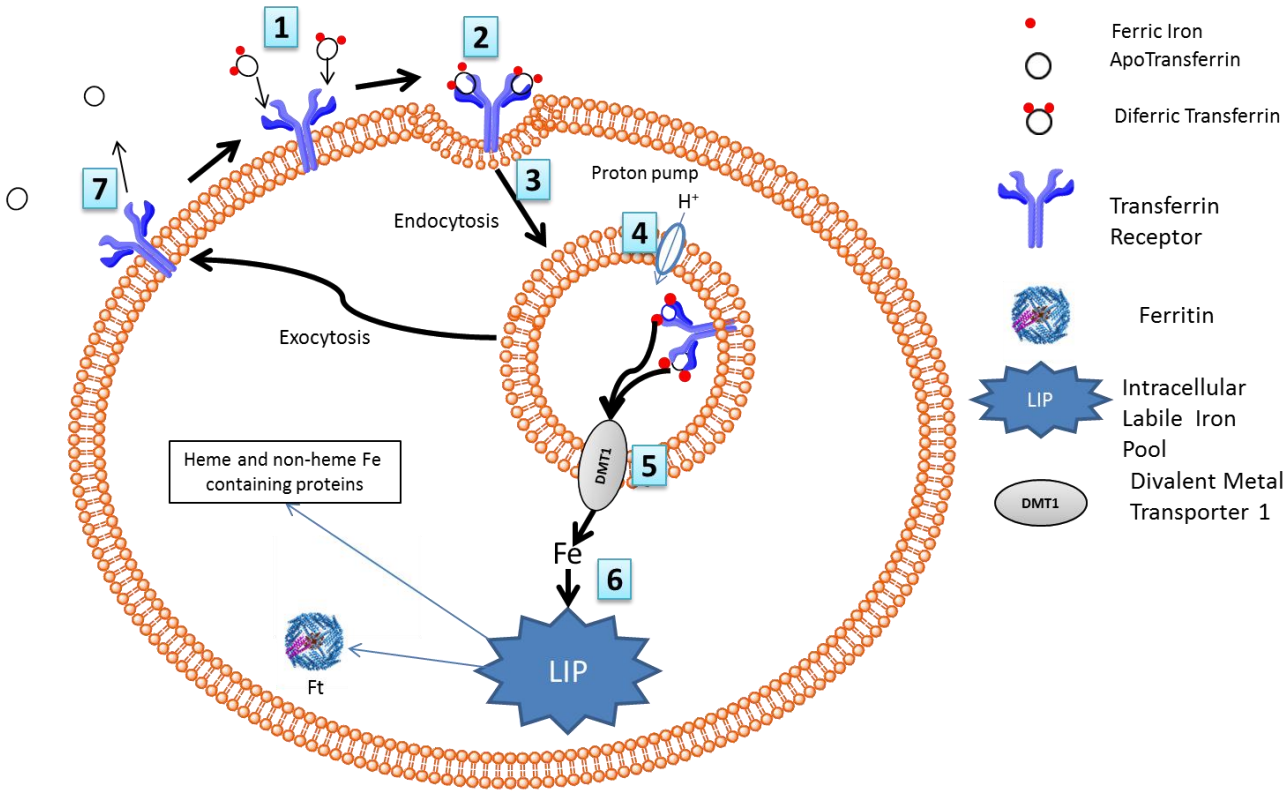

Figure 1.7: Schematic diagram illustrating the mechanisms involved in iron uptake. (Adapted from Kalinowski and Richardson, 2005)

1- Transferrin (Tf) binds two atoms of Fe^{3+} with high affinity. 2- Two molecules of diferric Tf bind to the Transferrin Receptor 1 (TfR1) on the cell surface. 3- The Tf-TfR1 complex formed is internalized into an endosome. 4- Within the endosome, iron is released from Tf following the decrease in intravesicular pH. 5- Iron transfers from Tf to Divalent Metal ion Transporter (DMT1) and is released in the Fe^{2+} form. 6- DMT1 transports Fe^{2+} across the endosomal membrane into the cytosol. 7- Apo-Tf is released into the plasma via exocytosis, whereby TfR1 returns to the cell surface.

1.5.3.3 Iron homeostasis

Mammalian cells maintain steady levels of metabolically active iron through the regulation of iron uptake and storage. The pathway of iron uptake via TfR and the iron storage in Ft are co-ordinately regulated at the post-transcriptional level by cytoplasmic factors known as iron regulatory proteins (IRPs). These regulatory mechanisms operate in order to prevent the expansion of the intracellular LIP, but still secure adequate supply of iron for the synthesis of iron-dependent proteins.

Transferrin (Tf)

Tf belongs to a family of related-binding proteins that includes: (a) serum Tf which binds iron in the circulation (b) lactoferrin, which is found both intracellularly and in secretions such as milk, tears and semen; (c) ovotransferrin, which is present in egg white and (d) melanotransferrin, which is formally known as tumour antigen p97. These proteins share a high degree of sequence homology.

Serum Tf is the plasma iron-binding glycoprotein, it is synthesised in hepatocytes and functions as the major vehicle for transfer of iron in the body between sites of absorption, storage and use. It is normally the only source of iron for hemoglobin synthesis.

Human serum Tf is a monomeric glycoprotein with a molecular weight of 80 kDa of which 6% is carbohydrate (MacGillivray *et al.*, 1983). It is encoded by gene on chromosome 3 (Yang *et al.*, 1984; Schaeffer *et al.*, 1987). Tf is a bilobal molecule and only one Fe^{3+} attaches to one of the two globular domains with high affinity at physiological pH (K_d=10^{-23} M) at sites located in the N and C lobes of the protein (Morgan, 1983; Richardson and Ponka, 1997). Transferrin exists as a mixture of iron-free (apoTf), one iron (monoTf) and two iron (difericTf) forms of the molecule. The binding of Fe^{+3} to Tf is a pH-dependent process (Chasteen, 1983).

In defined chemical systems iron can be released from Tf by three mechanisms i.e. (i) reduction of pH with resultant protonation of the iron-ligand bonds, (ii) reduction of Fe^{+3} to Fe^{+2}, and (iii) direct chelation by a stronger Fe-binding ligand (Aisen and Listowsky, 1980). There is strong evidence to indicate that Fe^{+3} is released from Tf via a decrease in pH in the endosome, leaving only apoTf (Huebers *et al.*, 1978).

Tf has three major functions: (1) it allows ferric iron to remain soluble i.e. in an aqueous and pH neutral plasma environment, (2) it allows iron to circulate in the safe form, and (3) it facilitates the cellular import of iron (Heeney and Andrews, 2004). The primary function of

Tf is to accept iron from plasma and to transport iron into various cells and tissues, by binding to membrane receptors (TfRs, see below).

There are several processes of iron uptake from Tf which have been identified in normal and neoplastic cells. The main process was consistent with saturable binding of Tf to the TfR1 and subsequent internalization of the protein via receptor mediated endocytosis (RME). However, a second process of iron uptake from Tf has also been identified which increases after saturation of the TfR1 (Page *et al.*, 1984; Trinder *et al.*, 1986; Richardson and Baker, 1990, 1994). It was suggested that this mechanism was consistent with adsorptive pinocytosis of Tf (Richardson and Baker, 1994). The control of iron uptake by the TfR1 is determined by the number of TfRs on the plasma membrane and the affinity of the TfR1 for Tf may play a role in controlling iron uptake in some cell types (Kwok and Richardson, 2002). It has been suggested that Tf may protect against oxidative damage by binding to iron and preventing oxidative reactions catalysed by iron (Klausner *et al.*, 1993; Kuhn, 1994).

Transferrin receptor (TfR)

Transferrin receptors (TfRs) provide controlled access of Tf to the cells. There are two forms of TfR, TfR1 and TfR2 (Kawabata *et al.*, 1999; Fleming *et al.*, 2000; Kawabata *et al.*, 2000) that have a distinct cell- and tissue-specific pattern. However, TfR2 was only described in 1999 in liver, liver-derived and human erythroleukemia K562 cell lines and is much less abundant than TfR1. So TfR1 has been the most studied one and was simply designated the TfR.

TfR is ubiquitously expressed in all cell types apart from mature erythrocytes and other terminally differentiated cells. It comprises two transmembrane glycoprotein subunits, covalently linked by S-S bonds. Each subunit has a MW of 90 kDa and binds one molecule of Tf (Enns and Sussman, 1981). The TfR subunits are encoded by genes on chromosome 3. Tf binds to the TfR at the cell surface and is internalised through clathrin-coated pits into endosomes.

Ferritin (Ft)

Most of the iron that is not metabolised is stored in Ft in order to prevent the formation of toxic free radical species (Kwok and Richardson, 2002). Therefore Ft plays a dual role in LIP homeostasis, acting on one hand as an iron-sequestering protein and on the other hand as a potential source of LIP. Ft is the major iron storage protein, ubiquitous in mammalian cells and is tightly regulated by IRPs and it is found in the cytoplasm, mitochondria and nucleus of cells (Arosio *et al.*, 2009).

Ft is composed of a protein shell (MW between 430 and 460 kDa) that can accommodate up to 4500 atoms of iron in the ferric form in its internal cavity as ferric-oxyhydroxide phosphate. Ft is made up of 24 subunits of two types, a light L-subunit (MW 19 kDa) and a heavy H-subunit (MW 21 kDa) (Munro and Linder, 1978; Theil, 1987; Drysdale, 1988). The Ft molecule has an internal diameter of 70–80 Å and an external diameter of 120–130 Å. The entry and exit of iron may occur via channels in the protein shell, and these are found on the three-fold and four-fold symmetry axes. There are six four-fold channels which are hydrophobic in nature plus eight three-fold channels that are hydrophilic, and all of these channels are approximately 3–4 Å in diameter (Richardson and Ponka, 1997).

Mammals have three functional Ft genes: *FTH* on human chromosome 11 encodes the cytosolic heavy chain (H-chain) of 183 amino acids, *FTL* on chromosome 19 encodes the cytosolic light chain (L-chain) of 175 amino acids, and the intronless *MtF* gene on chromosome 5 encodes the precursor of the mitochondrial ferritin (MtF) of 242 residues (the latter to be discussed below) (Richardson and Ponka, 1997).

Cytosolic Ft is composed of 2 subunits; H and L, which have approximately 50% sequence identity. The H-subunit has a high affinity for Fe^{3+} ($K_d = 10^{-25}$ mol/L), and has the catalytic site with ferroxidase activity that converts Fe^{+2} to Fe^{+3} (Lawson *et al.*, 1989). In contrast, the L-subunit has no ferroxidase activity but has a nucleation site that is involved in the formation of the iron core (Levi *et al.*, 1992) and has more iron storage capacity. The H- and L-chains co-assemble in different proportions generating a large number of isoferritins, probably formed by subunit homodimers, (H24L0, H22L2, H0L24) with tissue-specific distributions. Modification of the proportion of H- and L-subunits in the Ft shell may allow the cell to adjust to changes in iron requirement (Drysdale, 1988). An increase in the proportion of the L-subunit is associated with iron storage and is found mainly in spleen and liver, whereas the H-subunit is more abundant when iron is required for cellular metabolism and is found mainly in heart and brain (Jones *et al.*, 1978; Wagstaff *et al.*, 1978; Drysdale, 1988; McClarty *et al.*, 1990).

The process of iron release from Ft may involve iron reduction and/or chelation, and it has been suggested that the degradation of Ft is necessary for iron to be released (Raja *et al.*, 1986). Ft mRNA molecules are subjected to translational or "post-transcriptional" control by iron (Zahringer *et al.*, 1976; Aziz and Munro, 1986).

Studies on cytosolic Ft overexpression have revealed that H-Ft could regulate cell growth based on its potential to modulate the intracellular LIP levels (Epsztejn *et al.*, 1999; Cozzi *et al.*, 2000; Kakhlon *et al.*, 2001). Marked overexpression of H-Ft in HeLa cells attenuated cell growth in a manner that is dependent on its ferroxidase activity to incorporate iron (Cozzi *et al.*, 2000), whereas moderate overexpression of H-Ft, as well as partial repression of H- and L-Ft, produced no significant effect on cell growth (Epsztejn *et al.*, 1999; Cozzi *et al.*, 2000; Kakhlon *et al.*, 2001).

While Ft is mainly an intracellular protein, small amounts exist in the serum, and this is usually proportional to the quantity of iron in stores (Jacobs and Worwood, 1975). Serum Ft is increased in cases of iron overload and inflammation, but its function is obscure although it may play a role in regulating blood vessel formation (Coffman *et al.*, 2009). It is controversial whether serum Ft represents a different gene product or a glycosylated form of the intracellular protein that is routed along a secretory pathway (Linder *et al.*, 1996; Tran *et al.*, 1997).

In addition to Ft, iron overloaded cells, in conditions such as hereditary hemochromatosis, may contain another storage form of iron called hemosiderin. Hemosiderin is a degradation product of Ft under conditions of iron excess; Ft is taken-up by lysosomes where it undergoes a partial dissolution of the core resulting in the formation of insoluble hemosiderin (Hoffman *et al.*, 1991; Harrison and Arosio, 1996).

In 2001, Levi *et al.* reported a new Ft gene for mitochondrial Ft (MtF) (Levi *et al.*, 2001). It is known that the mitochondrion is vital for heme synthesis and for playing a critical role in the genesis of (Fe-S) clusters. The recently discovered MtF may store iron in ring sideroblasts and have a role to regulate the level of iron needed for these functions.

MtF is encoded by an intronless gene on chromosome 5q23.1, and shows 79% identity with H-Ft and 63% identity with L-Ft (Levi and Arosio, 2004). Its 3D structure is very similar to that of H-Ft with some differences in localization and presence of metal-binding sites (Langlois d'Estaintot *et al.*, 2004). The protein is synthesised as a 30 kDa precursor that is targeted to mitochondria by a leader sequence of 60 amino acids where it is processed into a

typical Ft shells. The leader sequence is cleaved in the mitochondrion to produce 22kDa subunits that have a ferroxidase center and form homopolymeric Ft shells that bind Fe like Ft H-chain (Corsi *et al.,* 2002). Unlike cytoplasmic Ft, MtF mRNA lacks an iron responsive element (IRE) and may be transcriptionally regulated by iron (Corsi *et al.*, 2002; Drysdale *et al.*, 2002).

MtFt expression is correlated with tissues that have high numbers of mitochondria (e.g. testis) rather than with tissues involved in iron storage (e.g. the liver and the spleen) (Napier *et al.,* 2005) which suggests that MtFt may play a protective role against iron-mediated oxidative damage (Santambrogio *et al.,* 2007). Interestingly, MtF was shown to be highly expressed in sideroblasts of patients with X-linked sideroblastic anemia (XLSA) but not in normal erythroblasts (Levi *et al.*, 2001; Cazzola *et al.*, 2003).

MtFt overexpression resulted in decreased cytoplasmic Ft, increased TfR1 expression, decreased heme synthesis, and increased iron-loading of MtFt. This effect not only alters mitochondrial iron metabolism, but also the whole-cell iron metabolism (Nie *et al.,* 2005), leading to a cytosolic iron-deficiency and reduced proliferation in neoplastic cells over-expressing MtFt *in vivo* (Nie *et al.,* 2006).

Iron Regulatory Proteins (IRPs)

As iron is required for a variety of cellular processes, a balance between iron uptake, usage, and storage must be maintained. Therefore alterations in LIP are normally sensed by the cytosolic iron regulatory proteins 1 and 2 (IRPs) which function as post-transcriptional regulators of both iron uptake via the TfR and iron sequestration by the iron-storage protein Ft (Klausner *et al.*, 1993; Kuhn, 1994; Guo *et al.*, 1995). IRP1 is a monomeric cytoplasmic protein (MW=90–95 kDa) (Leibold and Munro, 1988; Walden *et al.*, 1989; Barton *et al.*, 1990) that resembles mitochondrial aconitase in sequence (Hentze and Argos, 1991; Kaptain *et al.*, 1991; Rouault *et al.*, 1991; Haile *et al.*, 1992a; Haile *et al.*, 1992b), and has been found in all cells and tissues so far tested (Rothenberger *et al.*, 1990; Mullner *et al.*, 1992). IRP-1 can assemble an (4Fe–4S) cluster and is enzymatically active (Kaptain *et al.,* 1991). Depending on its iron content, IRP1 can act either as an RNA-binding protein or as a cytoplasmic aconitase (Kuhn, 1994). Whereas IRP2 that has a MW of 105 kDa (Henderson *et al.,* 1994) does not show any aconitase activity and does not accumulate an (4Fe–4S) cluster. Human IRP2 is 57% identical and 79% similar to IRP1 in amino acid sequence (Rouault *et al.*, 1992).

Both IRP1 and IRP2 regulate the expression of crucial proteins involved in iron homeostasis. This is attained by the binding of the IRPs to hairpin-loop structures known as iron-responsive elements (IREs) located in the 5' or 3'untranslated regions (UTRs) of several mRNAs including those encoding the Ft H- and L-subunits and TfR1 (Hentze *et al.*, 2004). The binding of IRP1 and IRP2 to the IRE is controlled by intracellular iron levels. This iron-mediated regulatory feedback mechanism allows cells to achieve and maintain a desired intracellular iron level (Hentze *et al.*, 2004). Under high intracellular iron levels, IRP1 assemble a (4Fe–4S) cluster, which results in the loss of IRE-binding ability, imparting aconitase activity (Hentze *et al.*, 2004). In contrast, IRP1 of iron-depleted cells does not contain this (4Fe–4S) cluster and hence is able to bind to IREs **(Fig. 1.8)**. The binding affinity of IRP2 to IREs is similar to that of IRP1, although this protein does not have a (4Fe–4S) cluster. IRP2 protein is rapidly degraded in iron-depleted cells via the proteasomes (Hentze *et al.*, 2004).

As mentioned previously, IRPs are able to bind to IREs located at the 3' or 5' end of mRNA, either increasing mRNA stability or inhibiting translation and consequently regulate protein expression (Richardson and Ponka, 1997; Hentze *et al.*, 2004). Under conditions of iron deficiency, IRPs are able to bind to IREs located at the 3' end of mRNA-encoding iron-uptake proteins, protecting the molecule from exonuclease activity and hence improving mRNA stability (Richardson and Ponka, 1997; Hentze *et al.*, 2004). This increases the expression of TfR1 and other proteins involved in iron uptake, thus elevating intracellular iron levels. In iron-replete cells, IRPs bind to IRE within the 5' untranslated region of Ft mRNA, sterically hindering translation, which allows the cell to use the iron that is present (Hentze *et al.*, 2004). On the other hand, when iron is abundant, IRPs cannot bind to IREs located at the 3'end of mRNA of iron-uptake proteins, allowing for mRNA degradation and subsequently a decrease in intracellular iron levels (Hentze *et al.*, 2004). Simultaneously, under high iron levels, IRPs can no longer bind to the 5' end of Ft mRNA, increasing Ft expression and levels of iron in storage (Kalinowski and Richardson, 2005).

Other proteins that process stem-loop structures either on the 5' or 3' untranslated portion of their mRNA include erythroid 5-aminolevulinic acid synthase (ALA-synthase, involved in heme biosynthesis; Cox *et al.*, 1991), mitochondrial aconitase (Dandekar *et al.*, 1991)and DMT-1 (reviewed by Sheth and Brittenham, 2000). Additional IRE sequences have also been identified in ferroportin1 (FP1, also known as IREG1 and MTP1) (Donovan *et al.*, 2000; McKie *et al.*, 2000) which plays a role in iron efflux across membranes to plasma but their function in IRP binding has not yet been determined. An important finding correlating IRP

and 5-ALA was also observed by (Pourzand *et al.*, 1999a). They demonstrated that there is a strict dependence on enhancement on LIP levels by photoporphyrin IX (PPIX) and the level of IRP activation. They proposed that the level of IRP activation could serve as a better marker for iron deficiencies than TfR expression since it is directly correlated with the level of intracellular LIP.

Relative ratios of IRP1/IRP2 differ between tissues, with IRP1 being the most abundant in liver, kidney, intestine and brain, and the least abundant in pituitary and pro-B-lymphocytic cell lines (Thomson *et al.*, 1999).

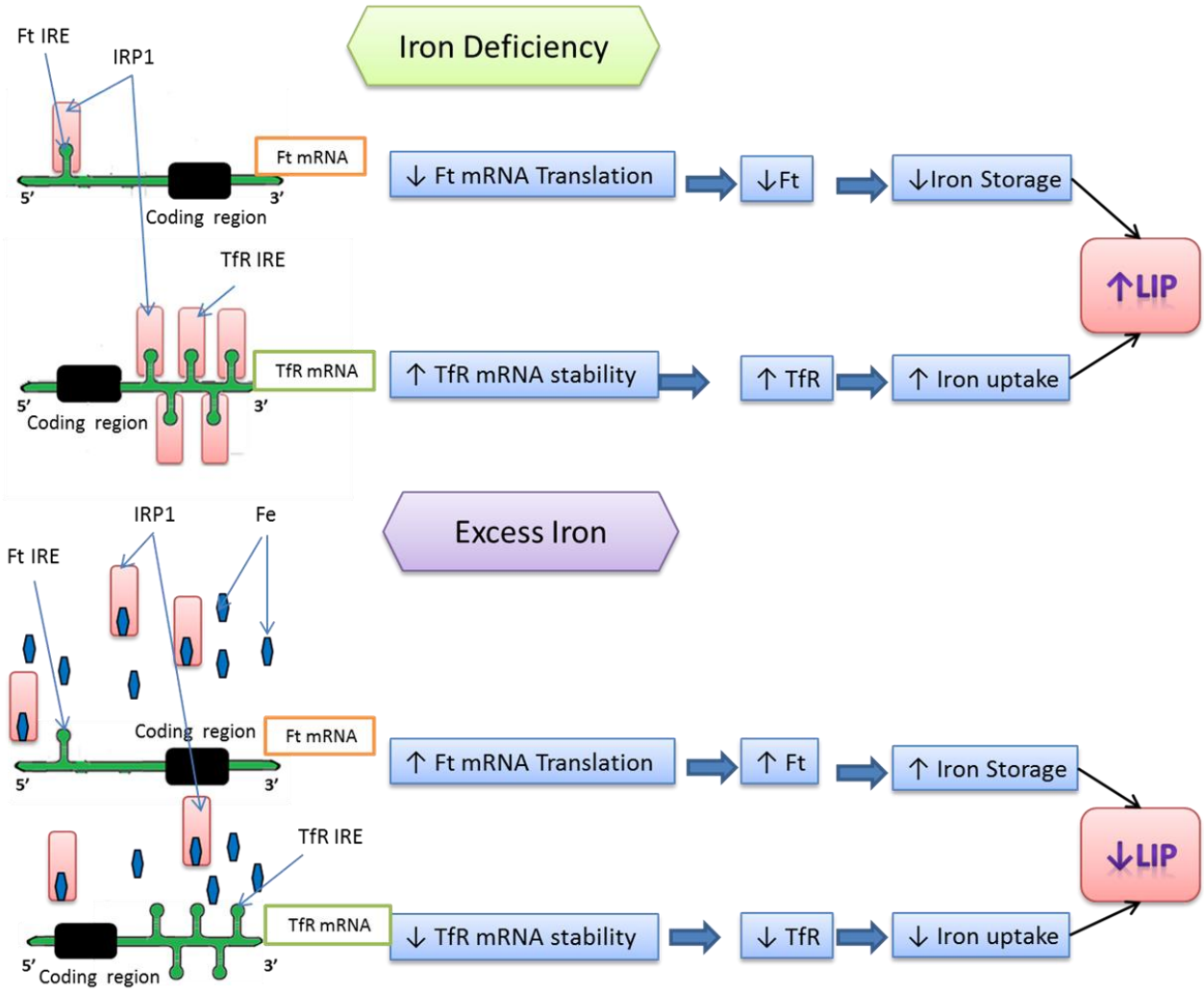

Figure 1.8: The schematic presentation of regulation of Ferritin and Transferrin receptor mRNAs translation during high and low intracellular labile iron conditions (Adapted from Kwok and Richardson, 2002).

An increase in iron supply will cause inactivation of IRP-1 (and degradation of IRP-2, not shown), leading to the induction of Ferritin (Ft) mRNA translation and degradation of Transferrein receptor (TfR) mRNA, resulting in decreased levels of intracellular labile iron pool (LIP). Conversely, under conditions of iron deprivation, IRPs bind to IREs, leading to inhibition of Ft mRNA translation and induction of TfR protein synthesis

1.5.4 Cancer cell iron metabolism

Compared to normal cells, neoplastic cells require a greater amount of iron because generally they proliferate at a greater rate than their normal counterparts (Le and Richardson 2002; Kalinowski and Richardson, 2005). Therefore there are a significant number of alterations in the metabolism of iron in tumour cells (reviewed by Kwok and Richardson, 2002).

1.5.4.1 Transferrin and cancer

Transferrin (Tf) which is the major iron transport protein in the plasma, is a growth factor required for all proliferating cells due to its high iron binding properties (Aisen and Listowsky, 1980; Richardson and Ponka, 1997). For this reason, Tf is a vital requirement in defined medium for the growth of cultured cells (Barnes and Sato, 1980). Furthermore, extra-hepatic tissues such as T4 lymphocytes and Sertoli cells synthesize Tf, which may permit specialised proliferation and differentiation (Skinner and Griswold, 1980; Lum *et al.*, 1986).
The human basal cell carcinoma (BCC) line MCF-7 secretes a factor which is immunologically identical to Tf, and its secretion is enhanced by 17β-oestradiol (OES) and reduced by the anti-oestrogen 4-hydroxy-tamoxifen (Vandewalle *et al*., 1989). It has been suggested that Tf secreted by BCC may act as an autocrine growth factor by conferring a selective advantage to rapidly proliferating BCC and permitting tumour growth in poorly vascularised areas (Vandewalle *et al*., 1989). Similarly, other cancer cell types, including small cell carcinoma (Vostrejs *et al.*, 1988) and T-lymphoma cells (Morrone *et al*., 1988), also secrete Tf and an autocrine function was proposed. In small cell carcinoma, Tf secretion increased more than 10-fold when the cells entered the active phase of the cell cycle (Vostrejs *et al*., 1988). However more studies are needed to determine whether Tf plays an important role in proliferation as an autocrine growth factor, or whether it represents a general up-regulation of gene expression related to neoplastic transformation (Kwok and Richardson, 2002).

1.5.4.2 Oestrogen-inducible transferrin-receptor-like protein

Poola and colleagues (Poola and Lucas, 1988; Poola et al., 1990; Poola and Kiang, 1994; Poola, 1997) identified an OES-inducible Tf-binding protein that had limited homology (10%) to the TfR1 in chick oviduct cells and BCC. This protein acts like TfR1 during RME (Poola et al., 1990) (i.e. in terms of binding to diferric Tf and releasing apoTf) which may

suggest a possible role in iron uptake. The TfR-like protein in chick oviduct cells is present in two forms with molecular weights of 104- and 116-kDa (Poola et al., 1990), and like the TfR1, it appears to form a dimer (Poola and Lucas 1988). Immunoprecipitation studies have shown that the 104kDa form was present in the OES-sensitive human BCC lines, MCF-7 and T-47D (Poola et al., 1990).

Since BCC cells secrete Tf (Vandewalle et al., 1989) and increase the expression of a TfR-like protein that can bind Tf in response to OES, it has been suggested that this autocrine-loop mechanism may enhance iron uptake (Kwok and Richardson, 2002). Nevertheless, more studies are required to determine its exact mechanism.

1.5.4.3 Transferrin receptor 1 and cancer

Several studies have demonstrated an increased TfR1 expression in cells with a high proliferation rate including tumour cells (Sutherland et al., 1981; Trowbridge and Lopez, 1982; Taetle and Honeysett, 1987).

As discussed above, TfR1 expression is regulated by intracellular iron levels by the IRP–IRE mechanism (Daniels et al., 2006). However, regulation of the expression of TfR1 at the transcriptional level seems to be important indicating that this molecule is a downstream target of the c-myc proto-oncogene (O'Donnell et al., 2006). Interestingly, microarray analysis also revealed that c-myc regulates the expression of other molecules involved in iron homeostasis, including the iron transporter DMT1 and frataxin (O'Donnell et al., 2006) that is thought to be involved in mitochondrial iron metabolism (Napier et al., 2005). Recent studies have also shown that colorectal cancer progression is accompanied with increased expression of iron import proteins (Dcytb, DMT1, and TfR1) and reduced expression of proteins involved in iron export (namely FP1 and hephaestin) (Brookes et al., 2006). Studies have also demonstrated that forced expression of TfR1 enhances cancer cells proliferation, while its down-regulation reduces cellular growth and alters expression of genes involved in cell cycle control e.g., growth arrest and DNA damage 45α (GADD45α) (O'Donnell et al., 2006). Interestingly, it has also been demonstrated that c-myc up-regulates the expression of IRP2 that is involved in regulating TfR1 (Wu et al., 1999). In addition, c-myc also represses the expression of the H-Ft. Collectively, these findings demonstrate that c-myc, which is regulated in a wide range of human cancers (Vita and Henriksson, 2006), coordinately regulates molecules involved in iron metabolism (Habel and Jung, 2006). This is important for understanding the alterations in iron metabolism in cancer cells that facilitate tumourigenesis.

1.5.4.4 The Transferrin receptor 2 and cancer

Recently, Kawabata and colleagues have cloned and functionally characterised another TfR-like molecule known as the TfR2 (Kawabata et al., 1999; Kawabata et al., 2000). This molecule has some structural and functional similarity to the TfR1, and its TfR2 gene has been located on chromosome 7 (7q22) (Kawabata et al., 2000). Two transcripts have been identified in cells, α and β, neither of which contains an IRE, and both are expressed in normal and cancer cells (Fleming et al., 2000; Kawabata et al., 2000). In normal tissues, studies have shown that the β-form was found in all human tissues tested. Whereas the expression of the α-form was limited to the liver, spleen, lung, muscle, prostate and peripheral blood mononuclear cells (Kawabata et al., 2000). However, in contrast to the TfR2-α transcript, the TfR2-β transcript does not contain the amino terminal portion or the putative transmembrane domain. The role of the TfR2-α in iron metabolism remains largely unknown, although its transfection into cells lacking the TfR1 results in iron uptake from Tf (Kawabata et al., 2000).

In contrast to TfR1 that is regulated by intracellular iron concentration, the TfR2 does not appear to be regulated in the same manner (Klausner et al., 1983a; Fleming et al., 2000). It has been suggested that TfR2-α expression may be regulated in accordance with the cell cycle (Fleming et al., 2000).

Interestingly, it has been demonstrated that desferrioxamine (DFO) reduces cell proliferation and DNA synthesis in CHO control cells, while it has little effect on cells expressing transfected TfR2-α (Fleming et al., 2000) suggesting that it may act as an additional source of iron (Kawabata et al., 2000).

Surprisingly, despite the fact that TfR2-α has a lower affinity for Tf than the TfR1, cells expressing TfR2-α grew into larger tumours than those expressing the TfR1 (Fleming et al., 2000).

Further studies on the function of the TfR2 are needed to be performed in order to understand the function of this molecule, and its possible role in the growth of normal and neoplastic cells (Kwok and Richardson, 2002).

1.5.4.5 Iron uptake mechanisms from low-molecular-weight iron complexes

In addition to the uptake of Tf-bound iron, cancer and normal cells can also efficiently take up iron from a variety of low MW iron complexes (Page *et al.*, 1984; Fuchs *et al.*, 1988; Richardson and Baker, 1990; Sturrock *et al.*, 1990; Kaplan *et al.*, 1991). This may represent a mechanism to bind and transport low MW iron complexes released from normal cells damaged by the invading tumour. Possible transport molecules involved in the uptake of low

MW iron complexes include DMT1 (Fleming *et al.*, 1998) and the stimulator of iron transport (SFT) (Gutierrez *et al.*, 1997; Yu and Wessling-Resnick, 1998). However the physiological significance of iron uptake from low MW iron complexes *in vivo* remains an important research question (Kwok and Richardson, 2002).

1.5.4.6 Melanotransferrin and cancer

Some malignant melanoma cells express a membrane-bound Tf homologue known as melanotransferrin (MTf) or p97 (Brown *et al.*, 1981a; Brown *et al.*, 1981b; Brown *et al.*, 1982; Rose *et al.*, 1986).

MTf shares a number of critical characteristics with serum Tf (reviewed by Kwok and Richardson, 2002), including: (i) MTf has a 37–39% sequence homology with human serum Tf, (ii) the MTf gene is on chromosome 3, as are those for Tf and the TfR1; (iii) many of the disulfide bonds present in serum Tf are also present in MTf; (iv) MTf has an N-terminal Fe-binding site that is very similar to that found in serum Tf; and (v) isolated and purified MTf can bind iron from iron citrate complexes (Brown *et al.*, 1981a; Plowman *et al.*, 1983; Rose *et al.*, 1986; Baker *et al.*, 1992).

However a variety of *in vitro* (Richardson and Baker, 1990; Richardson and Baker, 1991a; Richardson and Baker, 1991b) and *in vivo* investigations (Dunn *et al.*, 2006; Sekyere *et al.*, 2006) have demonstrated that MTf plays little role in Fe metabolism (Dunn *et al.*, 2007; Suryo Rahmanto *et al.*, 2007). In fact, MTf has been shown to be involved in the proliferation, migration and invasion of melanoma cells *in vitro* and their growth *in vivo* (Dunn *et al.*, 2006; Bertrand *et al.*, 2007; Suryo Rahmanto *et al.*, 2007). Further studies using gene knockout technology are essential to clearly determine the biological role of MTf.

1.5.4.7 Ferritin and cancer

Several studies have suggested that some relationship may exist between Ft and cancer. It has been demonstrated that serum Ft is increased in patients suffering a number of neoplasms, despite no increase in Fe stores (Marcus and Zinberg, 1975; Kew *et al.*, 1978; Hann *et al.*, 1980). Tumour cells, when compared to their normal counterparts, usually contain low quantities of Ft, poor in iron (Munro and Linder, 1978). This fact is somewhat of a paradox considering the high rate of iron uptake by tumours via the TfR1. However, it has been reported that cells from the childhood tumour neuroblastoma (NB) contain Fe-rich Ft and hemosiderin (Iancu, *et al.*, 1988; Iancu, 1989). This finding, together with the fact that

NB appears sensitive to iron depletion with DFO (Richardson, 2002) may indicate that the Fe metabolism of this tumour is altered compared to other cell types.

Serum Ft is markedly increased in NB at stages III and IV, but not in stages I or II (Hann *et al.*, 1980; Hann *et al.*, 1981; Hann *et al.*, 1985). It has been suggested that the neoplasm is the source of increased serum Ft levels as: (A) NB cells contain Fe-rich Ft and patients with advanced NB have increased amounts of Ft within the tumour (Hann *et al.*, 1980; Iancu *et al.*, 1988; Iancu, 1989); (B) human Ft has been detected in the sera of nude mice bearing NB xenografts (Hann, 1984); (C) serum Ft levels become normal with remission (Hann *et al.*, 1980), and (D) most Ft released from NB is glycosylated, indicating active secretion (Hann *et al.*, 1984).

The H-type Fts may suppress immunological responses (Broxmeyer *et al.*, 1981; Broxmeyer *et al.*, 1991), that may aid cancer cell proliferation. However, other properties may be important as most Ft secreted by NB cells is of the L-type (Hann *et al.*, 1988).

Ft may act as an autocrine growth factor, since Ft secreted by NB cells is rich in iron (Iancu *et al.*, 1988; Iancu, 1989), which suggests that it could possibly be used as an iron source by other NB cells. However, addition of Ft to serum-free medium only slightly stimulated NB growth and DNA synthesis. In addition, specific Ft-binding sites were not identified on these cells (Blatt and Wharton, 1992). It has been suggested that Ft has mitogenic activity for NB cells (Kwok and Richardson, 2002).

Also it is of interest that an autocrine growth factor released from leukaemic cells has immunological identity with Ft. Interestingly, Ft antibody inhibited the proliferation of these cells, suggesting a role for Ft in stimulating cellular growth (Kikyo *et al.*, 1994a; Kikyo *et al.*, 1994b). Moreover, binding sites for Ft (Covell *et al.*, 1987; Covell and Cook, 1988; Konijn *et al.*, 1990; Fargion *et al.*, 1991) and the endocytosis of Ft (Bretscher and Thomson, 1983) have been identified in cancer cells, suggesting that Ft iron uptake could occur by receptor-mediated endocytosis. However, more studies are required to determine the role of secreted Ft as a mitogenic factor for cancer cells (Richardson *et al.*, 2009).

On the other hand, studies have demonstrated that neoplastic transformation can result in changes in the expression of Ft and other molecules involved in cellular Fe metabolism. For example, E1A oncogene has been found to modulate the expression of *H-Ft* at the transcriptional level (Tsuji *et al.*, 1993). In growing cells the transcription factor encoded by c-*myc*, a proto-oncogene, represses the expression of H-Ft and increases the expression IRP2 (Wu *et al.*, 1999). Additionally, *H-Ft* down-regulation was necessary for transformation via *c-myc*. The increase in the expression of *IRP2* may enhance its RNA-binding activity that

could cause an elevation in the expression of TfR1 and Fe uptake from Tf that is essential for tumour proliferation (Wu *et al.*, 1999).

In contrast, Modjtahedi et al. (Modjtahedi *et al.*, 1992) demonstrated that cells' transfection with *c-myc* gene copies lead to *H-Ft* over-expression due to an increase in the transcription rate. This latter study revealed that the *H-Ft* and *cytokeratin* expressions were increased in tumourigenic compared to non-tumourigenic clones of the SW 613-S human carcinoma cell line (Modjtahedi *et al.*, 1992).

Interestingly, *N-myc* amplification and secretion of Ft co-exist in patients with advanced NB (Brodeur *et al.*, 1984; Hann *et al.*, 1985). A study examining Ft secretion and synthesis in three NB cell lines demonstrated that the cell line secreting the highest concentration of Ft, also had the highest number of N-*myc* copies (Selig *et al.*, 1993).

1.6 Cell Cycle

1.6.1 General definitions

The cell cycle is the series of events that take place in a cell leading to its division and duplication (replication). The cell-division cycle is a vital process by which hair, skin, blood cells, and some internal organs are renewed. This process consists of five distinct phases: G0; G1 phase, S phase (synthesis), G2 phase (collectively known as interphase) and M phase (mitotic phase) **(Fig. 1.9).**

G0 phase (also known as post-mitotic)

The term "post-mitotic" is sometimes used to refer to both '*quiescent'* and '*senescent'* cells.

'Quiescent' cells: non-proliferative cells in multicellular eukaryotes generally enter the quiescent G0 state from G1 and may remain quiescent for long periods of time, possibly indefinitely (as is often the case for neurons).

'Scenescent' cells: Cellular senescence is a state that occurs in response to DNA damage or degradation that would make a cell's progeny non-viable; it is often a biochemical alternative to the self-destruction of a damaged cell by apoptosis.

Interphase

Before a cell can enter cell division, it needs to prepare itself by replicating its genetic information and all of the organelles. All of the preparations are done during the interphase. Interphase proceeds in three stages, i.e. G1 (Gap1), S (Synthesis), and G2 (Gap2). Cell division operates in a cycle; therefore, interphase is preceded by the previous cycle of mitosis and cytokinesis - the process in which the cytoplasm of a single eukaryotic cell is divided to form two daughter cells.

G1 phase (~12h) is the first phase within interphase, from the end of the previous M phase until the beginning of DNA synthesis (is called G1). During this phase – which is also called 'growth phase'- the biosynthetic activities of the cell, which had been considerably slowed down during M phase, resume at a high rate. This phase is marked by synthesis of various enzymes that are required in S phase, mainly those needed for DNA replication. Duration of G1 is highly variable, even among different cells of the same species (Lodish, 2008).

S phase (~6h) starts when DNA synthesis commences; when it is complete, all of the chromosomes have been replicated, i.e. each chromosome has two (sister) chromatids. Thus, during this phase, the amount of DNA in the cell has effectively doubled, although the number of single sets of chromosomes in a cell (the ploidy) remains the same. Rates of RNA transcription and protein synthesis are very low during this phase. An exception to this is histone production, most of which occurs during the S phase (Lodish, 2008).

G2 phase (~6h): the cell then enters the G2 phase, which lasts until the cell enters mitosis. Significant protein synthesis occurs during this phase, mainly involving the production of microtubules, which are required during the process of mitosis. Inhibition of protein synthesis during G2 phase prevents the cell from undergoing mitosis (Lodish, 2008).

M (Mitotic) phase is the brief process (~30min) by which a eukaryotic cell separates the chromosomes in its cell nucleus into two identical sets in two nuclei. The process of mitosis is complex and highly regulated. The sequence of events is divided into prophase, prometaphase, metaphase, anaphase and telophase. During the process of mitosis the pairs of chromosomes condense and attach to fibres that pull the sister chromatids to opposite sides of the cell. It is generally followed immediately by cytokinesis (in conjunction with telophase), which divides the nuclei, cytoplasm, organelles and cell membrane into two genetically identical daughter cells (Cordon-Cardo, 1995).

It is known that errors in cell cycle can either kill a cell through apoptosis or cause mutations that may lead to cancer. Therefore the cell cycle is tightly controlled by many regulatory mechanisms that either permit or restrain its progression.

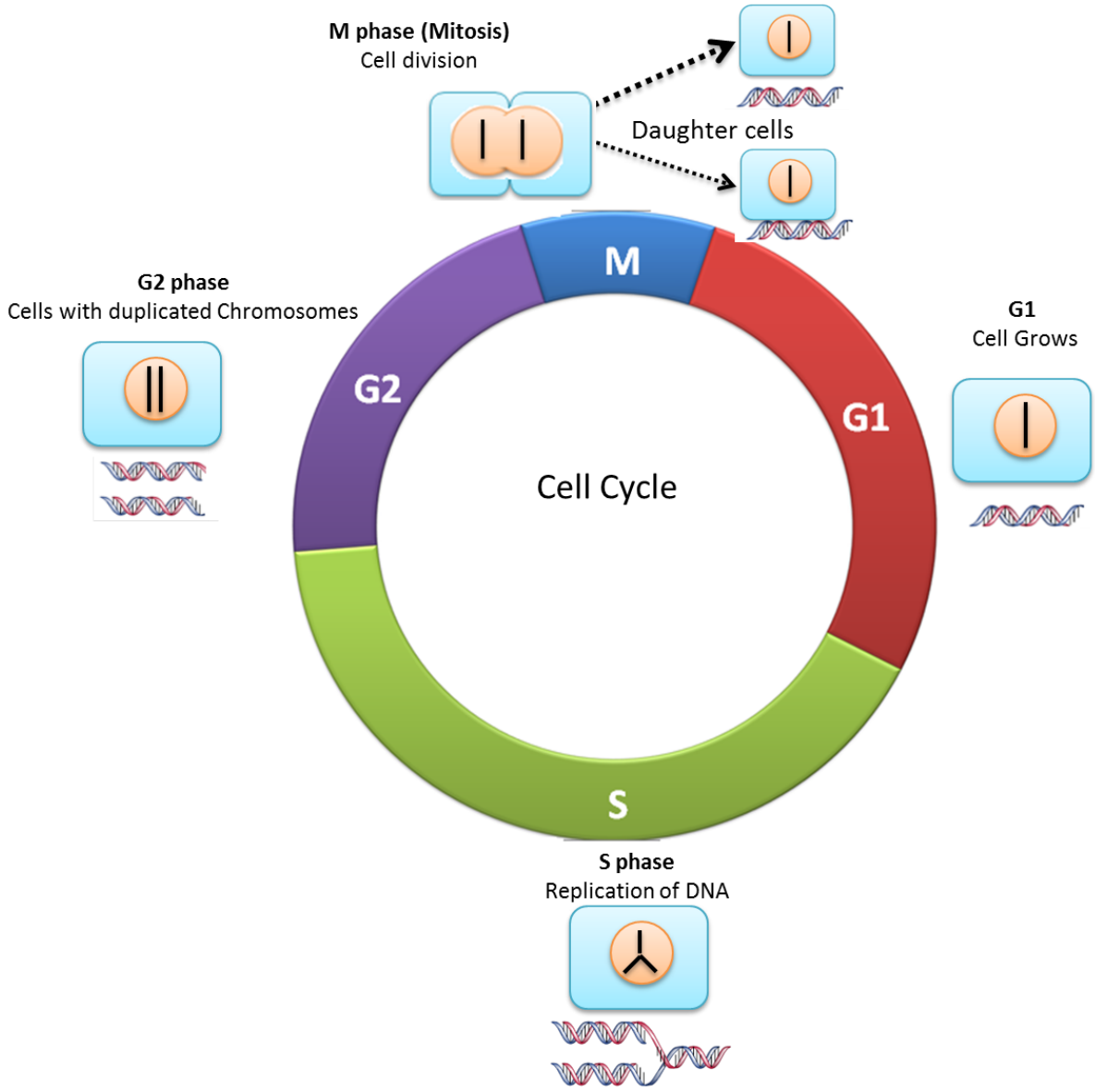

Figure 1.9: The cell cycle (Adapted from Cerqueira *et al.*, 2007).

Cell division operates in a cycle and consists of four distinct phases: G_1 phase, S phase (synthesis), G_2 phase (collectively known as interphase) and M phase (mitosis). G1 phase (Growth phase): is marked by synthesis of various enzymes that are required in S phase for DNA replication. S phase (Synthesis phase): involves DNA synthesis; when it is complete, all of the chromosomes have been replicated, i.e. each chromosome has two (sister) chromatids. the amount of DNA in the cell has effectively doubled. G2 phase: Protein synthesis involving the production of microtubules, which are required during the process of mitosis. M (Mitotic) phase: a cell separates the chromosomes in its cell nucleus into two identical sets in two nuclei. The pairs of chromosomes condense and attach to fibres that pull the sister chromatids to opposite sides of the cell . It is followed by which divides the nuclei, cytoplasm, organelles and cell membrane into two genetically identical daughter cells.

1.6.2 Cell Cycle regulation

The cell cycle is a very complex and tightly regulated process that can result in cell division, differentiation, or growth, or contribute to programmed cell death through apoptosis (Elsayed and Sausville, 2001).

The main families of regulatory proteins that play key roles in controlling cell-cycle progression are the cyclins, the cyclin-dependent kinases (Cdks), the Cdk inhibitors (CKI) and tumour suppressor genes such as p53 and the retinoblastoma susceptibility gene product (pRb) (**Fig. 1.10**). These families comprise the basic regulatory machinery responsible for catalysing cell cycle transition and checkpoint traversation (Elsayed and Sausville, 2001).

1.6.2.1 Cyclins and Cyclin-dependent kinases (Cdks)

Cell cycle transitions depend on the activity of the Cyclin-dependent kinases (Cdks). The active forms of these kinases occur as heterodimers that are composed of a regulatory subunit called a cyclin, and its catalytic counterpart, the Cdk (Sherr, 2000). It is the up-regulation and degradation of the cyclins and their subsequent interaction with Cdks that mediate progression through the cell cycle (Zetterberg *et al.*, 1995; Reed, 1997) (**Fig. 1.10**).

Cyclins are a family of proteins that are structurally identified by conserved 'cyclin box' regions (Joyce *et al.*, 2001). They are 56 kDa proteins and are implicated in the mitosis of all eukaryotes (Elsayed and Sausville, 2001).

Cyclins activate specific Cdks through a 1:1 non-covalent binding and trigger and coordinate the transition between the different phases of the cell cycle.

To date, nine Cdks (Cdk1-9) and at least15 preferentially binding cyclins have been identified (see **Table 1.1**) (Draetta, 1990; Sherr and Roberts, 1999; Sausville *et al.*, 2000). Cdks are typically small proteins of 300 amino acids in length and molecular weight of 33-40 kDa.

The Cyclin–Cdk complexes are activated by phosphorylation via cyclin-activating kinases (CAKs) (Vidal and Koff, 2000) that activates or inactivates target proteins to orchestrate coordinated entry into the next phase of the cell cycle.

Different cyclin-Cdk combinations determine the downstream proteins targeted. Cdks are constitutively expressed in cells whereas cyclins are synthesised at specific stages of the cell cycle, in response to various molecular signals (Prather *et al.*, 1999).

An important regulatory mechanism performed by Cdk molecules involves the phosphorylation of the retinoblastoma protein (pRb) (Sherr, 2000). This molecule mediates

progression of cells from G_1 to the S phase of the cell cycle. In its hypophosphorylated form, pRb suppresses cellular growth by binding to E2Fs. In addition to that, the mechanism of pRb-mediated inhibition involves recruitment of proteins that are repressive for transcription, such as histone deacetylases. Following Cyclin D/Cdk4 or Cdk6–mediated phosphorylation, however, pRb releases E2Fs that subsequently activate downstream transcriptional targets involved in S phase, including DNA polymerase- alpha, Cyclin A, Cyclin E and Cdk1. CyclinE/Cdk2 complexes further phosphorylate pRb at the G1-to-S transition, enabling cells to pass through a "restriction point" from which the cell proceeds through the remainder of the cycle irrespective of mitogenic stimuli. CyclinA/Cdk2 and CyclinB/Cdk1 activities are required for S-to-G2 and G2-to-M transitions, respectively (Corn and El-Deiry, 2002).

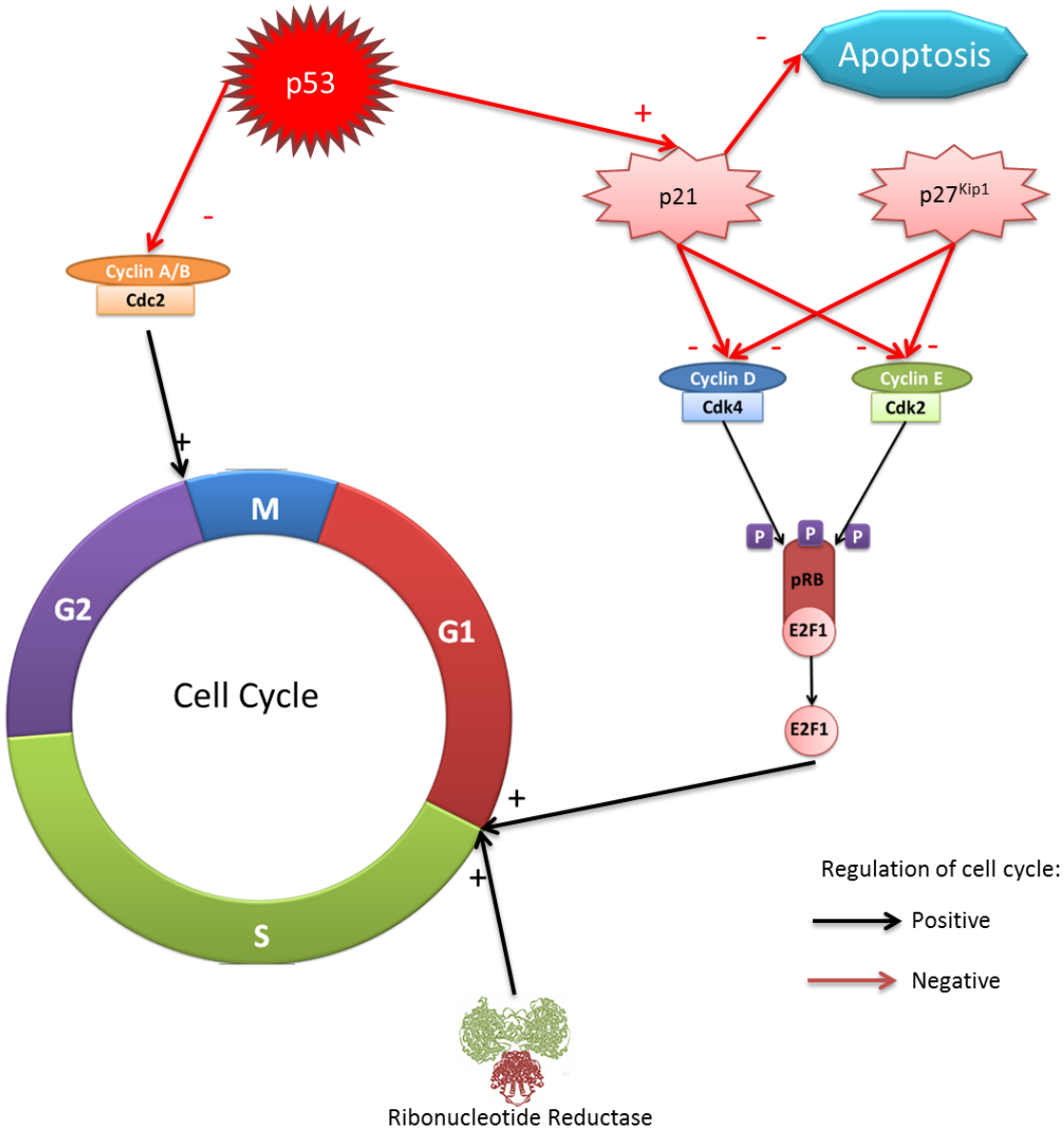

Figure 1.10: The cell cycle in normal cells (Adapted from Yu *et al.*, 2007).

The cell cycle consists of four main phases: G1, S, G2 and M phases. Under normal conditions, the progression of the cell cycle controlled mainly by cyclins A, B, D and E, and the cyclin-dependent kinases (cdks). Cyclin D1 forms a complex with cdk4, while cyclin E binds with cdk2. These complexes are then involved in hyper-phosphorylation of the retinoblastoma susceptibility gene product (pRb), which allows it to release the transcription factor, E2F1. Once free, E2F1 is able to translocate to the nucleus where it mediates the transcription of a range of genes vital for S-phase progression. One of the most important mediators of this G1/S checkpoint is p53, which is able to cause G1/S arrest under conditions of cell stress or DNA damage. One function of p53 is to transactivate the expression of the cdk inhibitor, p21CIP1/WAF1, which then inhibits the activity of cyclin D1/cdk4- and cyclin E/cdk2 complexes, thereby preventing entry into S-phase. However, the activity of p21CIP1/WAF1 can be paradoxical and under some conditions can aid in cell cycle progression (see section on p21CIP1/WAF1). In addition, p53 is also able to inhibit cyclins A and B leading to G2/M arrest.

Table 1.1 Mammalian cyclin-dependent kinase complexes (Carnero, 2002)

Kinase	**Regulatory subunit**	**Substrate**	**Function**
CDC2	cyclin A & B	pRb, NF, histone H1	G2/M
Cdk2	cyclin A, E	pRb, p27	G1/S, S
Cdk3	cyclin E	E2F1/DP1	G1/S
Cdk4	cyclin D1, D2 & D3	pRb	G1/S
Cdk5	p35, cyclin D1 & D3	NF, Tau	Neuronal differentiation
Cdk6	cyclin D1, D2 & D3	pRb	G1/S
Cdk7	cyclin H	CDC2, Cdk2/4/6	CAK
Cdk8	cyclin C	RNA pol II	Transcript. Regulation
Cdk9	cyclin T	pRb, MBP	G1/S

1.6.2.2 Cdk Inhibitors (CKIs)

The activity of cyclin-Cdk complexes are negatively regulated by Cdk inhibitors (CKI), which in turn act in response to growth inhibitory signals. Based on structural and functional homologies (Corn and El-Deiry, 2002), CKIs are classed into two families , the inhibitors of Cdk4 (INK4) or the kinase inhibitor proteins (CIP/KIP) (Vidal and Koff, 2000).

The CIP/KIP family consists of three proteins: namely $p21^{WAF1/CIP1}$, $p27^{KIP1}$ and $p57^{KIP2}$. These molecules prevent cell cycle progression and exert their influence during most periods of the cell cycle by binding directly to the Cdk/cyclin complex to inhibit their activity (Vidal and Koff, 2000).While the CIP/KIP CKIs bind all Cdks, their affinity is much lower for Cyclin B/Cdk1.

More recent studies have demonstrated that CIP/KIP proteins are required for the assembly of active CyclinD/Cdk enzyme complexes. Thus, although they were initially recognized as inhibitors, the CIP/KIP proteins actually appear to have both positive and negative regulatory effects on G1 cell-cycle progression. This is in part influenced by their stoichiometry with the kinase complexes and the regulation of their expression by cell-cycle checkpoints or cell-cycle position (Corn and El-Deiry, 2002).

In contrast to the CIP/KIP family of CKIs, the inhibitory activities of INK4 are restricted to Cdk4 and Cdk6 (Ruas and Peters, 1998). As a consequence, the INK4 family is thought to play a major role in G_1/S arrest. This family of CKI includes $p15^{INK4B}$, $p16^{INK4A}$, $p18^{INK4C}$ and $p19^{INK4D}$(Ruas and Peters, 1998).

1.6.2.3 The p53 tumour suppressor protein

The p53 tumour suppressor protein plays a pivotal role in preventing cancer development by acting as a critical transcription factor to induce cellular cycle arrest to initiate repair mechanism and when damage is irreparable it will activate apoptosis (Le and Richardson, 2002).

Many stress factors can initiate the stabilization, accumulation and activation of p53. These include DNA damage, decreased dNTP levels, hypoxia, loss of a cell survival signal, oncogene activation, abnormal cell growth and, more recently, iron chelation (Fuchs *et al.*, 1988; Linke *et al.*, 1996; An *et al.*, 1998; Vousden and Woude, 2000).

Once activated, p53 can initiate the transcription and subsequent expression of various downstream genes that commit the cell to differentiation, senescence, DNA repair, cellular

arrest and/or apoptosis (**Table 1.2**) (Vousden and Woude, 2000). Consequently, p53 transcription, translation, protein stabilization, subcellular localization and activation are tightly regulated.

Murine double minute-2 (mdm-2) protein acts as an ubiquitin ligase to mediate p53 degradation (Honda *et al.*, 1997). And any increase in p53 results in increased mdm-2 expression (Honda *et al.*, 1997) to form an auto-regulatory feedback loop.

Several pathways can activate and stabilize p53:

- For instance DNA damage caused by cells exposure to ionising radiation leads to the expression of the ataxia telangiectasia mutated (ATM) protein and check-point kinase 2 (CHK2) phosphokinase which stabilize p53 by phosphorylation (Carr, 2000).
- Other forms of DNA damage (e.g. chemotherapeutic drugs, ultraviolet light or protein kinase inhibitors) can stabilize p53 by phosphorylation via the ataxia telangiectasia-related (ATR) phosphokinase) (Tibbetts *et al.*, 1999).
- On the other hand, oncogenes such as c-myc and ras, can increase the levels of p53 via the expression of the alternative reading frame of the INK4A locus (ARF) protein (Sherr, 2000; Elliott *et al.*, 2001; Lin and Lowe, 2001).

As a result of cellular damage, either p53 or mdm-2 can be post-translationally modified to stabilize p53 for nuclear accumulation (Le and Richardson, 2002).

Table1.2 p53-inducible proteins involved in apoptosis, cell arrest and DNA repair (Le and Richardson, 2002).

p53-inducible molecule	Comments
BAX	Well Characterised pro-apoptotic protein. BAX is inactivated by bcl-2 Overexpression of BAX induces mitochondrial apoptosis.
NOXA *(for damage)*	Member of the bcl family of pro- and anti-apoptotic proteins. Cells exposed to X-ray inrradiation express NOXA to induce mitochondrial apoptosis.
PUMA (p53 up-regulated modulator of apotosis)	Consists of an alpha and beta form with similar apoptosis functions. Localizes to mitochondria to induce apoptosis.
p53AIPI (p53 mediated apoptosis inducing protein 1)	Pro-apoptotic protein. Localizes to mitochondria to induce apoptosis. Requires p53 to be phosphorylated at serine 46.
p53 DINPI (p53-dependent damage-inducible nuclear protein 1)	Apoptosis induced after double-stranded DNA breaks via p53AIPI expression. This protein in associated with the phosphorylation of p53 at serine 46 to initiate apoptosis
p21 WAF1/CIP1	Cell cycle inhibitor of the CIP//KIP family. Can arrest cell during all stages of the cell cycle.
GADD45	Protein causes cellular arrest and DNA excision repair
p53R2 (p53-inducible R2)	Shares 80% homology to R2. This protein is probably required for RR activity during DNA repair
MDM-2	Involved in the targeting of p53 via ubiquitination for proteasomal degradation.

1.6.3 Ribonucleotide Reductase

Ribonucleotide reductase (RR) is a ubiquitous radical-containing enzyme, which belongs to a family of enzymes that are involved in the conversion of both purine and pyrimidine ribonucleotide diphosphates into their corresponding deoxyribonucleotide (dNTPs) by replacing the C2'-hydroxyl group on the ribose moiety by a hydrogen atom. After phosphorylation, the resulting molecules are the precursors needed for DNA replication, cell cycle progression and cellular repair **(Fig. 1.11)** (Cerqueira *et al.*, 2007).

The discovery of this enzyme was reported in 1961 by Peter Reichard. The first RR enzyme was discovered in *E. coli* but later on it was found in all growing cells of every living organism and even several species of viruses carry their own copy of RR (Jordan and Reichard, 1998).

All RR enzymes contain two components; an R1 subunit i.e. the reductase component that is involved in the binding of ribonucleotides and allosteric effectors, and an R2 subunit i.e. the radical generator, that contains a tyrosyl radical that is stabilised by iron **(Fig. 1.11)** (Thelander and Reichard, 1979; Thelander *et al.*, 1983; Guittet *et al.*, 2001; Shao *et al.*, 2004). The R1 subunit is somewhat similar between all RR classes, whereas the R2 subunit is not the same within all the RR enzymes and is deeply buried inside the protein, in order to be protected from the environment (Cerqueira *et al.*, 2007).

The RR enzyme is classified into three classes (Yu *et al.*, 2009):

Class I RRs are found in all eukaryotic organisms and in some prokaryotic and viruses (Yu *et al.*, 2009). They are characterized by a tyrosyl radical that is stabilized by an oxo-bridged binuclear Fe^{+3} complex and requires oxygen for its generation. This class is further divided into three subclasses (Ia, Ib and Ic) based on polypeptide sequence homology and allosteric behaviour (Jordan *et al.*, 1994). Human RR is a tetramer that belongs to class Ia (Yu *et al.*, 2007).

Class II RRs are restricted to prokaryotes (both aerobic and anaerobic) whereas class III RRs, only function in anaerobic conditions. (Cerqueira *et al.*, 2007).

For the purpose of my thesis, RR is referred to as human RR i.e. Class Ia.

1.6.3.1 Ribonucleotide Reductase regulation

The levels and activity of RR are highly regulated by the cell cycle and DNA checkpoints which maintain optimal dNTP pools required for genetic fidelity. The enzyme can be regulated by two factors: by transcription of the genes or by allosteric control of RR by triphosphate effectors. The genes of each subunit are located on separate chromosomes and the corresponding mRNAs are similarly expressed during the S-Phase of the cell cycle.

During the normal cell cycle the levels of the R1 protein do not change substantially and can be detected throughout the whole cycle. In contrast, protein R2 can only be truly detected between the S phases, where it slowly accumulates, up to late mitosis, where it is rapidly degraded. This mechanism ensures an adequate supply of dNTPs for replication and/or repair during the S and G2 phase of the cell cycle.

Recently, Guittet *et al* (2001) found that when DNA damage occurs, a transcriptional induction of a new protein called p53R2 is observed in a p53-dependant manner (Thelander and Reichard, 1979; Thelander *et al.*, 1983; Guittet *et al.*, 2001; Shao *et al.*, 2004). It has been reported that there is also an additional p53-independent induction of p53R2, because cells with mutated p53 still express this molecule in response to DNA-damaging agents. In fact, p53R2 can be a transcriptional target of the p53 family member, p73 (Nakano *et al.*, 2000). Furthermore, it has been demonstrated that protein R1 can form a functional complex either with protein R2 or protein p53R2. Therefore, R2 protein appears to be responsible for the maintenance of dNTPs levels for replication in S/G2 phase, whereas p53R2 is responsible for production of dNTPs in response to DNA damage (Cerqueira *et al.*, 2007) in G0/G1 phase (Renton and Jeitner, 1996).

1.6.3.2 Ribonucleotide Reductase and iron

A series of reactions between the di-iron centre and tyrosyl radicals of the R2 subunit and conserved cysteine residues of the R1 subunit are required before effective catalysis takes place (Ke and Costa, 2006).

The mechanism by which the substrate-binding site of the R1subunit is activated involves the generation of radicals at the tyrosine residues of the R2 subunit(Kolberg *et al.*, 2004). These radicals are subsequently transferred to the cysteine residues in the active site of the R1 subunit (Kolberg *et al.*, 2004). The role of iron in this process is the generation of tyrosyl radicals in the R2 subunit through reactions with molecular oxygen (Kolberg *et al.*, 2004). Once the radicals have been formed, iron is also involved in the radical transfer chain formed between the R1 and R2 subunit (Levy *et al.*, 1995).

In the absence of a constant supply of iron to R2, the R1 subunit is inactive and thus, RR cannot function (Thelander and Reichard, 1979; Thelander *et al.*, 1983), therefore the activity of RR is iron-dependent (Le and Richardson, 2002). Both the R2 and p53R2 subunits possess an iron-binding site that is important for their enzymatic function (Shao *et al.*, 2004), and hence are susceptible to the action of iron chelators (Nyholm *et al.*, 1993; Cooper *et al.*, 1996).

In comparison to several key enzymes, RR shows the greatest increase in activity in tumours compared to normal cells (Witt *et al.*, 1978; Takeda and Weber, 1981). This means that this Fe-containing enzyme is an important target for anti-tumour drugs.

The potential of RR as a therapeutic target for the treatment of cancer is illustrated by the cytotoxic drug hydroxyurea (HU) that acts to scavenge the tyrosyl radical of this enzyme (Nyholm *et al.*, 1993). However, HU has limited potency due to its short half-life, low affinity for RR, and the development if HU resistanc (Beckloff *et al.*, 1965; Gwilt and Tracewell, 1998).

Therefore, iron chelation may provide an alternative mechanism to inhibit RR activity in HU-resistant tumours. In fact, *in vitro* studies have shown that some chelators that are RR inhibitors can overcome HU-resistance via their ability to bind iron (Green *et al.*, 2001). Indeed, several iron chelators such as pyridoxal isonicotinoyl hydrazone (PIH), deferoxamine, and thiosemicarbazone derivatives inhibit enzymatic activity, either by chelation of the cofactors, which precludes the incorporation of the cofactor in the enzyme or directly at the enzyme-bound metallic center. The success of these iron chelators, particularly DFO (Deferrioxamine mesylate; Desferal®, Novartis, Switzerland), Triapine (3-aminopyridine-2-carboxaldehydethiosemicarbazone) and 2-hydroxy-1-naphthyl-aldehyde-isonicotinoyl hydrazone (van Reyk *et al.*, 2000) in *in vitro*, *in vivo* and in some clinical trials, together with their selective antitumour activity, confirms their potential as anti-cancer drugs (Cerqueira *et al.*, 2007). This is discussed in more detail below.

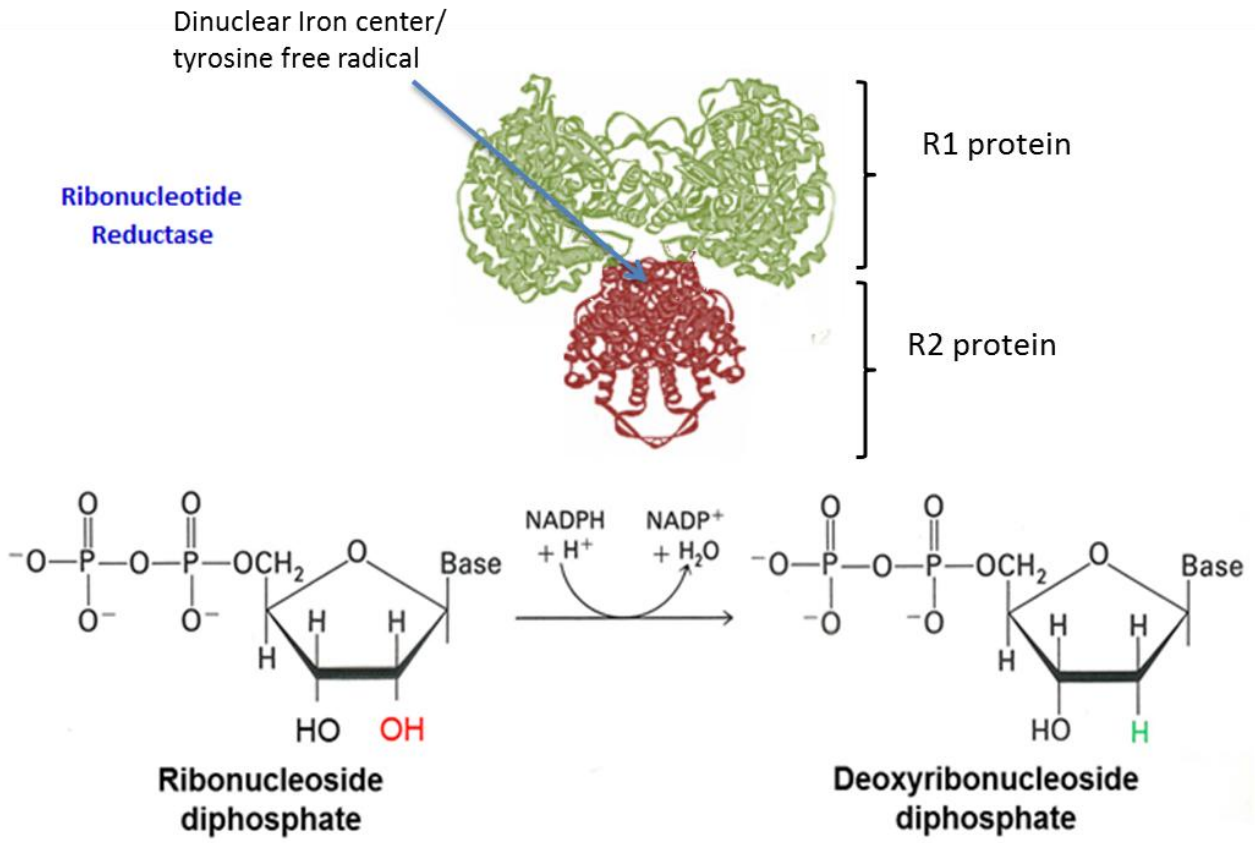

Figure 1.11: The Structure of protein R1 and R2 of Ribonucleotide reductases (RR) and the reaction that provides the building blocks for DNA in all living cells. (Adapted from Cerqueira *et al.*, 2007).

1.6.4 Cell Growth Regulation in cancer

Human neoplasms develop following the progressive accumulation of genetic and epigenetic alterations to oncogenes and tumour suppressor genes. These alterations confer a growth advantage to the cancer cell. Genes that are altered in neoplasia affect three major biologic pathways that normally regulate cell growth and tissue homeostasis, i.e. the cell cycle, apoptosis, and differentiation (Corn and El-Deiry, 2002).

1.6.4.1 Disturbance of cell-cycle control in oncogenesis

As mentioned above, the fundamental task of the cell cycle is to ensure that DNA is faithfully replicated once during S phase and that identical chromosomal copies are distributed equally to two daughter cells during M phase (Heichman and Roberts, 1994; Wuarin and Nurse, 1996). However, defects in cell cycle control may lead to abnormal proliferation of cancer cells. Indeed, two regulatory pathways of the cell cycle that are disrupted in virtually all human tumours are the p53- and Rb-dependent pathways (Corn and El-Deiry, 2002).

Oncogenic alterations of the components of pRB-dependent pathway such as cyclins, Cdks and CKIs, have been reported in more than 90% of human neoplasms and are summarized in **Table 1.3** (Elsayed and Sausville, 2001).

- The cyclin D1 gene is induced by various oncogenic signals including activating mutations in ras, src, and mitogen-activated protein kinases (MAPK) (Albanese *et al.*, 1995; Lee *et al.*, 1999). Cyclin D1 promotes transformation and malignancy (Daksis, Lu *et al*., 1994; Lovec, Grzeschiczek *et al*., 1994), and in transgenic mice it facilitates development of breast adenocarcinoma (Wang *et al.*, 1994) and lymphoma (Bodrug *et al.*, 1994). It is also associated with higher incidence of recurrence in head and neck cancers (Michalides *et al.*, 1995).
- Cyclin E dysregulation is associated with hyperproliferation and malignant transformation (Keyomarsi and Herliczek, 1997). Overexpression of cyclin E correlated well with breast tumour aggressiveness and independently predicted the risk of distant visceral relapse (Kim *et al.*, 2000).
- Inactivation of the CKIs p16 or p21 by mutation, deletion, or p53-mediated inactivation might result in aberrant activity of Cdks, and in turn phosphorylation within activation of pRB. The loss of $p16^{INK4A}$, $p27^{KIP1}$, and $p21^{WAF1}$ was a predictor of poor outcome in several

tumour types (Tsihlias *et al.*, 1999). Similarly, mutations in the p53 gene are found in more than half of all human cancers, and the 'p53 pathway' appears to be disrupted in the vast majority of the remaining tumours. Loss of p53 function has consequences on pathways of cell-cycle control ($p21^{Cip/Waf1}$, 14-3-3 sigma), DNA repair (Gadd45, p53R2) and apoptosis (Bax, KILLER/DR5, p53AIP1) (Vogelstein *et al.*, 2000).

Table 1 3. Abnormalities of cyclins, cyclin-dependent kinases, and cyclin-dependent kinase inhibitors in various human cancers (Elsayed and Sausville, 2001)

Cyclin/Cdk/CKI	**Phase/activity**	**Tumour types**
Cyclin D1	G_1	Lymphoma, mantle cell lymphoma 95%, breast 35%-81%, esophagus 40%, lung 10%-20%, parathyroid, myeloma, head and neck 40%, sarcoma 33%, hepatocellular 10%, bladder 15%
Cyclin D2	G_1	Colorectal, testicular, CLL
Cyclin D3	G_1	Lymphoma 50%, ALL 50%, retinoblastoma
Cyclin K (D-like)	G_1	Kaposi sarcoma
Cyclin E	late G_1, early S	Colorectal, breast, prostate, ovarian, gastric, lung, CLL, renal, pancreatic
Cyclin E2	G_1/S	Breast, small cell lung, cervical
Cyclin B1	G_2/M	Colorectal, breast
Cyclin A	mid S/G_2	Hepatocellular, breast
Cdk2	G_1/S	Colorectal
Cdk4	G_1/S	Sarcoma 8%-36%, glioma 10%, melanoma, Colorectal, breast
Cdk6	G_1/S	Glioma
$p16^{INK4}$	inhibits Cdk4/6	Melanoma, ALL 30%, bladder 30%, head and neck 10%, lung 30%, breast, ovary 20%, esophagus 30%, pancreas 40%, glioma 50%, mesothelioma 50%, nasopharyngeal 40%, sarcoma 10%, biliary tract 50%
$p15^{INK4}$	inhibits Cdk4/6	Melanoma, T-cell ALL, lung, head and neck
$p21^{WAF1/CIP1}$	inhibits all Cdks	Brain, colorectal, leukemia, melanoma
$p27^{kip}$	inhibits all Cdks	Breast, colon, melanoma

1.6.4.1.1 Disturbance of apoptotic pathway in oncogenesis

In normal tissues, there is a tightly regulated balance between cellular proliferation and cellular death. If this balance is disturbed, tumours may develop.

While increased cellular proliferation has long been regarded as the predominant cause of neoplasia, in more recent years a growing body of evidence supports the alternative hypothesis that cancer cells survive because they fail to undergo normal apoptosis, or programmed cell death (Corn and El-Deiry, 2002).

Apoptosis involves an orchestrated series of biochemical events leading to cell death (Lawen, 2003). There are two principal molecular pathways that signal apoptosis by cleaving the initiator caspases; the intrinsic mitochondrial pathway and the extrinsic death receptor pathway**:**

- The mitochondrial pathway is triggered by a number of stimuli, such as DNA damage, ischemia and oxidative stress (Lawen, 2003). This pathway is initialized with the permeabilisation of the mitochondrial outer membrane leading to protein release, such as cytochrome c and apoptosis-inducing factor (AIF) (Lawen, 2003). The release of cytochrome c leads to the induction of Apaf-1 that activates caspase-9 by the formation of the apoptosome. Caspase-9 then proceeds to activate caspases-3 and -7 resulting in the induction of apoptosis (Lawen, 2003). Permeability of the mitochondrial membrane is regulated by the Bcl-2 family of proteins that consist of pro-apoptotic molecules (Bax, Bid, Bad, Puma and Bim) and anti-apoptotic molecules (Bcl-2 and Bcl-xL). Apoptosis induced by p53 is mediated through the mitochondrial pathway and is linked to pro-apoptotic signals directed from certain Bcl-2 members. For example, Bax is a p53-induced pro-apoptotic molecule and the loss of p53, which is common in human tumours, results in decreased Bax activity (Amundson *et al.*, 1998; LaCasse *et al.*, 1998).

- The second major apoptosis pathway is the death-receptor pathway (Hengartner, 2000) Examples of cell-surface death receptors are Fas/APO1/CD95, tumour necrosis factor receptor-1 (TNFR1), and KILLER/DR5, and their natural ligands are FasL, TNF, and TRAIL respectively. When these receptors are engaged by their ligands, they aggregate to form a potent death-inducing signaling complex (DISC) that uses an adaptor protein (e.g., FADD) to recruit and activate caspase-8, which in turn activates caspase-3 to carry out the remainder of the death program.

There is cross talk between the death-receptor and mitochondrial pathways through Bid, a proapoptotic Bcl-2 member that is cleaved by caspase-8 and translocates to the mitochondria to enhance cytochrome c release. The death-receptor pathway is subject to regulation by Fas (DcR3), TRAIL (TRID and TRUNDD), c-FLIP, and IAPs (inhibitors of apoptosis) (for review see (Corn and El-Deiry, 2002).

1.6.4.1.2 Disturbance of apoptotic pathway in skin hyperproliferative diseases

Skin cancer and hyperproliferative disease such as psoriasis are the most notable examples of that involve decreased keratinocytes' (KC) apoptosis. A common feature of these diseases is expression of Survivin (Bowen *et al.,* 2004). Survivin is generally not expressed in normal skin. Interestingly, in psoriasis survivin expression is localized to the upper third of the epidermis, whereas in actinic keratoses (AK), basal-cell carcinoma (BCC), and squamous-cell carcinoma (SCC) reveal staining in all epidermal layers (Bowen *et al.*, 2004).

In psoriasis, there is decreased spontaneous KC apoptosis in lesional skin (Laporte *et al.*, 2000), which correlates with decreased levels of caspase-14 (Lippens *et al.*, 2000). KCs in psoriatic plaques exhibit a phenotype reminiscent of that of senescent KCs, characterized by resistance to apoptosis compared with normal KCs and lack of p53 activation (Wrone-Smith *et al.*, 1997; Qin *et al.*, 2002). In addition to Survivin, multiple studies consistently demonstrated increased levels of Bcl-xL in psoriasis (Fukuya *et al.*, 2002).

Non-melanoma skin cancers (e.g. SCC and BCC) demonstrate multiple examples of apoptotic dysregulation in which proapoptotic regulatory molecules are reduced or antiapoptotic molecules are overexpressed. Mutation or deletion of *p53* occurs in many skin cancers. Moreover, in BCC there is a concomitant decrease in Bax expression (Tomkova *et al.*, 1998) that coincides with increased Bcl-2 expression (Morales-Ducret *et al.*, 1995). In addition, Bcl-xL is overexpressed in SCC (Wrone-Smith *et al.*, 1999). The presence of Survivin in pre-malignant lesions (Bowen *et al.*, 2004) suggests that its expression represents an early step in KC transformation. In SCC, expression of Bcl-2 (Hantschmann and Kurzl, 2000; Matsumoto *et al.*, 2001), Bcl-xL (Matsumoto *et al.*, 2001), and Survivin (Lo Muzio *et al.*, 2001) is associated with metastasis or poor prognosis (Raj *et al.*, 2006). These dysregulations have important implications for cancer therapies. Since it has been shown that cells with inactivated p53 or Bax could be resistant to chemotherapy (Bunz *et al.*, 1999; Zhang *et al.*, 2000).

1.6.4.1.3 Disturbance of cell differentiation in oncogenesis

Cellular differentiation as a biologic process appears to be quite distinct from the cell cycle or apoptosis. However it is closely linked to both processes. Differentiation entails a definitive withdrawal from the cell cycle, thus cells that cannot arrest will not be able to differentiate. The two cell-cycle proteins that have been closely linked to differentiation are pRb and $p21^{Cip/Waf1}$(Corn and El-Deiry, 2002). Additionally, there is an important relationship between dysregulated apoptosis and abnormal differentiation (Corn and El-Deiry, 2002). Indeed using the small intestine as a model, differentiation and apoptosis have been linked as integral pathways for normal cellular homeostasis. The antiapoptotic protein Bcl-2 has been proposed to be a candidate protein that inhibits differentiation (Von Wangenheim and Peterson, 2001). Cancer cells that overexpress Bcl-2 often retain their clonogenic potential when exposed to a variety of differentiating agents. This has important implications for the use of differentiation agents in cancer therapy, since many tumours overexpress Bcl-2.

Skin cancer and some pathologic disorders such as psoriasis are characterised by incomplete differentiation of the *stratum granulosum* and SC (Lippens *et al.*, 2009).

1.7 Role of iron in cell cycle and related molecules

Iron depletion may alter the expression and/or function of molecules that are critical in regulating progression of the cell cycle. Some of these include: RR, cyclins, Cdks p53, $p21^{CIP1/WAF1}$, $p27^{Kip}$, GADD45α, hypoxia inducible factor-1α (HIF-1α), N-myc downstream regulatory gene-1 (Ndrg-1), and pRb. By altering the expression and/or function of the above molecules, iron-depletion is able to effectively inhibit the growth of tumour cells (reviewed by Yu *et al.,* 2007). Therefore iron chelation has been proposed as an alternative therapy for cancer **(see section 1.9)**.

1.7.1 Cyclins and Cdk

As previously described, it is the regulated alterations in the availability and activity of cyclins and Cdks that allows the transition between the cell cycle phases (Sherr, 1994).

Studies have demonstrated that iron-chelation in SK-N-MC neurblastoma (NB) cells can markedly decrease the expression of cyclins D1, D2 and D3, while having a lesser effect on reducing the levels of cyclin A and B (Gao and Richardson, 2001). It has also been shown that there was a reduction in cyclin A protein and its kinase activity in normal T lymphocytes after incubation with DFO (Lucas *et al.*, 1995).

A more recent study has confirmed that the mechanism of the iron-depletion-mediated reduction in cyclin D1 protein expression is due to its proteasomal degradation, there being no decrease in *cyclin D1* mRNA levels (Nurtjahja-Tjendraputra *et al.*, 2007).

Iron-chelation has also been shown to reduce the expression of Cdk2 (Gao and Richardson, 2001; Chaston *et al.*, 2003) or Cdk4 (Kulp *et al.*, 1996) protein depending on the cell type. Furthermore, DFO was found to decrease the protein levels and kinase activity of $p34^{cdc2}$ in NB cells (Brodie *et al.*, 1993). This is important, as $p34^{cdc2}$ functions in the G2/M and potentially G1/S phase transitions, by forming complexes with cyclin A, B and E (Aleem *et al.*, 2005; Kaldis and Aleem, 2005). This may explain the G1/S and G2/M arrest seen after iron depletion under some experimental conditions. In contrast to other cyclins, cyclin E protein expression was found to be elevated in response to iron-depletion in NB cells (Gao and Richardson, 2001).

Several studies have shown that following iron-depletion, pRb becomes hypo-phosphorylated leading to G1/S arrest (Hollstein *et al.*, 1991; Terada *et al.*, 1991). Indeed, as mentioned above, iron-depletion reduces cyclin D1 and Cdk2 expression (Gao and Richardson, 2001; Chaston *et al.*, 2003; Nurtjahja-Tjendraputra *et al.*, 2007) which prevents

cyclin-Cdk complexes formation leading to pRb hypophosphorylation that will contribute to cell G1/S arrest (Gao and Richardson, 2001). This observation was further confirmed by studies on NB cells (Gao and Richardson, 2001), human breast cancer cells (Kulp *et al.*, 1996) and T lymphocytes (Terada *et al*., 1991), where iron chelation resulted in the pRb hypo-phosphorylation (Gao and Richardson, 2001; Terada *et al*., 1991). Hypo-phosphorylation of pRb during mid to late G1 phase by Cdk4- or Cdk6-cyclin D complexes prevents the release of transcription factor E2F1 from pRb that is necessary for cell cycle arrest (Hatakeyama and Weinberg, 1995; Weinberg, 1995).

1.7.2 p53

Iron-depletion was found to elevate the level of p53 protein expression (Fukuchi *et al.*, 1995; Sun *et al.*, 1997; Liang and Richardson, 2003) at the post-transcriptional level but there is no change in *p53* mRNA (Fukuchi *et al.*, 1995; Gao and Richardson, 2001). In cellular studies, it has been shown that iron-chelation induced the transactivational activity of p53 and its sequence-specific DNA binding in a dose- and time-dependent manner (Sun *et al.*, 1997; Liang and Richardson, 2003). Many mechanisms may be involved in the p53 activation by iron depletion (Yu *et al.*, 2007). These include: (i) an increase in the expression of p53 protein (Liang and Richardson, 2003); (ii) an increase in the conversion of latent p53 to its active DNA-binding form (Ashcroft *et al.*, 2000); (iii) p53 phosphorylation at serine-15 which increases p53 stability and prevents mdm-2-mediated proteasomal degradation (Ashcroft *et al.*, 2000). The elevated phosphorylation of p53 at serine-15 may indicate up-regulation of ataxia telangiectasia mutated (ATM) and/or ATM-Rad3 related (ATR) genes or proteins after iron-chelation (Ashcroft *et al.*, 2000); (iv) other target-molecules of iron-chelation that can also increase the expression of p53, such as the transcription factor hypoxia inducible factor-1α (HIF-1α) (Golias *et al.*, 2004). However, it is unclear which of the p53 molecular targets that are affected by iron-depletion. The expression of both $p21^{CIP1/WAF1}$ and *GADD45 mRNA* are increased after iron depletion, but this occurs in both p53-dependant and independent pathways (Darnell and Richardson, 1999)

1.7.3 Cdk inhibitors

Investigations in this field have focussed on the effects of iron chelators on the more well-characterised Cdk inhibitors (e.g, $p21^{WAF1/CIP1}$, $p27^{KIP1}$) (Darnell and Richardson, 1999; Ashcroft *et al.*, 2000; Gao and Richardson, 2001). Iron-depletion mediated by DFO and 311 markedly upregulates $p21^{WAF1/CIP1}$ mRNA by a p53-independent pathway (Darnell and Richardson, 1999; Le and Richardson, 2004). This effect has been observed in a variety of cell types (Fukuchi *et al.*, 1995; Darnell and Richardson, 1999; Gao and Richardson, 2001; Becker *et al.*, 2003; Le and Richardson, 2003) and is relevant to the pharmacological effects of chelators as anti-tumour agents (Yu *et al.*, 2007). However, $p21^{WAF1/CIP1}$ protein expression decreased after iron-depletion (Fu and Richardson, 2007). This downregulation of $p21^{WAF1/CIP1}$ is important, as apart from being a Cdk inhibitor and positive regulator of the cell cycle, this protein has also anti-apoptotic activity.

On the other hand, iron-depletion mediated by the iron chelator 'mimosine' upregulates $p27^{KIP1}$ at both mRNA and protein levels (Wang *et al.*, 2000; Yoon *et al.*, 2002; Dong and Zhang, 2003; Wang *et al.*, 2004). It was suggested that iron-depletion also increased the expression of transforming growth factor β1 (TGF- β1) (Yoon *et al.*, 2002). Interestingly, the upregulation of $p27^{KIP1}$ was prevented when TGF- β1was neutralized using a TGF- β1antibody (Yoon *et al.*, 2002).

1.7.4 The growth arrest and DNA-damage-inducible genes(GADD) family

The GADD group of genes are stress response molecules comprising of GADD34, GADD45 and GADD153. Their expression is increased when cells are subjected to a stress such as nutrient deprivation (e.g., glucose, glutamine, zinc) (Carlson *et al.*, 1993; Abcouwer *et al.*, 1999; Fanzo *et al.*, 2001) or exposed to DNA-damaging agents (e.g., peroxynitrite) (Oh-Hashi, Maruyama *et al.*, 2001) leading to cell cycle arrest and/or apoptosis.

The GADD45 group of genes encodes three proteins, GADD45α, GADD45β and GADD45γ. Although these proteins are structurally-related , only GADD45α has been demonstrated to cause p53-dependent G2/M arrest and inhibit cdc2 kinase (Zerbini and Libermann, 2005). GADD45α has also been shown to interact with cell cycle regulatory molecules, such as $p21^{CIP1/WAF1}$ (Kearsey *et al.*, 1995), cdc2/cyclin B1 (Vairapandi *et al.*, 2002) and p38 mitogen-activated protein kinase (MAPK; see section **1.7.5**) (Bulavin *et al.*, 2003). The GADD45α cellular activity also depends on its interacting partner. For instance,

interaction between GADD45α and p38 MAPK has been shown to regulate p53 which prevent, in part, oncogene-induced growth (Bulavin *et al*., 2003).

It has been suggested that GADD34 and GADD153 may directly initiate apoptosis rather than inducing cell cycle arrest (Hollander *et al.*, 2001; Maytin *et al.*, 2001). Overexpression of each *GADD* gene leads to the inhibition of growth and/or apoptosis, whereas combined overexpression of the three *GADD* genes causes synergistic or cooperative effects on antiproliferative activity (Zhan *et al.*, 1994).

Interestingly, studies have demonstrated that DFO or 311-mediated iron chelation has caused a marked increase in the *GADD45* mRNA expression in BE-2 neuroblastoma, SK-N-MC neuroepithelioma and K562 erythroleukemia cell lines, in a concentration- and time-dependent manners (Darnell and Richardson, 1999). Iron-depletion has also been found to increase *GADD153* mRNA (Yu *et al.,* 2007). Further studies are required to assess the GADD45 protein level in cells after iron-depletion since one study has shown there was no appreciable increase in the GADD45 protein level in cells after iron-depletion (Gao and Richardson, 2001).

Similarly, both *GADD45* and *GADD153* mRNAs have been found to be up-regulated during hypoxia (Price and Calderwood, 1992). This suggests that the transcription factor HIF-1α plays a role in the up-regulation of these genes that may be activated by both hypoxia and iron-chelation via prolyl hydroxylases (see section **1.7.5**).

It has been suggested that GADD45 may cause growth arrest by inhibiting the activity of cyclin B and Cdk2 (Vairapandi *et al.*, 2002) and studies have demonstrated that iron-chelation causes a reduction in the expression of these regulatory molecules (Gao and Richardson, 2001).

1.7.5 p38 MAPK

The p38 MAPK signalling molecule is a member of the MAPK family which also includes extracellular signal-regulated kinase (ERK) and c-Jun N-terminal protein kinase/stress-activated protein kinase (JNK/SAPK). These proteins affect processes such as cell differentiation and apoptosis and are activated by many environmental stresses and inflammatory cytokines (Bulavin *et al.*, 2003).

It has been shown that iron-chelation with DFO strongly activated p38 MAPK and ERK, but did not activate JNK (Lee *et al.*, 2006).

Interestingly, growth inhibition mediated by p38 has been suggested to involve p53 activation (Bulavin *et al.*, 1999) and reduce cyclin D1 expression (Lavoie *et al.*, 1996), both of which also occur upon iron-chelation (Fukuchi *et al.*, 1995; Kulp *et al.*, 1996; Gao and Richardson, 2001; Nurtjahja-Tjendraputra *et al.*, 2007).

1.7.6 Hypoxia inducible factor-1 (HIF-1)

HIF-1 is a transcription factor that is activated under hypoxic conditions and acts to initiate a signalling pathway leading to cell survival (Semenza, 1999; Greijer *et al.*, 2005). This protein is a heterodimer composed of an "α" subunit which is regulated by the hypoxic state, and a "β" subunit which is constitutively expressed (Wang *et al.*, 1995). Under normal conditions, HIF-1α is regulated by prolyl hydroxylase enzymes (Ivan *et al.*, 2001; Stockmann and Fandrey, 2006) which mediates its degradation (Semenza, 1999; Ivan *et al.*, 2001; Greijer *et al.*, 2005). However, under conditions of oxygen-deprivation and/or iron-depletion, prolyl hydroxylases does not function, causing HIF-1α accumulation in the cell (Ivan *et al.*, 2001; Stockmann and Fandrey, 2006). HIF-1α then translocates to the nucleus where it binds to HIF-1β to form the HIF-1 complex (Wang *et al.*, 1995; Caro, 2001).

Once formed, HIF-1 can upregulate TfR1 transcriptionally (Bianchi *et al.*, 1999; Tacchini *et al.*, 1999) leading to an increase in intracellular iron levels. HIF-1 can also target Ndrg-1 (**see section 1.7.7**) (Kovacevic and Richardson, 2006). Moreover, under conditions of severe hypoxia, HIF-1α can stabilise p53 expression (An *et al.*, 1998) and upregulate proapoptotic factors such as BNIP3 (Bruick, 2000; Guo *et al.*, 2001) that may lead to apoptosis.

Iron-depletion results in the activation of HIF-1α and its down-stream targets, ultimately leading to cell cycle arrest, apoptosis, metastasis suppression and inhibition of growth (Le and Richardson, 2004). Although HIF-1α up-regulation may lead to growth and angiogenesis (e.g., through vascular endothelial factor-1 VEGF1), potent iron chelators have been shown to override this and activate apoptotic pathways (Gao and Richardson, 2001; Le and Richardson, 2004).

1.7.7 N-myc downstream regulated gene 1 (Ndrg-1)

Ndrg-1 is a metastasis suppressor gene that is involved in cell differentiation and proliferation (Bandyopadhyay *et al.*, 2004; Kovacevic and Richardson, 2006; Maruyama *et*

al., 2006). Iron-chelation markedly upregulates *Ndrg-1* mRNA and the expression of the protein in a number of cancer cell types. It has been found that in prostate cancer patients, high expression of Ndrg-1 is associated with greater survival and less aggressive tumours (Bandyopadhyay *et al.*, 2003). Additionally, in pancreatic adenocarcinoma patients, there is a significant inverse correlation of Ndrg-1 expression with depth of invasion (Maruyama *et al.*, 2006). Moreover, in breast and prostate cancer patients with lymph node or bone metastasis, Ndrg-1 expression was significantly reduced when compared to those with localized disease (Bandyopadhyay *et al.*, 2003; Bandyopadhyay *et al.*, 2004). Furthermore, studies *in vivo* and *in vitro* have demonstrated that over-expression of Ndrg-1 protein results in smaller tumours that are less aggressive (Kurdistani *et al.*, 1998; Bandyopadhyay *et al.*, 2003; Maruyama *et al.*, 2006). Hence, the up-regulation of Ndrg-1 after iron depletion may, in part, play an important role in inhibiting the proliferation observed after treatment with these agents.

The Ndrg-1 expression in normal breast epithelial cells was found to be high during G1 and G2/M phases and low during the S-phase, suggesting a potential role in regulating the cell cycle. In contrast, in breast cancer cells, Ndrg-1 levels remains constant throughout the cell cycle (Kurdistani *et al.*, 1998).

It has been suggested that Ndrg-1 plays a role in cell cycle regulation. Analysis of the nucleotide sequence of the Ndrg-1 promoter has revealed a motif for the transcription factor E2F1 (Kovacevic and Richardson, 2006), which plays a pivotal role in the G1 to S-phase transition. Furthermore, it has been found that Ndrg-1 was induced by p53 following DNA damage, which suggests that Ndrg-1 is necessary for p53-dependent apoptosis (Stein *et al.*, 2004).

Recently, it has been found that DFO, 311 and Dp44mT up-regulate the Ndrg-1 level in a range of cancer cell types in an iron-dependent but p53-independent manner (Le and Richardson, 2004). Interestingly the degree of Ndrg-1 up-regulation was proportional to the efficacy of the anti-proliferative activity of the chelator assessed. Furthermore the up-regulation of Ndrg-1 following iron-chelation was found to be due to both HIF-1α-dependent and -independent mechanisms (Le and Richardson, 2004).

Since Ndrg-1 potentially plays a pivotal role in cell cycle regulation, its up-regulation following iron-chelation may be one mechanism by which iron chelators cause cell cycle arrest and apoptosis (Yu *et al.*, 2007).

1.7.8 CDC14A

Sanchez et al. (2006) have identified a novel IRE in the 3' UTR of *CDC14A* mRNA that binds IRPs. Iron-chelation using DFO lead to an increase in the expression of the CDC14A transcript that contains the IRE (Sanchez *et al.*, 2006). Interestingly, it has been demonstrated that CDC14A de-phosphorylates $p27^{Kip1}$ and cyclin E, which are critical for the G1 to S transition (Kaiser *et al.*, 2002). Therefore, it was suggested that CDC14A may play a role in the cell cycle arrest seen after iron-chelation. However, the effect of iron-chelation on CDC14A expression was only reported at the mRNA level. Further studies are necessary to determine whether iron-depletion affects the protein expression of CDC14A.

1.7.9 Iron-depletion and apoptosis

Many studies have demonstrated the ability of iron chelators to induce apoptosis (Hileti *et al.*, 1995). For example, DFO induced apoptosis in a number of cancer cells including ovarian cancer (Brard *et al.*, 2006) , NB (Fan *et al.*, 2001), Kaposi's sarcoma (Simonart *et al.*, 2000) malignant oral KC (Lee *et al.*, 2006) and cervical carcinomas (Simonart *et al.*, 2002). Silmilarly, iron chelators such as Triapine (Alvero *et al.*, 2006), Tachpyridine (Greene *et al.*, 2002; Zhao *et al.*, 2004), O-Trensox (Rakba *et al.*, 1998) and Dp44mT (Yuan *et al.*, 2004) have also been shown to induce apoptosis in a variety of neoplastic cell types both *in vitro* and *in vivo*.

Furthermore, it has been shown that DFO increased the activity of caspase-3, -8 and -9 (Brard *et al.*, 2006; Lee *et al.*, 2006; Wang *et al.*, 2006), while Dp44mT markedly increased the activity of caspase-3 (Yuan *et al*., 2004). Numerous studies have demonstrated that iron chelators induce apoptosis through the mitochondrial pathway. For instance, Triapine-induced apoptosis was mediated by Bid activation (Alvero *et al.*, 2006). Moreover, apoptosis caused by Tachpyridine was not inhibited by blocking the CD95 death receptor pathway with a Fas-associated death domain protein dominant-negative mutant (Greene *et al*., 2002). Furthermore, apoptosis induction by Dp44mT and DFO was associated with a reduction in Bcl-2 expression, an increase in Bax and efflux of cytochrome c from the mitochondrion (Yuan *et al.*, 2004; Lee *et al.*, 2006). Additionally, DFO has been found to cause the nuclear accumulation of pleomorphic adenoma gene like 2 (PLAGL2) which results in the expression of the proapoptotic factor, BNIP3 (Mizutani *et al.*, 2002). The BNIP3 overexpression increases Bax and Bak levels which leads to the release of cytochrome c and apoptosis (Kubli *et al.*, 2007).

It still remains unclear whether p53 accumulation upon iron-deprivation is necessary for apoptosis. For instance, incubation of cells with Tachpyridine led to rapid accumulation of p53 and death but this did not require p53 activation (Abeysinghe *et al.*, 2001). In contrast, other mechanisms have been suggested where iron-depletion activates p38 and ERK MAPK to transduce signals for induction of the apoptotic cascade (Lee *et al.*, 2006).

1.8 Skin Hyper-proliferative Disease

1.8.1 Skin cancer

In the United Kingdom, the incidence of skin cancer is greater than that of all other cancers. According to Cancer Research UK, it is estimated that at least 100,000 new cases are diagnosed each year (Cancer Research UK, 2008).

The common skin cancers, which are also named after the type of skin cell they arise from, are basal cell carcinoma (BCC) and squamous cell carcinoma (SCC), known together as Non-Melanoma Skin Cancer (NMSC) which is the most common cancer in UK with official figures reporting over 72400 cases diagnosed only in 2004. In addition to malignant melanoma which is substantially less common but often fatal, BCC comprises 75% of all NMSC cases.

BCC may be categorized into three major growth patterns: nodular (nBCC), superficial (sBCC) and morphoeiform (or sclerotic; mBCC). Nodular BCC is the most frequent form of BCC. It usually presents as a waxy, pearly or translucent papule/nodule with overlying fine telangiectasias, with frequent ulceration or erosion of the surface. Tumours may occasionally be pigmented to varying degrees. Superficial BCC most commonly arise on the trunk and extremities, but may be seen anywhere on the body. The tumours are characterized by an erythematous macule or patch, which may be variably pigmented. There may also be an overlying fine scale, a superficial erosion or hemorrhagic scale crust. mBCC is frequently seen in chronic arsenism and as late sequelae of radiation therapy. Morpheaform or sclerosing

has a scar-like appearance. It consists of a dermal plaque with overlying epidermal atrophy in a sun-exposed distribution (Toro *et al.*, 2009).

Squamous cell carcinoma (SCC) is the second most common type of skin cancer in this country after BCC, accounting for 20% of all skin cancers. It commonly presents as a red, scaling, thickened patch on sun-exposed skin. Some are firm hard nodules and dome shaped like keratoacanthomas. Ulceration and bleeding may occur. When SCC is not treated, it may develop into a large mass. SCC metastasis rate is quite low, with the exception of SCCs of the lip, ear, and in immunosuppressed patients.

Melanoma is the least frequent of the 3 common skin cancers. However it frequently metastasises, and is deadly once spread. Most skin cancer deaths (i.e. more than 1800 each year), are from malignant melanoma. The mortality related to melanoma has quadrupled since the 1970s and its rate has risen faster than any other cancer in the UK in the last 25 years. Melanoma is also the most common cancer in young adults aged 15-34 (Bruce and Brodland, 2000). Most melanomas are brown to black-looking lesions. Unfortunately, a few melanomas are pink, red or fleshy in colour. These are called amelanotic melanomas and tend to be more aggressive. Warning signs of malignant melanoma include change in the size, shape, colour or elevation of a mole. Other signs are the appearance of a new mole during adulthood or new pain, itching, ulceration or bleeding.

The rising incidence rates of NMSC and melanoma is probably due to a combination of increased exposure to UV light primarily from sunlight (Rigel, 2008) and from the recreational use of sunbeds, increased outdoor activities, changes in clothing style, increased longevity and ozone depletion (Bruce and Brodland, 2000).

1.8.1.1 Current therapies for skin cancer

Surgery is the most common approach with the Mohs micrographic surgery being the best treatment so far, but owing to the time and expenses involved with this procedure, it is indicated only in patients with aggressive tumours. In addition to the potential for disfigurement and the inherent risks associated with any surgical procedure (Martinez and Otley, 2001). Radiation therapy (external beam radiotherapy or brachytherapy) is also effective. However this treatment requires several sessions and is the most expensive. It is not considered for patients under 55 years because it predisposes the treated area to radiation-induced skin cancer and cosmesis can worsen over time (Neville *et al.*, 2007).

Further non-invasive options for NMSC include topical chemotherapeutics (imiquimod or 5-fluorouracil), cryotherapy (freezing the tumour off), biological immune response modifiers (e.g. imiquimod), retinoids and photodynamic therapy (PDT), using photosensitizing porphyrin 5-ALA or the methyl ester of ALA (mALA) together with a light source in the 450–750 nm wavelength range (Neville *et al.*, 2007).

Several regimens of chemotherapy have been clinically applied for the treatment of NMSC but have turned out to be insufficient at improving the prognosis (Cassileth and Chapman, 1996; McCann, 1997).

Treatments so far are tailored to tumour type, location, size and histological pattern but with increasing incidence of NMSC, there is a clear need to design new non-invasive treatments to target cancer cells more generally at all stages of tumourigenesis.

As mentioned previously, iron is essential for cell proliferation due to its important role in the active sites of a wide range of proteins involved in energy metabolism, respiration and DNA synthesis; and neoplastic cells, in particular, have a high iron requirement due to their rapid proliferation (Richardson and Baker, 1990; Richardson and Ponka, 1994; Le and Richardson, 2002). Moreover, in both animals and humans, primary neoplasms develop at body sites of excessive iron deposits such as skin, which is potentially the target of significant oxidative damage due to its constant exposure to high oxygen tensions, and frequent exposure to UV light. These observations, in addition to the critical roles of iron and iron proteins in cell proliferation, highlight the importance of iron chelation as a suitable therapeutic strategy for cancer treatment.

1.8.2 Psoriasis

Psoriasis is a well-recognised, chronic skin condition affecting approximately 3% of the population in the UK, commonly presenting before the age of 35 years. It is a chronic life-long condition which has significant effects on the patient's quality of life as well as detrimentally affecting their physical and emotional well-being. Several clinical phenotypes of psoriasis are recognised, of which chronic plaque psoriasis (*psoriasis vulgaris*) is the most common, presenting in approximately 90% of cases. The rest of phenotypes include chronic plaque psoriasis, guttate psoriasis, pustular psoriasis, flextural psoriasis, erythrodermic psoriasis (Myers *et al.*, 2006).

Chronic plaque psoriasis presents as slightly raised, reddish and well demarcated papulo-squamous lesions of varying dimensions, covered with silvery white scales. Peeling of the scales reveals characteristic pin-point bleeding in the underlying dermis. The lesions are usually distributed symmetrically over the body, especially presenting on the extensor aspects of elbows and knees, the scalp, genitals and soles and palms. Up to 15% of sufferers may develop a potentially destructive and disabling arthritis called psoriatic arthritis that can attack the joints, mainly the distal inter-phalangeal joints of the hands and feet.

Psoriasis is characterized by hyperproliferation of epidermal keratinocytes and hyperkeratosis (Champion, 1981; Stevenson and Zaki, 2002). The normal turnover of epidermis is between 3-4weeks and in psoriasis this is reduced to 2-5 weeks (Champion, 1981; Stevenson and Zaki, 2002). The hyperproliferation of epidermis in psoriatic lesion leads to thickening of the superficial layers of the skin.

Psoriasis is also known to involve lymphocytic infiltration that consists mainly of T lymphocytes (Stevenson and Zaki, 2002). Activation of T lymphocytes, migration of T lymphocytes to the skin, and T lymphocyte mediated production of cytokines such as interferon gamma, interleukin-2, and tumour necrosis factor alpha is important in the pathogenesis. Interferon gamma inhibits apoptosis of keratinocytes, interleukin-2 stimulates growth of T lymphocytes and tumour necrosis factor alpha increases proliferation of pro-inflammatory cytokines and adhesion molecules. The adhesion molecules further stimulate T lymphocytes to produce cytokines.

Angiogenic factors produced by epidermal keratinocytes may also play a role in causing abnormal dermal vascular proliferation and angiogenesis, with levels of VEGF (vascular
endothelial growth factor) being found to be significantly raised in psoriasis plaques**.**
This is therefore a potential area for future research to investigate the role of angiogenic factors further.

There is a great body of evidence indicating that oxidative stress and antioxidant imbalance could play a pivotal role in the pathogenesis of psoriasis (Briganti and Picardo, 2003; Wojas-Pelc and Marcinkiewicz, 2007). It has been shown that in psoriatic lesions ROS are generated by both keratinocytes and activated inflammatory cells (mostly neutrophiles) (Pelle *et al.*, 2005). Under such conditions the natural antioxidant defense system is overwhelmed by a prolonged production of ROS, and the resulting free radicals cause damage to proteins, lipids and DNA (Kohen, 1999). Furthermore, it has been reported that in

psoriatic skin there is a decreased level of natural antioxidants namely SOD, GPx and ascorbic acid (Trenam *et al.*, 1992).

Interestingly, elevated iron levels have been detected in psoriatic epidermis (Trenam *et al.*, 1992; Morris *et al.*, 1995) and dermis (Leveque *et al.*, 2004) that act almost certainly to exacerbate both proliferation and inflammatory sides of the disease.

Psoriasis is a relapsing remitting condition that can flare up at any time. Predisposing factors include the use of chloroquine, withdrawal of corticosteroid in a susceptible individual, emotional stress, alcohol or tobacco consumption, trauma (Köebner phenomenon), hypocalcaemia, and sunburn. Streptococcal infection can precipitate guttate psoriasis via a mechanism that involves activation of CD4+ T cells by a superantigen (Clark, 2004).

At present there is no satisfactory method to cure psoriasis. The common methods available at present to control this disease are topical therapies aided by natural sunlight or UVB in mild and moderate cases (Clark, 2004). In severe cases, the combination of photosensitizing drugs known as psoralens and UVA (PUVA) has been used, as well as systemic therapy. However since chronic plaque psoriasis is a lifelong condition, long-term therapy is indicated which limits the use of many of these therapies due to unacceptable side-effects.

Bath solutions and moisturizers, mineral oil, and petroleum jelly may help soothe affected skin and reduce the dryness which accompanies the build-up of skin on psoriatic plaques. Ointment and creams containing coal tar, dithranol (anthralin), corticosteroids like desoximetasone (Topicort), fluocinonide, vitamin D3 analogues, calcipotriol, and retinoids are routinely used. The mechanism of action of each is probably different but they all help to normalise skin cell production and reduce inflammation. Corticosteroids are most commonly prescribed agents due to their anti-inflammatory effects. However their accompanying adverse side effects such as skin thinning, iatrogenic Cushing's disease, etc, limit their use to short term only. Vitamin D analogues, Calcitriol (the active vitamin D metabolite) and its synthetic analogues Talcalcitriol and Calcipotriol, are thought to exert their effect by inhibiting KC proliferation and inducing terminal differentiation of psoriatic cell (Menter, 2009). They are used often in combination with corticosteroids as first line treatment for psoriasis. With a better long term safety profile they are much more amenable for maintenance therapy than the corticosteroids. Calcineurin inhibitors (Tacrolimus and

Pimecrolimus) are also used topically. However due to inefficient skin penetration, they are used only under occlusion or on thinner skin such as the face and genitals (Menter, 2009). Topical Retinoids such as Tazarotene are available for therapy of psoriasis, however they are only moderately effective (Menter, 2009) and cause local irritation and so are usually only used in combination with other topical therapy such as vitamin D analogues and topical corticosteroids. Tazarotenes potential for teratogenicity precludes its use in pregnancy.

Some topical agents are used in conjunction with other therapies, especially phototherapy. PUVA photo-chemotherapy which consists of ingested psoralen (P) photosensitiser and UVA light has been shown to facilitate clearance of psoriatic plaques (James *et al.,* 2006). PUVA is thought to modulate the expression of cellular adhesion molecules and induce T cell apoptosis (Clark, 2005). However its use is limited by its associated adverse gastro-intestinal side effects and headaches. It was also found to cause structural damage to DNA and can generate ROS such as $O_2^{\bullet-}$ that are clastogenic. This may contribute to the increased risk for developing SCC and melanoma in the skin of PUVA-treated patients (Bickers and Athar, 2006).

Psoriasis that is resistant to topical treatment and phototherapy is treated by systemic medications. Patients undergoing systemic treatment are required to have regular blood and liver function tests because of the toxicity of the medication. Methotrexate is the mainstay of systemic treatment for psoriasis at present. It is a folic acid antagonist and therefore works by inhibiting DNA synthesis and cell replication. Thus KC hyper-proliferation is halted. It also suppresses T-cell. However severe adverse effects of methotrexate including nephrotoxicity, bone marrow suppression and teratogenicity, limits its use long term (Clark, 2005). Cyclosporine is a calcineurin inhibitor inhibiting the synthesis and release of TH-1 and TH-2 type cytokines in T cells which play a pivotal role in the inflammatory response mechanism leading to the formation of psoriatic plaques. However as with methotrexate, severe nephrotoxicity associated with systemic cyclosporin therapy precludes its use long term, with the FDA administration recommending that cyclosporine should not be given for duration of longer than 1 year of continuous treatment (Clark, 2005). Oral Retinoids such as acitretin are vitamin A derivatives which bind to nuclear retinoid receptors altering gene transcription and returning keratinocyte proliferation and differentiation to normal. However its use is limited by its adverse effects on liver and kidney function and teratogenicity especially to women of child bearing age (Clark, 2005). One approach may be to use anti-proliferative agents either

systematically or topically but such drugs have extremely potent side-effects and their use must be strictly controlled.

In principle, RR could provide a suitable target to prevent proliferation, and topical use could minimize systemic exposure to potentially toxic molecules. Furthermore elevated iron levels have been detected in psoriatic skin that almost certainly act to exacerbate both proliferation and inflammatory side of the disease. As a result iron chelators that inhibit both RR and residual excess of iron in psoriatic skin should have great potential for the treatment of psoriasis.

1.9 Iron Chelation Therapy for Hyperproliferative Diseases

Iron chelators are ligating drugs that avidly bind iron depriving cells from essential nutrient iron (Kalinowski and Richardson, 2005). Selective iron chelators can play an important role in treating situations where a local increase in iron concentration causes an unfavourable pathology:

- For example elevated iron levels detected in psoriatic skin will almost certainly act to exacerbate both proliferation and inflammation. As a result, iron chelators that inhibit both RR and residual excess of iron in psoriatic skin should have great potential for its treatment (Singh *et al.*, 1995; Finch *et al.*, 2000; Chaston *et al.*, 2003). Systemic application of iron chelators such as ICRF-159 (razoxane) was found to be remarkably successful for the treatment of psoriasis. Unfortunately, prolonged exposure of patients to such chelators was associated with high incidence of epitheliomas and leukemia (Horton *et al.*, 1983; Horton *et al.*, 1984).
- The higher utilization of iron by cancer cells compared to their normal counterparts provides also a rationale for the selective anti-tumour activity of iron chelator molecules.

Because of the crucial role of iron in hyperproliferative diseases, 'iron chelation therapy' (ICT) which uses iron-trapping drugs (i.e. iron chelators) to reduce harmful levels of iron in cells, has been recognized as an attractive alternative to the existing drug-based approaches. Indeed iron chelators are powerful tools in the context of cancer and psoriasis, to prevent cell division by depleting essential nutrient iron and by inhibiting RR the key enzyme involved in DNA synthesis.

ICT should also have distinct advantages over conventional cancer chemotherapy as problems associated with resistance and unresponsive of cancer cells to such agents may be avoided (Whitnall *et al.*, 2006).

1.9.1 Iron chelators and cancer

The selectivity of the iron chelators in the context of cancer is based upon the fact that rapidly growing tumour cells have a higher iron requirement than normal cells (Le and Richardson, 2004). Therefore these agents theoretically have little effect on normal cells while inhibiting neoplastic cell growth. Numerous studies have demonstrated that tumour cells are responsive to iron deprivation by chelation treatment (Gao and Richardson, 2001; Becker *et al*., 2003).

Iron chelators consist of bi-dentate, tri-dentate or hexadentate ligands in which two, three, or six atoms respectively, bind with iron (Richardson and Kalinowski, 2005).

In addition to leukaemia and NB (Chaston *et al*., 2004; Chaston *et al*., 2003; Donfrancesco *et al*., 1990; Donfrancesco *et al*., 1995; Estrov *et al*., 1987) ICT has been shown to inhibit the growth and/or induce the apoptosis of malignant cell lines from patients with melanoma, hepatoma, Kaposi's sarcoma and cervical cancer (Hann *et al.*, 1990; Richardson *et al.*, 1994; Simonart *et al.*, 2000; Simonart *et al.*, 2002).

1.9.1.1 Desferrioxamine (DFO)

DFO **(Fig. 1.12)**, a hexadentate siderophore isolated from *Streptomyces pilosus*, is the current clinical chelator of choice for the treatment of iron overload diseases such as β-thalassemia (Kalinowski and Richardson, 2005).

Interestingly, various studies have shown that DFO possess anti-proliferative activity against a wide variety of tumour cells (Buss *et al.*, 2003; Kalinowski and Richardson, 2005; Pahl and Horwitz, 2005; Richardson, 2005) . Some examples are outlined below:

- Upon DFO treatment, NB cells displayed a 10-fold higher sensitivity to iron-depletion than normal bone-marrow cells (Becton and Bryles, 1988).
- An *in vitro* study found 90% cell death in two NB cell lines (CHP 126 and CHP 100) and minimal effects in non-NB cells treated with DFO (Blatt and Stitely, 1987). Importantly the anti-proliferative activity of DFO was found to be due to iron deprivation (Blatt and Stitely 1987).

- A clinical trial study showed a 50% decrease in bone-marrow infiltration in 7 out of 9 NB patients, while one patient experienced a 48% reduction in tumour size (Donfrancesco *et al*., 1990).
- Another trial with 57 NB patients treated with DFO in combination with a series of other anti-cancer agents, including cyclophosphamide, etoposide, carboplatin and thio-TEPA, resulted in complete responses in 24 patients, 26 partial responses, 3 minor responses and 4 showing no response (Donfrancesco *et al*., 1995).
- A case study of an infant patient with acute leukaemia (Estrov *et al*., 1987) showed no rise in peripheral blood blast cell numbers after DFO administration, while an increase in the growth of normal haematopoietic progenitor cells was observed (Estrov *et al.*, 1987).
- Animal studies demonstrated the efficacy of DFO at inhibiting the growth of tumours. For example, DFO inhibited or caused total regression of hepatocellular carcinoma xenografts (Hann *et al.*, 1992), it inhibited the growth of mammary carcinoma transplanted in Fischer rats (Wang *et al.*, 1999), and it prolonged the life of mice with L1210 leukemia (Yu *et al.*, 2006).
- In addition, there are much *in vitro* cell culture-based studies demonstrating that DFO can inhibit tumour cell growth (for reviews see Donfrancesco *et al.*, 1996; Richardson, 1997).

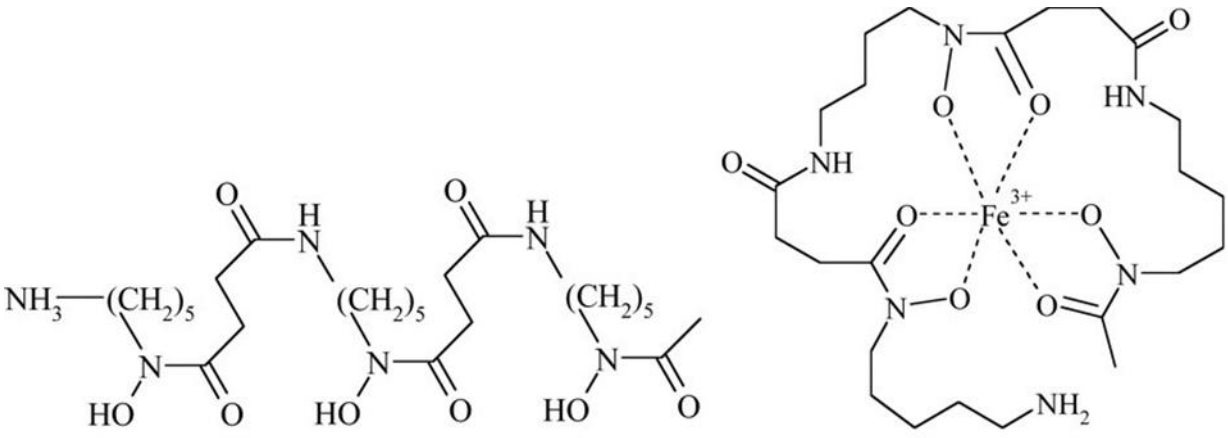

Figure 1.12: Chemical structures of free (DFO) and its complex with iron**.**

The anti-proliferative activity caused by iron depletion mediated by DFO is thought to be related to its effect on RR, the rate-limiting enzyme in the formation of deoxyribonucleotides for DNA synthesis. Nevertheless DFO has also a significant effect on cellular energy metabolism which was evident in a study done by Oexle and colleagues (Oexle *et al.*, 1999) in which DFO decreased the expression of mitochondrial aconitase, citrate synthase, isocitrate dehydrogenase, and succinate dehydrogenase (Oexle *et al.*, 1999). This resulted in decreased mitochondrial oxygen consumption and ATP formation via oxidative phosphorylation and an increase in glycolysis (Oexle *et al.*, 1999). Other targets of DFO include proteins involved in cell cycle control which are discussed in the Aroyl Hydrazone section **(section 1.9.1.3)**.

Despite the preclinical *in vivo* and *in vitro* studies, as well as clinical trials that gave evidence of the potential of DFO in cancer therapy; in other studies the anti-proliferative activity of DFO has not been so marked. For instance, DFO treatment failed to produce a response in 10 children with recurrent NB (Blatt, 1994). It also failed to inhibit the growth of human tumour xenografts in mice (Selig *et al.*, 1998). The lack of an effect of DFO in these studies is probably due to its short plasma half-life and its low efficiency at permeating biological membranes (Frazer *et al.*, 2005; Mims and Prchal, 2005; Dunn *et al.*, 2006). Such studies highlight the fact that DFO was never designed for cancer treatment but rather for the therapy of iron overload diseases. Moreover DFO is expensive to produce and not suitable for topical application, since it is hydrophilic in nature (the calculated n-Octanol-Water partition coefficient log P_{calc} = -0.14) and therefore suffers from poor plasma membrane permeability.

In cellular studies, it has been shown that DFO takes several hours to enter the cells via the slow process of endocytosis. Then it is transported into the lysosomal compartment where it remains intact (i.e. undegraded) and acts as a sink for iron, decreasing rapidly the cytosolic LIP (Lloyd *et al.*, 1991; Glickstein *et al.*, 2005; Kurz *et al.*, 2006; Kurz *et al.*, 2008). Furthermore prolonged exposure to DFO provokes severe iron starvation in cells, resulting in removal of essential iron from various sites including iron-containing enzymes leading to clinical complications (Porter and Huehns, 1989). At the cellular level, prolonged DFO treatment results in cell cycle arrest and cell death (Doulias *et al.*, 2003; Yu *et al.*, 2006).

As a result of DFO limitations, there is a great need to develop more effective iron chelators for cancer therapy.

1.9.1.2 Thiosemicarbazones

The thiosemicarbazone class of chelators were one of the first groups of ligands to be characterised for potent anti-tumour activity (Sartorelli and Booth, 1967; Sartorelli *et al.*, 1971; Antholine *et al.*, 1977; Agrawal and Sartorelli, 1978).

The best characterised member of this family of chelators is the 3-aminopyridine-2-carboxyaldehyde thiosemicarbazone (Triapine®, **Fig. 1.13**; Vion Pharmaceuticals Inc, New Haven, CT),

Triapine®; is a tridentate chelator that ligates iron via a sulfur and two nitrogen donor atoms. It is the one of the most potent RR inhibitors (Wadler *et al.*, 2004). Unlike the clinically used RR inhibitor, hydroxyurea, that inhibits R2 only, Triapine can equally inhibit both R2 and p53R2 (Shao *et al.*, 2004) preventing DNA repair and synthesis (Shao *et al.*, 2006) both *in vivo* and *in vitro* (Finch *et al.*, 2000; Chaston *et al.*, 2003; Shao *et al.*, 2006). Triapine exerts its antiproliferative activity mainly by forming a complex with iron. The Triapine-iron complex is redox active (Chaston *et al.*, 2003), and has been shown to be more active at inhibiting RR than free Triapine. Indeed Triapine forms a complex with Fe^{3+}, which is then reduced to Fe^{2+} that acts as a catalyst to form ROS. The generated ROS quench the RR tyrosyl radical and cause its inactivation (Shao *et al.*, 2006).

Over the last few years, Triapine® has been developed as an anti-cancer agent and is currently undergoing Phase I and II clinical trials (Gojo *et al.*, 2007; Knox *et al.*, 2007; Mackenzie *et al.*, 2007).

In a Phase I clinical trial conducted in 21 patients, a decrease in tumour markers associated with stable disease was observed in four patients (Wadler *et al.*, 2004) (**Table 1.4**). Triapine® administered at a dose of 120 mg/m^2/day once per fortnight was well-tolerated, but at 160 mg/m^2/day, 3 out of 6 patients suffered from toxic effects including anaemia, thrombocytopenia, leucopenia and met-haemoglobinemia (Wadler *et al.*, 2004). One trial reported that patients with deficiencies in glucose-6-phosphate dehydrogenase (G6PD) experienced severe met-haemoglobinemia and hemolysis after Triapine® treatment (Foltz *et al.*, 2006). Another Phase I clinical trial demonstrated that Triapine® administered by infusion had anti-leukaemia activity (Gojo *et al.*, 2007). Although no patients were observed to have complete or partial remission, 76% of patients were found to have a > 50% decrease in white blood cell counts (Gojo *et al.*, 2007).

A Triapine® dose of 96 mg/m^2 administered using daily 2 h infusions for 5 days every other week was found to be well-tolerated. However one patient developed met-

haemoglobinemia, diarrhoea, dyspnoea and hypoxia when triapine was administered at a dose of 85 mg/m^2 twice daily by the same schedule, (Gojo *et al.*, 2007).

A Phase II clinical trial of Triapine® in patients with metastatic renal cell carcinoma demonstrated that when patients were administered with 2 h infusions of 96 mg/m^2 Triapine® every 2 weeks, adverse effects were observed including fatigue, nausea and vomiting in 74%, 68% and 58% of patients, respectively (Knox *et al.*, 2007). Adverse events of greater severity, such as neutropenia, hypoxia, hypotension and met-haemoglobinaemia were also noted. Consequently, only 47% of patients received at least 90% of the planned Triapine® dose (Knox *et al.*, 2007). The study was early terminated due to a failure to meet minimal efficacy criteria (Knox *et al.*, 2007).

Another recent two-step Phase II clinical trial examined the anti-tumour activity of Triapine® in combination with gemcitabine in patients with advanced pancreatic adenocarcinoma (Mackenzie *et al.*, 2007). Patients were treated with Triapine® at 105 mg/m^2 over a 2 h infusion. Gemcitabine was subsequently administered 4 h after the Triapine® infusion at 1000 mg/m^2 and this treatment schedule was given on days 1, 8 and 15 of a 28-day cycle (Mackenzie *et al.*, 2007). Of the 25 patients assessed, 4 discontinued treatment due to adverse effects including myocardial infarction, hypertension, vomiting and hypoxia. While no objective responses were observed, 11 patients had stable disease. However, this two-stage trial was stopped after stage 1 due to the lack of anti-tumour activity (Mackenzie *et al.*, 2007).

Triapine® continues to be examined in clinical trials, particularly in combination with standard chemotherapy drugs. However, the deleterious effects associated with it must be considered when designing future studies with compounds of this class.

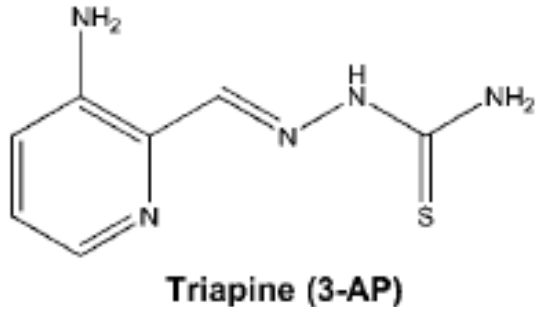

Triapine (3-AP)

Figure 1.13 Chemical structures of 3-aminopyridine-2- carboxaldehyde (3-AP or Triapine) (Yu *et al*., 2006).

Table 1.4 : Summary of clinical trials with DFO and Triapine (Yu *et al.*, 2006).

Treatment	No. of patients	Outcome	References
DFO	9 patients with NB	7 patients showed decrease in bone marrow infiltration; 1 patient showed a 50% reduction in tumour mass	Donfrancesco *et al.*, 1995
DFO	10 children with recurrent NB	No partial or complete responses, although decreased serum ferritin were noted in 4 patients	Blatt, 1994
DFO	14 patients with advanced hormone-refractory prostate cancer	13 patients had disease progression, although 9 had stable measurable or evaluable disease	Dreicer *et al.*, 1997
DFO Cyclophosphamide Etoposide Carboplatin Thiotepa (D-CECaT)	23 patients with advanced NB and 2 patients with PNET	In previously untreated patients, there were 15 complete responses and 2 partial responses. In patients who had a different drug regimen previously, there were 2 very good partial responses and 4 partial responses. Median survival for most patients was 22 mo	Donfrancesco *et al.*, 1995
D-CECaT	57 patients with advanced NB	Following four treatment courses, almost all patients underwent surgery. After surgery there were 24 complete responses, 26 partial responses, 3 minor responses and 4 with disease progression	Donfrancesco *et al.*, 1995
DFO IFN α (Roferon) Adriamycin Tamoxifen Ascorbic acid	7 patients with inoperable hepatocellular carcinoma	Compared with 5 untreated patients, the treated patients had a longer survival rate, increased tumour regression and less progressive disease	Kountouras *et al.*, 1995
DFO Doxorubicin or CHOP regimen Iron sorbitol citrate	9 patients with refractory malignant disease	Partial responses were observed in 2 of 4 patients with refractory non-Hodgkin's lymphoma	Voest *et al.*, 1993
Triapine	27 patients with advanced cancer	8 patients experienced stabilization of disease for 2-4 mo, the remaining patients experienced progression. No objective tumour responses were observed	Feun *et al.*, 2002
Triapine	24 patients with refractory leukemia	No patient had an objective response. Over 70% of patients had >50% reduction of WBC count	Giles *et al.*, 2003
Triapine	32 patients with different tumour types	No partial or complete responses were observed; 5 patients showed a positive antitumour effect, in which 2 achieved disease stabilization; 4 of the 5 patients had metastatic disease	Murren *et al.*, 2003
Triapine gemcitabine	26 patients with progressive metastatic or locally advanced cancer	3 patients had objective responses; 2 other patients achieved a partial response; another patient achieved tumour size reduction without meeting the criteria for a partial response	Yen *et al.*, 2004
Triapine	21 patients with advanced or metastatic cancer	No partial or complete responses of tumour size reduction were observed; 2 patients remained progression-free for 6 and 10 mo, whereas 4 others achieved stable disease for 3-4 mo	Wadler *et al.*, 2004
Triapine Cytarabine (ara-C)	31 patients with refractory acute leukemia and high-risk MDS	4 patients achieved a complete response after the first cycle of therapy	Yee *et al*,. 2006

1.9.1.3 Aroylhydrazones

Novel aroylhydrazone chelators such as pyridoxal isonicotinoyl hydrazone (PIH) and salicaldehyde isonicotinoyl hydrazone (SIH) have shown promise as effective iron chelators for cancer therapy (Richardson and Ponka, 1994; Richardson *et al.*, 1995) and skin photoprotection (Yiakouvaki *et al.*, 2006).

PIH and SIH **(Fig 1.14)** are tridentate iron chelators which binds iron octahedrally in a ligand/iron ratio of 2:1(Ponka *et al.*, 1979a) through the carbonyl oxygen, imine nitrogen, and phenolic oxygen (Kalinowski and Richardson, 2005). Both SIH and PIH have high affinity and selectivity for Fe^{3+} that is comparable to that of DFO (Richardson *et al.*, 1995). They also bind Fe^{2+} but with a lower affinity (Kalinowski and Richardson, 2005). The efficiency of both PIH and SIH in preventing iron uptake and mobilization is superior to DFO (Richardson *et al.*, 1995).

An acid dissociation constant study of PIH and SIH revealed that at physiological pH, the majority (~80%) of PIH and (~86%) of SIH are present in a neutral state, with a small proportion being found as a singly charged anionic species (Kalinowski and Richardson, 2005). These results, in combination with the lipophilicity of these ligands (Baker *et al.*, 1985) (Clog P= 0.69 for PIH and 2.04 for SIH), indicate that both iron chelators are able to readily permeate cell membranes and tissues (Ponka *et al.*, 1979b; Huang and Ponka, 1983; Richardson and Baker, 1990; Epsztejn *et al.*, 1997). The chelator SIH is sufficiently lipophilic to readily cross the cell membrane and even transport iron to the extracellular media (Yiakouvaki *et al.*, 2006).

Importantly the high lipophilicity of PIH and SIH make these iron chelators ideal candidates for topical therapy of iron-related hyperproliferative skin disorders, notably skin cancer and psoriasis. Furthermore these chelators have already shown promising protection against UVA-induced iron damage in skin (Yiakouvaki *et al.*, 2006), as they readily enter cells and firmly chelate the redox-active LIP and block the production of iron-catalysed ROS formation.

Indeed numerous studies with PIH and SIH used under conditions of limited exposure time have shown the protective effect of these compounds in a series of iron-related oxidative stress conditions and pathologies (Richardson *et al.*, 1995; Horackova *et al.*, 2000; Simunek

et al., 2005; Kurz *et al.*, 2006). However, prolonged exposure of cells to these strong iron chelators induces cell death due to severe iron starvation (Gao and Richardson, 2001; Buss *et al.*, 2004). This property of PIH, SIH and their derivatives has been exploited in iron chelation therapy of cancer (Yu *et al.*, 2006).

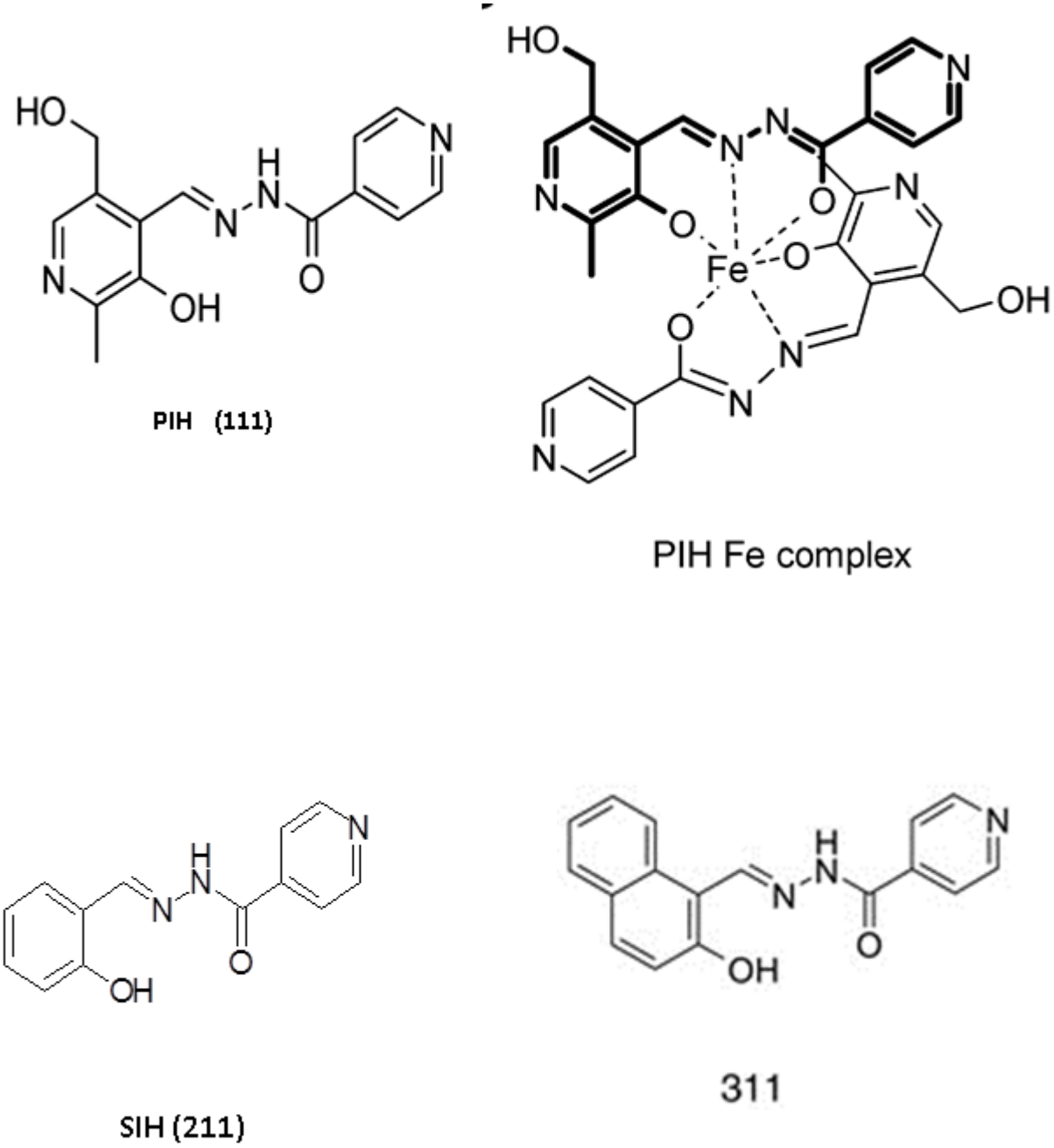

Figure 1.14: Chemical Structures of PIH, PIH-Fe Complex, SIH and 311.

Well before any of these aroylhydrazones were demonstrated to be highly efficient iron chelators in cellular or whole animal systems, Sah (Sah and Peoples, 1954) noted that PIH has distinct activity against mammary tumours and certain leukemias in mice.

In an *in vitro* study involving human melanoma, bladder, and lung epithelial carcinoma cell lines, Johnson and colleagues (Johnson 1982)demonstrated that both SIH and its derivative ligand 201 possess higher iron chelation-dependent anti-tumour activity than their corresponding 100 series analogs, PIH and 101 (Johnson *et al*., 1982). The study also demonstrated that the Cu^{2+} complexes of these ligands, in particular that of analog 201, contain higher anti-tumour activity than the chelators alone (Johnson *et al*., 1982).

Considering the high activity of PIH and its analogues and the ability of DFO to inhibit the proliferation of tumour cells, studies were initiated to determine the iron chelation efficacy of DFO, PIH, and 5 of their analogues in SK-N-MC NB cells (Richardson and Ponka, 1994) . This study demonstrated that PIH was more effective than DFO at mobilizing ^{59}Fe from the SK-N-MC NB cells and preventing ^{59}Fe uptake from Fe-Tf . However PIH was equally or far less effective than DFO at preventing [^{3}H]-thymidine incorporation. (Richardson and Ponka, 1994) .

Interestingly, 3 analogues of PIH, namely, pyridoxal benzoyl hydrazone (101), pyridoxal p-methoxybenzoyl hydrazone (107), and pyridoxal m-fluorobenzoyl hydrazone (109), had chelation activities comparable to PIH but were more effective than either DFO or PIH at inhibiting [^{3}H]-thymidine incorporation (Richardson and Ponka, 1994) . These results suggested that these iron chelators target different iron pools (Richardson and Ponka, 1994; Richardson *et al.*, 1995).
Considering the high activity of these latter analogues it was deemed worthwhile to investigate the effect of a wide range of the aroyl hydrazone class of chelators on the growth of NB cells *in vitro.*

Richardson and colleagues examined a range of PIH analogues with systematic substitutions to examine the structure–activity relationships of the aroylhydrazone ligands.
These chelators were synthesised from various acid hydrazides and three parent aromatic aldehydes, namely: pyridoxal, salicylaldehyde and 2-hydroxy-1-naphthylaldehyde and were termed the 100, 200 and 300 series, respectively (**Fig. 1.15)** (Richardson *et al.*, 1995;

Richardson and Milnes, 1997), (for IC 50 values see **Table 1.5**). The study demonstrated that out of 15 members of the 100 series examined, only 3 exhibited higher antiproliferative effects than DFO, and this highlights the suitability of the 100 series for the treatment of iron overload disease (Richardson *et al.*, 1995). The ligand (106) (p-tert-butyl-substituted), the most lipophilic derivative of the 100 series, demonstrated increased antiproliferative effect over other more hydrophilic members, such as the p-hydroxy substituted chelator (102) (Richardson *et al.*, 1995)The antiproliferative effect of these ligands was shown to be caused by their ability to bind iron as the addition of ferric ammonium citrate was found to prevent their cytotoxic effects (Richardson *et al*., 1995). Interestingly, the analysis of the relationship between the lipophilicity of the PIH analogs and their antitumour effects illustrated a weak linear relationship (Richardson *et al*., 1995; Johnson *et al*., 1982). The same study illustrated the increased cytotoxic effects of the (200) series in comparison to the (100) series of ligands (Richardson *et al*., 1995). Out of the (11) of (200) series analogs examined, SIH and (9) other derivative possessed higher antiproliferative activity than their 100 series counterparts (Richardson *et al*., 1995). This study also demonstrated a clear linear relationship between antiproliferative activity and the ability of the chelator to either prevent iron uptake from Tf or induce iron mobilization from pre-labeled cells (Richardson *et al*., 1995).

Another range of PIH analogs developed, namely the 300 series, showed even higher lipophilicity than that of the 100 and 200 series by incorporating a 2-hydroxy-1-naphthaldehyde group (Richardson *et al*., 1995). The analysis of the cytotoxic effects demonstrated that from all of the 100, 200, and 300 series of analogs, the latter group of chelators had the highest lipophilicity and greatest antiproliferative activity (Richardson *et al*., 1995). All members of the 300 series were found to have antiproliferative activity markedly higher than that DFO (**Table 1.5**) (Richardson *et al*., 1995). This study also highlighted the 2-hydroxy-1-naphthylaldehyde isonicotinoyl hydrazone, also known as 311 (**Fig. 1.14**) as one of the most active chelators (Richardson *et al.*, 1995; Richardson and Milnes, 1997).

Complexation of 311 with iron resulted in the inhibition of its cytotoxic effects, indicating that its antitumour activity relies on its ability to bind iron (Richardson and Bernhardt, 1999). The effects of 311 were also studied in CCRF-CEM, breast, bladder, and head and neck cancer cell lines, and the chelator again showed strong growth inhibitory effect (Green *et al*., 2001). Studies from the Richardson laboratory have also illustrated that 311 is

able to increase the RNA-binding activity of the IRPs far more effectively than DFO (Darnell and Richardson, 1999). This in turn results in a marked increase of TfR1 mRNA and protein levels (Chaston *et al*., 2003).

From the screening study described above (Richardson *et al.*, 1995), 5 of the most effective, PIH analogues: (206), (308), (309), (311) and (315), were examined further for their mechanism of action (Richardson and Milnes, 1997). These studies demonstrated that all these analogues were far more effective than DFO at inhibiting cellular proliferation and [^{3}H]thymidine, [^{3}H]leucine and [^{3}H]uridine incorporation and the marked inhibition of DNA, RNA, and protein synthesis (Richardson and Milnes, 1997)
Compared to other types of cytotoxic drugs, these PIH analogues also showed comparable activity to cisplatin, bleomycin, although they were less effective than doxorubicin (Richardson and Milnes, 1997).

In the above study on SK-N-MC NB cells, Richardson and colleagues clearly demonstrated that chelators that were derived from pyridoxal had high iron chelation activity but poor anti-proliferative effects, suggesting that these compounds may be more suitable as effective agents to treat iron overload disease (Richardson *et al.*, 1995; Richardson and Milnes, 1997). In contrast, the more lipophilic ligands derived from salicylaldehyde or 2-hydroxy-1-naphthylaldehyde that had both high iron chelation activity and marked antiproliferative efficacy may be more suitable for the treatment of cancer. These latter compounds also showed much greater iron chelation-dependent anti-tumour activity than DFO (Richardson *et al.*, 1995; Richardson and Milnes, 1997).

To better understand the effects of PIH analogs on molecular targets involved in proliferation, the effects of 311 on the expression of molecules necessary for cell cycle progression have also been assessed. Treatment of different cell lines with 311 has been shown to increase WAF1 and GADD45 mRNA expression, but not mdm2. The increase in GADD45 and WAF1 mRNA was seen only after a 20h exposure to the ligands and was reversible upon removal of the chelators and re-incubation with iron (Darnell and Richardson, 1999). These effects were observed not only in cells with native p53 but also in those that lack p53 expression. Interestingly, much higher levels of DFO were required to increase WAF1 and GADD45 mRNA levels (Darnell and Richardson 1999).

However, despite the marked increase in WAF1 mRNA after iron chelation with 311 (Darnell and Richardson, 1999; Gao and Richardson, 2001), the nuclear levels of its protein product, $p21^{CIP1/WAF1}$, were found to decrease (Le and Richardson, 2003; Liang and Richardson, 2003), illustrating the inhibition of its translation or its increased degradation after iron chelation. Incubation with ferric ammonium citrate was observed to reverse the effects of this chelator, indicating that $p21^{CIP1/WAF1}$ protein levels are dependent upon the intracellular iron concentration (Le and Richardson, 2003).

The mechanism by which 311 mediates its anti-proliferative activity was found to be related to the ability of the chelator to deplete iron pools required for the activity of RR and other processes (Green *et al.*, 2001; Chaston and Richardson, 2003). This resulted in a decrease in the RR tyrosyl radical, leading to enzyme inhibition and subsequent apoptotic cell death (Green *et al.*, 2001; Chaston and Richardson, 2003).

Apart from the activity of chelators at inhibiting RR, several studies have shown that their effect on the expression of molecules involved in cell cycle control could be a factor in their antitumour activity. For instance, DFO and 311 decreased levels of the cell cycle regulators cyclins D1, D2, and D3 (Gao and Richardson, 2001). Additionally, 311 reduced expression of CDK2 and the cyclins A and B1 (Gao and Richardson, 2001). Inhibition of expression of these molecules would be effective in inducing cell cycle arrest. This activity was not observed after incubation of cells with the iron complexes of DFO or 311, or the RR inhibitor hydroxyurea (Gao and Richardson, 2001).

Interestingly the level of cyclin E was found to increase after treatment with 311 or DFO, although the effect of 311 was more marked. The latter observation may reflect the cell-cycle dysregulation induced by chelators. Alternatively, the ligands may inhibit progression through G1 at approximately the G1/S transition, when cyclin E proteins are at their maximum and Cyclin D levels have fallen (Gao and Richardson, 2001).

Recently, a gene array study demonstrated that iron chelation up-regulated the expression of Ndrg-1, which has been characterised as a metastasis suppressor protein (Wadler *et al.*, 2004). Although the exact function of this gene remains unclear, it is thought that Ndrg-1 acts as a potent metastasis suppressor as the incubation of cells with 311 resulted in an increase in both mRNA and protein levels, a result not induced by incubation with the iron complex (Le and Richardson, 2004). Based on these observations, Richardson and

coworkers suggest that Ndrg1 may act as a novel link between the effect of iron chelation therapy by 311 and the inhibition of cellular proliferation (Le and Richardson, 2004).

Collectively, the above results clearly demonstrate the many molecular targets of iron chelators. These effects were absent upon treatment with the 311-Fe complex, indicating that changes induced by 311 were a direct result of the ability of 311 to chelate cellular iron (Gao and Richardson, 2001; Shao *et al.*, 2004) .

The significantly greater antitumour activity of 311 and the success of Triapine led to studies assessing the structure-activity relationships of several new series of aroylhydrazone/thiosemicarbazone hybrid ligands. These included the di-2-pyridylketone isonicotinoyl hydrazone series (Becker *et al.*, 2003), and the di-2-pyridylketonethiosemicarbazone series (Yuan *et al.*, 2004).

Table 1.5: the Effects of PIH Analogues on Cellular Proliferation of SK-N-MC NB Cells

	IC50 (μM)		
	Pyridoxal (100 series)	Isonicotinoyl (200 series)	2-Hydroxy -1-Naphthylaldehyde (300 series)
Benzoyl (1)	35	5	3
p- Hydrozybenzoyl (2)	>80	36	4
p- Methylbenzoyl (3)	28		
p- Nitrobenzoyl (4)	>80	49	
p- Aminobenzoyl (5)	>80	76	8
p- Butylbenzoyl (6)	7	1	
p- Methoxybenzoyl (7)	52	8	2
m-Chlorobenzoyl (8)	24	20	1
m-Fluorobenzoyl (9)	17	2	1
m-Bromobenzoyl (10)	41		2
Isonicotinoyl (11)	75	21	1
Acetyl (12)	>80	>80	7
2-Pyridyl(13)	7		
2-Furoyl (14)	>80		
2-Thiophenecarboxyl (15)	30	8	1
IC50 (μM)			
DFO	22		

The iron chelators were incubated with cells for 72h, at the end of this incubation period, cells density was determined by the MTT assay (Richardson *et al.*, 1995).

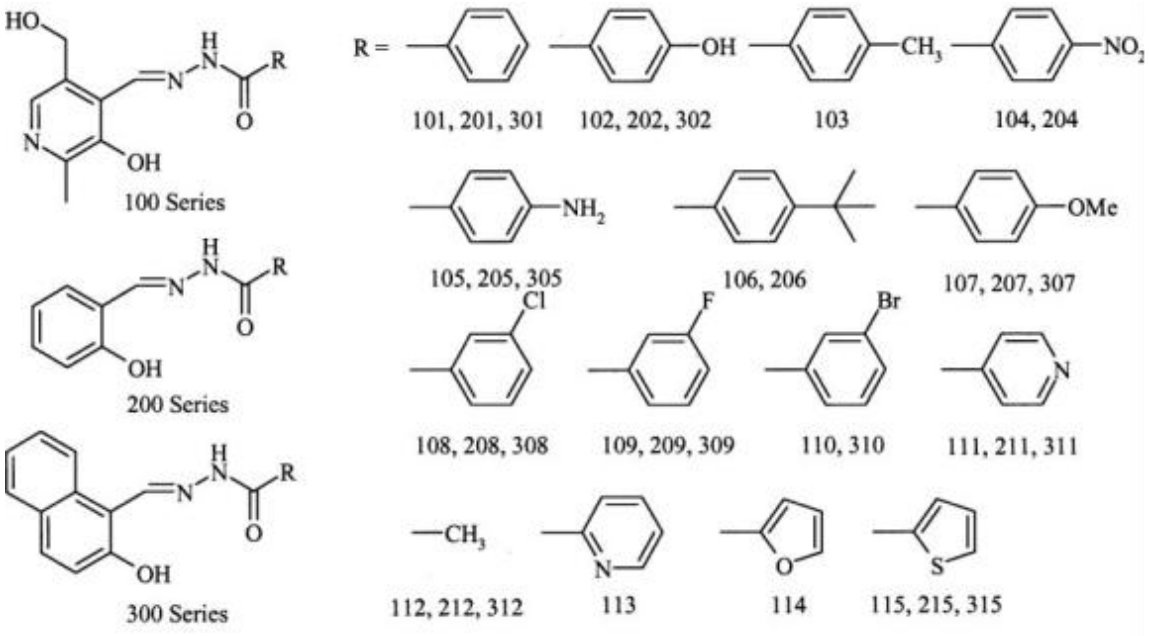

Figure 1.15: PIH analogs illustrating the 100, 200, 300 series backbone and their corresponding R groups as used by Richardson *et al.*, 1995.

1.9.1.4 Di-2-pyridylketone isonicotinoyl hydrazone analogs:

Following development of the PIH analogues, an additional range of aroylhydrazones known as the di-2-pyridylketone isonicotinoyl hydrazone (PKIH) series was synthesised **(Fig. 1.16)** (Bernhardt *et al.*, 2003). These iron chelators have been shown to readily cross the cell membrane due to their lipophilicity, and they predominately remain neutral at physiological pH (Bernhardt *et al.*, 2003). Studies on SK-N-MC cells demonstrated that all PKIH analogues, apart from di-2-pyridylketone 3-bromobenzoyl hydrazone (PK3BBH) were efficient in both increasing iron efflux from pre-labeled cells and preventing iron uptake from Tf (Becker *et al*., 2003). Of the chelators examined, PKIH, di-2-pyridylketone thiophenecarboxyl hydrazone, di-2-pyridylketone benzoyl hydrazone, and PK3BBH , were found to have the highest antiproliferative activity in SK-N-MC cells similar to that of 311 **(Table 1.6)** (Becker *et al*., 2003).

The Fe^{2+}-PKIH series complexes demonstrated anti-proliferative activity similar to that of the uncomplexed PKIH ligand, suggesting that they act through other mechanisms in addition to iron chelation (Becker *et al.*, 2003). Subsequent investigations demonstrated that the Fe^{2+}-PKIH complexes were redox-active leading to the hydroxylation of benzoate and the degradation of DNA in the presence of $Fe^{2+}$and H_2O_2 (Bernhardt *et al.*, 2003; Chaston *et al.*, 2003). Additionally, this series of ligands showed selectivity toward tumour cells as their activity against MRC-5 fibroblasts was much less pronounced (Becker *et al*., 2003).

PKIH analogs were found to decrease [^{3}H] thymidine, [^{3}H]leucine, and [^{3}H]uridine incorporation (Becker *et al*., 2003). They were also found to increase the expression of both GADD45 and WAF1 mRNA levels leading to G1/S arrest, to a higher extent than 311 (Becker *et al*., 2003). Investigations into the structure activity relationship of this series of ligands demonstrated no strong correlation between their log P values and their antiproliferative activity (Becker *et al*., 2003).

Table 1.6: The Effects of PKIH Analogues on Cellular Proliferation of SK-N-MC NB Cells (Becker *et al*., 2003).

Iron Chelators	IC50 (μM)
DFO	>50
311	3±2
PKIH	2±1
PKTH	3±1
PKBH	3±1
PKBBH	1±1
PKAH	42±9
PKHH	38±10

Cell density was determined by the MTT assay.

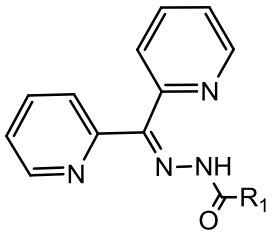

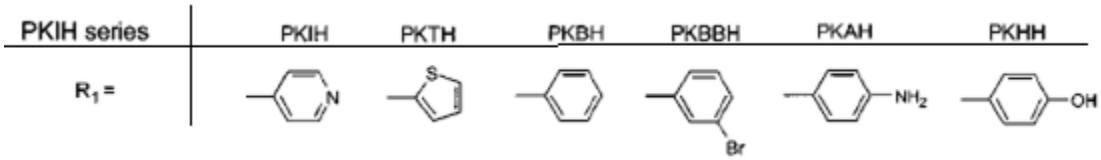

Figure 1.16: The Molecular Structure of PKIH analogs (Becker *et al.*, 2003).

1.9.1.5 Di-2-pyridylketone thiosemicarbazone (DpT) series

Structure–activity relationship studies of aroyl hadrazone led to the identification of a number of structural characteristics important for iron chelating efficacy and potent anti-proliferative activity and development of hybrid Iron chelators notably the di-2-pyridylketone thiosemicarbazone (DpT, **Fig 1.17**) series (Yuan *et al.*, 2004). These chelators are hybrids of the PKIH (Becker *et al.*, 2003) and 2-hydroxy-1-napthylaldehyde thiosemicarbazone series of ligands (Lovejoy and Richardson, 2002). The resulting ligands were assessed in terms of their antiproliferative activity both in *in vitro* and *in vivo* experiments against DFO, 311 and Triapine. The IC50 values for DpT analogues in SK-N-MC NB cells were between 0.03 and 0.06 µM compared to 5 µM ,0.3 µM and 0.26 µM for DFO, 311 and Triapine, respectively, **(Table 1.7)** (Yuan *et al.*, 2004) as analysed by the MTT assay 72 h after incubation with the compounds.

Similar results were also observed when the chelators were examined in SK-Mel-28 melanoma and MCF-7 breast cancer cells (Yuan *et al.*, 2004) . These iron chelators were far less efficient in inhibiting normal cells' proliferation (IC50 > 25 µM) **(Table 1.7).**

A further *in vivo* study was performed on Dp44mT to examine its ability to inhibit the growth of a cytotoxic drug-resistant lung carcinoma M109 cell line (Yuan *et al.*, 2004). After a treatment period of 5 days at a dose of 0.4 mg/kg, it was observed that Dp44mT could reduce tumour growth up to 47% of the control. In the same mouse model, Triapine® was found to be more effective at a much higher dose of 6 mg/kg, being able to reduce tumour size to 10% of the control (Yuan *et al.*, 2004). However, it was found that unlike Dp44mT, Triapine® significantly decreased animal weight, haemoglobin concentration, haematocrit, erythrocyte and leukocyte cell counts (Yuan *et al.*, 2004).

In a study by Whitnall and coworkers, the antiproliferative activity of Dp44mT was compared to that of Triapine® both *in vitro* and *in vivo* (Whitnall *et al.*, 2006). The anti-proliferative activity of both ligands was examined for both ligands across a range of 28 tumour cell lines. This study indicated that Dp44mT had a significantly higher antiproliferative effect than Triapine, and a much greater activity than DFO in the tested cell lines (Whitnall *et al*., 2006). Furthermore, in this study, Dp44mT could overcome resistance to other anti-tumour agents, by exerting its antiproliferative effect *via* a p53-independent mechanism. The latter highlighted the suitability of Dp44mT as a potential anti-cancer agent, as approximately 50% of tumours have a mutated p53.

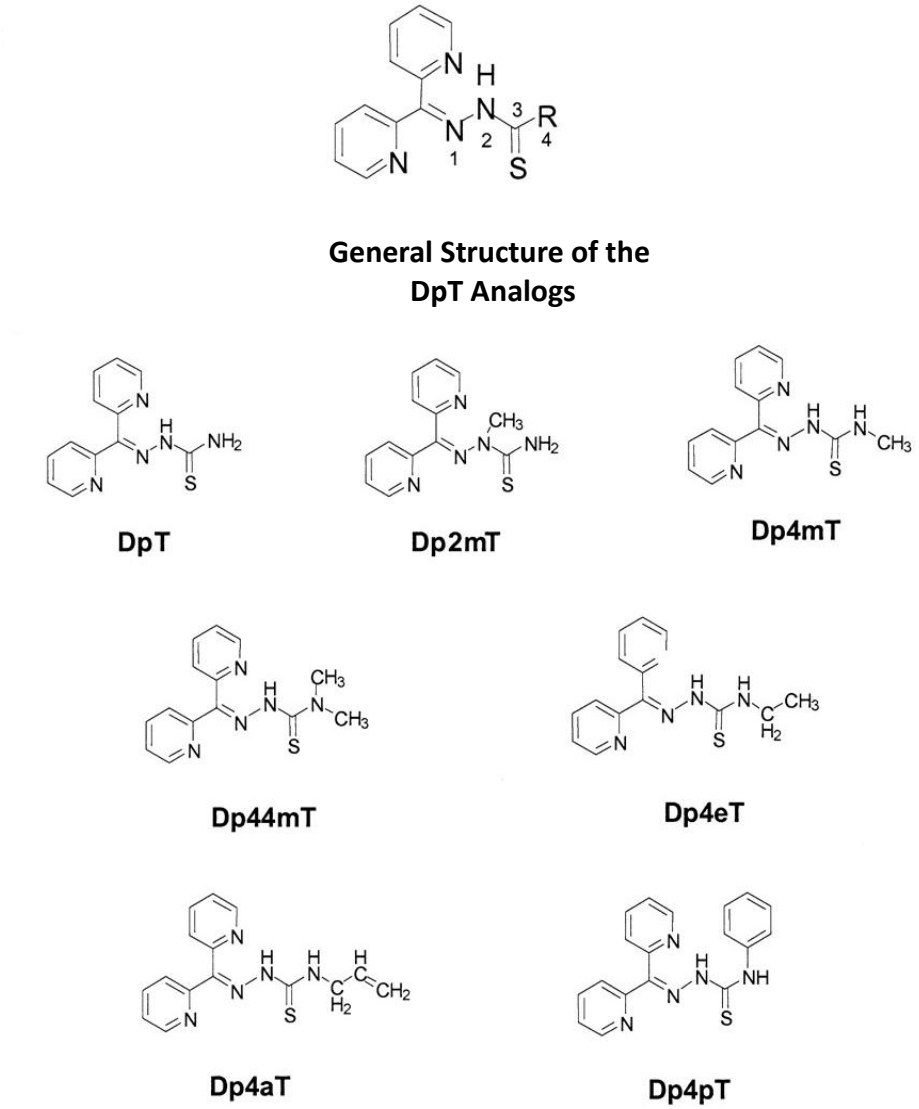

Figure 1.17: Molecular Structure of Dpt Analogs (Yuan *et al*., 2004).

In accordance with previous *in vivo* studies using a murine tumour (Yuan *et al*., 2004), Whitnall and coworkers demonstrated that Dp44mT can inhibit the growth of a variety of solid human tumour xenografts in nude mice (Whitnall *et al*., 2006). The results of this study confirmed the growth inhibitory efficacy of Dp44mT both in *in vitro* and *in vivo* models under short- and long-term treatment regimens. For example, under a short-term regimen (i.e. administration of Dp44mT for 14 days at a dose of 0.75 mg/kg), the tumour burden in treated mice was on average 5.6% of the control (Whitnall *et al*., 2006). However under long term regimen (i.e. 7 weeks of treatment at a dose of 0.4 mg/kg), the tumours of the treated mice were 92% smaller than those of the control group (Whitnall *et al.*, 2006).

Interestingly, this study showed that *in vivo* iron-depletion was not a major mechanism of the anti-tumour activity of this compound, since under the experiments' conditions, Dp44mT did not lead to iron-depletion within the tumour (Whitnall *et al*., 2006) nor in the whole body (Whitnall *et al*., 2006). It was suggested that the redox activity of the Dp44mT-Fe complex (Yuan *et al*., 2004; Richardson *et al*., 2006) played a significant role in its anti-cancer effects. At high non-optimal doses, Dp44mT was shown to result in post-necrotic cardiac fibrosis (Whitnall *et al*., 2006).

Studies on the mechanism of action of the DpT series and Dp44mT in particular, revealed that the antiproliferative effect of Dp44mT was mediated by its activity against multiple molecular targets, which is a desirable characteristic of potential anti-cancer therapeutics (Lilenbaum *et al*., 1999). The effect of this series was also due to their ability to gain access and bind intracellular iron, forming redox-active complexes which are able to generate ROS. Hence, the DpT series of chelators act *via* a "double punch" mechanism, depleting cellular iron and forming redox-active iron complexes (Richardson *et al.*, 2006).

Interestingly Dp44mT and other iron chelators, including 311 and DFO markedly up-regulate the expression of the metastasis suppressor gene N-myc downstream regulated gene-1 (Ndrg1) in tumour cells *in vitro* (Wadler *et al*., 2004) and *in vivo* (Whitnall *et al*., 2006).
Increased Ndrg1 expression was correlated to chelator antiproliferative activity and was reversed by iron repletion (Wadler *et al*., 2004). These results on the effect of iron chelator on Ndrg1 suggest another link between iron metabolism and proliferation and points to a novel mode of anticancer activity.

Table 1.7: The Effects of Dpt Analogues on cellular proliferation of cancer cells

	Neoplastic cells			Normal cells
	SK-N-MC neuroblastoma	**SK-Mel-28 melanoma**	**MCF-7 breast cancer**	**MRC-5 fibroblasts**
DFO	5 ± 2	15 ± 7	14 ± 9	> 25
311	0.3 ± 0.2	0.9 ± 0.5	—	> 25
Triapine	0.26 ± 0.01	2.6 ± 0.6	3.0 ± 1.5	—
Dp2mT	> 25	> 25	> 25	> 25
Dp4mT	0.19 ± 0.1	0.6 ± 0.5	0.3 ± 0.2	> 25
Dp44mT	0.03 ± 0.01	0.06 ± 0.03	0.06 ± 0.01	> 25
Dp4eT	0.06 ± 0.01	0.09 ± 0.06	0.08 ± 0.01	> 25
Dp4aT	0.06 ± 0.01	0.10 ± 0.06	0.07 ± 0.01	> 25
Dp4pT	0.05 ± 0.006	0.09 ± 0.05	0.07 ± 0.01	> 25
Doxorubicin	0.02 ± 0.01	0.35 ± 0.09	0.6 ± 0.2	—

The Chelators were incubated with cells for 72h, at the end of this incubation period, cells density was determined by the MTT assay (Yuan *et al*., 2004).

1.9.1.6 Tachypyridine

N,*N*′,*N*″-tris(2-pyridylmethyl)-*cis*,*cis*-1,3,5-triaminocyclohexane (tachpyridine or tachpyr, **Fig. 1.18**) is a hexadentate chelator with higher antiproliferative activity than DFO (Torti *et al*., 1998). A study by Torti and co workers have demostrated that tachpyridine inhibits Ft synthesis and the proliferation of bladder cancer cells in culture with an IC_{50} of 4.6 μmol/L compared with 70 μmol/L for DFO (Torti *et al*., 1998). Toxicity studies with tachypyridine complexes suggest that iron depletion mediates its cytotoxic effects (Torti *et al*., 1998).

Similar to Triapine and Dp44mT, tachpyridine induces apoptotic cell death via a p53-independent pathway (Abeysinghe *et al*., 2001; Greene *et al*., 2002). Additionally, tachpyridine-induced death was prevented in cells microinjected with Bcl-X_L and a dominant-negative caspase-9 expression vector, suggesting the involvement of the mitochondrial apoptotic pathway (Greene *et al*., 2002). Furthermore, tachpyridine-Fe complexes produce $OH^{\cdot}$ or hypervalent Fe through the Haber-Weiss reaction, which contributes to its anti-tumour activity (Samuni *et al*., 2002). Interestingly, unlike most iron chelators that arrest cells at the G1-S interface due to RR inhibition, tachpyridine arrests cells at G_2, which is a radiosensitive phase of the cell cycle (Turner *et al*., 2005). In fact, radiation increased the sensitivity of tumour cells to the action of tachpyridine (Turner *et al*., 2005).
Tachpyridine binds iron, but it can also bind Cu^{+2} and Zn^{+2}, which may underlie its ability to arrest cells in G_2 (Torti *et al*., 1998).
Currently, tachpyridine is in preclinical development with the National Cancer Institute (Turner *et al*., 2005), and evaluation of tachpyridine derivatives, such as trenpyr, are under way (Torti *et al*., 2005).

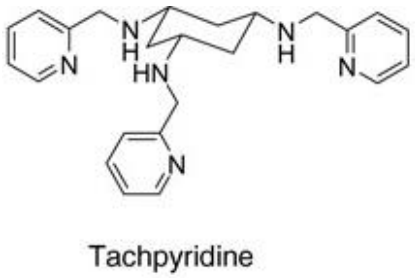

Tachpyridine

Figure 1.18: Molecular Structure of Tachypyridine (Torti *et al*., 1998).

1.10 Caged Iron Chelators

The extensive *in vitro* and *in vivo* studies provided in this section clearly demonstrate the enormous anti-tumour potential of ICT, but a new approach is required that will avoid problems of toxicity that accompany the prolonged and repeated exposure of a patient to "classical" iron chelators. Ideally, smart chelating agents are required that possess appropriate physicochemical properties for effective cellular uptake, and that may be selectively activated *in situ* within tumours. One way to achieve such *in situ* activation is to apply caged iron chelators (CICs) that are ordinarily inactive as chelators, but which upon exposure to a physiologically relevant light source (e.g.UVA, 320-400 nm), are converted to the free iron-binding molecule in a highly spatially selective and dose-controlled fashion. Such a strategy most readily lends itself to topical administration of CICs, which is ideally suited to the challenge of treating external lesions as in NMSC. Indeed, although the promise of antitumour ICT is widely recognised, the potential of iron chelators in skin cancer has yet to be properly explored. The use of light-activated CICs for treatment of NMSC would allow for specific localised release of a given therapeutic chelator within the targeted tissue, while substantially decreasing the need for systemic repeated exposure of the patient to strong ICs and their obvious toxic side effects. Topical CICs therapy might also provide a powerfull alternative for treatment of other iron-related hyperproliferatve skin disorders such as psoriasis.

Pourzand and colleagues from our laboratory have recently developed two prototype photo-activatable and photo-controlled 'caged' iron chelators derived from SIH and PIH **(see Fig. 1.19).** The caging group blocks the critical iron-binding function of the iron chelators PIH and SIH. Initial proof of concept of this approach was delivered with the 2-nitrophenyl ethyl (2-NPE) caging group for the purpose of skin photoprotection (Yiakouvaki *et al.*, 2006). In these studies the prototypes were examined for (i) uncaging by broad spectrum UVA radiation at a physiologically relevant dose; (ii) iron chelation by caged and uncaged products *in vitro*; (iii) modulation of the intracellular labile iron concentration prior to, and following UVA irradiation of a human skin fibroblast cell line, FEK4; (iv) protection of skin cells from oxidative damage following radiation treatment. These initial testings revealed that exposure to UVA light (320-400 nm) cleaves the caging function to generate the parent chelator and an inactive fragment **(Fig. 1.19)**. Furthermore, unlike the parent compounds, the caged chelators 2NPE-SIH and 2NPE-PIH did not diminish the normal labile iron pool in cells. However, exposure to a physiologically relevant UVA dose subsequently provided promising levels of

protection of skin fibroblast cells against UVA-mediated oxidative damage and necrotic cell death in monolayer cultures (Yiakouvaki *et al.*, 2006). Highly localised topical application of light-activated caged-iron chelators could not only be beneficial for skin photoprotection but could also provide a powerful alternative therapeutic strategy for hyperproliferative skin disease states in which elevated iron levels are implicated such as psoriasis and NMSC (Yu *et al.*, 2006).

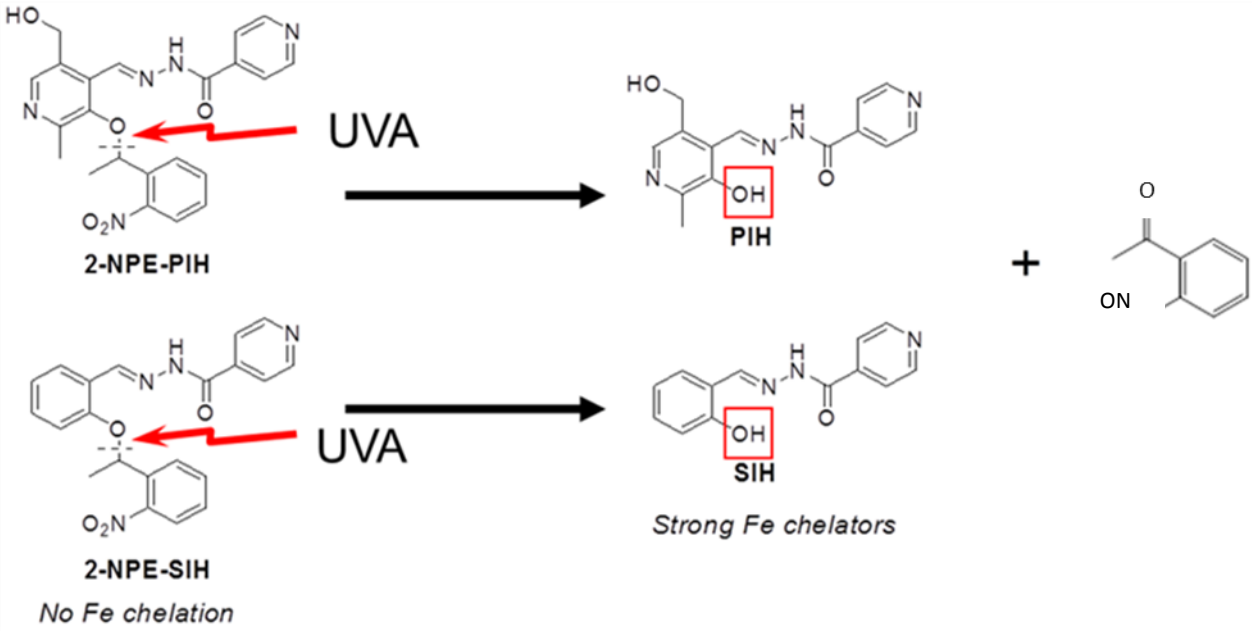

Figure 1.19: Prototype phoactivatable CICs. Reproduced with the permission of Dr Ian Eggleston.

1.11 Aims and objectives of the study

The purpose of this study was to evaluate the growth inhibitory potential of iron chelators SIH, PIH and their caged-derivatives (+/- UVA) in monolayer cultures of normal, psoriatic and skin cancer cells (SCC) isolated from the patients. The primary objective was to provide evidence for the efficient and selective antiproliferative activity of the caged-chelators as powerful alternatives to existing therapies against skin hyperproliferative disorders notably NMSC and psoriasis.

The project workplan was split into 4 periods:

(1) Synthesis and *in vitro* characterisation of PIH, SIH and their caged derivatives 2NPE-PIH and 2NPE-SIH. Synthesised compounds were fully characterised by NMR, MS, and dark stability in PBS buffer, pH 7.4, assessed by RP-HPLC. Kinetics of uncaging upon UVA irradiation was assessed by HPLC, and quantum efficiency of release determined.

(2) Evaluation of the rate of proliferation of skin cell models and elucidation of the role of intracellular LIP in cell proliferation. The growth rate of cells was evaluated by cell counting assay and light microscopy. The intracellular LIP was evaluated by Calcein-fluorescent assay.

(3) Comparison of the antiproliferative activity of 'classical' PIH/SIH in normal, psoriatic and cancer-derived SCC cell lines: Cell growth retardation/inhibition of the chelators was evaluated by MTT and then the effect of those compounds was further examined by BrdU assay (i.e. to monitor the rate of DNA synthesis) and Annexin V/PI assay (i.e. to monitor cell death). The antiproliferative/antitumour activity of the chelators was then confirmed with colony-forming ability assay.

(4) Comparison of the antiproliferative activity of caged iron chelators in absence or presence of UVA. The caged chelators were either uncaged *in vitro* or *in situ* (inside the cells) with UVA. Their antiproliferative activity was then evaluated using MTT assay.

CHAPTER TWO

MATERIALS AND METHODS

2.1 Chemicals and Reagents

Cell culture materials were obtained from Gibco (Germany) except for Foetal Calf Serum (FCS) that was purchased from PAA Laboratories (Austria). All chemicals were from Sigma-Aldrich Chemical (Poole, UK) unless otherwise indicated. Annexin-V-FLUOS and Bovine Serum Albumin (BSA) were supplied from Roche (Mannheim, Germany). CA-AM (Calcein-acetoxymethyl ester) was purchased from Molecular Probes (Leiden, Netherlands). Desferrioxamine mesylate Ph. Eur. (Desferal, DFO) was purchased from Ciba-Geigy laboratories (Basel, Switzerland). MilliQ water used to prepare phosphate buffered saline (PBS) and other stock solutions were issued from a Millipore purification system (MilliQ cartridge: Millipore, Bedford, MA) in order to minimize the presence of trace elements such as transition metals.

2.2. Cell culture

All the cell lines outlined below were cultured routinely and incubated in a humidified atmosphere at 37^{o}C with 5% $CO_{2.}$

2.2.1 FEK4

FEK4 cells are human primary forskin fibroblasts (a kind gift from Prof R. M. Tyrrell). The FEK4 fibroblasts are passage-dependent and in this project were used between passages 11 to16.

The growth medium was composed of 15% FCS (heat-inactivated at 56^{o}C for 45 min before use)-EMEM (Earle's modified minimum essential medium) supplemented with 0.25% sodium bicarbonate, 2 mM L-glutamine and 50 IU/ml of each of penicillin/ streptomycin (P/S).

The stock FEK4 cells were passaged by trypsinisation once a week and then seeded in tissue culture plates for experiments as detailed below:

- For MTT and clonogenic assays, 2 x 10^4 cells were seeded per 3 cm plate in 3ml media.
- For flow cytometry, LIP and BrdU assays, 12 x 10^4 cells were seeded per 10 cm plate in 12 ml media.

2.2.2 HaCaT

Human spontaneously immortalised skin keratinocyte (KC) cell line (a kind gift from Prof R. M. Tyrrell). This cell line maintains full epidermal differentiation capacity, but remains non-tumourigenic (Boukamp *et al.,* 1988) .

The growth medium was 10% FCS-DMEM (high-glucose Dulbecco's modified eagles medium) containing 50 IU/ml P/S.

Cells were passaged once a week and seeded for experiments as follows:

- For MTT and clonogenic assays, 2 x 10^4 cells were seeded per 3 cm plate in 3 ml media.
- For flow cytometry, LIP and BrdU assays, 8 x 10^4 cells were seeded per 10 cm plate in 12 ml of media..

2.2.3 Swiss 3T3

The Swiss 3T3 are spontaneously immortalized mouse embryonic fibroblasts (a kind gift from Prof I. Leigh, Dundee). This cell line is used as a feeder layer for the cultivation of keratinocytes (Proby *et al.*, 2000). The 3T3 cells secrete both extracellular matrix proteins that aid KC attachment, and growth factors that stimulate proliferation.

3T3 Feeder layer preparation: Cells were first grown in 10% FCS DMEM containing 50 IU/ml P/S. When the cells reached 80% confluency, mitomycin C (stock 0.2 g/ml in PBS) was added to cultured media at 4 µg/mL final concentration, and incubated for 2 h at 37^0C. Mitomycin C is a DNA cross-linker that inhibits DNA replication in 3T3 cells to avoid their overgrowth when used with keratinocytes (KCs). After incubation, medium was aspirated and cells were washed thoroughly (three times) with warm PBS to ensure that no mitomycin C remained to inhibit the growth of the keratinocytes. The mitomycin-treated 3T3 fibroblasts were then trypsinised and resuspended in RM+ media (see below). This fibroblast cell suspension was then used as a feeder layer for matrix-dependent KC cultures (i.e. KCP7, KCP8, PM1, Met2 and MKPS cells) .

2.2.4 KCP7 and KCP8

The KCP7 and KCP8 are human primary skin KCs derived from infant foreskin (Zhong *et al.*, 2004).

Cells were grown in a rich medium called RM+ (i.e. DMEM and Ham's F12 medium in a ratio of 3:1 (v/v) supplemented with 10% FCS, hydrocortisone (0.4 µg/ml), cholera toxin (10^{-10} M), epidermal growth factor (10 ng/ml), insulin(5 µg/ml), transferrin (5 µg/ml), liothyronine (2×10^{-11} M), 0.25% sodium bicarbonate, 2 mM L-glutamine and 50 IU/ml of each of penicillin/ streptomycin (P/S).

These primary KC cells were seeded at a density of 1×10^5 cells per 3 cm plate in the presence of 3T3 feeder layer seeded at a density of 4×10^5 cells per 3 cm plate. The primary KCs were used at passage 3.

2.2.5 PM1 and Met 2

PM1 is an epidermal KC cell line, clonally derived from forehead skin showing dysplasia.

Met2 is a Squamous Cell Carcinoma (SCC) KC cell line, clonally derived from a local recurrence of invasive SCC.

PM1 and Met 2 are isogenic cell lines isolated from the same patient. (a kind gift from Prof Irene Leigh, Dundee, see Popp *et al.*, 2000; Proby *et al.*, 2000).

- For the MTT assay, 5×10^4 cells were seeded per 3 cm plates containing 3ml of RM+ media.
- For BrdU and LIP assays, 25×10^4 cells were seeded per 10 cm plates containing 12 ml of RM+ media.

2.2.6 MKPS

MKPS is an immortalised KC cell line derived from the skin of a male patient with chronic plaque psoriasis. (a kind gift from Prof Irene Leigh, Dundee).

MKPS cells stock was grown in RM+ media in the presence of 3T3 feeder layer.

For the MTT assay, the MKPS cells were seeded in RM+ media without 3T3 in 3 cm dishes at a density of 5×10^4 cells/ plate in 5 ml of media.

For BrdU and LIP assays, MKPS cells were seeded in 10 cm plates containing 15ml of RM+ media at a density of 25×10^4 cells per plate.

2.3 Chemical treatments

The compounds were added to media of cells grown for 2 or 3 days (i.e. conditioned media, CM) at the required final concentrations. The cells were incubated with the compounds for 24-72 h, depending on the experimental requirement.

2.3.1. Stock solutions:

DFO (MW 657): The DFO stock solution was prepared at the final concentration of 150 mM in H_2O. Aliquots were kept at -20^oC until required.

BIH (MW 225): The BIH stock solution was prepared at the final concentration of 100 mM in dimethyl sulphoxide (DMSO). Aliquots were kept at -20^oC until required.

PIH (MW 286): PIH powder was first dissolved in 1N HCl at the final concentration of 500 mM and then further diluted in PBS to obtain a 25 mM stock solution. Because of the tendency of the stock solution to precipitate over time, for experiments involving PIH treatment, the stock solution was prepared freshly on the day of treatments.

SIH (MW 241): The SIH stock solution was prepared at the final concentration of 100 mM or 200 mM in DMSO, depending on the experimental condition.

2NPE PIH (MW 435) and 2NPE SIH (MW 390): The stock solutions were prepared at the final concentrations of 4, 100, or 200 mM in DMSO, depending on the experimental requirement.

To avoid the toxicity of DMSO in cell treatments with stock solutions made in DMSO (i.e. BIH, SIH, 2NPE-PIH and 2NPE-SIH), for cell treatments, the DMSO's final concentration in CM was kept to less than 01%.

2.4 Iron saturation assay

The Fe^{3+} complexes of the chelators were prepared by adding Fe^{3+} (as $FeCl_3$) to the ligands in a 1:1 ligand:metal ratio for the hexadentate chelators (*i.e.*, DFO) and in a 2:1 ligand:metal ratio for the tridentate chelators (*i.e.*, PIH, SIH, UVA irradiated 2NPE-PIH and -SIH). The solutions were then mixed thoroughly and incubated for 1h at 37°C prior to addition to cell culture media. Cells were incubated with the iron-complexed chelator for 72 h at a concentration equivalent to their IC50 for relevant ligands. Then the MTT assay was performed as described in section **2.9**.

2.5. UVA irradiation

2.5.1 Irradiation of cells in plates

Prior to irradiation, the CM medium was removed from the plates, and the cells were washed thoroughly with PBS. Cells were then covered with PBS (i.e. 2 ml for 3 cm plate). This was followed by irradiation of cells at doses of 50, 100 and 250 kJ/m^2.

The UVA doses were measured using an IL1700 radiometer (International Light, Newbury, MA). All irradiations were performed with a broad-spectrum Sellas 4kW UVA lamp (Sellas, Germany). This lamp emits primarily UVA radiation (significant emission in the range of 350–400 nm) and some near-visible radiation longer than 400 nm. The incident dose rate was $150W/m^2$. The spectrum of the lamp is shown in **Fig 2.1**.

Irradiation was carried out in an air-conditioned room at 18^oC in order to maintain the temperature of the cells to approximately 25^0C throughout the irradiation procedure**.**

The PBS was then removed, and cells were incubated in CM with or without the compound for the appropriate incubation time (e. g. 4 h to 72 h) at 37^oC.

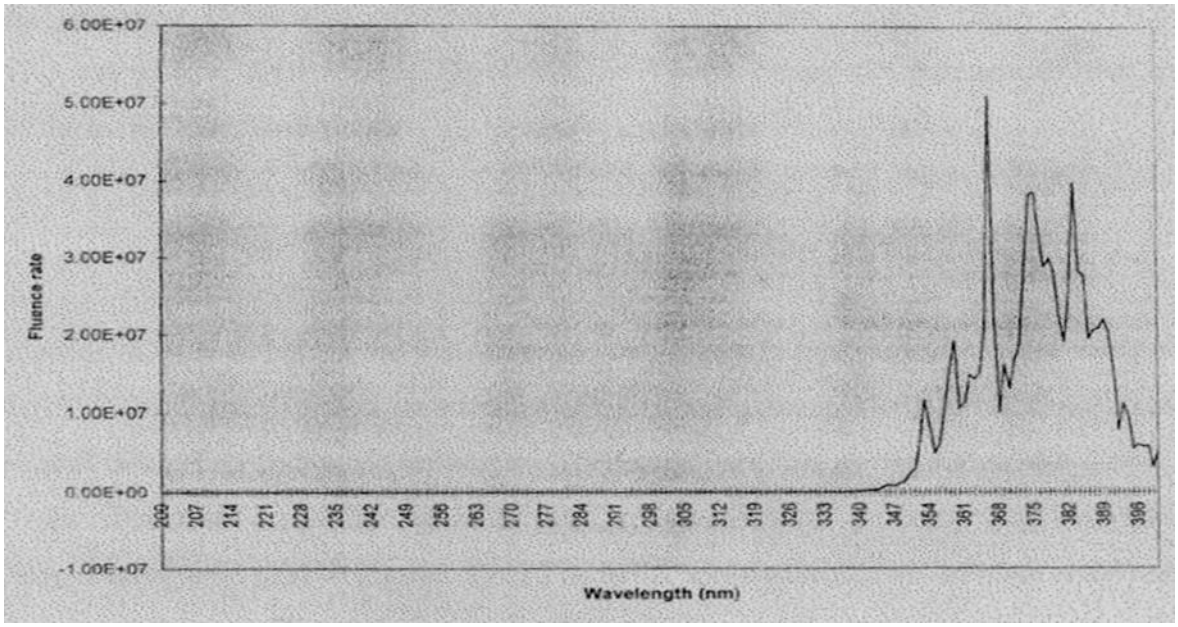

Figure 2.1.: Spectrum of the Sellas 4kW UVA lamp.

2.5.2 Irradiation of 2-NPE-PIH and 2-NPE-SIH

For cell culture treatments, 2-NPE-PIH and 2-NPE-SIH stock solutions were prepared in DMSO at final concentrations of 100 mM or 200 mM, depending on the experimental requirement and then irradiated at in quartz cuvettes at a UVA dose 250 kJ/m^2. The cells were then treated with the UVA-irradiated (uncaged) compounds for 24-72 h.

To generate the uncaged profile for 2-NPE-PIH and 2-NPE-SIH by reverse phase HPLC, 2NPE-PIH and 2NPE-SIH were prepared in DMSO at a final concentration of 1 mg/ml and then irradiated in quartz cuvettes with increasing UVA doses of 5, 10, 20, 50, 100, 250 and 500 kJ/m^2.

2.6 Reverse Phase HPLC analysis of 2NPE-PIH and 2NPE-SIH following *in vitro* uncaging with UVA irradiation

HPLC profiles of 2NPE-PIH and 2NPE-SIH and SIH were monitored at 280nm, 1h following UVA irradiation.

HPLC: Dionex UltiMate 3000 HPLC system was equipped with a Phenomenex Gemini 5 µm C-18 (150 x 4.6 mm) column with a flow rate of 1 ml/min.

Mobile phase A was MeCN (Acetonitrile) containing 0.1% TFA (Trifluoroacetic acid), B H_2O containing 0.1% TFA using a HPLC gradient of 5% A to 60% A over a period of 10 min.

2.7 Cell Growth Curve

FEK4 and HaCaT cells were seeded in 3cm plates containing 3ml media at a density of 2×10^4. Over a period of 7 days cells were trypsinised and counted on a hemocytometer every 24 h in triplicate.

The mean cell counts at each time point were then used to plot the growth curve, based on which the cells' doubling time was calculated.

2.8. BrdU assay

2.8.1 Principle of the assay

During cell proliferation the DNA has to be replicated before the cell is divided into two daughter cells. This close association between DNA synthesis and cell doubling makes the measurement of DNA synthesis very attractive for assessing cell proliferation. If labelled DNA precursors are added to the cell culture, cells that are about to divide incorporate the labelled nucleotide into their DNA.

The thymidine analogue 5-bromo-2'-deoxy-uridine (BrdU) is a synthetic nucleotide that can be incorporated into the newly synthesized DNA of replicating cells (during the S phase of the cell cycle), by substituting for thymidine during DNA replication.

Antibodies specific for BrdU can then be used to detect the incorporated chemical, thus indicating cells that were actively replicating their DNA. Binding of the antibody requires the denaturation of the DNA by exposing the cells to acid. FITC-conjugated second antibodies will then allow the detection of the "newly synthesized" DNA that will fluoresce green. The denatured DNA can be stained with propidium iodide (PI) and will fluoresce red.

2.8.2 BrdU Pulsing

To pulse cells, 10 µM BrdU was added to cells for 1 h at 37^{o}C. For the negative control no BrdU was added. After incubation, cells were washed with PBS, then harvested with 0.25% (w/v %) trypsin, and collected in the CM and kept on ice. Cells were then centrifuged at 1000 rpm (120 *x g)* for 8 min in a Falcon 6/300 MSE centrifuge pre-cooled to 4^{o}C. Medium was then removed. To permeabilise the cells, 5ml of ice-cold 70% ethanol was added slowly, drop-wise onto them while vortexing to avoid formation of clumps. The cells were left on ice for a minimum of 30 min and then stored at 4^{o}C prior to BrdU staining.

2.8.3 BrdU Staining

Cells were first centrifuged at 2000 rpm (120 *x g*) to remove ethanol and then washed twice with PBS. Then the DNA was denatured by resuspending the cell suspension in 2M hydrochloric acid (HCl), for 30min with occasional mixing. This step allows the access of the anti-BrdU antibody to its epitope in the DNA. Cells were then centrifuged at 1000 rpm (120 *x g*) to remove the HCl, followed by washing with PBS-T (PBS + 0.1% BSA + 0.2% Tween20, pH7.4). Cells were then stained with the anti-BrdU primary antibody (Beckton Dickinson), for 20min at room temperature (RT) in the dark. Following a second wash with PBS-T, the cell suspension was incubated with the FITC-conjugated secondary antibody (DAKO) for 20 min (at RT in the dark). Cells were then washed with PBS-T and then RNAs were eliminated, by treating the cells with RNAse (DNAse-free) for 15min at RT. Then PI was added and cells were further incubated in the dark for 30min.

RNAse treatment is necessary because PI incorporates into both DNA and RNA. But we are only interested in the signal coming from PI incorporated into DNA.

Cells were then analyzed by flow cytometry. Fluorochromes were excited by a 488nm laser. The FITC fluorescence was collected between 515 and 545nm and the PI fluorescence was collected above 580nm. Pulse processing of the PI signal was used to distinguish true G2 from G1 doublets and to eliminate the latter (i.e to gate G2 in our experiment). 20,000 events were collected, at a low flow rate setup.

Plan of Experiments to evaluate the antiproliferative effects of Compounds

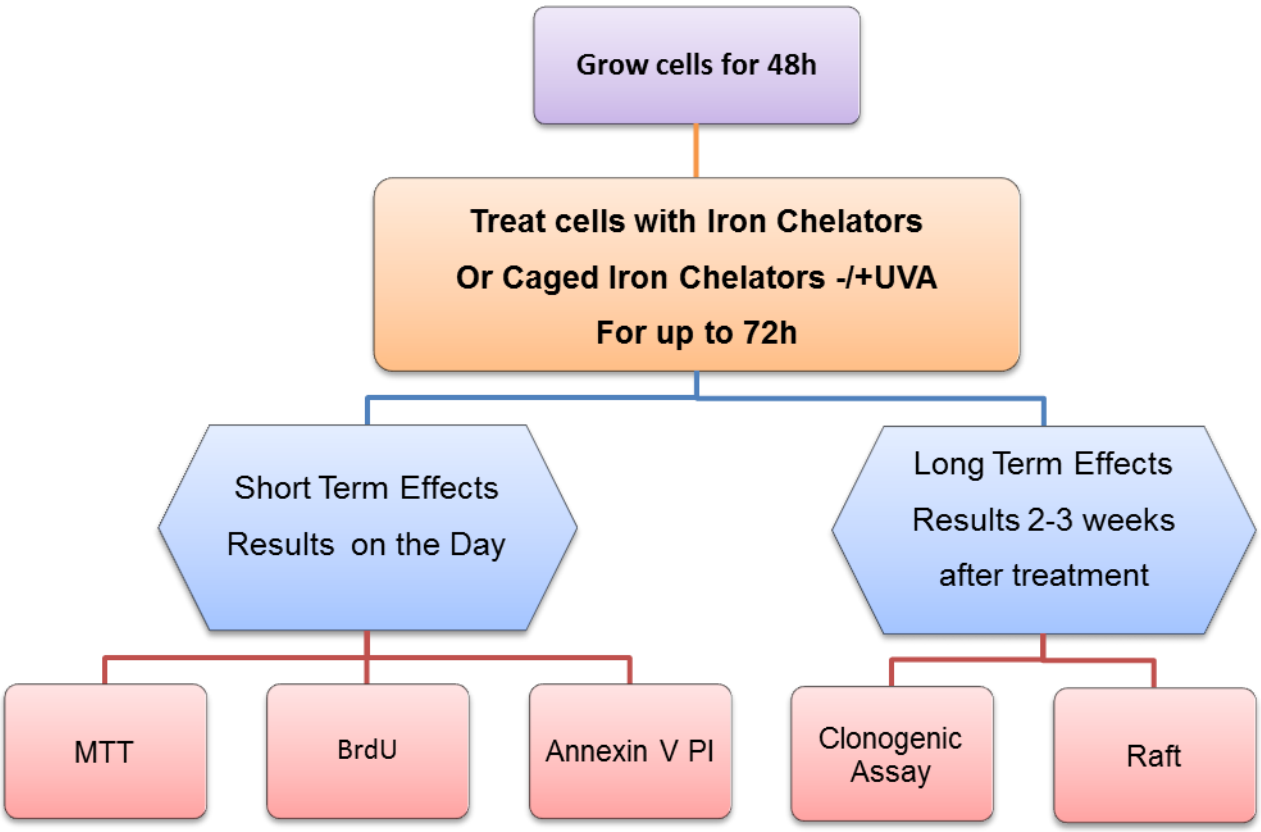

2.9 MTT Assay

2.9.1 Principle of the assay

The MTT assay is widely used in cell proliferation and cytotoxicity assays (Berridge *et al.*, 1996). It is a sensitive colorimetric assay (Mosmann, 1983; Doyle and Griffiths, 1998) that is performed to determine the viability of cells after relevant treatments. The principle of this assay is based on the capacity of cellular and mitochondrial dehydrogenase enzyme to convert MTT [3-(4,5-dimethylthiazol-2-yl)-2,5-diphenyl tetrazolium bromide], a yellow water-soluble substrate, into a dark blue formazan product that is water-insoluble. The amount of formazan produced is directly proportional to the viable cell number.

2.9.2. Procedure

The procedure involves the preparation of the MTT stock solution in PBS at 5mg/ml, which was then filtered through a 0.2 μm filter (Ministart®, Germany) for sterilisation and stored at –20ºC.

MTT/SFM stock solution: The fresh MTT solution in serum free media (SFM) was prepared at a final concentration of 0.5 mg/ml.

On the day of the assay (24 to 72 h post-treatment with compounds +/- UVA) cells were washed with PBS and incubated with 500 μl of MTT/SFM for 3 h at 37°C. After incubation, MTT/SFM solution was aspirated and 500 μl of DMSO was added to each plate. Then the plates were swirled for 3 minutes on 3D rocking platform (Stuart Scientific, UK). Finally, 100 μl of each sample (for FEK4) or 20 μl of sample diluted in 80μl DMSO for the rest of keratinocytes, was added in duplicate to a 96-well micro-plate. Absorbance was read by VERSAmaxTM (Molecular devices,California) at 570 nm.

2.10 Clonogenic Assay (Colony Forming Assay)

2.10.1 Principle of the assay

This assay is the most reliable method for assessing viable cell number. It is based on the ability of a single cell to grow into a colony and its ability to undergo “unlimited” division. The colony is defined to consist of at least 50 cells (Doyle and Griffiths, 1998).

2.10.2 Procedure

Cells were grown and treated with compounds as described above for 24, 48, and 72h. On the day of experiments, cells were trypsinised and re-seeded as single cell suspension at a density of 500 cells/ 3cm plate for FEK4, and 250 cells/ 3 cm plate for HaCaT in fresh media in triplicates. Cells were then allowed to grow for 12 days by replacing thr media every 3-4 days. At day 12 media was removed, and colonies were fixed and stained with 0.2% w/v crystal violet solution (in 20% v/v methanol, 2% w/v paraform aldehyde) for 15min. Then the plates were washed twice with PBS and colonies were counted. Data were expressed as percent survival relative to the control.

2.11 Annexin V / Propidium Iodide Dual Staining Assay

2.11. 1 Principle of the assay

Quantification of apoptotic, necrotic, and live cells was evaluated by flow cytometry. Apoptotic cells were shown to express phosphatidyl serine (PS) on the outer layer of the plasma membrane (Fadok *et al.*, 1992). In the early stages of apoptosis, PS translocates from the inner part of the plasma membrane to the outer layer. Annexin-V-FLUOS is a phospholipid-binding protein with a high affinity for PS. Therefore it is suitable for the detection of apoptotic cells. On the other hand, necrotic cells that lose cell membrane integrity are stained with both Annexin-VFLUOS and PI. Therefore, Annexin-V-FLUOS and PI double-staining can differentiate between necrotic and apoptotic cells.

2.11.2 Procedure

After relevant treatments and incubation periods (i.e. 4h to 72h), cells were collected and washed with incubation buffer (10 mM Hepes/NaOH, pH 7.4, 5 M NaCl, 100 mM $CaCl_2$). Then 5 x 10^5 cells were resuspendded in 100 µl of incubation buffer containing Annexin-V-FLUOS (20 µl/ml) and PI (20 µg/ml). Samples were then transferred to a 5 ml polystyrene round-bottom tube and incubated for 20 min at RT under dark condition. Finally 400 µl of incubation buffer was added. Data analysis was performed using FACSDiva software (Becton-Dickinson, Erembodegem, Belgium).

2.12 Organotypic 3D raft culture using de-epidermalised dermis (DED)

Glycerol preserved skin (Euro Skin Bank, Netherlands) was washed and incubated in PBS at 37^{o}C for up to 10 days. Epidermis was then mechanically removed using Forceps and the de-epidermalized dermis was cut into 2 x 2 cm squares and placed in culture plates with the papillary dermal surface on the underside. Stainless steel rings were placed on top of the dermis, and 5x 10^5 FEK4 were inoculated into the rings on the reticular dermal surface. Following an overnight incubation, the depidermalized dermis was inverted to orient the papillary dermal surface on top before the rings were replaced. Then 3 x 10^5 HaCaT KCs were seeded inside the rings onto the dermis. After 2 days, the dermis was raised to the air-liquid interface in the same orientation, by placing the comosites on stainless steel grids **(Fig. 2.2).**

After 7 days of raising the HaCaT Raft-DEDs, the 3D cultures were treated with DFO, PIH or 2NPE-PIH (+/- UVA) at a final concentration of 100 µM for 72 h. The cultures were then incubated for an additional 10 days (in the absence of compounds). On the 10^{th} day, HaCaT Raft-DEDs were removed from the grids, fixed in 10% formalin and embedded in paraffin.

Deparafinized sections were stained with haematoxylin and Eosin for histologic examination.The medium used for this experiment was the rich RM+ that allows the skin cell to achieve a higher proliferative state, and was refreshed every 3 days.

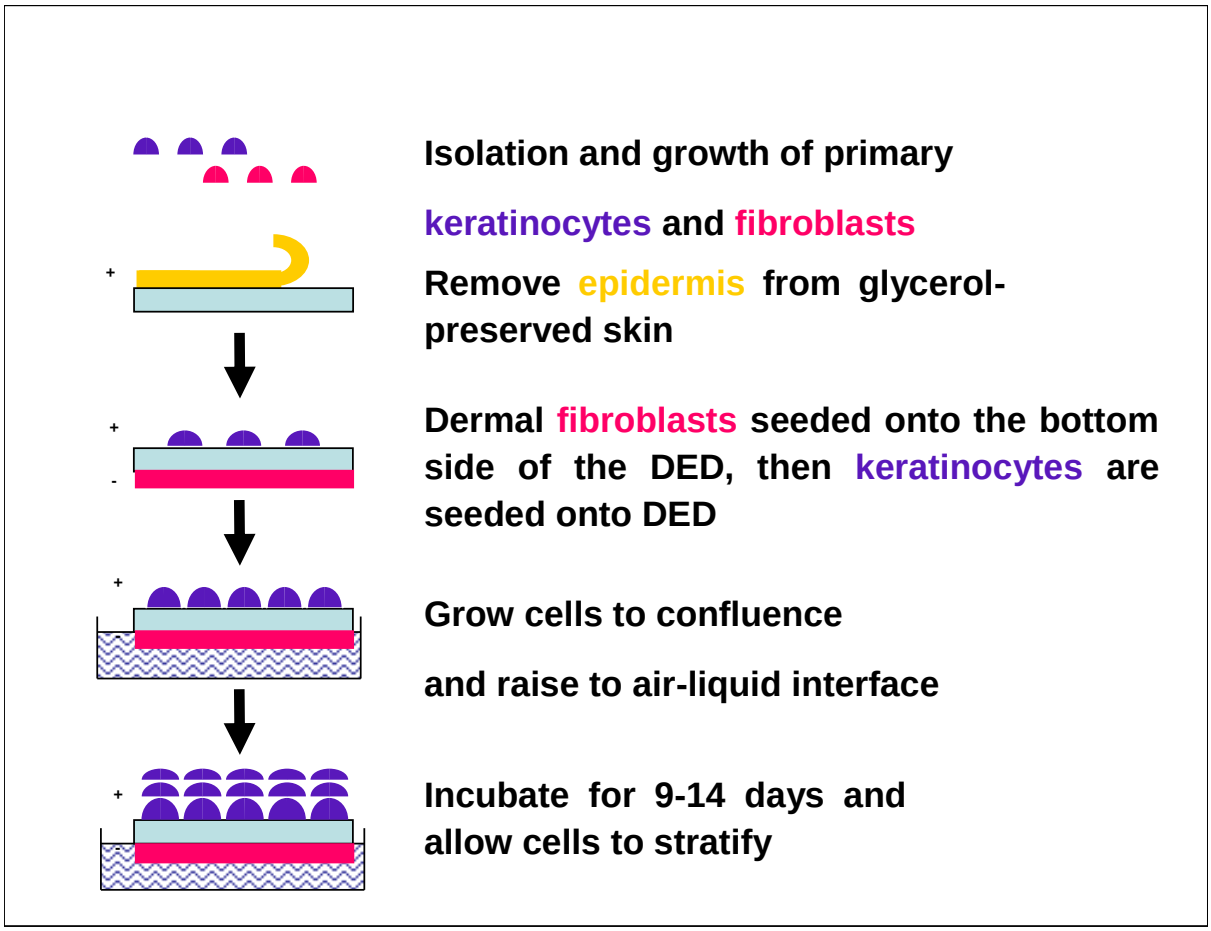

Figure 2.2: Organotypic raft culture using de-epidermalised dermis (DED). Provided by Dr Reelfs with thanks.

2.13 LIP determination in 96 well-plates

2.13.1 Principle of the assay

The level of LIP was determined by an adaptation of the method developed by (Epsztejn *et al.*, 1999; Petrat *et al.*, 1999).

The cytochemical calcein acetoxymethyl ester (CA-AM) assay is well established as a technique for the assay of cellular LIP. The principle of this assay is that non-fluorescent lipophilic CA-AM that easily penetrates cellular membranes produces fluorescent CA when rapidly cleaved by unspecific cytosolic esterases. The fluorescent CA is a fluorochromic alcohol that chelates labile iron (Tenopoulou *et al.*, 2007). The level of intracellular CA-Fe complexes is determined by the increase in fluorescence produced by the addition of the fast membrane permeable iron chelator, SIH. SIH is a lipophilic strong chelator that restores the fluorescence by removing the complexed iron (Glickstein *et al.*, 2005).

2.13.2 Procedure

Step I: CA Loading

Cells were grown for 72, 96 or 120 h as indicated in the cells section. On the day of treatment, the CM was aspirated and the cells were washed with PBS. Cells were then harvested by treatment with 0.125% trypsin and neutralised with 10% FCS PBS to avoid interference with fluorescence. Bovine serum albumin (BSA) was then added at a final concentration of 3 mg/ml to keep the osmotic integrity of the cells. Next, the cell suspension was centrifuged at 1000rpm (120 *x g*) for 2min in a Falcon 6/300 MSE centrifuge.The supernatant was then aspirated and the cells were loaded with 0.25 μM CA-AM for 15 min at 37°C in Earle's minimum essential media, containing 20 mM HEPES (pH 7.3) and 3 mg/ml BSA .

Step II: washing

This step allows the elimination of the excess CA-AM from the cell suspension. After loading, the cell suspension was centrifuged at 1000rpm (120 *x g*) for 2 min. The supernatant was then aspirated and the cells were resuspended in 4 ml of BSA (3 mg/ml in PBS) and centrifuged for 2 min at 1000 rpm (120 *x g*). The supernatant was then aspirated.

Step III: fluorescence monitoring

This step allows the measurement of basal fluorescence intensity of free CA, CA-Fe and total CA. After washing, the cell pellet was re-suspended in 300 µl of fixing solution [10 mM HEPES buffer containing 150 mM NaCl and 2 mM diethyltriamine-pentaacetic acid (DTPA) which is a non-permeable iron chelator, affinity > 10^{27}]. At this point the cell suspension was transferred to 96 well plates (Costar 3603) (i.e.100µl cell suspension per well in triplicate).The fluorescence (F1) was then measured (excitation 485 – emission 535) by a Fluoroskan Ascents microplate reader (Labsystems, OY). Next, 5 µl of SIH (4 mM stock solutions) was then added to obtain the final concentration of 0.2 mM. The 96 well plate was then placed on a rocking platform (Stuart Scientific, UK) for 15 min to allow chelation. The fluorescence (F2) was then recorded at an excitation wavelength of 485 nm and an emission wavelength of 535 nm. The fractional increase of fluorescence (ΔF = (F2-F1) / F2) was first determined by the calibration curve and then normalised to total cellular protein. This correlates with the LIP (µM / µg) within the cells (Duarte and Jones, 2007).

The calibration curve was prepared with ferrous ammonium sulphate (Petrat *et al.*, 2000). It was initially diluted with PBS to 1 mM and then to a final concentration of 1 µM (final). From this solution, a series of 1:1 serial dilutions were prepared up to the final concentration of 2.44 x 10^{-4} µM (i.e. in total 12 concentrations were used). Next, 0.25 µM of CA stock solution (Sigma, C0875) was added to the 12 serial dilutions and the fluorescence (F1) was recoded (Excitation 485 – Emission 535) by a Fluoroskan Ascents microplate reader (Labsystems, OY).

To each well, 5 µl of SIH (4 mM stock solutions) was added and the plate was placed on a rocking platform (Stuart Scientific, UK) for 15 min to allow chelation. After the 15 min, the fluorescence (F2) was measured (Excitation 485 – Emission 535). For the calibration curve (Darbari *et al*, 2003), the fractional increase of fluorescence (ΔF = (F2-F1) / F2) was plotted against the iron concentration used (y = 9.981x + 0.088, is the linear equation of the trendline).

Step IV: Protein measurements:

Protein concentrations were then measured according to the method of Bradford (Bradford, 1976) with slight modification. This modification was performed to enable the measurements of the protein content to be carried out in the 96-well plate to decrease the amount of protein extract used. To calibrate the standard curve, BSA (2 mg/ml) was first diluted (1:1) with MilliQ water (i.e. to 1 mg/ml) and then used at final concentrations of 0, 1, 2, 3, 4, 6, 8, 10 mg/ml.

The total volume of cellular extract (1 µl) or BSA (0-10 µl) with MilliQ water used in the each well was 160 µl, done in duplicates. Finally 40 µl of Bio-rad Protein Reagent (Bio-rad. 500-0006) was added, and the solution was thoroughly mixed with a pipette (preferably, a multichannel pipette). The absorbance was read using a VERSAmax^{TM} (Molecular devices, California) at 595 nm.

The schematic presentation of the steps for measuring CA-Fe by CA-assay

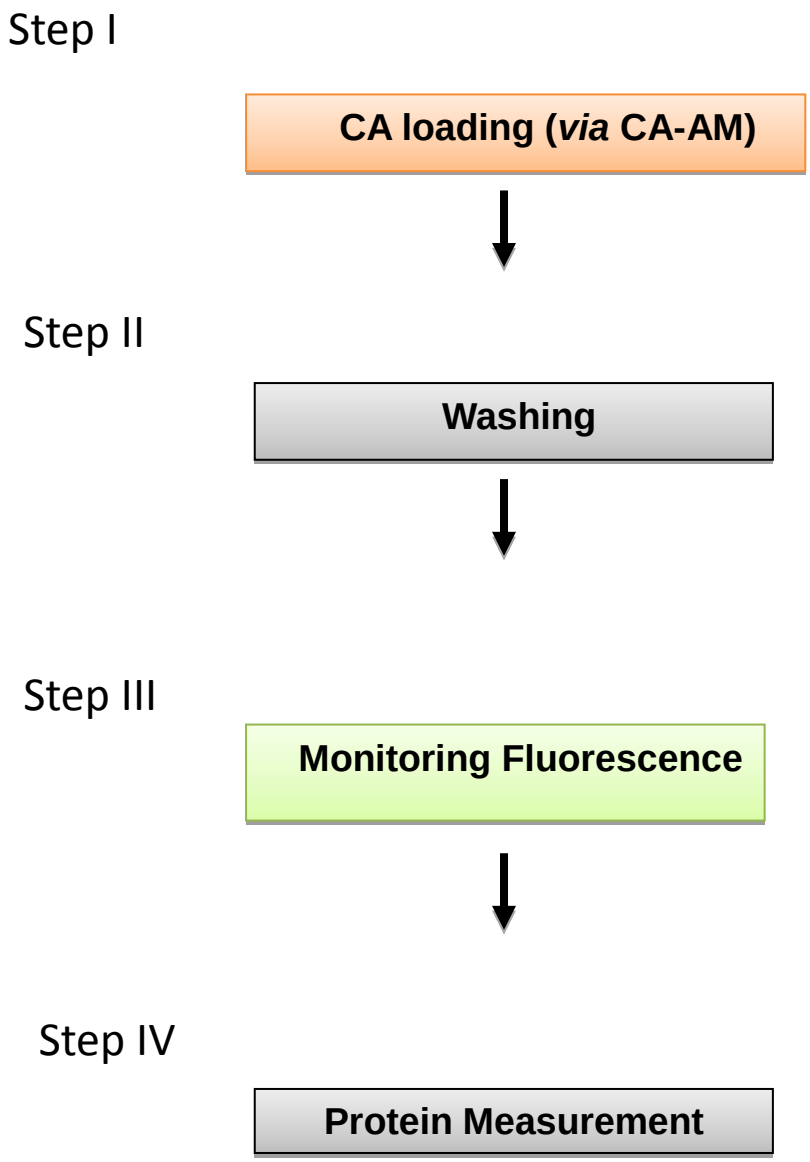

2.14 Statistical analysis

Results are expressed as mean ± standard deviation (SD). Paired or unpaired Student's one-tailed *t*-test was used as appropriate to test differences between groups of data. Note that the rejection p value is 0.05. Statistical analysis was performed using Microsoft Excel.

2.15 Synthesis of Caged –iron chelators and analogues

All compounds were synthesised in the School of Chemistry, University of Nottingham under the supervision of Dr James Dowden, according to Yiakouvaki *et al.* (2006) and unpublished procedures by Dr Savovic (Pourzand and Dowden's laboratories).

2.15.1 Solvents, reagents, equipments

All solvents and reagents were purchased from commercial sources and used as received.
^{1}H and ^{13}C NMR (nuclear magnetic resonance) were obtained on a Varian EX-400 NMR spectrometer at 400 and 100 MHz, respectively.

2.15.2 General procedure for phenol alkylation (2NPE-SIH precursor a and 2-NPE-PIH precursor b)

A solution of the phenol (salycilaldehyde or pyridoxal HCl) (2.5 mmol), 1-(1-bromo-ethyl)-2-nitro-benzene, and K_2CO_3 anhydrous (for precursor **a**) or Cs_2CO_3 (for precursor **b**) in dimethyl formamide was stirred at 60°C for 12 h and then concentrated under vacuum. The obtained crude extracts were separated as outlined in the following table:

Aimed Product	Residue Partitioned between	Column chromatography	Recrystalisation
2-NPE-SIH precursur (**a**)	DCM x 3 and H2O	EtOAc:Hexane (7:3)	-
2-NPE-PIH precursor (**b**)	EtOAc x 3 and H2O	Et_2O: Hexane (2:8)	EtOAc:Hexane

2.15.3 General procedure for hydrazide formation (to synthesise 2NPE-SIH and 2-NPE-PIH, BIH, SIH, PIH)

A solution of aldehyde (1 mmol) and isonicotinic acid hydrazide (1 mmol) in ethanol (10 ml) or ethanol: water (9:1, 10 ml) for PIH and 2-NPE-PIH, was heated at reflux for 24 h.

The reaction to make 2-NPE-PIH (final product) was performed in presence of filtered Dowex® 50WX4-100 acidic resin.

The obtained crude extracts were separated as outlined in the following table:

Aimed Product	Column chromatography	Recrystalisation
2NPE-SIH	EtOAc:Hexane (7:3)	EtOAc:EtOH
2-NPE-PIH	MeOH:DCM (0.3: 9.7) to (0.6:9.4)	EtOAc: EtOH: Et_2O
SIH	-	EtOAc:EtOH
PIH	-	EtOH: H_2O (9:1)
BIH	-	MeOH:EtOH

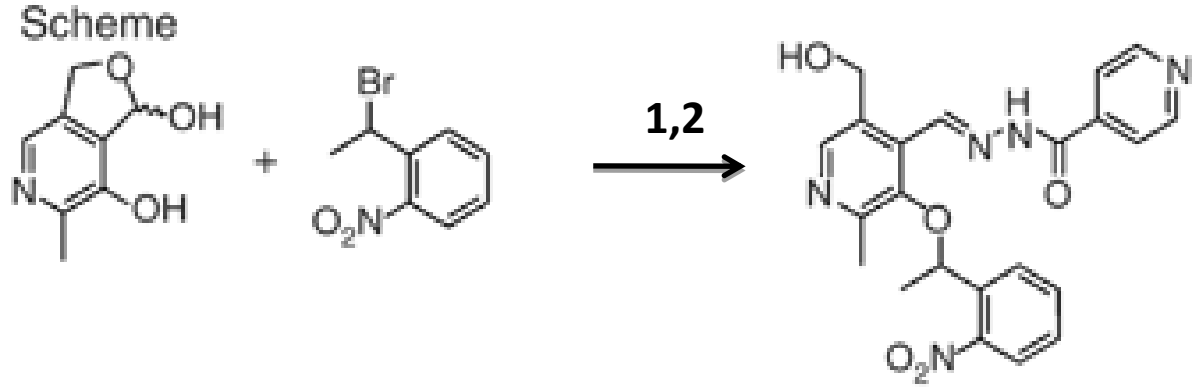

Pyridoxal

(2-nitrophenyl)ethyl pyridoxal isonicotinoyl hydrazone **(2NPE PIH)**

Figure 2.3: Structures of caged iron chelators and control compounds. (**1**) Cs_2CO_3, DMF; (**2**) isonicotinic acid hydrazide, Dowex® 50WX4-100, EtOH/H_2O (9:1).
(Adapted from Yiakouvaki *et al.*, 2006)(Yiakouvaki *et al.*, 2006).

CHAPTER THREE

RESULTS AND DISCUSSION

3.1. The Choice of Cell Lines

To investigate the antiproliferative potential of Fe chelation as a powerful alternative therapy for skin hyperproliferative diseases such as NMSC or psoriasis, a series of experiments was performed to evaluate the impact of the parental compounds (PIH and SIH) and their caged derivatives (+/-UVA) on cell growth and cell cycle. The Fe chelator DFO was used as a positive control and the SIH derivative BIH, which lacks the iron binding moiety, was used as a negative control.

The proof of concept studies were carried out using FEK4 fibroblasts and HaCaT keratinocytes (KCs) as cell models. FEK4 cells are human primary skin fibroblasts that were originally isolated from the foreskin of a newborn baby in Tyrrell's laboratory (ISREC, Switzerland). FEK4 fibroblasts are not immortalised and are therefore passage-dependent. HaCaT KCs are spontaneously immortalised cells and were originally isolated from a male human in Boukamp's laboratory (1988). The HaCaT cell line has proved to be a useful and reliable *in vitro* model of human skin cell carcinoma. Furthermore as a cell line, it shows high genomic stability with successive passaging and provides reproducible results with time. This cell line is hyperproliferative and has a significantly higher proliferation rate than normal human skin KCs and fibroblasts (unpublished data, this laboratory). Both FEK4 and HaCaT cells are well characterised in Pourzand's laboratory in terms of their molecular and enzymatic antioxidant defence capacity, susceptibility to UVA and H_2O_2, labile iron profile (+/- UVA), intracellular content of Ft, HO-1, HO-2 (+/- UVA) and short-term response to Fe chelators DFO, PIH, SIH and their caged-derivatives (+/- UVA) (Pourzand and Tyrrell, 1999; Pourzand *et al.*, 2000; Zhong *et al.*, 2004; Yiakouvaki *et al.*, 2006; Reelfs *et al.*, 2010).

The proof of concept experiments described in this section was first carried out with FEK4 and HaCaT cells. The obtained results were then further confirmed in a series of hyperproliferative cancerous and psoriatic cell lines. The cancer cell models used in this

study consisted of one keratinocyte cell line (i.e. PM1), clonally derived from forehead skin showing dysplasia, and one SCC line (i.e. Met 2) derived from a local recurrent cutaneous tumour. PM1 and Met 2 are isogenic KC cell lines isolated from the same patient (a kind gift from Prof Irene Leigh, Dundee, see Proby *et al.*, 2000 and Popp *et al.*, 2000). As additional model of hyperproliferative cell line, we also used the MKPS cell line. MKPS is an immortalised KC cell line derived from the psoriatic lesion of a male patient (a kind gift from Prof Irene Leigh, Dundee). Other control cells also included human primary cultured KC cells KCP7 and KCP8 that were passage-dependent and were used between passages 3-5 after which they usually differentiate.

3.1.1 Comparison of the Growth Rate of Skin Cells

3.1.1.1 Cell Count Assay

For the purpose of this PhD project, the growth rate of HaCaT KCs was compared to that of human primary skin fibroblasts FEK4, using the cell count assay. HaCaT and FEK4 cells were seeded at low confluency (i.e. 2 x 10^4 cells per 3cm plate) and the doubling time was calculated for both cell lines by counting the number of cells every 24 h in triplicates over a period of 7 days. The results (**Fig 3.1A**) showed that both in FEK4 and HaCaT cultures, there was a lag period of about 24 h after seeding, corresponding to the adaptation and recovery of the cells. However from 24 h onwards, the cells started to proliferate and rapidly entered the exponential phase, as evidenced by the logarithmic straight line plot in **Fig 3.1A**. As the cell density increased, the proliferation rate receded as a result of cell-cell contact inhibition and the cells entered the plateau phase after the 7^{th} day (data not shown). Further comparison, revealed significant difference in proliferation rates of both cell types (i.e. 0.01754 versus 0.01056 for HaCaT and FEK4 cells respectively, p=0.01513). The doubling time for HaCaT was found to be ~17h, against ~28h for FEK4. The latter is in agreement with previous findings from this laboratory (unpublished).

The differential growth rate of FEK4 and HaCaT cells made them suitable as models of slow and fast growing cells for comparative studies aiming at evaluating the growth inhibitory effects of Fe chelators used in our study. Also since under conditions used in this study, both cell types maintained their exponential growth phase profile over the period of 24-120 h after seeding (see **Fig 3.1A**), it was possible to monitor the antiproliferative potential of Fe chelators in a time-dependent manner within this period.

3.1.1.2 BrdU Assay

The BrdU incorporation assay was used to compare the growth rate of FEK4, HaCaT and MKPS cells with that of cancer cell models PM1 and Met2 (all in exponential phase of their growth). The BrdU incorporation assay coupled with flow cytometry is a highly sensitive and reproducible technique particularly for determining the proportion of cells in the S phase of the cell cycle and provides both quantitative and qualitative data. The results (**Fig. 3.1B**) showed that in the exponential growth phase of cells, only 18% ± 2of FEK4 cells were in S phase. In contrast in PM1 and Met 2 cancer cell models, the percentages of cells in S phase were much higher than FEK4 (i.e. 49% and 38%, respectively). In comparison, the percentage of HaCaT cells in S phase was even higher (i.e. 55% ± 8). The psoriatic MKPS cells had the highest proliferation rate with 79% of cells in S phase. In summary, these results illustrated that compared to FEK4 control cells, all other cell lines have much higher growth rate.

3.1.1.3 Growth rate of primary keratinocytes

Previous unpublished work from this laboratory has already established that in comparison to the immortalised HaCaT KCs, the primary human KC cells KCP7 and KCP8 have much slower growth rate (i.e. several fold-lower than HaCaT cells). However these cell lines were not suitable as cell models for routine experiments. This is because the culture of KCP primary KCs is very time consuming and for experimental set up they often require 3-4 weeks of growth in culture before reaching the appropriate cell density for methodologies used in the study. In comparison, FEK4 and HaCaT experimental set up required only 2-3 days of growth in culture to reach the appropriate stage. Furthermore KCP cell culture is not only matrix-dependent (i.e. requires feeder layer for growth similar to PM1, Met2 and MKPS) but also extremely passage-dependent, since as primary KCs, KCP 7 and KCP8 can only be used between passages 1-5 after which they differentiate. The latter reason was also a major limitation for the number of repeats of the experiments. Therefore in this PhD project, KCP7 and KCP8 cells were only used as checkpoints in some of the experiments to compare the results obtained with other cell models.

1A.

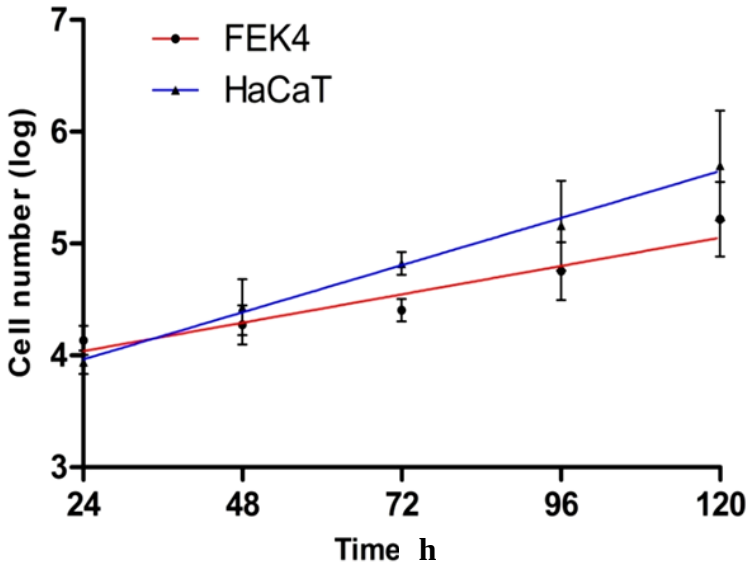

1B.

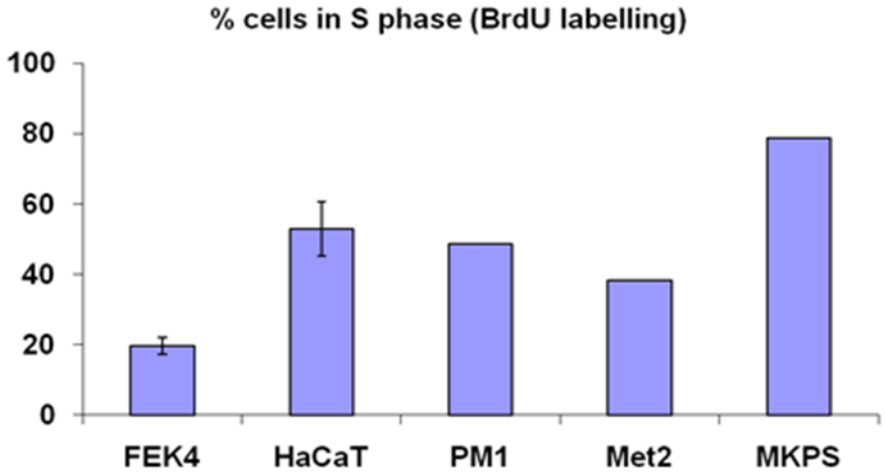

Figure 3.1: Comparison of growth rate of a series of skin cell lines.

1A. Combined logarithmic plot of growth curves data for HaCaT keratinocytes and human primary skin fibroblasts FEK4 cells. Log values of average cell counts were plotted and the best fit line was plotted using linear regression analysis. Statistical analysis was carried out using Graphpad Prism 5.0. (n=3).

1B. Cell proliferation rate of FEK4 fibroblasts and HaCaT, PM1, Met2 and MKPS KCs as measured by BrdU-assay. Exponentially-growing cells were first pulsed with BrdU (10 µM) for 1 h, and then harvested and processed by flow cytometry for determination of the percentage of cells in S phase. 20'000 events were collected and analysed (n=2-3).

3.1.2 Comparison of the Basal LIP Level in Skin Cells

Numerous studies have highlighted that compared to normal cells, the cancer cells are more sensitive to Fe-depletion. It has been suggested that this sensitivity relates to their high requirement for iron which is necessary for the rapid cancer cell multiplication. However to our knowledge, no study has demonstrated to date a clear relationship between the high turnover of iron in cancer cells and their high rate of proliferation. This information is also missing for skin-related hyperproliferative disorders notably NMSC and psoriasis. Nevertheless it is known that iron is involved in the pathology of skin diseases as the presence of excess iron has been demonstrated in a variety of skin disorders such as psoriasis, venous ulceration and atopic eczema.

Our cell models provided us with an opportunity to investigate whether there is a correlation between the intracellular level of labile iron and the proliferation rate of the cells. Such studies could provide valuable clues to understand the modulation of intracellular iron levels during progression of normal skin cells towards early and late stages of carcinogenesis.

Zhong *et al.* (2004), from this laboratory, have already demonstrated that epidermal keratinocytes (e.g. HaCaT, KCP7 and KCP8) are more resistant to UVA-induced oxidative damage and cell death than dermal fibroblasts (e.g. FEK4, FCP7 and FCP8) presumably because both the 'basal' and 'UVA- induced' level of labile iron is considerably lower in keratinocytes than in fibroblasts. Indeed this study has revealed that the basal intracellular LIP level of primary skin KCs, KCP7 and KCP8, is 3-4-fold lower than their respective matched primary skin fibroblasts FCP7 and FCP8. The basal intracellular level of LIP in HaCaT KCs was also found to be 2.5-fold lower than that of FEK4 fibroblasts (see **Table I** and (Zhong *et al.*, 2004).

For the purpose of this PhD project, the intracellular level of LIP was evaluated with the highly sensitive CA fluorescence assay in PM1, Met2, MKPS and HaCaT KC cell lines over a period of 120 h after seeding. The results (**Table II**) demonstrated that in exponential growth phase, the basal LIP levels of PM1, Met2 and MKPS KCs are on average 1.6-2-fold higher than that of HaCaT cells. The comparison of data obtained in this study (**Table II**) with that of Zhong *et al.* (2004; **Table I**) further revealed that the basal LIP levels of cancer

cell lines PM1 and Met 2 as well as the psoriatic cell line MKPS are on average 3-4 fold higher than primary KCs, KCP7 and KCP8.
The higher labile iron content of the PM1, Met2 and MKPS (**Table II**) appeared to correlate with their proliferation rate, since the intracellular LIP levels of these fast growing cells were significantly higher than that of primary KCs (**Table I** and unpublished data, this laboratory). Nevertheless primary FEK4 fibroblasts that had comparable basal level of LIP to PM1, Met2 and MKPS, showed much lower growth rate as shown in **Fig 3.1B**.

These observations suggested that although the basal LIP level might not always correlate with cell proliferation rate, it might however be a useful parameter to measure as it could provide valuable information about the sensitivity of the cell lines to Fe-depletion for instance during ICT. The PM1, Met2 and MKPS cell lines were therefore used as models of high proliferating cells to evaluate the antiproliferative potential of SIH, PIH and their caged derivatives i.e. 2NPE−PIH and 2NPE−SIH, followed or not by exposure to low to moderate doses of UVA. Sections **3.2** and **3.3** provide the summary of these findings.

Table I. The comparison of the basal intracellular level of LIP in skin cell lines

Cell-line	LIP= [Fe] + [CA-Fe] (μM)
Fibroblast: FCP7	2.01 ± 0.06
Keratinocyte: KCP7	0.27 ± 0.03
Fibroblast: FCP8	1.67 ± 0.21
Keratinocyte: KCP8	0.31 ± 0.17
Fibroblast: FEK4	1.21 ± 0.45
Keratinocyte:Hacat	0.50 ± 0.06

Note: reproduced from Zhong *et al*, 2004.

Table II. Fold difference in basal LIP of PM1, Met2 and MKPS as compared to HaCaT cells

Ratio of LIP/protein (uM/ug)	Time After Seeding		
	72h	96h	120h
HaCaT	1.00	1.00	1.00
PM1	1.44	1.58	1.75
Met2	2.05	1.94	2.61
MKPS	2.42	2.06	2.31

Note: Average from 2-3 experiments.

3.2. The Antiproliferative Effect of Parental Iron Chelators

3.2.1. Comparison of the Growth Inhibitory Effect of Equimolar Concentration of PIH, SIH, DFO and BIH in skin cells

Prolonged exposure of cells to strong Fe chelators has been associated with severe toxicity and cell death due to iron starvation. Previous studies from this laboratory have demonstrated that short term treatment (i.e. 4-18 h) of FEK4 cells with Fe chelators Desferal (DFO) as well as parental PIH, SIH compounds and their caged-derivatives (at a final concentration of 100 μM) successfully depletes the basal and UVA-induced transit labile iron in cells but has no significant toxicity to the cells (Pourzand *et al.*, 1999b; Reelfs *et al.*, 2004; Zhong *et al.*, 2004; Yiakouvaki *et al.*, 2006). This was also confirmed for HaCaT KCs when treated for 4-18 h with DFO at a final concentration of 100 μM (Zhong *et al.*, 2004).

In the present study we extended these observations by incubating the exponentially growing cultures of HaCaT and FEK4 cells for longer periods (up to 72 h) with Fe Chelators DFO, PIH and SIH at a final concentration of 100 μM. The SIH derivative 'BIH' that lacks the iron binding moiety was used as a non-chelating analogue control compound. A study performed by Yiakouvaki *et al.* (2006, this laboratory) has already demonstrated that overnight treatment of FEK4 cells with BIH at a final concentration of 100 μM triggers no toxicity to cells and unlike its analogues PIH and SIH, it does not modulate the basal or UVA-induced level of LIP in the cells.

3.2.1.1 MTT Assay

We first evaluated the cytotoxicity of the compounds with the MTT assay 24, 48 and 72 h after addition of compounds to exponentially growing HaCaT and FEK4 cells. The MTT assay monitors the ability of cellular dehydrogenases to convert the yellow soluble MTT (3-(4,5-Dimethylthiazol-2-yl)-2,5-diphenyltetrazolium bromide) into a insoluble purple formazan product. The intensity of the production of this purple product is directly proportional to cell density as well as cellular reductive capacity and subsequently cell viability. Therefore this rapid and sensitive assay is often used as the first line of evaluation and screening of novel compounds in both cell proliferation and cytotoxicity studies.

The MTT assay (**Fig 3.2**) demonstrated a significant reduction in cellular enzymatic activity of both FEK4 and HaCaT cells following prolonged treatment with Fe chelators. Nevertheless while with DFO and SIH, this effect occurred in both cell lines in a time-dependent manner, with PIH, the time-dependent reduction in activity could only be observed in FEK4 cells (**Fig 3.2A**). Indeed in PIH-treated HaCaT cells the observed reduction in enzymatic activities at 24h did not significantly change on progressing to 48 and 72 h time points (**Fig 3.2B**). Nevertheless, compared to FEK4 cells, SIH- and DFO-treatment had a more pronounced effect on HaCaT cells, as reflected by a more significant reduction in enzymatic activity at all time points used in the study. In contrast, the effect observed with PIH was less impressive and comparable in both cell lines (**Fig 3.2A** and **3.2B**). For example at the 72 h post-treatment time point, the percentage control enzymatic activities calculated for both PIH-treated HaCaT and FEK4 cells were 54% ± 8 and 46% ± 9, respectively (see **Fig 3.2A** and **3.2B**). For the same time point, the observed percentage control activity in SIH- and DFO-treated FEK4 cells was slightly lower (i.e. 34% ±7 and 35% ± 4, respectively) than the corresponding PIH-treated cells (**Fig 3.2A**). In contrast in SIH- and DFO-treated HaCaT cells, the respective percentage control activities were substantially lower (i.e. 4% ± 1 and 3% ± 2, respectively) than the corresponding PIH-treated cells (**Fig 3.2B).**

The treatment of both cell lines with BIH, a SIH derivative lacking the iron-binding moiety, did not have a significant effect in both cell lines (**Fig 3.2**), suggesting that the observed reduction in activity with its analogues PIH and SIH might be related to their Fe chelation property.

Overall HaCaT cells were found to be more sensitive to Fe chelators DFO and SIH than FEK4. The lower basal LIP level of HaCaT cells might play a role in their increased sensitivity to Fe-depletion when compared to FEK4 cells (**Table I** and (Zhong *et al.*, 2004). Finally the lower response of both cell types to PIH when compared to that of SIH and DFO, suggested that PIH might not be a suitable candidate chelator for iron chelation therapy.

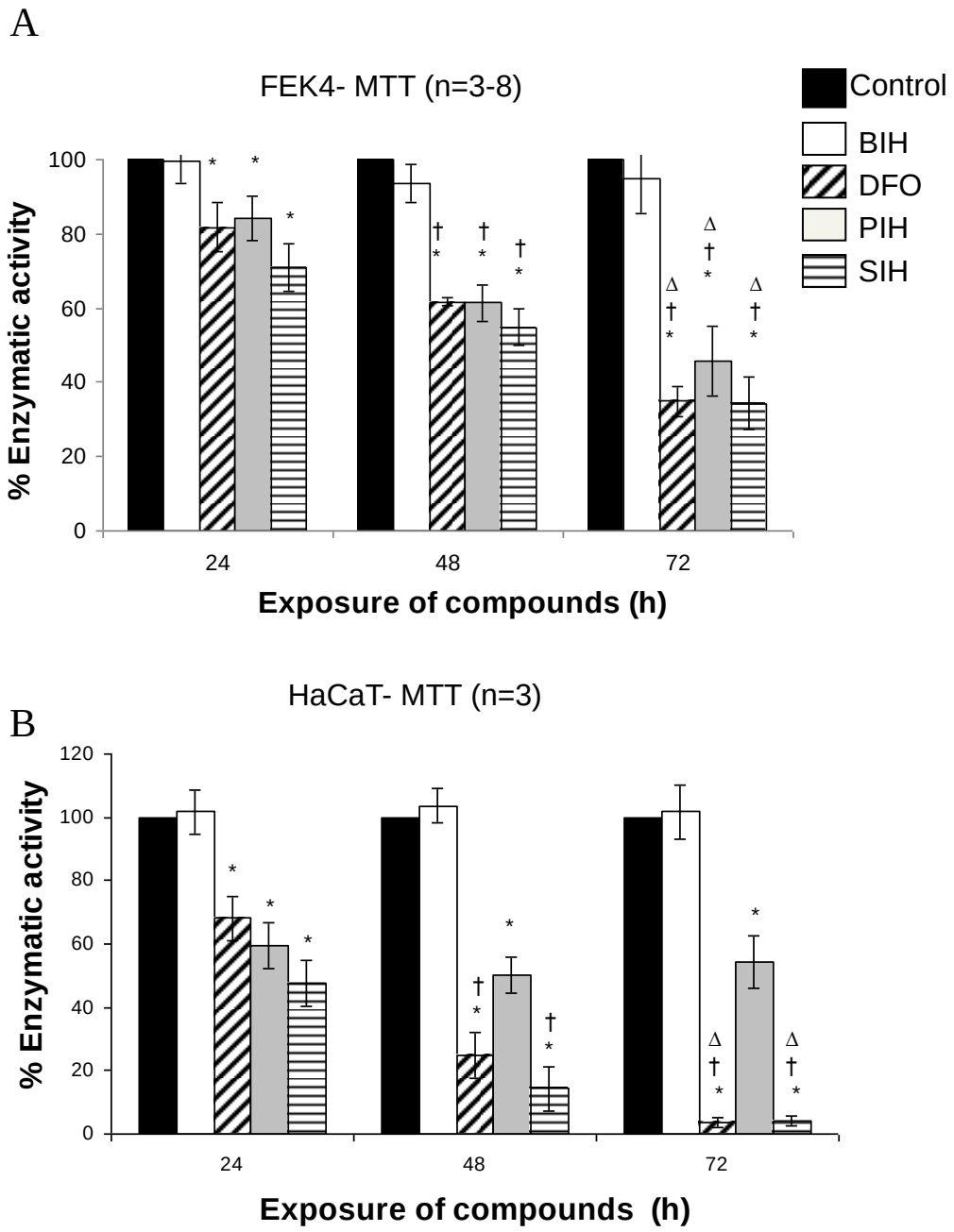

Figure 3.2: The evaluation of growth inhibitory effect of PIH, SIH, and DFO on FEK4 (A) HaCaT (B) cells with MTT assay.

Exponentially growing cells were incubated for 24, 48, and 72 h with compounds prior to MTT assay, as described in **Materials and Methods** section. The results were expressed as percentage of control (Mean ±SD; n=3-8)

* : p< 0.05 Significant difference between value and corresponding untreated control.

┼ : p< 0.05 Significant difference between value and corresponding 24h treatment

Δ : p< 0.05 Significant difference between value and corresponding 48h treatment.

3.2.1.2 Cell Count Assay

To ascertain that the observed reduction in enzymatic activity in MTT assay was related to decrease in cell density due to the growth inhibitory effect of the chelators rather than direct impact on cellular dehydrogenases enzymatic activity, we used the cell count assay as a control methodology to evaluate the change in cell density 24, 48 and 72 h following treatment of HaCaT cells with 100 µM DFO and PIH. While the MTT assay is invariably more sensitive than the cell count assay, there are a number of benefits associated with the latter. Namely, cell counting provides a direct measure of cell proliferation rates and it can give a clear indication of compound cytotoxicity. On a par with the benefits of cell counting, its drawbacks include an inherently increased risk of error (the procedure involves many more steps than the MTT assay), a reduced sensitivity and a much more labour intensive procedure. The results (**Fig 3.3**) showed that the trend of PIH and DFO cell count data are similar to those obtained with the MTT assay. Namely, both PIH and DFO treatments at a final concentration of 100 µM, substantially decreased the HaCaT cell proliferation rate, as reflected by the decrease in the number of viable cells. However the effect was much smaller with PIH. Also, there was again evidence of much reduced time-dependence with PIH.

A.

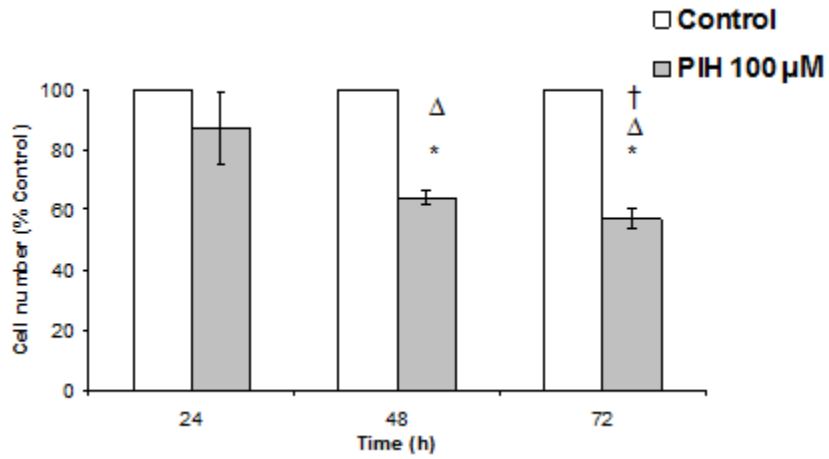

B.

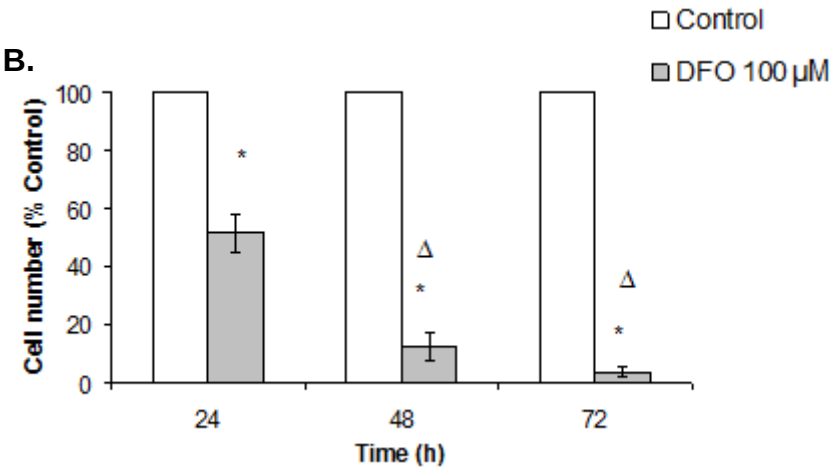

Figure 3.3: The evaluation of growth inhibitory effect of PIH (A) and DFO (B) on HaCaT cells, with the cell count assay.

Exponentially growing cells were incubated for 24, 48, and 72 h with compounds prior to the cell count assay, as described in **Materials and Methods** section.

The results were expressed as percentage of control (Mean ± SD; n=3)

* : $p < 0.05$ Significant difference between value and corresponding control.

Δ : $p < 0.05$ Significant difference between value and corresponding 24h treatment.

┼ : $p < 0.05$ Significant difference between value and corresponding 48h treatment.

3.2.1.3 Light Microscopy

The relative reduction in cell density was also visualized by light microscopy in both FEK4 (**Fig 3.4A**) and HaCaT cells (**Fig 3.4B**), 72 h following treatment of cells with DFO, SIH and PIH at a final concentration of 100 µM. With the BIH-treated cells, there was again no evidence of reduction in cell density.

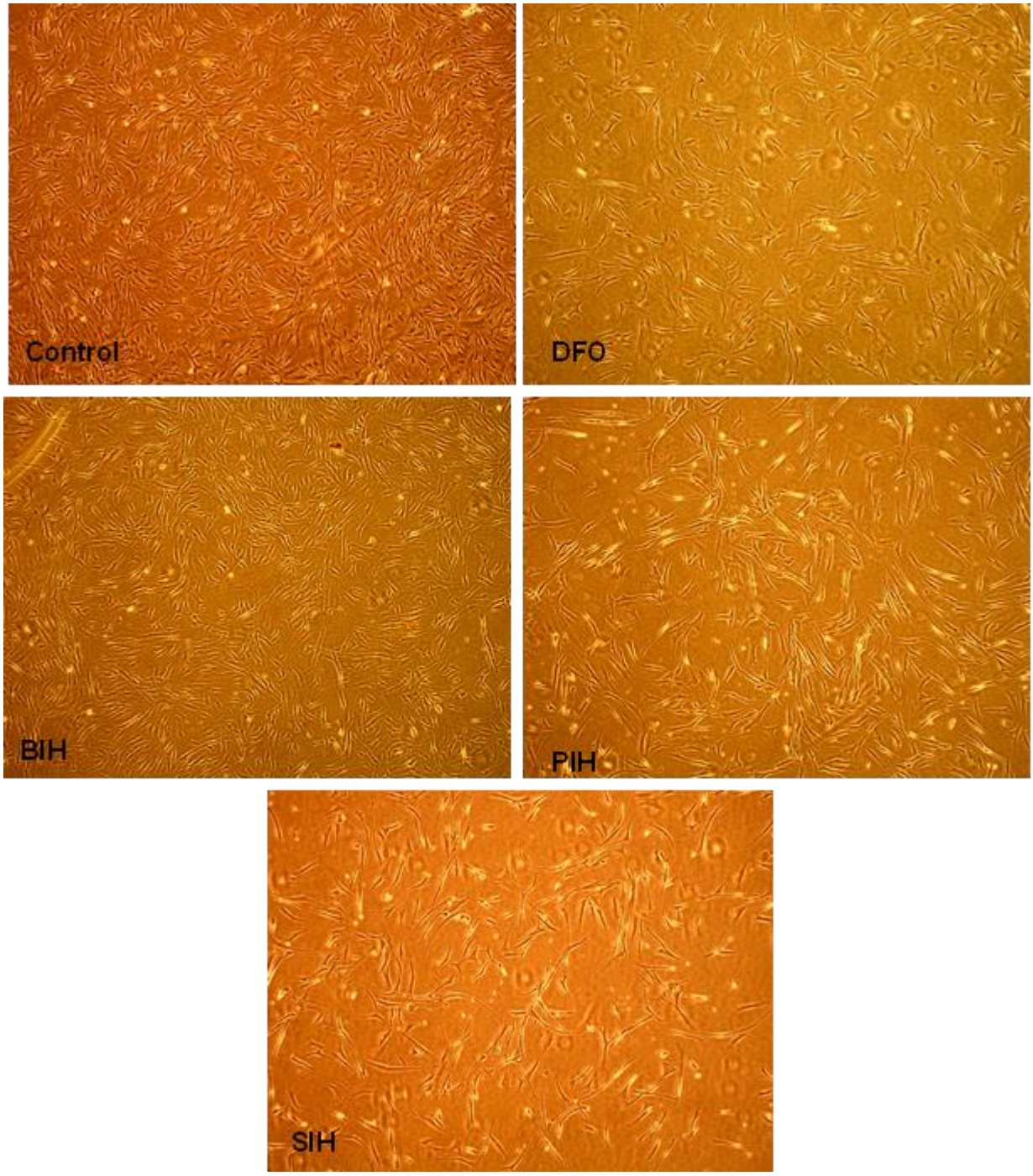

Figure 3.4A. The microscopic evaluation of cell confluency in FEK4 cells treated (or not) with Fe chelators DFO, PIH and SIH.

The microscopic photography was taken 72 h following treatment of the cells with compounds at a final concentration of 100 µM. BIH was used as a non-chelating control compound.

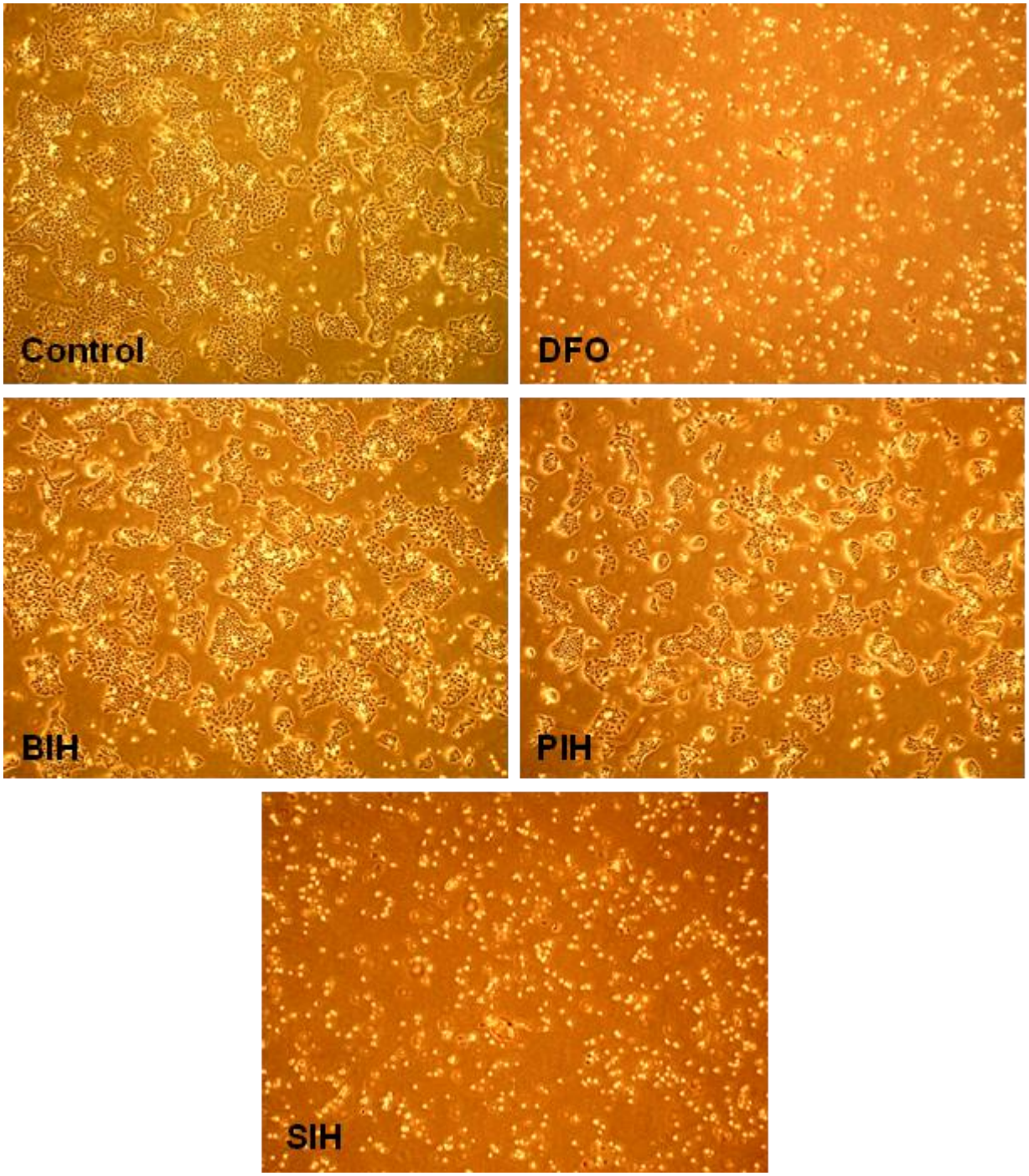

Figure 3.4B: The microscopic evaluation of cell confluency in HaCaT cells treated (or not) with Fe chelators DFO, PIH and SIH.

The microscopic photography was taken 72 h following treatment of the cells with compounds at a final concentration of 100 µM. BIH was used as a non-chelating control compound.

3.2.2 Effect of PIH, SIH and DFO on Skin Cell Survival Using Colony Forming Ability Assay

The results obtained with the MTT assay provided information about the short term effect of Fe chelators on HaCaT cells' proliferation (i.e. up to 72 h post-treatment). In an attempt to relate these findings to an *in vivo* setting, the colony forming ability (CFA) assay was also performed in parallel with the MTT assay in HaCaT cells. The CFA assay is a useful methodology for monitoring the antiproliferative behaviour of the Fe chelators since unlike the MTT assay, it monitors the long term toxic/growth-inhibitory effect of the compounds. The CFA assay assesses the ability of a single cell to plate, divide and form colonies 14 days following treatment with compounds of interest (e.g. Fe-chelators in this study). The CFA assay has been recognized as a reliable and powerful first line *in vitro* method (i.e. prior to *in vivo* testing) for evaluation of the anticancer effects of the chemotherapeutic agents in terms of inhibition of cancer cell proliferation and their ability to form a colony. Furthermore the CFA assay has been used to reliably predict treatment outcomes *in vivo*.

For the purpose of this study, the exponentially growing HaCaT cells were treated with SIH, PIH and DFO at a final concentration of 100 μM for 24, 48 or 72 h. After each treatment, the cells were trypsinised and then seeded at single cell density and allowed to grow for 14 days in the absence of the compounds. At day 14^{th}, the colonies were counted and expressed as percentage colony formation of the untreated control. The results (**Fig 3.5**) showed that in HaCaT cells, SIH and DFO have a much higher antiproliferative activity than PIH. Indeed the counting of colonies revealed that SIH and DFO treatments considerably reduce the percentage of colony formation in a time-dependent manner. Briefly, compared to control HaCaT cells, the 24 h treatment of cells with DFO and SIH decreased the percentage of colonies from 100% (i.e. control) to 74% ± 3 and 48%, respectively, and the 48 h treatment reduced further the DFO and SIH values to 14% ± 8 and 19%, respectively. Interestingly, only very few colonies were formed in cell culture plates that were originally treated with both compounds for 72 h. These results were in agreement with those of the MTT assay, although the effects observed with CFA were more pronounced.

Surprisingly, PIH treatment did not have a significant effect on colony formation in HaCaT cells, even after 72 h pre-treatment. The latter observation did not correlate with the MTT and cell count data, suggesting that the short term decrease in cell proliferation in PIH-treated

HaCaT cells must have been a transient effect that only occurred in the presence of the compound, and that presumably after removal of the compounds and addition of fresh media, cells have re-started to proliferate. In other words, the Fe chelating property of PIH might only cause 'growth retardation' in cells due to a transient Fe depletion rather than 'growth inhibition'. Growth retardation due to transient iron starvation could translate as a longer S phase in the cell cycle, since the iron required for RR implicated in DNA synthesis is scarce. In this scenario, the removal of the Fe chelator should restore the DNA synthesis and cell division as a whole. In contrast growth inhibition may occur when RR activity is inhibited by the Fe chelator, so that the cell cycle stops at G1/S phase. The G1/S arrest in cell cycle usually leads to cell death. To distinguish between these two phenomena, it was therefore necessary to monitor both the percentage of cells in S phase of the cell cycle and cell death following Fe chelator treatments. Section **3.2.3** and **3.2.4** provide the summary of these analyses.

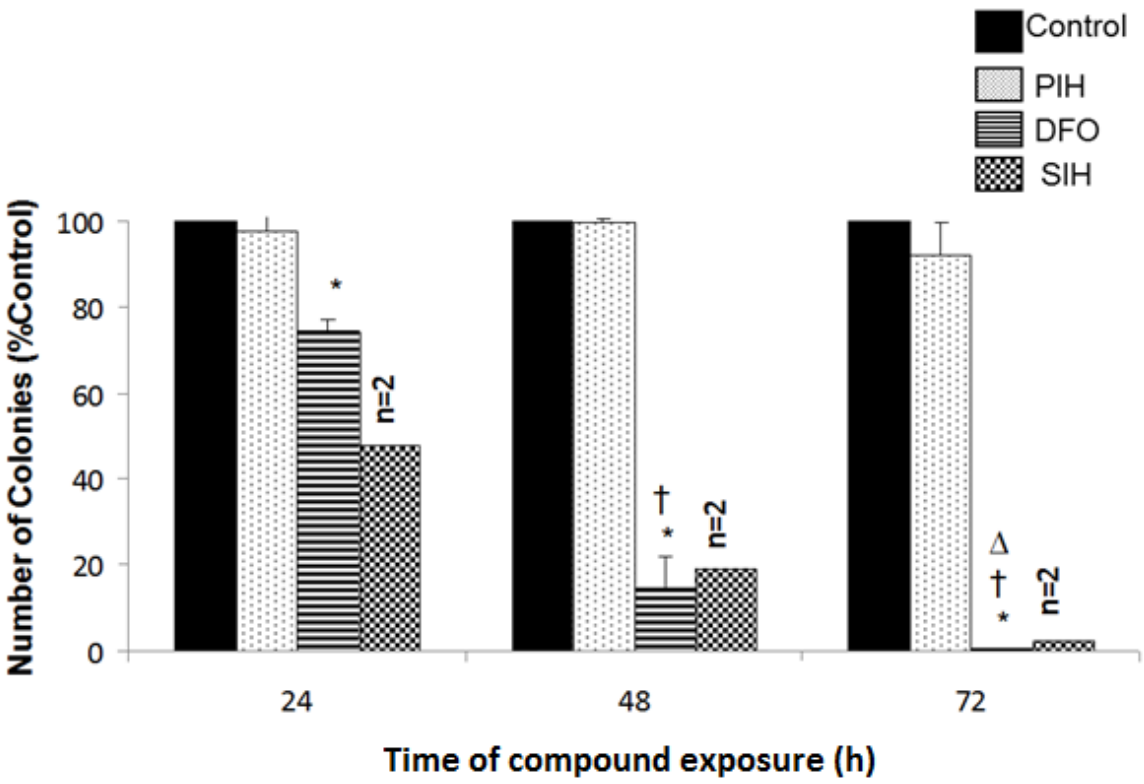

Figure 3.5*:* The evaluation of growth inhibitory effect of PIH, SIH, and DFO on HaCaT cells with the clony forming ability assay.

Exponentially growing cells were incubated for 24, 48, and 72 h with Fe chelators at a concentration of 100 µM. Cells were then seeded at single cell density, incubated for 14 days, stained and counted. The values are expressed as percentage of control (Mean ± SD) n=2-3.

* : $p < 0.05$ Significant difference between value and control.

┼ : $p < 0.05$ Significant difference between value and corresponding 24h

Δ : $p < 0.05$ Significant difference between value and corresponding 48h.

3.2.3 Effect of PIH, SIH and DFO on HaCaT Cell Proliferation as Measured by BrdU Incorporation Assay

To verify the above hypothesis, we evaluated the percentage of HaCaT cells in S phase of the cell cycle with BrdU incorporation assay following 72 h treatment with DFO, SIH and PIH at a final concentration of 100 µM. The results (**Fig 3.6**) revealed that both SIH and DFO are capable of efficiently decreasing the percentage of cells in S phase, although the effect with DFO was more pronounced than SIH. In contrast, compared to control cells, PIH-treatment did not show any change in the percentage of cells in S phase. These results implied that the observed decrease in percentage colony formation with DFO and SIH in CFA experiments (**Fig 3.5**) might be due to the fact that these compounds provoke a significant G1/S arrest in HaCaT cell cycle, leading to cell death as reflected by reduced colony formation. In contrast, the PIH-treated cells progress to S phase and therefore fully survive (**Fig 3.5** and **3.6**).

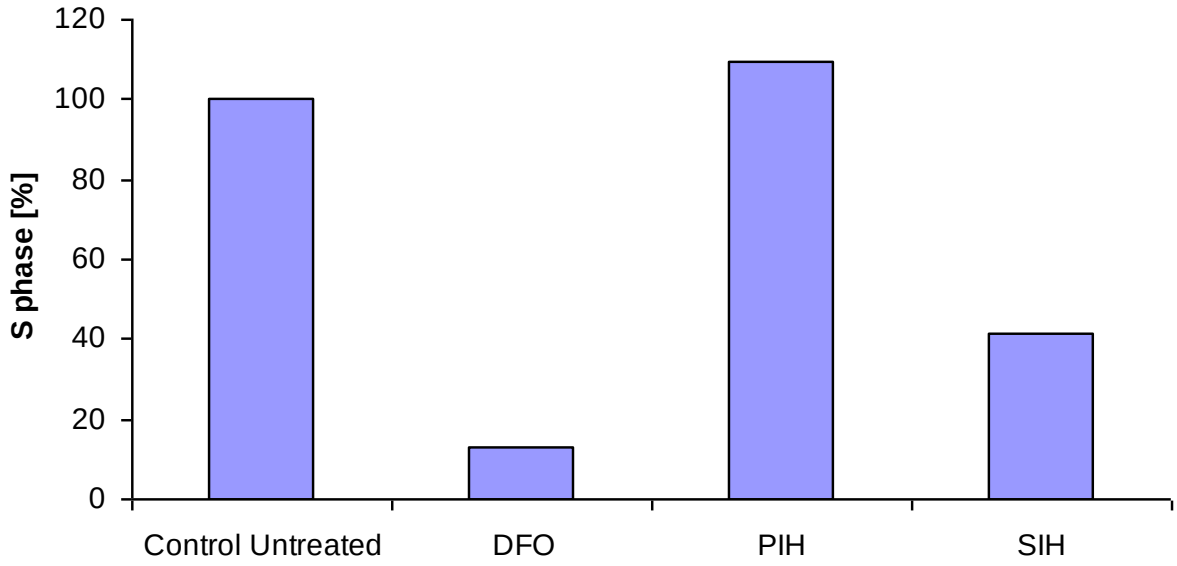

Figure 3.6: The evaluation of growth inhibitory effect of DFO, PIH and SIH HaCaT cells as measured by the BrdU-assay.

Exponentially growing cells were incubated for 72 h with the indicated compounds at a concentration of 100 µM prior to pulsing with BrdU (10 µM) for 1h, then harvested and processed by flow cytometry for determination of the percentage of cells in S phase. 20,000 events were collected and analysed.
The results were expressed as percentage of control (n=2).

3.2.4 Effect of PIH, SIH and DFO on HaCaT Cell Death as Measured by Annexin V / PI Dual Staining Assay

To further verify the above assumption, it was decided to quantify the percentage of cell death using the sensitive flow cytometry-based Annexin V / PI dual staining assay. For this purpose, the exponentially growing HaCaT cells were treated for 24, 48 or 72 h with SIH, PIH and DFO at a final concentration of 100 µM. The flow cytometry analysis (**Fig 3.7**) demonstrated that in agreement with CFA (**Fig 3.5**) and BrdU data (**Fig 3.6**), prolonged exposure of HaCaT keratinocytes to DFO and SIH provokes a time-dependent increase in cell death and at the 72 h time point, only 8% and 5% of cells survive, respectively. However the percentage of dead cells remained extremely low in cells exposed to PIH for the same period of time (**Fig 3.7**).

These results suggested that in contrast to PIH, DFO and SIH should have much higher inhibitory effect on the RR enzyme, since treatment of cells with both of these chelators led to substantial G1/S arrest of cells in cell cycle leading to cell death. This assumption is in agreement with previous findings by Richardson and coworkers who demonstrated that compared to PIH, SIH and DFO have much higher antiproliferative activity presumably because they are more potent inhibitors of RR (Richardson *et al*., 1995; Yu *et al*., 2006). Furthermore they demonstrated that in general, the pyridoxal (PIH) analogues show high Fe chelation efficacy but low anti-proliferative activity (Richardson *et al.*, 1995). Using the hepatocyte and reticulocyte cell models, they further demonstrated that among the PIH analogues, the least cytotoxic chelators (i.e. PIH, 101, and 107) were highly effective Fe chelators but lacked anti-proliferative activity (Richardson *et al.*, 1995).

A recent study on both normal and immortalized skin keratinocyte (HaCaT) versus oral normal and SCC cancer cell lines has also demonstrated that prolonged Fe chelation with DFO (72-96 h) induces cell death in all cell lines used (Lee *et al*., 2006). In the same study, the reduction in cell proliferation with DFO was also demonstrated in HaCaT cells grown in 3-dimensional (3D) organotypic collagen-based culture. DFO caused severe growth inhibition in the form of less epithelial maturation, decreased epithelial thickness and decreased surface keratinisation compared to controls.

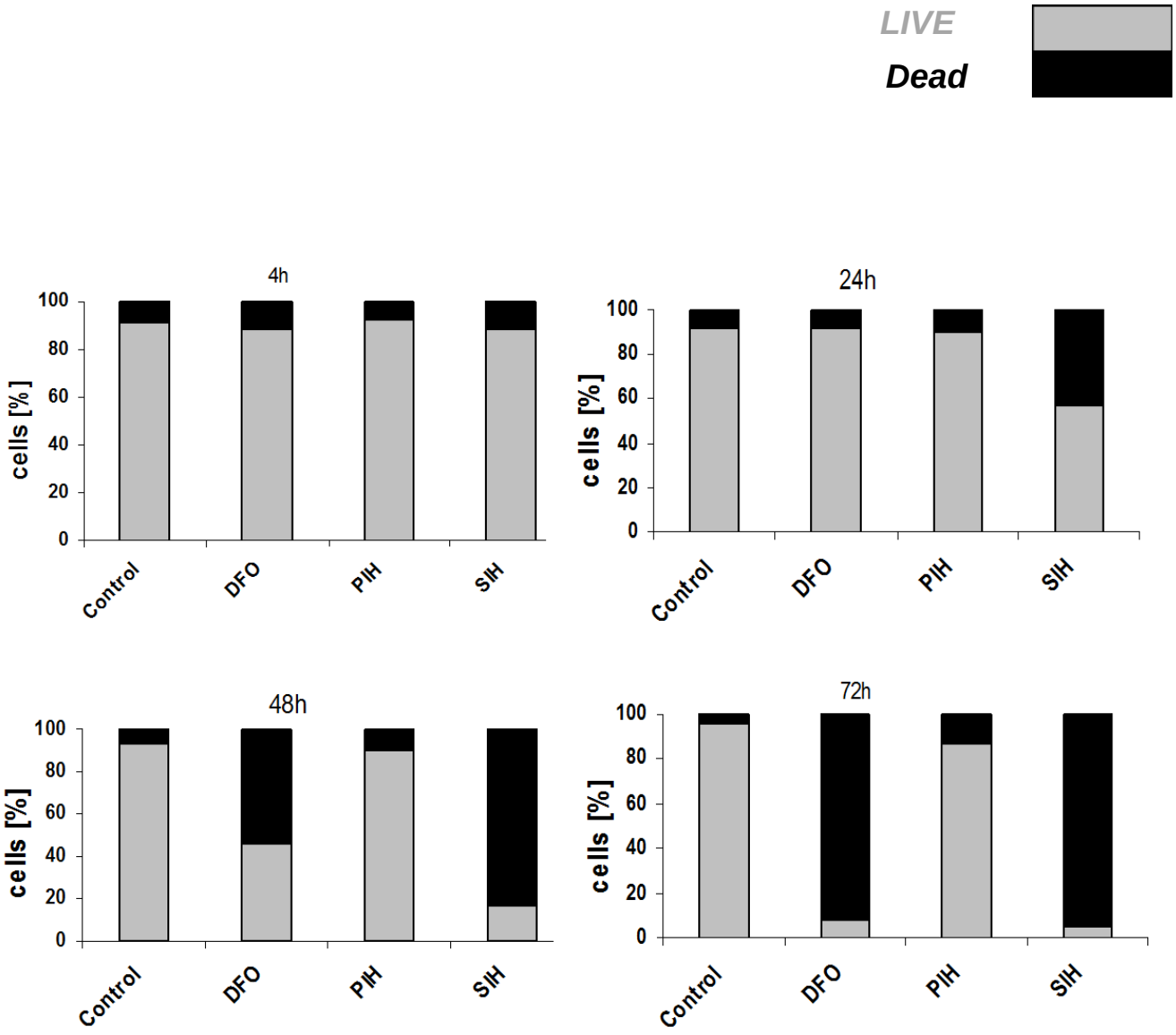

Figure 3.7: The evaluation of percentage of 'live' (grey) and 'dead' (black) HaCaT cells by flow cytometry 4, 24, 48 and 72 h following treatment with DFO, PIH and SIH.

Exponentially growing cells were incubated for 4, 24, 48 and 72 h with the indicated compounds at a concentration of 100 µM prior harvesting and dual Annexin-V/ PI staining, and processed by flow cytometry for determination of the percentage of dead cells. 10,000 events were scored . The results were expressed as percentage of total events recorded (n=1).

3.2.5 Effect of PIH and DFO on HaCaT Epidermal Cells in 3D De-epidermalised Dermis Raft Organotypic Culture

The low antiproliferative activity of PIH was further verified with morphological studies in a HaCaT 3D organotypic skin equivalent raft culture. **Fig 3.8** illustrates a typical section of a primary human keratinocyte raft made with DED and grown for 17 days.

For the purpose of this experiment, HaCaT cells were raised on a series of 3D de-epidermalised dermis (DED) and at day 7 of growth, they were treated with 100 µM DFO or PIH for 72 h. The media containing the chelators was then removed and replaced with fresh media. The cultures were then incubated for an additional 10 days and then stained with haematoxylin–Eosin for microscopic view. As it can be seen in **Fig 3.9**, the DED-raft cultures of the untreated HaCaTcells as well as those treated with PIH produced epithelial stratification with well-preserved morphologic differentiation and distinct *stratum corneum* that was comparable to that of normal keratinocytes illustrated in **Fig 3.8**. In contrast the DFO-treated culture produced a very thin *stratum corneum* (or at least invisible) and the epidermis thickness on average was lower when compared to that of control or PIH-treated cells. Furthermore the epidermal layer in DFO-treated epidermis appeared significantly damaged with the appearance of considerable holes within the tissue. Also the damaged cells appeared to have condensed chromatin, presumably due to their propensity to undergo apoptotic cell death as a result of G1/S cycle arrest by DFO (see **Fig 3.10**). These results further confirmed that in contrast to DFO, PIH lacks effective antiproliferative activity.

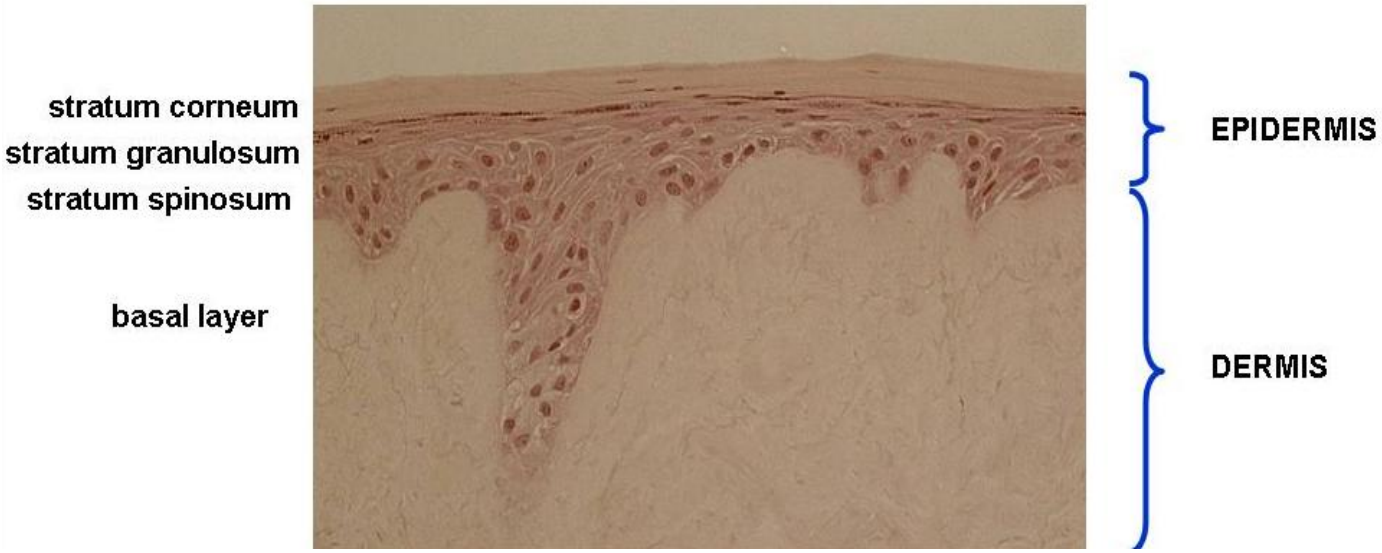

Figure 3.8: Typical section of a primary human keratinocyte raft made with DED and grown for 17 days.

The epidermal and dermal layers are clearly indicated for information.

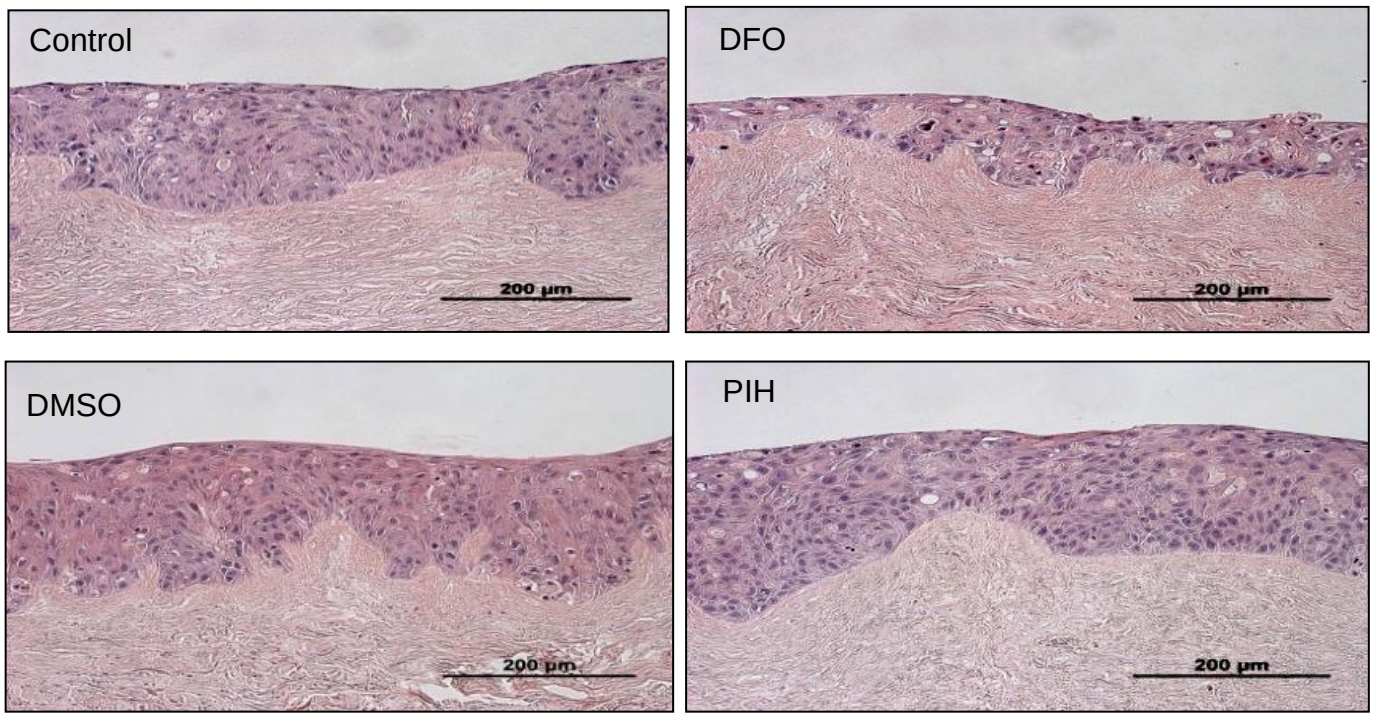

Figure 3.9: Morphological study of DED-Raft HaCaT cultures treated with 100 µM DFO and PIH for 72 h.

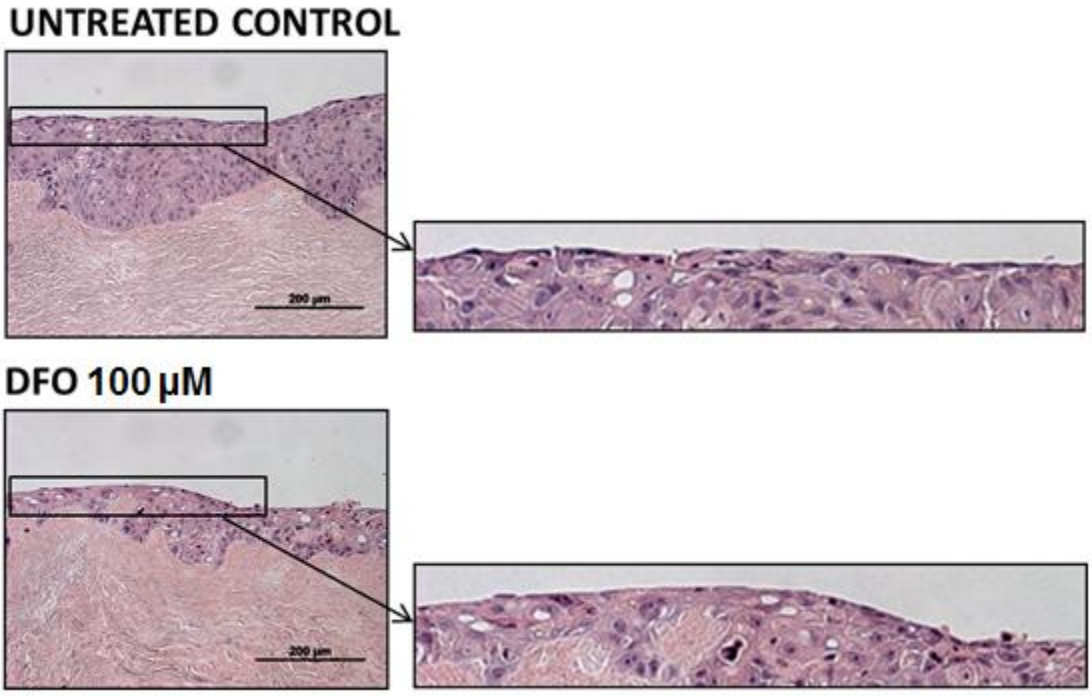

Figure 3.10: Magnification of the epidermal layer of control and DFO-treated DED-rafts of Figure 3.9.

3.2.6 Determination of IC50 for PIH, SIH and DFO

All the chelators used in this study are known to have similar strong iron binding activities but DFO and SIH were found to have more potent antiproliferative activity than PIH. Therefore it was of particular interest to determine the IC50 values of these chelators (i.e. the Fe chelator doses necessary to inhibit the proliferation of cells by 50%) as a mean to evaluate the extent of their growth inhibitory effect in skin cells. For this purpose FEK4 and HaCaT cells were analyzed by the MTT assay 72 h following treatment with a range of doses of PIH, SIH, and DFO, as detailed in the **Materials and Methods** section. The results were expressed as a percentage of the control values.

Table III summarises the IC50 values obtained by the MTT assay for PIH, SIH and DFO in the skin cell models of the study. As it can be seen, the IC50 values for PIH were overall much higher that SIH and DFO for all the cell lines used, consistent with the notion that this chelator is the least effective antiproliferative agent. Furthermore as it was demonstrated above, the decrease in cell proliferation with PIH was transient as it only occured in the MTT assay in the presence of the compound. In contrast, SIH and DFO appeared to have a much stronger growth inhibitory effect than PIH as reflected by their lower IC50 values obtained for all the cell lines, except PM1 that required a much higher concentration of these chelators to achieve the IC50 value. These results suggested that the response of cells to the antiproliferative action of Fe-chelators depends not only on the chelator identity but also on the cell type.

Table III. Comparison of the IC50 values of Fe chelators in skin cell models

Cell line	PIH (μM)	SIH (μM)	DFO (μM)
FEK4	100	50	50
HaCaT	100	20	10
KCP7	200	50	10
KCP8	200	20	20
PM1	200	200	200
Met 2	200	50	10
MKPS	200	10	20

Note: Average from 2-8 experiments.

3.2.7 Effect of Fe^{3+}-Chelator Complexes on Cellular Proliferation

To confirm that the observed growth retardation / inhibitory effects of the Fe chelators used in the study were related to their Fe chelating property, additional MTT assays were performed with DFO, SIH and PIH where the chelators were complexed (or not) with Fe^{3+} (Fe-citrate). The compounds were then added to the cells at their corresponding IC50 (see **Table III**) and higher concentrations, so that the observed effect could also be verified in a dose-dependent context.

As it can be seen in **Fig 3.11**, the treatment of FEK4 cells with iron saturated PIH, SIH and DFO reversed significantly the observed decrease in enzymatic activity (as measured by MTT assay) of the cells treated with Fe chelators alone at both their IC50 and higher concentrations. For example the comparison at IC50 concentrations revealed that iron saturation of PIH could substantially increase the enzymatic activity of cells treated with PIH alone from 46% ± 9 to 85% ± 10. Also iron saturation of SIH increased the enzymatic activity of SIH-treated cells from 48% ± 5 to 94% ± 5. Finally iron saturation of DFO increased the enzymatic activity of DFO-treated cells from 52% ± 4 to 84% ± 12, respectively.

Similarly when HaCaT cells were treated with 100 μM PIH, 20 μM SIH and 10 μM DFO complexed with Fe^{3+}, the cellular enzymatic activity also significantly increased when compared to treatment with Fe chelatros alone (**Fig 3.12**) (i.e. from 54% ±8 in PIH-treated cells to 75% ± 9 in PIH+ Fe^{3+}-treated cells; from 37% ± 13 in SIH-treated cells to 97% ± 6 in SIH+ Fe^{3+}-treated cells and from 53% ±8 in DFO-treated cells to 91% ± 16 in DFO+ Fe^{3+}-treated cells, respectively.

Interestingly in both FEK4 and HaCaT cells, the iron saturation of Fe chelators at the IC50 or at higher concentrations yielded the same increase in enzymatic activity.

We also checked the response of PM1 and Met2 to DFO, PIH and SIH saturated or not with Fe^{3+} at their corresponding IC50 concentrations (**Fig 3.13**), results for PIH are demonstrated in **Fig 3.18**. Again here, the iron saturation of Fe chelators substantially reversed the observed decrease in enzymatic activity of the chelator-treated cells, although the effect was more pronounced with DFO-Fe^{3+} than SIH- and PIH-Fe^{3+}.

Overall the results confirmed that saturation of Fe chelators with iron reverses the antiproliferative activities of the chelators at both IC50 and higher concentrations, so the growth retardation/inhibitory effects of Fe chelators were iron-related. These results were in agreement with previous studies carried out with these chelators in other cell models (Richardson *et al.*, 2005)

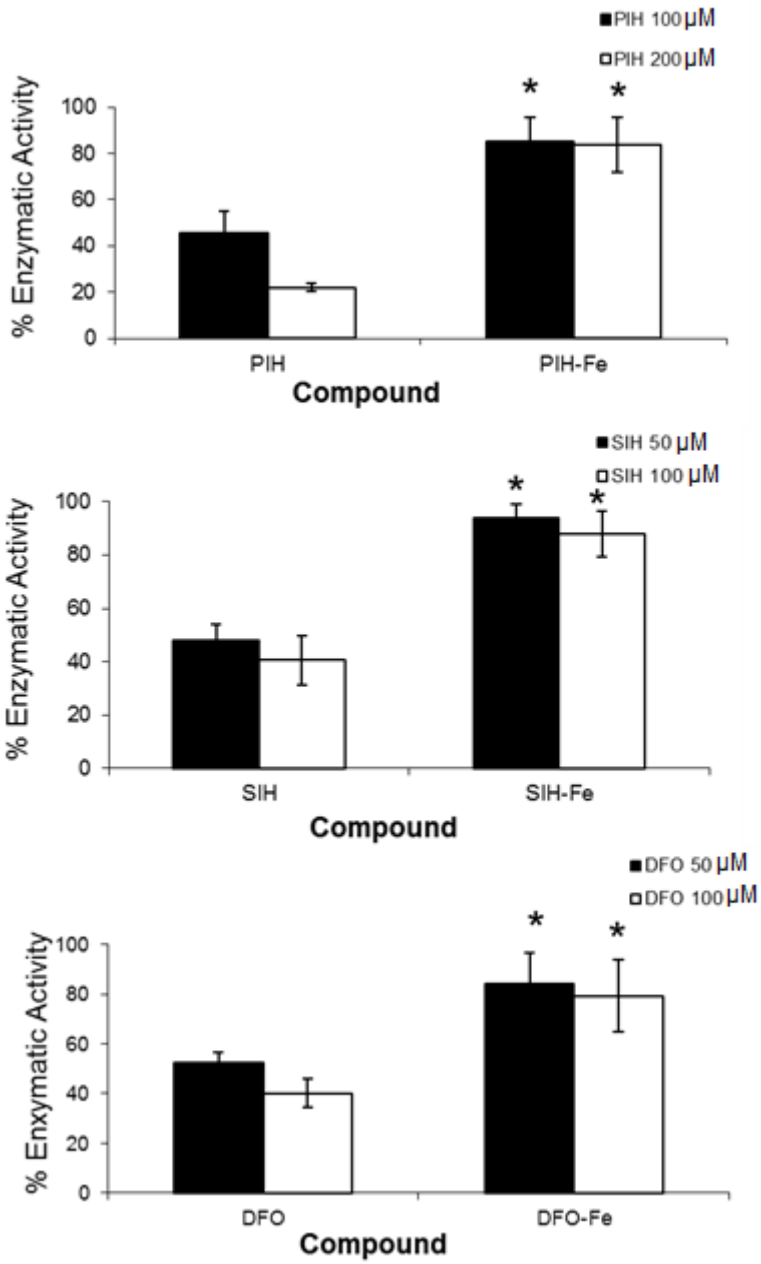

DFO:Iron = 1:1

SIH:Iron = 2:1

PIH:Iron = 2:1

Figure 3.11: Growth inhibitory effect of PIH, SIH, and DFO (+/- iron-citrate) on FEK4 cells as measured by the MTT assay.

Exponentially growing cells were incubated for 72 h with compounds complexed (or not) with iron, prior to the MTT assay, as described in the **Materials and Methods** section. The results were expressed as the percentage of untreated control (Mean ± SD; n=3-5)

* : $p < 0.05$ Significant difference from the corresponding untreated control.

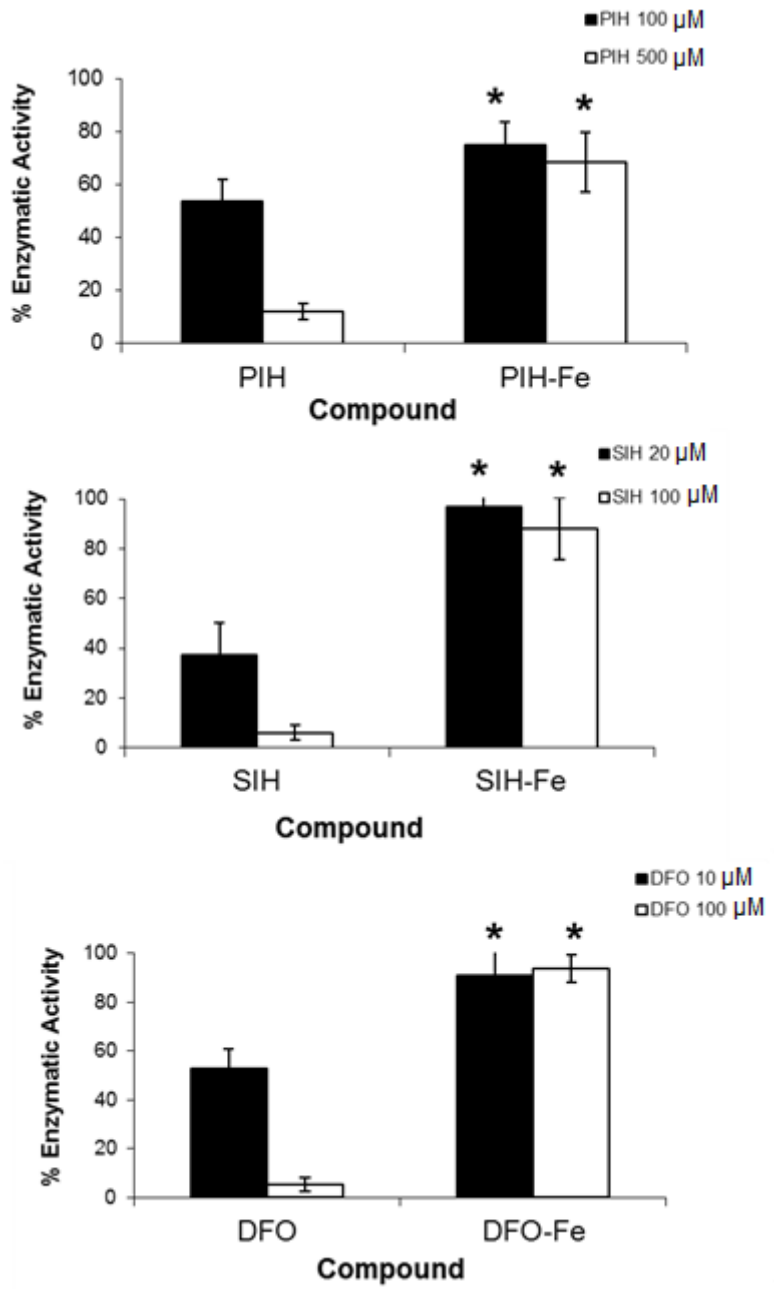

DFO:Iron = 1:1

SIH:Iron = 2:1

PIH:Iron = 2:1

Figure 3.12: Growth inhibitory effect of PIH, SIH, and DFO (+/- iron-citrate) on HaCaT cells (MTT assay).

Exponentially growing cells were incubated for 72h with compounds complexed (or not) with iron, prior to the MTT assay, as described in **Materials and Methods** section. The results were expressed as a percentage of the untreated control (Mean ± SD; n=3-5).

*: $p < 0.05$: Significant difference from the corresponding untreated control.

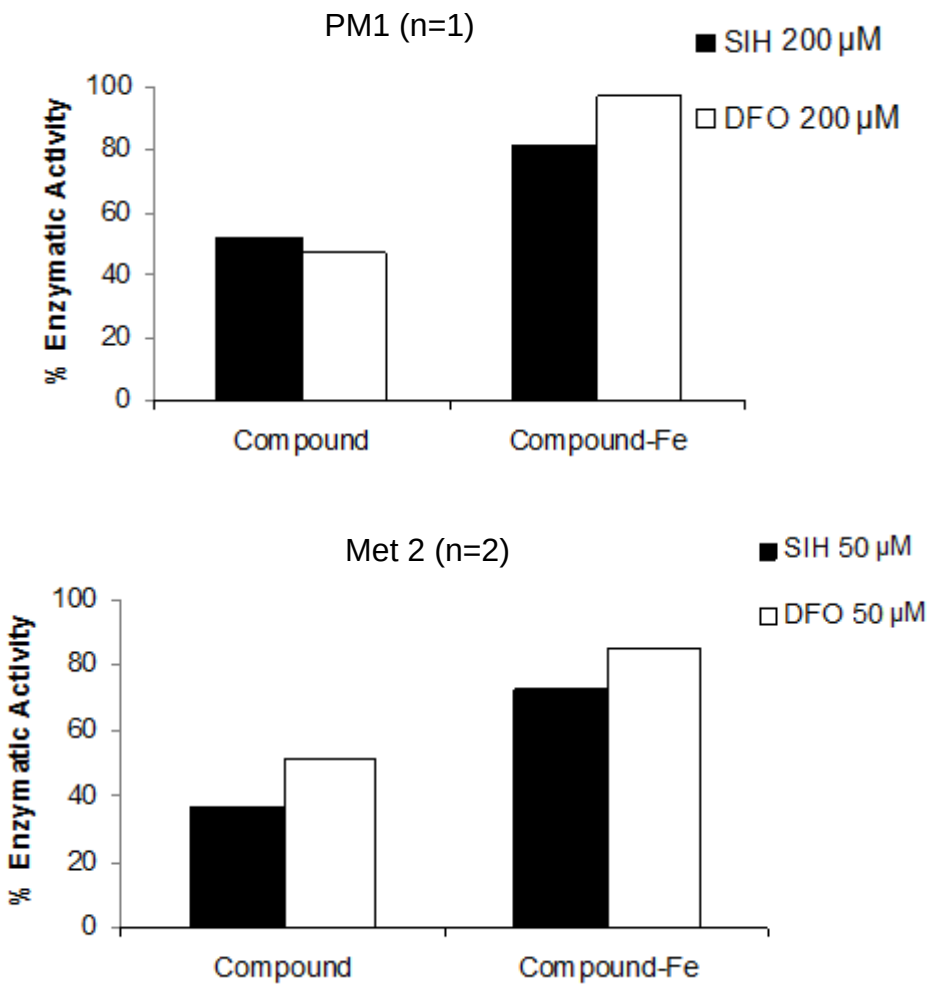

DFO:Iron = 1:1

SIH:Iron = 2:1

Figure 3.13: Growth inhibitory effect of SIH, and DFO (+/- iron-citrate) on PM1 and MET2 cells (MTT assay).

Exponentially growing cells were incubated for 72 h with compounds complexed (or not) with iron, prior to the MTT assay, as described in **Materials and Methods** section. The results were expressed as a percentage of the untreated control.

3.3 Antiproliferative Effect of Caged Iron Chelators

While SIH as a lipophilic Fe chelator with strong antiproliferative activity appears to be suitable for topical Fe chelation therapy of skin hyperproliferative diseases such as skin cancer, the prolonged topical application of SIH *per se* may be harmful as it could locally cause starvation of the normal skin cells surrounding the skin tumour/lesion from the essential nutrient iron. Our novelly designed light-activatable caged iron chelators (CICs) should circumvent this problem, as in practice the compounds will be first applied topically and then switched on selectively *in situ* within the tumour in a dose- and context-dependent manner. This section provides the summary of the pilot study performed with the aim of evaluating the antiproliferative activity of CICs derived from PIH and SIH (i.e. 2NPE−PIH and 2NPE−SIH, respectively) following uncaging with UVA radiation.

3.3.1 *In vitro* Characterisation of 2NPE-PIH and 2NPE-SIH (+/- UVA) by Reverse Phase HPLC

The first stage of this project involved the chemical synthesis of 2NPE-PIH and 2NPE-SIH in Nottingham under supervision of Dr James Dowden who initially designed and synthesized these CICs in collaboration with Dr Pourzand (see (Yiakouvaki *et al.*, 2006). Following synthesis and evaluation of the purity of the compounds in Nottingham with NMR and MS analyses, the decaging profile of the CICs (+/- UVA or ambient light) was further characterised in the Bath laboratory in collaboration with Dr Ian Eggleston:

Fig 3.14A illustrates the reverse HPLC profile of 2NPE-PIH and PIH with or without irradiation with a UVA dose of 250kJ/m^2 as compared to the previously obtained profile of 2NPE-SIH and SIH (+/-UVA, 250kJ/m^2) by Yiakouvaki *et al.* (2006) (**Fig 3.14B**). As can be seen, UVA irradiation triggers the uncaging of the 2NPE-PIH and 2NPE-SIH CICs and converts them to parental compounds PIH and SIH, respectively. This is further illustrated by co-injection of UVA-irradiated CICs with pure parental compounds (**Fig 3.14A** and **3.14B**). The uncaging of 2NPE-PIH and 2NPE-SIH by UVA and the release of active PIH and SIH is schematised in **Fig 3.15**.

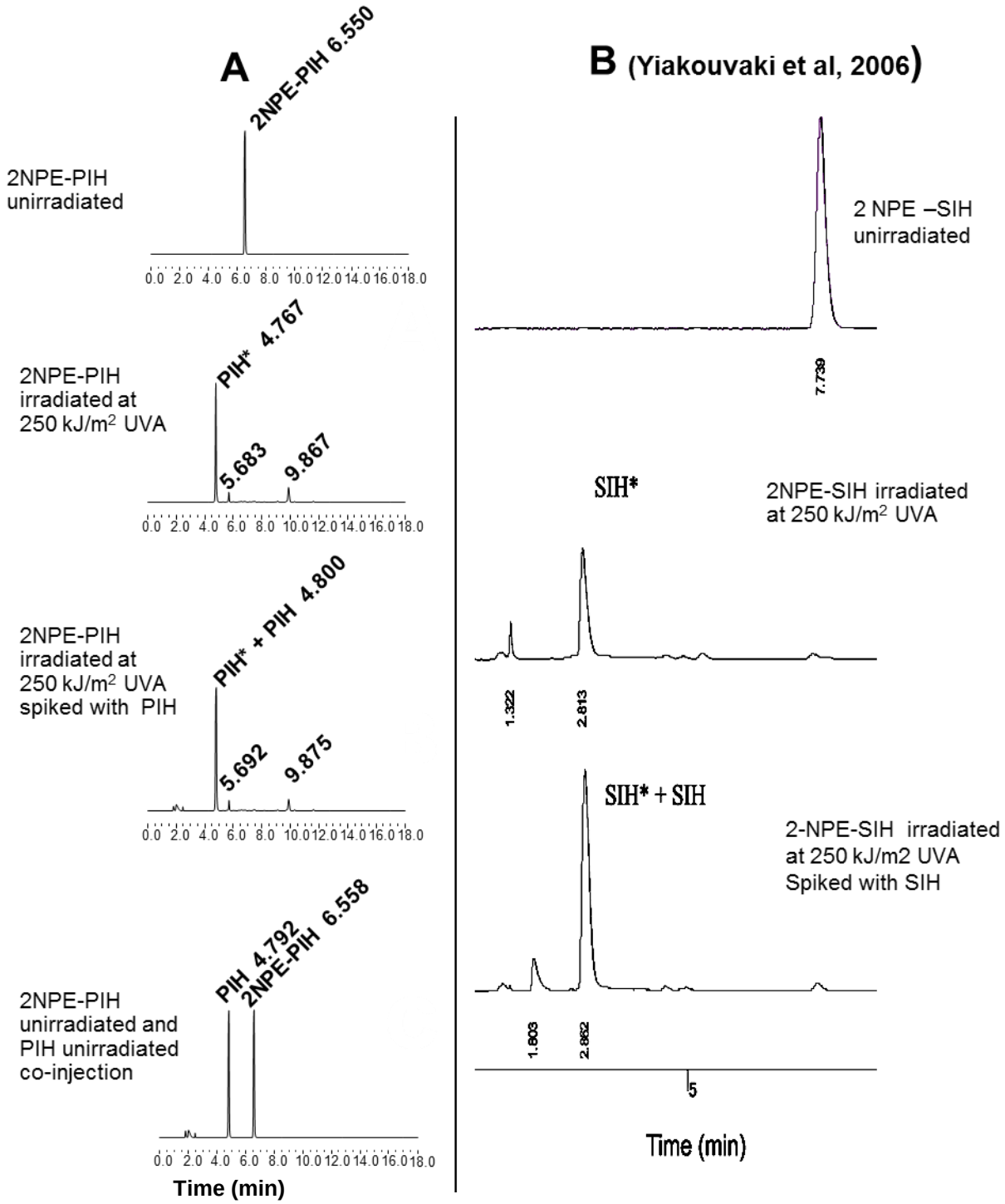

PIH*: UVA-irradiated 2NPE-PIH

Figure 3.14: Prototype photo-activatable CICs (in collaboration with Dr Ian Eggleston).

2-NPE-SIH /PIH were run first (0.1mm in CH3CN/aq 1:1); then same samples were run after irradiation with 250kJ/m2 UVA; and irradiated samples were run with parental compounds i.e. with SIH or PIH co-injection.

To evaluate the minimum UVA dose necessary for uncaging of 2NPE-SIH and 2NPE-PIH caged-chelators and release of parental compounds, the CICs were exposed to a range of doses of UVA (i.e. 5, 10, 20, 50, 100 and 250 kJ/m^2) and then the relative peak areas of the reverse-HPLC profiles were quantified 1h following irradiation. The results (**Fig 3.16**) revealed that even at very low doses of 5-10 kJ/m^2, UVA could trigger the uncaging of the CICs. For 2NPE-SIH a low dose of 50 kJ/m^2 was sufficient to fully release the uncaged compound i.e. SIH. At natural exposure level, 50 kJ/m^2 will be equivalent to 10-15 min exposure to sunlight at sea level (i.e. a sub-erythemal non-damaging dose). Typically with a fluence rate of 150 W/cm^2, and a distance of 15 cm, the irradiation time for this dose will be around 2-3min in the laboratory setting (or during CIC-based therapy in the clinical setting). For 2-NPE-PIH however higher doses of 100-250 kJ/m^2 were necessary for clean conversion of the caged-PIH to parental PIH. In comparison, in psoralen-UVA (PUVA) therapy, the typical UVA dose applied for sensitisation of skin is between 5-50 kJ/m^2 depending on the skin type of the patients. However PUVA is not an effective single therapy and usually necessitates multiple treatments that would cause an accumulation of the UVA doses applied. The cumulative doses in PUVA treatments of psoriatic patients could reach values up to 500kJ/m^2. The single and lower UVA dose treatment necessary to uncage the CIC compounds might therefore provide a clear advantage for caged-iron chelation therapy of skin hyperproliferative disease when compared to PUVA.

To evaluate the stability of the prototype CICs, additional reverse-HPLC analyses were performed with samples of 2NPE-PIH and –SIH kept for a few days at room temperature under ambient light. These results (not shown) revealed that the compounds are fully stable at ambient light and uncaging of the compounds occurs only upon exposure to a UVA broad spectrum lamp (i.e. 340-400nm with maximum peak at 364nm)

To exclude partial uncaging of the CICs, a UVA dose of 250kJ/m^2 was used for experiments involving CIC uncaging by UVA.

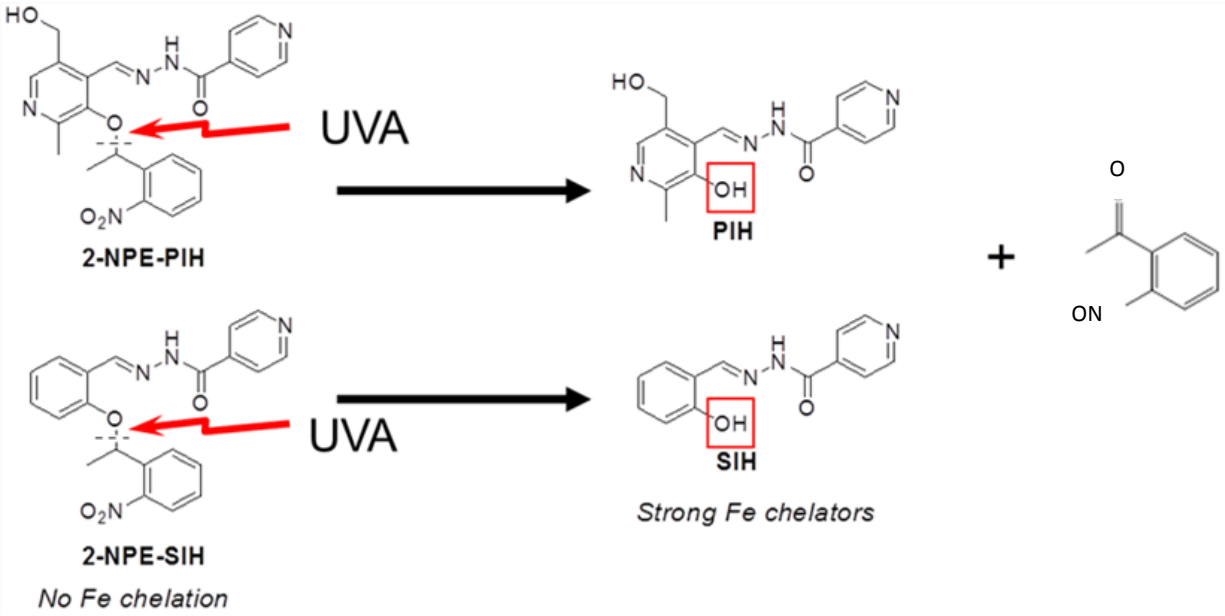

Figure 3.15: Prototype photoactivatable CICs. Reproduced with the permission of Dr Ian Eggleston

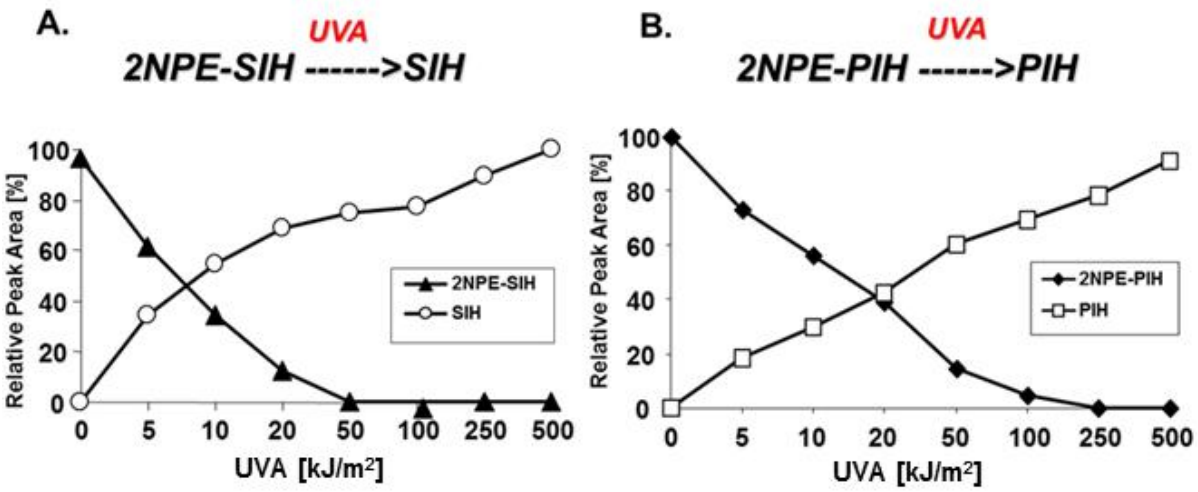

Figure 3.16: Reverse-HPLC analysis of UVA-induced uncaging of 2NPE-SIH and 2NPE-PIH.

Quantifications of relative peak areas of reverse-HPLC analysis of (A) 2NPE-SIH and SIH;

(B) 2NPE-PIH and PIH (collected at 280nm 1h post-UVA treatment).

3.3.2 Comparative IC50 Values for Parental PIH, SIH and their UVA-irradiated Caged Derivatives

To compare the antiproliferative activity of uncaged CICs versus the parental compounds, a series of MTT assays in FEK4 and HaCaT cells 72 h following treatment with a range of concentrations of the compounds (see a representative example in **Fig 3.17**) was performed. These experiments allowed determination of the IC50 values of both parental and their UVA-irradiated caged derivatives. **Table IV** provides the summary of the main findings as outlined below:

- The IC50 values calculated for UVA irradiated 2-NPE-PIH-treated FEK4 and HaCaT cells were similar to that of parental PIH (i.e. 100 μM). Furthermore the unirradiated 2-NPE-PIH had no antiproliferative activity, consistent with the notion that the UVA-mediated release of PIH from the caged-compound is necessary for its antiproliferative action (**Fig 3.17**).
- The IC50 values calculated for SIH and its UVA-irradiated caged derivative were found to be around 50 μM and 20 μM, respectively for FEK4, and 20 μM for HaCaT cells. Again the unirradiated 2-NPE-SIH had no apparent antiproliferative activity, consistent with the notion that the UVA-mediated release of SIH from the caged-compound is necessary for its antiproliferative action (**Fig 3.17**).

To ascertain that the antiproliferative activity of UVA-irradiated CICs is related to their Fe chelation properties as a result of their conversion to their respective parental compounds, the UVA-irradiated 2NPE-PIH were complexed with Fe^{+3} using iron citrate and then performed MTT assays were then carried out 72 h following addition of the compound (at its IC50 concentration) to HaCaT cell cultures. The results (**Fig 3.18**) revealed that iron saturation of both parental PIH and its UVA-irradiated caged version significantly reduced the decrease in enzymatic activity following treatment of cells with PIH and UVA-irradiated 2NPE-PIH alone.

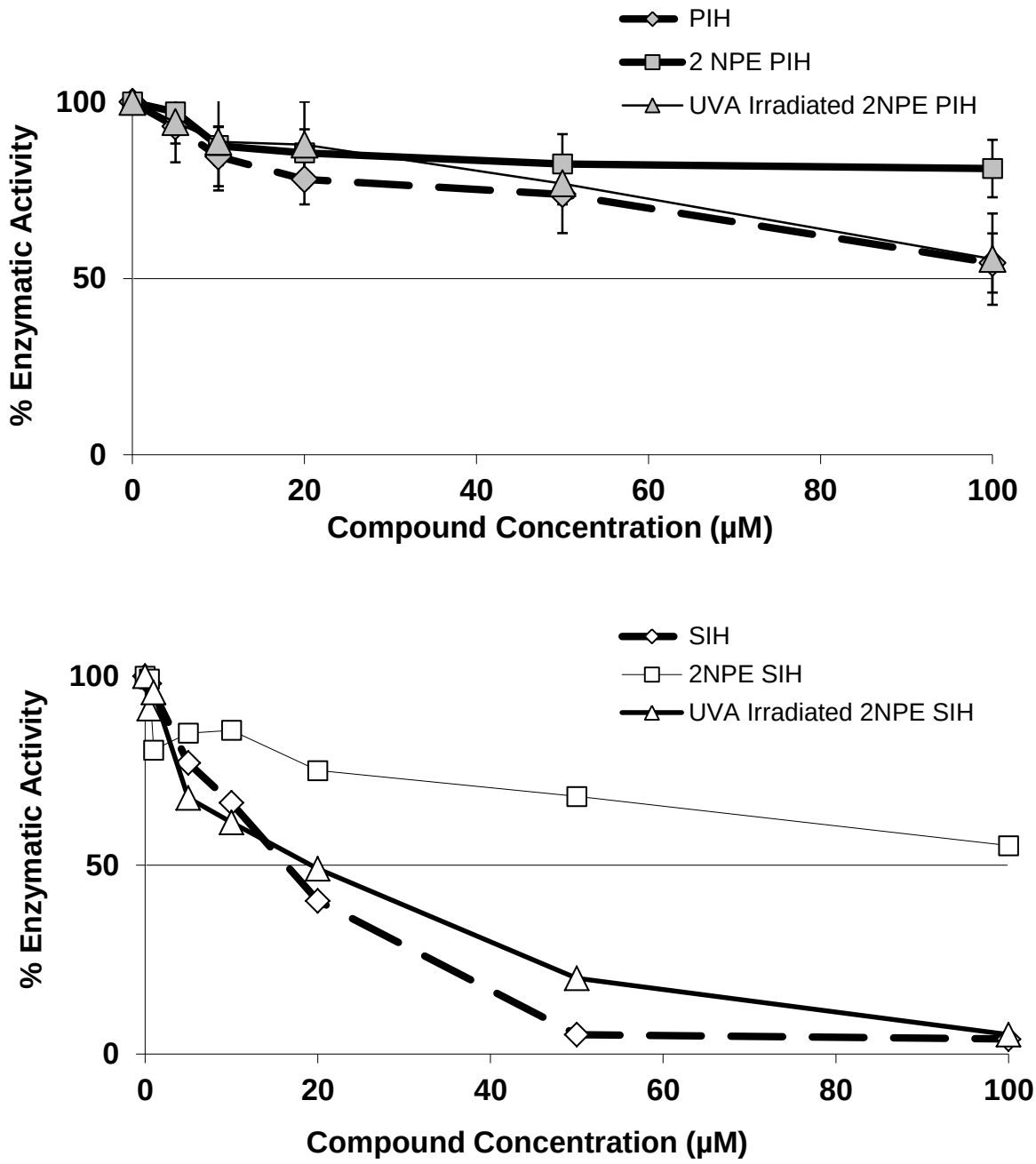

Figure 3.17: The deterimation of IC50 values for PIH/ SIH and 2NPE-PIH/-SIH (+/- UVA, 250 kJ/m^2) HaCaT cells with the MTT assay.

The results are expressed as mean ± SD, (n=3) for PIH and its derivatives, and (n=2) for SIH and its derivatives.

Table IV. The comparison of IC50 values of PIH, SIH to UVA-irradiated 2NPE-PIH and 2NPE-SIH in FEK4 and HaCaTcells (MTT assay- 72h post treatment)

Cell line	Compound	IC50 (μM)
FEK4	PIH	100
FEK4	UVA-irradiated 2NPE-PIH	100
FEK4	SIH	50
FEK4	UVA-irradiated 2NPE-SIH	20
HaCaT	PIH	100
HaCaT	UVA-irradiated 2NPE-PIH	Above 100
HaCaT	SIH	20
HaCaT	UVA-irradiated 2NPE-SIH	20

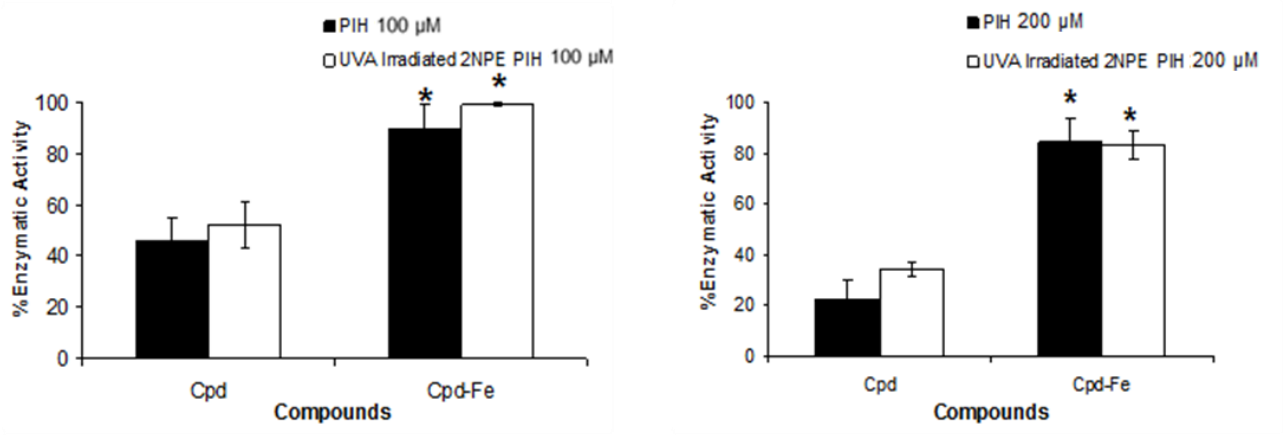

DFO:Iron = 1:1

SIH:Iron = 2:1

PIH:Iron = 2:1

Figure 3.18: Growth inhibitory effect of PIH and UVA irradiated 2NPE PIH(+/- iron-citrate) on FEK4 cells (MTT assay).

Exponentially growing cells were incubated for 72 h at concentrations of 100 µM or 200 µM of compounds complexed (or not) with iron, prior to MTT assay, as described in **Material and Methods** section. The results were expressed as percentage of the untreated control (Mean ± SD; n=3)

* : $p < 0.05$ Significant difference from the corresponding free ligand.

3.3.3 Effect of PIH/SIH, 2-NPE-PIH/SIH and Subsequent UVA Irradiation on the Proliferation of Skin Cells

After assessing the antiproliferative effect of parental PIH/SIH and their UVA-irradiated caged derivatives, it was important to assess the antiproliferative activity of the CICs uncaged *in situ* inside the cells. For this purpose, exponentially growing FEK4 and HaCaT cells were first treated for 18 h with 2NPE-SIH or SIH and 2NPE-PIH or PIH, respectively, at a final concentration of 100μM and then irradiated with a range of UVA doses. Following UVA irradiation, the cells were incubated for 72 h in the absence of compounds and then analysed with the MTT assay.

The results (**Fig 3.19A**) demonstrated that in the absence of UVA, caged-PIH does not alter the cellular enzymatic activity of HaCaT cells, but following UVA irradiation provides a significant decrease in the observed activity of cells. UVA-irradiated controls only marginally altered the enzymatic activity of HaCaT cells, indicating that the effect observed in caged-treated irradiated cells is unrelated to radiation but rather related to uncaging of the 2NPE-caging group and release of active antiproliferative PIH compound. The antiproliferative activities of UVA-irradiated PIH- treated cells were quite similar to those obtained with caged-PIH, implying efficient *in situ* uncaging of caged-PIH by UVA even at lower doses of 50 and 100kJ/m^2. Similarly, when SIH and 2NPE-SIH were tested in FEK4 cells, the antiproliferative activity of UVA-irradiated SIH-treated cells was also quite similar to that obtained with UVA-irradiated caged-SIH (**Fig 3.19 B**). Nevertheless UVA irradiation of FEK4 cells in the absence of compounds revealed higher toxicity at 250 kJ/m^2. This is in agreement with previous findings from this laboratory that have shown that FEK4 fibroblasts are more susceptible to UVA irradiation than HaCaT cells (Zhong *et al.*, 2004). Nevertheless the lower non-damaging UVA dose of 50 kJ/m^2 appeared to be sufficient to uncage the 2NPE-SIH in agreement with the *in vitro* uncaging UVA dose evaluated by the reverse HPLC data. Furthermore the results of **Fig 3.19B** suggested that for 2NPE-PIH the lower UVA doses of 50 and 100 kJ/m^2 are also effective in *in situ* uncaging as the effect observed with the caged-PIH using the MTT assay was quite similar to that obtained with parental compound upon low doses of UVA.

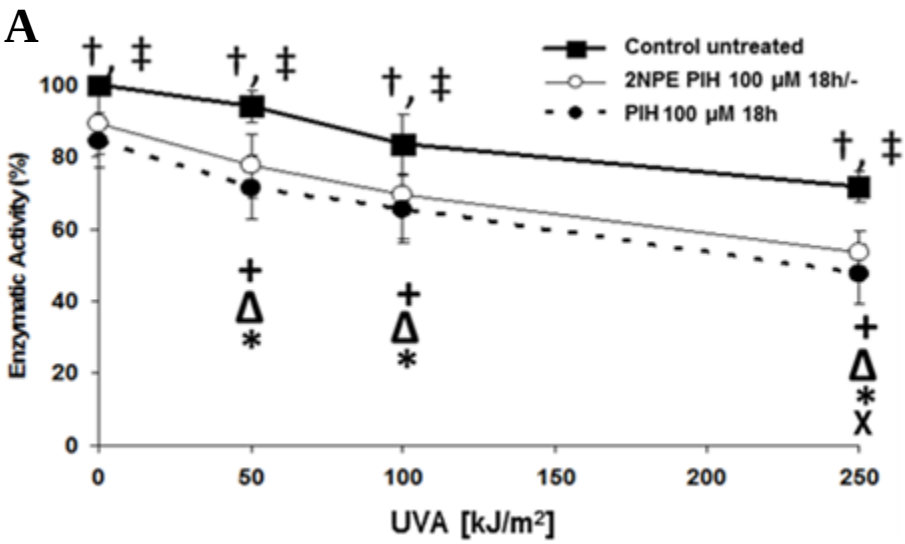

PIH 100µM 18h: PIH was added for 18h prior to UVA irradiation and then removed.

2NPE PIH 100µM 18h : Caged PIH was added for 18h prior to UVA irradiation and then removed.

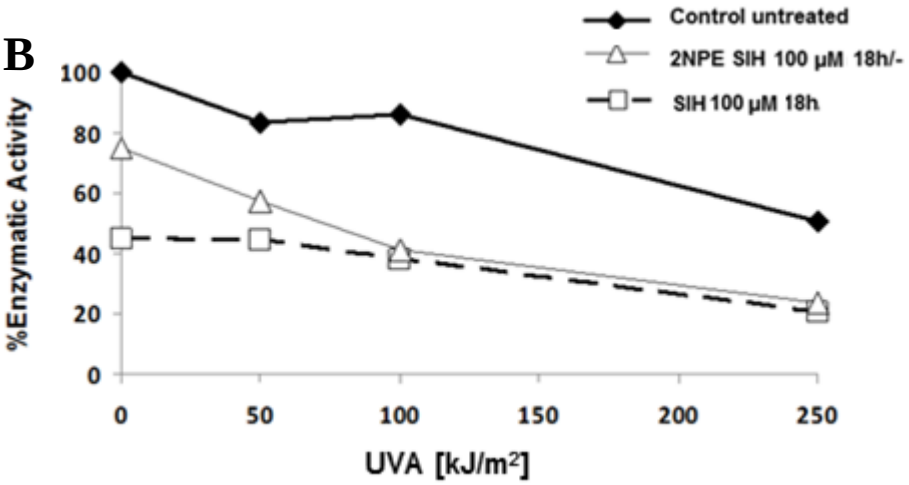

SIH 100µM 18h: SIH was added for 18h prior to UVA irradiation and then removed.

2NPE SIH 100µM 18h : Caged PIH was added 18 h prior to UVA irradiation then removed.

Figure 3.19: The evaluation of cell proliferation following treatment of **(A) HaCaT** cells with PIH and 2NPE-PIH +/-UVA (n=3) and treatment of **(B) FEK4** cells with SIH and 2NPE-SIH +/-UVA (n=2) with MTT assay. *The results are expressed as mean ± SD.*

T-test (vertical comparisons):

†: ($p < 0.05$), significant difference between caged PIH treated -/+UV and untreated cells -/+UV.

‡ : ($p < 0.05$), significant difference between PIH treated -/+UV and untreated cells -/+UV.

□: ($p < 0.05$), significant difference between PIH treated -/+UV and Caged PIH treated cells -/+UV.

T-test (horizontal comparisons):

+: ($p < 0.05$), significant difference between unirradiated and irradiated cells.

Δ : ($p < 0.05$), significant difference between Caged PIH treated and Caged PIH + UV treated cells.

* : ($p < 0.05$), significant difference between PIH treated and PIH + UV treated cells.

3.4Concluding remarks

The evaluation of the antiproliferative activity of PIH and SIH and their caged derivatives in our cell models revealed that while short-term (i.e. 4 -18 h post - UVA) exposure of cells to 2NPE-based CICs provides protection against UVA-induced oxidative damage with no apparent toxicity (see Yiakouvaki *et al.*, 2006), the prolonged (i.e. 24 – 72 h) exposure of cells to parental SIH or UVA-irradiated 2NPE-SIH triggers growth inhibition because of G1/S arrest in the cell cycle leading to substantial cell death. PIH and UVA-irradiated PIH on the other hand only caused transient growth retardation in cells in the form of a delayed S phase but had no apparent toxicity to skin cells, since the percentage of dead cells remained extremely low in cells exposed to these compounds for the same length of time. These results highlighted the importance of the choice of the parental Fe chelators in determining the level of toxicity of cells. Based on these results, 2NPE-PIH, that had very low toxicity, appeared to be the best candidate for skin photoprotection. In contrast, 2NPE-SIH that triggered high levels of cell death upon UVA light appeared to have potential for topical caged-iron chelation therapy of iron-related skin disorders, notably skin cancer. The low toxicity of UVA-irradiated 2NPE-PIH was further confirmed in morphological studies in 3D organotypic raft cultures using the DED dermis.

The growth-retardation or -inhibitory effects observed with Fe chelators or uncaged CICs were related to their iron-chelating property, as their saturation with iron, could reverse their antiproliferative activity in analysed skin cells. Finally, the studies aimed at evaluating the antiproliferative activity of CICs upon *in situ* uncaging with low doses of UVA revealed that in the absence of UVA, 2NPE−PIH and –SIH do not alter the cell growth, but following 'low' UVA radiation doses, they provide a significant decrease in growth rate of cells that is comparable to the effects observed with the parental chelators alone.

Taken together, these data indicated that 2NPE-PIH, which possesses very high iron chelating potential, but low antiproliferative activity (i.e. upon uncaging by UVA), is more suitable for skin photoprotection. In contrast, 2NPE-SIH which remains inactive inside the cells until its strong iron binding activity and high antiproliferative properties are activated by UVA, offers a highly selective and dose-controlled alternative for the treatment of hyperproliferative skin disorders such as skin cancer and psoriasis.

3.5 Future Work

Although the pilot study performed in this PhD project provided the first evidence for the suitability of 2NPE-SIH for caged-iron chelation therapy of skin hyperproliferative disease, it is clear that more data are still required to validate this approach. One of the essential requirements for the continuation of this project is to study the antiproliferative potential of this promising prototype CIC in additional cell models of cancerous and psoriatic cell lines. Also the effect observed in monolayer cultures should be further validated in 3D DED raft cultures so that the long-term antiproliferative action of the CIC could be clearly demonstrated. At this point, it will also be necessary to evaluate the minimum UVA dose necessary to uncage the CIC compound in the epidermal layer of the 3D raft culture. Dr Reelfs from this laboratory has already established an enzymatic protocol that would allow the separation of the epidermal layer of the rafts and further digestions in order to obtain the KC cell suspension. This cell suspension can be analysed with the CA assay by flow cytometry to evaluate the modulation of LIP in epidermal layers treated with CICs + UVA. Furthermore Dr Eggleston's laboratory are presently designing a series of fluorescent 2NPE-SIH molecules that could allow the visualization of the depth of penetration of the CICs in epidermal layer of rafts with fluorescence microscopy. Such studies are necessary to complement the studies performed in this thesis.

Following the above investigations, the antiproliferative action of 2-NPE-SIH-type CICs should then be validated in skin xenografts of cancerous and psoriatic cell lines in animal models. At this point further measures have also to be taken to find out the best topical formulation for efficient administration of the CICs.

Future work should also include the design of more improved CICs with new Fe chelators and new caging groups allowing uncaging at lower UVA doses while keeping the high lipophilicity, high iron-binding activity and high antiproliferative activity upon uncaging. An in-depth analysis of novel and improved CICS might allow then the selection of CICs with the most efficient growth inhibitory/ iron binding ability for subsequent *in vivo* testing in order to identify the most promising CIC(s) for topical caged iron-chelation therapy of iron-related skin hyperproliferative diseases, notably skin cancer and psoriasis.

Furthermore the prototype CICs studied in this thesis offer considerable scope for optimisation/fine tuning, with respect to wavelength of release (by varying the caging group),

lipophilicity and toxicity (by varying the chelators and/or caging group). For instance, chemical fine-tuning of either chelator or caging moieties to enhance either cytotoxic or protective functions upon release from the inactive caged structure could offer a wide range of medical and healthcare applications. This is a major advantage for several applications, and cannot be achieved with systemic iron chelation approaches currently in development.

REFERENCES

Abcouwer, S.F., Schwarz, C., Meguid, R.A., **1999**. Glutamine deprivation induces the expression of GADD45 and GADD153 primarily by mRNA stabilization. J Biol Chem 274, 28645-28651.

Abeysinghe, R.D., Greene, B.T., Haynes, R., Willingham, M.C., Turner, J., Planalp, R.P., Brechbiel, M.W., Torti, F.M., Torti, S.V., **2001**. p53-independent apoptosis mediated by tachpyridine, an anti-cancer iron chelator. Carcinogenesis 22, 1607-1614.

Ackerman, Z., Seidenbaum, M., Loewenthal, E., Rubinow, A., **1988**. Overload of iron in the skin of patients with varicose ulcers. Possible contributing role of iron accumulation in progression of the disease. Arch Dermatol 124, 1376-1378.

Agrawal, K.C., Sartorelli, A.C., **1978**. The chemistry and biological activity of alpha -(N)-heterocyclic carboxaldehyde thiosemicarbazones. Prog Med Chem 15, 321-356.

Aisen, P., Listowsky, I., **1980**. Iron transport and storage proteins. Annu Rev Biochem 49, 357-393.

Albanese, C., Johnson, J., Watanabe, G., Eklund, N., Vu, D., Arnold, A., Pestell, R.G., **1995**. Transforming p21ras mutants and c-Ets-2 activate the cyclin D1 promoter through distinguishable regions. J Biol Chem 270, 23589-23597.

Aleem, E., Kiyokawa, H., Kaldis, P., **2005**. Cdc2-cyclin E complexes regulate the G1/S phase transition. Nat Cell Biol 7, 831-836.

Alvero, A.B., Chen, W., Sartorelli, A.C., Schwartz, P., Rutherford, T., Mor, G., **2006**. Triapine (3-aminopyridine-2-carboxaldehyde thiosemicarbazone) induces apoptosis in ovarian cancer cells. J Soc Gynecol Investig 13, 145-152.

Amstad, P., Peskin, A., Shah, G., Mirault, M.E., Moret, R., Zbinden, I., Cerutti, P., **1991**. The balance between Cu,Zn-superoxide dismutase and catalase affects the sensitivity of mouse epidermal cells to oxidative stress. Biochemistry 30, 9305-9313.

Amundson, S.A., Myers, T.G., Fornace, A.J., Jr., **1998**. Roles for p53 in growth arrest and apoptosis: putting on the brakes after genotoxic stress. Oncogene 17, 3287-3299.

An, W.G., Kanekal, M., Simon, M.C., Maltepe, E., Blagosklonny, M.V., Neckers, L.M., **1998**. Stabilization of wild-type p53 by hypoxia-inducible factor 1alpha. Nature 392, 405-408.

Anderson, R.R., Parrish, J.A., **1981**. The optics of human skin. J Invest Dermatol 77, 13-19.

Andrews, N.C., **2007**. When is a heme transporter not a heme transporter? When it's a folate transporter. Cell Metab 5, 5-6.

Andrews, N.C., **2008**. Forging a field: the golden age of iron biology. Blood 112, 219-230.

Antholine, W., Knight, J., Whelan, H., Petering, D.H., **1977**. Studies of the reaction of 2-formylpyridine thiosemicarbazone and its iron and copper complexes with biological systems. Mol Pharmacol 13, 89-98.

Applegate, L.A., Frenk, E., Gibbs, N., Johnson, B., Ferguson, J., Tyrrell, R.M., **1994**. Cellular sensitivity to oxidative stress in the photosensitivity dermatitis/actinic reticuloid syndrome. J Invest Dermatol 102, 762-767.

Applegate, L.A., Lautier, D., Frenk, E., Tyrrell, R.M., **1992**. Endogenous glutathione levels modulate the frequency of both spontaneous and long wavelength ultraviolet induced mutations in human cells. Carcinogenesis 13, 1557-1560.

Applegate, L.A., Noel, A., Vile, G., Frenk, E., Tyrrell, R.M., **1995**. Two genes contribute to different extents to the heme oxygenase enzyme activity measured in cultured human skin fibroblasts and keratinocytes: implications for protection against oxidant stress. Photochem Photobiol 61, 285-291.

Applegate, L.A., Scaletta, C., Labidi, F., Vile, G.F., Frenk, E., **1996**. Susceptibility of human melanoma cells to oxidative stress including UVA radiation. Int J Cancer 67, 430-434.

Applegate, L.A., Scaletta, C., Panizzon, R., Frenk, E., **1998**. Evidence that ferritin is UV inducible in human skin: part of a putative defense mechanism. J Invest Dermatol 111, 159-163.

Arosio, P., Ingrassia, R., Cavadini, P., **2009**. Ferritins: a family of molecules for iron storage, antioxidation and more. Biochim Biophys Acta 1790, 589-599.

Arosio, P., Levi, S., **2002**. Ferritin, iron homeostasis, and oxidative damage. Free Radic Biol Med 33, 457-463.

Ashcroft, M., Taya, Y., Vousden, K.H., **2000**. Stress signals utilize multiple pathways to stabilize p53. Mol Cell Biol 20, 3224-3233.

Auletta, M., Gange, R.W., Tan, O.T., Matzinger, E., **1986**. Effect of cutaneous hypoxia upon erythema and pigment responses to UVA, UVB, and PUVA (8-MOP + UVA) in human skin. J Invest Dermatol 86, 649-652.

Aust, S.D., Morehouse, L.A., Thomas, C.E., **1985**. Role of metals in oxygen radical reactions. J Free Radic Biol Med 1, 3-25.

Aziz, N., Munro, H.N., **1986**. Both subunits of rat liver ferritin are regulated at a translational level by iron induction. Nucleic Acids Res 14, 915-927.

Bacon, B.R., Britton, R.S., **1990**. The pathology of hepatic iron overload: a free radical--mediated process? Hepatology 11, 127-137.

Baker, B., Peatfield, A.C., Richardson, P.S., **1985**. Nervous control of mucin secretion into human bronchi. J Physiol 365, 297-305.

Baker, E.N., Baker, H.M., Smith, C.A., Stebbins, M.R., Kahn, M., Hellstrom, K.E., Hellstrom, I., **1992**. Human melanotransferrin (p97) has only one functional iron-binding site. FEBS Lett 298, 215-218.

Balla, G., Jacob, H.S., Balla, J., Rosenberg, M., Nath, K., Apple, F., Eaton, J.W., Vercellotti, G.M., **1992**. Ferritin: a cytoprotective antioxidant strategem of endothelium. J Biol Chem 267, 18148-18153.

Balla, J., Jacob, H.S., Balla, G., Nath, K., Eaton, J.W., Vercellotti, G.M., **1993**. Endothelial-cell heme uptake from heme proteins: induction of sensitization and desensitization to oxidant damage. Proc Natl Acad Sci U S A 90, 9285-9289.

Bandyopadhyay, S., Pai, S.K., Gross, S.C., Hirota, S., Hosobe, S., Miura, K., Saito, K., Commes, T., Hayashi, S., Watabe, M., Watabe, K., **2003**. The Drg-1 gene suppresses tumor metastasis in prostate cancer. Cancer Res 63, 1731-1736.

Bandyopadhyay, S., Pai, S.K., Hirota, S., Hosobe, S., Takano, Y., Saito, K., Piquemal, D., Commes, T., Watabe, M., Gross, S.C., Wang, Y., Ran, S., Watabe, K., **2004**. Role of the putative tumor metastasis suppressor gene Drg-1 in breast cancer progression. Oncogene 23, 5675-5681.

Barber, L.A., Spandau, D.F., Rathman, S.C., Murphy, R.C., Johnson, C.A., Kelley, S.W., Hurwitz, S.A., Travers, J.B., **1998**. Expression of the platelet-activating factor receptor results in enhanced ultraviolet B radiation-induced apoptosis in a human epidermal cell line. J Biol Chem 273, 18891-18897.

Barnes, D., Sato, G., **1980**. Methods for growth of cultured cells in serum-free medium. Anal Biochem 102, 255-270.

Barry, B.W., 1983. Dermatological formulations : percutaneous absorption. Marcel Dekker, New York.

Barton, H.A., Eisenstein, R.S., Bomford, A., Munro, H.N., **1990**. Determinants of the interaction between the iron-responsive element-binding protein and its binding site in rat L-ferritin mRNA. J Biol Chem 265, 7000-7008.

Basu-Modak, S., Luscher, P., Tyrrell, R.M., **1996**. Lipid metabolite involvement in the activation of the human heme oxygenase-1 gene. Free Radic Biol Med 20, 887-897.

Basu-Modak, S., Tyrrell, R.M., **1993**. Singlet oxygen: a primary effector in the ultraviolet A/near-visible light induction of the human heme oxygenase gene. Cancer Res 53, 4505-4510.

Beauchamp, C., Fridovich, I., **1970**. A mechanism for the production of ethylene from methional. The generation of the hydroxyl radical by xanthine oxidase. J Biol Chem 245, 4641-4646.

Becker, E.M., Lovejoy, D.B., Greer, J.M., Watts, R., Richardson, D.R., **2003**. Identification of the di-pyridyl ketone isonicotinoyl hydrazone (PKIH) analogues as potent iron chelators and anti-tumour agents. Br J Pharmacol 138, 819-830.

Beckloff, G.L., Lerner, H.J., Frost, D., Russo-Alesi, F.M., Gitomer, S., **1965**. Hydroxyurea (NSC-32065) in biologic fluids: dose-concentration relationship. Cancer Chemother Rep 48, 57-58.

Becton, D.L., Bryles, P., **1988**. Deferoxamine inhibition of human neuroblastoma viability and proliferation. Cancer Res 48, 7189-7192.

Benjamin, C.L., Ullrich, S.E., Kripke, M.L., Ananthaswamy, H.N., **2008**. p53 tumor suppressor gene: a critical molecular target for UV induction and prevention of skin cancer. Photochem Photobiol 84, 55-62.

Bernhardt, P.V., Caldwell, L.M., Chaston, T.B., Chin, P., Richardson, D.R., **2003**. Cytotoxic iron chelators: characterization of the structure, solution chemistry and redox activity of ligands and iron complexes of the di-2-pyridyl ketone isonicotinoyl hydrazone (HPKIH) analogues. J Biol Inorg Chem 8, 866-880.

Berridge, M.V., Tan, A.S., McCoy, K.D., Kansara, M., Rudert, F., **1996**. CD95 (Fas/Apo-1)-induced apoptosis results in loss of glucose transporter function. J Immunol 156, 4092-4099.

Bertling, C.J., Lin, F., Girotti, A.W., **1996**. Role of hydrogen peroxide in the cytotoxic effects of UVA/B radiation on mammalian cells. Photochem Photobiol 64, 137-142.

Bertrand, Y., Demeule, M., Michaud-Levesque, J., Beliveau, R., **2007**. Melanotransferrin induces human melanoma SK-Mel-28 cell invasion in vivo. Biochem Biophys Res Commun 353, 418-423.

Bianchi, L., Tacchini, L., Cairo, G., **1999**. HIF-1-mediated activation of transferrin receptor gene transcription by iron chelation. Nucleic Acids Res 27, 4223-4227.

Bickers, D.R., Athar, M., **2006**. Oxidative stress in the pathogenesis of skin disease. J Invest Dermatol 126, 2565-2575.

Biro, T., Toth, B.I., Hasko, G., Paus, R., Pacher, P., **2009**. The endocannabinoid system of the skin in health and disease: novel perspectives and therapeutic opportunities. Trends Pharmacol Sci 30, 411-420.

Bissett, D.L., Chatterjee, R., Hannon, D.P., **1990**. Photoprotective effect of superoxide-scavenging antioxidants against ultraviolet radiation-induced chronic skin damage in the hairless mouse. Photodermatol Photoimmunol Photomed 7, 56-62.

Bissett, D.L., Chatterjee, R., Hannon, D.P., **1991**. Chronic ultraviolet radiation-induced increase in skin iron and the photoprotective effect of topically applied iron chelators. Photochem Photobiol 54, 215-223.

Black, G., Matzinger, E., Gange, R.W., **1985**. Lack of photoprotection against UVB-induced erythema by immediate pigmentation induced by 382 nm radiation. J Invest Dermatol 85, 448-449.

Blatt, J., **1994**. Deferoxamine in children with recurrent neuroblastoma. Anticancer Res 14, 2109-2112.

Blatt, J., Stitely, S., **1987**. Antineuroblastoma activity of desferoxamine in human cell lines. Cancer Res 47, 1749-1750.

Blatt, J., Wharton, V., **1992**. Stimulation of growth of neuroblastoma cells by ferritin in vitro. J Lab Clin Med 119, 139-143.

Bodrug, S.E., Warner, B.J., Bath, M.L., Lindeman, G.J., Harris, A.W., Adams, J.M., **1994**. Cyclin D1 transgene impedes lymphocyte maturation and collaborates in lymphomagenesis with the myc gene. EMBO J 13, 2124-2130.

Boukamp, P., Petrussevska, R.T., Breitkreutz, D., Hornung, J., Markham, A., Fusenig, N.E., **1988**. Normal keratinization in a spontaneously immortalized aneuploid human keratinocyte cell line. J Cell Biol 106, 761-771.

Bowen, A.R., Hanks, A.N., Murphy, K.J., Florell, S.R., Grossman, D., **2004**. Proliferation, apoptosis, and survivin expression in keratinocytic neoplasms and hyperplasias. Am J Dermatopathol 26, 177-181.

Boyer, R.F., Schori, B.E., **1983**. The incorporation of iron into apoferritin as mediated by ceruloplasmin. Biochem Biophys Res Commun 116, 244-250.

Bradford, M.M., **1976**. A rapid and sensitive method for the quantitation of microgram quantities of protein utilizing the principle of protein-dye binding. Anal Biochem 72, 248-254.

Brard, L., Granai, C.O., Swamy, N., **2006**. Iron chelators deferoxamine and diethylenetriamine pentaacetic acid induce apoptosis in ovarian carcinoma. Gynecol Oncol 100, 116-127.

Bretscher, M.S., Thomson, J.N., **1983**. Distribution of ferritin receptors and coated pits on giant HeLa cells. EMBO J 2, 599-603.

Breuer, W., Epsztejn, S., Cabantchik, Z.I., **1996**. Dynamics of the cytosolic chelatable iron pool of K562 cells. FEBS Lett 382, 304-308.

Brewer, G.J., **2007**. Iron and copper toxicity in diseases of aging, particularly atherosclerosis and Alzheimer's disease. Exp Biol Med (Maywood) 232, 323-335.

Briganti, S., Picardo, M., **2003**. Antioxidant activity, lipid peroxidation and skin diseases. What's new. J Eur Acad Dermatol Venereol 17, 663-669.

Brodeur, G.M., Seeger, R.C., Schwab, M., Varmus, H.E., Bishop, J.M., **1984**. Amplification of N-myc in untreated human neuroblastomas correlates with advanced disease stage. Science 224, 1121-1124.

Brodie, C., Siriwardana, G., Lucas, J., Schleicher, R., Terada, N., Szepesi, A., Gelfand, E., Seligman, P., **1993**. Neuroblastoma sensitivity to growth inhibition by deferrioxamine: evidence for a block in G1 phase of the cell cycle. Cancer Res 53, 3968-3975.

Brookes, M.J., Hughes, S., Turner, F.E., Reynolds, G., Sharma, N., Ismail, T., Berx, G., McKie, A.T., Hotchin, N., Anderson, G.J., Iqbal, T., Tselepis, C., **2006**. Modulation of iron transport proteins in human colorectal carcinogenesis. Gut 55, 1449-1460.

Brown, J.P., Hewick, R.M., Hellstrom, I., Hellstrom, K.E., Doolittle, R.F., Dreyer, W.J., **1982**. Human melanoma-associated antigen p97 is structurally and functionally related to transferrin. Nature 296, 171-173.

Brown, J.P., Nishiyama, K., Hellstrom, I., Hellstrom, K.E., **1981a**. Structural characterization of human melanoma-associated antigen p97 with monoclonal antibodies. J Immunol 127, 539-546.

Brown, J.P., Woodbury, R.G., Hart, C.E., Hellstrom, I., Hellstrom, K.E., **1981b**. Quantitative analysis of melanoma-associated antigen p97 in normal and neoplastic tissues. Proc Natl Acad Sci U S A 78, 539-543.

Broxmeyer, H.E., Bognacki, J., Dorner, M.H., de Sousa, M., **1981**. Identification of leukemia-associated inhibitory activity as acidic isoferritins. A regulatory role for acidic isoferritins in the production of granulocytes and macrophages. J Exp Med 153, 1426-1444.

Broxmeyer, H.E., Cooper, S., Levi, S., Arosio, P., **1991**. Mutated recombinant human heavy-chain ferritins and myelosuppression in vitro and in vivo: a link between ferritin ferroxidase activity and biological function. Proc Natl Acad Sci U S A 88, 770-774.

Bruce, A.J., Brodland, D.G., **2000**. Overview of skin cancer detection and prevention for the primary care physician. Mayo Clin Proc 75, 491-500.

Bruick, R.K., **2000**. Expression of the gene encoding the proapoptotic Nip3 protein is induced by hypoxia. Proc Natl Acad Sci U S A 97, 9082-9087.

Bruls, W.A., Slaper, H., van der Leun, J.C., Berrens, L., **1984**. Transmission of human epidermis and stratum corneum as a function of thickness in the ultraviolet and visible wavelengths. Photochem Photobiol 40, 485-494.

Bulavin, D.V., Kovalsky, O., Hollander, M.C., Fornace, A.J., Jr., **2003**. Loss of oncogenic H-ras-induced cell cycle arrest and p38 mitogen-activated protein kinase activation by disruption of Gadd45a. Mol Cell Biol 23, 3859-3871.

Bulavin, D.V., Saito, S., Hollander, M.C., Sakaguchi, K., Anderson, C.W., Appella, E., Fornace, A.J., Jr., **1999**. Phosphorylation of human p53 by p38 kinase coordinates N-terminal phosphorylation and apoptosis in response to UV radiation. EMBO J 18, 6845-6854.

Bunz, F., Hwang, P.M., Torrance, C., Waldman, T., Zhang, Y., Dillehay, L., Williams, J., Lengauer, C., Kinzler, K.W., Vogelstein, B., **1999**. Disruption of p53 in human cancer cells alters the responses to therapeutic agents. J Clin Invest 104, 263-269.

Burren, R., Scaletta, C., Frenk, E., Panizzon, R.G., Applegate, L.A., **1998**. Sunlight and carcinogenesis: expression of p53 and pyrimidine dimers in human skin following UVA I, UVA I + II and solar simulating radiations. Int J Cancer 76, 201-206.

Buss, J.L., Neuzil, J., Ponka, P., **2004**. Oxidative stress mediates toxicity of pyridoxal isonicotinoyl hydrazone analogs. Arch Biochem Biophys 421, 1-9.

Buss, J.L., Torti, F.M., Torti, S.V., **2003**. The role of iron chelation in cancer therapy. Curr Med Chem 10, 1021-1034.

Cadogan, J.I.G., 1973. Principles of free radical chemistry. Chemical Society, London.

Cairo, G., Bernuzzi, F., Recalcati, S., **2006**. A precious metal: Iron, an essential nutrient for all cells. Genes Nutr 1, 25-39.

Cairo, G., Pietrangelo, A., **2000**. Iron regulatory proteins in pathobiology. Biochem J 352 Pt 2, 241-250.

Cairo, G., Tacchini, L., Pogliaghi, G., Anzon, E., Tomasi, A., Bernelli-Zazzera, A., **1995**. Induction of ferritin synthesis by oxidative stress. Transcriptional and post-transcriptional regulation by expansion of the "free" iron pool. J Biol Chem 270, 700-703.

Camaschella, C., **2005**. Understanding iron homeostasis through genetic analysis of hemochromatosis and related disorders. Blood 106, 3710-3717.

Carlson, S.G., Fawcett, T.W., Bartlett, J.D., Bernier, M., Holbrook, N.J., **1993**. Regulation of the C/EBP-related gene gadd153 by glucose deprivation. Mol Cell Biol 13, 4736-4744.

Carnero, A., **2002**. Targeting the cell cycle for cancer therapy. Br J Cancer 87, 129-133.

Caro, J., **2001**. Hypoxia regulation of gene transcription. High Alt Med Biol 2, 145-154.

Carr, A.M., **2000**. Cell cycle. Piecing together the p53 puzzle. Science 287, 1765-1766.

Cassileth, B.R., Chapman, C.C., **1996**. Alternative and complementary cancer therapies. Cancer 77, 1026-1034.

Cazzola, M., Invernizzi, R., Bergamaschi, G., Levi, S., Corsi, B., Travaglino, E., Rolandi, V., Biasiotto, G., Drysdale, J., Arosio, P., **2003**. Mitochondrial ferritin expression in erythroid cells from patients with sideroblastic anemia. Blood 101, 1996-2000.

Cerqueira, N.M., Fernandes, P.A., Ramos, M.J., **2007**. Ribonucleotide reductase: a critical enzyme for cancer chemotherapy and antiviral agents. Recent Pat Anticancer Drug Discov 2, 11-29.

Champion, R.H., **1981**. Psoriasis and its treatment. Br Med J (Clin Res Ed) 282, 343-346.

Chasteen, N.D., **1983**. Transferrin: a perspective. Adv Inorg Biochem 5, 201-233.

Chaston, T.B., Lovejoy, D.B., Watts, R.N., Richardson, D.R., **2003**. Examination of the antiproliferative activity of iron chelators: multiple cellular targets and the different mechanism of action of triapine compared with desferrioxamine and the potent pyridoxal isonicotinoyl hydrazone analogue 311. Clin Cancer Res 9, 402-414.

Chaston, T.B., Richardson, D.R., **2003**. Interactions of the pyridine-2-carboxaldehyde isonicotinoyl hydrazone class of chelators with iron and DNA: implications for toxicity in the treatment of iron overload disease. J Biol Inorg Chem 8, 427-438.

Cheeseman, K.H., Slater, T.F., **1993**. An introduction to free radical biochemistry. Br Med Bull 49, 481-493.

Chou, P.T., Khan, A.U., **1983**. L-ascorbic acid quenching of singlet delta molecular oxygen in aqueous media: generalized antioxidant property of vitamin C. Biochem Biophys Res Commun 115, 932-937.

Clark, C., **2004**. Psoriasis : First line treatment The Pharmaceutical Journal 274, 623-626.

Clark, C., **2005**. Management of severe psoriasis The Pharmaceutical Journal 274, 689-692.

Coffman, L.G., Parsonage, D., D'Agostino, R., Jr., Torti, F.M., Torti, S.V., **2009**. Regulatory effects of ferritin on angiogenesis. Proc Natl Acad Sci U S A 106, 570-575.

Connor, M.J., Wheeler, L.A., **1987**. Depletion of cutaneous glutathione by ultraviolet radiation. Photochem Photobiol 46, 239-245.

Cooper, C.E., Lynagh, G.R., Hoyes, K.P., Hider, R.C., Cammack, R., Porter, J.B., **1996**. The relationship of intracellular iron chelation to the inhibition and regeneration of human ribonucleotide reductase. J Biol Chem 271, 20291-20299.

Cordon-Cardo, C., **1995**. Mutations of cell cycle regulators. Biological and clinical implications for human neoplasia. Am J Pathol 147, 545-560.

Corn, P.G., El-Deiry, W.S., **2002**. Derangement of growth and differentiation control in oncogenesis. Bioessays 24, 83-90.

Corsi, B., Cozzi, A., Arosio, P., Drysdale, J., Santambrogio, P., Campanella, A., Biasiotto, G., Albertini, A., Levi, S., **2002**. Human mitochondrial ferritin expressed in HeLa cells incorporates iron and affects cellular iron metabolism. J Biol Chem 277, 22430-22437.

Covell, A.M., Cook, J.D., **1988**. Interaction of acidic isoferritins with human promyelocytic HL60 cells. Br J Haematol 69, 559-563.

Covell, A.M., Einspahr, D.E., Skikne, B.S., Cook, J.D., **1987**. Specific binding of acidic isoferritins to erythroleukemia K562 cells. J Lab Clin Med 110, 784-790.

Cox, T.C., Bawden, M.J., Martin, A., May, B.K., **1991**. Human erythroid 5-aminolevulinate synthase: promoter analysis and identification of an iron-responsive element in the mRNA. EMBO J 10, 1891-1902.

Cozzi, A., Corsi, B., Levi, S., Santambrogio, P., Albertini, A., Arosio, P., **2000**. Overexpression of wild type and mutated human ferritin H-chain in HeLa cells: in vivo role of ferritin ferroxidase activity. J Biol Chem 275, 25122-25129.

Dandekar, T., Stripecke, R., Gray, N.K., Goossen, B., Constable, A., Johansson, H.E., Hentze, M.W., **1991**. Identification of a novel iron-responsive element in murine and human erythroid delta-aminolevulinic acid synthase mRNA. EMBO J 10, 1903-1909.

Daniels, T.R., Delgado, T., Rodriguez, J.A., Helguera, G., Penichet, M.L., **2006**. The transferrin receptor part I: Biology and targeting with cytotoxic antibodies for the treatment of cancer. Clin Immunol 121, 144-158.

Danpure, H.J., Tyrrell, R.M., **1976**. Oxygen-dependence of near UV (365 NM) lethality and the interaction of near UV and X-rays in two mammalian cell lines. Photochem Photobiol 23, 171-177.

Darnell, G., Richardson, D.R., **1999**. The potential of iron chelators of the pyridoxal isonicotinoyl hydrazone class as effective antiproliferative agents III: the effect of the ligands on molecular targets involved in proliferation. Blood 94, 781-792.

David, T.J., Wells, F.E., Sharpe, T.C., Gibbs, A.C., Devlin, J., **1990**. Serum levels of trace metals in children with atopic eczema. Br J Dermatol 122, 485-489.

Davies, K.J., **1986**. Intracellular proteolytic systems may function as secondary antioxidant defenses: an hypothesis. J Free Radic Biol Med 2, 155-173.

De Domenico, I., McVey Ward, D., Kaplan, J., **2008**. Regulation of iron acquisition and storage: consequences for iron-linked disorders. Nat Rev Mol Cell Biol 9, 72-81.

Dean, R.T., Gieseg, S., Davies, M.J., **1993**. Reactive species and their accumulation on radical-damaged proteins. Trends Biochem Sci 18, 437-441.

Dennery, P.A., Spitz, D.R., Yang, G., Tatarov, A., Lee, C.S., Shegog, M.L., Poss, K.D., **1998**. Oxygen toxicity and iron accumulation in the lungs of mice lacking heme oxygenase-2. J Clin Invest 101, 1001-1011.

Dethmers, J.K., Meister, A., **1981**. Glutathione export by human lymphoid cells: depletion of glutathione by inhibition of its synthesis decreases export and increases sensitivity to irradiation. Proc Natl Acad Sci U S A 78, 7492-7496.

Diffey, B.L., **2002**. Human exposure to solar ultraviolet radiation. J Cosmet Dermatol 1, 124-130.

Djavaheri-Mergny, M., Maziere, J.C., Santus, R., Mora, L., Maziere, C., Auclair, M., Dubertret, L., **1993**. Exposure to long wavelength ultraviolet radiation decreases processing of low density lipoprotein by cultured human fibroblasts. Photochem Photobiol 57, 302-305.

Djavaheri-Mergny, M., Mergny, J.L., Bertrand, F., Santus, R., Maziere, C., Dubertret, L., Maziere, J.C., **1996**. Ultraviolet-A induces activation of AP-1 in cultured human keratinocytes. FEBS Lett 384, 92-96.

Donfrancesco, A., De Bernardi, B., Carli, M., Mancini, A., Nigro, M., De Sio, L., Casale, F., Bagnulo, S., Helson, L., Deb, G., **1995**. Deferoxamine followed by cyclophosphamide, etoposide, carboplatin, thiotepa, induction regimen in advanced neuroblastoma: preliminary results. Italian Neuroblastoma Cooperative Group. Eur J Cancer 31A, 612-615.

Donfrancesco, A., Deb, G., De Sio, L., Cozza, R., Castellano, A., **1996**. Role of deferoxamine in tumor therapy. Acta Haematol 95, 66-69.

Donfrancesco, A., Deb, G., Dominici, C., Pileggi, D., Castello, M.A., Helson, L., **1990**. Effects of a single course of deferoxamine in neuroblastoma patients. Cancer Res 50, 4929-4930.

Dong, Z., Zhang, J.T., **2003**. EIF3 p170, a mediator of mimosine effect on protein synthesis and cell cycle progression. Mol Biol Cell 14, 3942-3951.

Donovan, A., Brownlie, A., Zhou, Y., Shepard, J., Pratt, S.J., Moynihan, J., Paw, B.H., Drejer, A., Barut, B., Zapata, A., Law, T.C., Brugnara, C., Lux, S.E., Pinkus, G.S., Pinkus, J.L., Kingsley, P.D., Palis, J., Fleming, M.D., Andrews, N.C., Zon, L.I., **2000**. Positional cloning of zebrafish ferroportin1 identifies a conserved vertebrate iron exporter. Nature 403, 776-781.

Doulias, P.T., Christoforidis, S., Brunk, U.T., Galaris, D., **2003**. Endosomal and lysosomal effects of desferrioxamine: protection of HeLa cells from hydrogen peroxide-induced DNA damage and induction of cell-cycle arrest. Free Radic Biol Med 35, 719-728.

Doyle, A., Griffiths, J.B., 1998. Cell and tissue culture : laboratory procedures in biotechnology. Wiley, Chichester.

Draetta, G., **1990**. Cell cycle control in eukaryotes: molecular mechanisms of cdc2 activation. Trends Biochem Sci 15, 378-383.

Dreicer, R., Kemp, J.D., Stegink, L.D., Cardillo, T., Davis, C.S., Forest, P.K., See, W.A., **1997**. A phase II trial of deferoxamine in patients with hormone-refractory metastatic prostate cancer. Cancer Invest 15, 311-317.

Drysdale, J., Arosio, P., Invernizzi, R., Cazzola, M., Volz, A., Corsi, B., Biasiotto, G., Levi, S., **2002**. Mitochondrial ferritin: a new player in iron metabolism. Blood Cells Mol Dis 29, 376-383.

Drysdale, J.W., **1988**. Human ferritin gene expression. Prog Nucleic Acid Res Mol Biol 35, 127-172.

Duarte, T.L., Jones, G.D., **2007**. Vitamin C modulation of H2O2-induced damage and iron homeostasis in human cells. Free Radic Biol Med 43, 1165-1175.

Dudek, E.J., Peak, J.G., Roth, R.M., Peak, M.J., **1993**. Isolation of V79 fibroblast cell lines containing elevated metallothionein levels that have increased resistance to the cytotoxic effects of ultraviolet-A radiation. Photochem Photobiol 58, 836-840.

Dunn, L.L., Rahmanto, Y.S., Richardson, D.R., **2007**. Iron uptake and metabolism in the new millennium. Trends Cell Biol 17, 93-100.

Dunn, L.L., Sekyere, E.O., Rahmanto, Y.S., Richardson, D.R., **2006**. The function of melanotransferrin: a role in melanoma cell proliferation and tumorigenesis. Carcinogenesis 27, 2157-2169.

Eisenstein, R.S., **2000**. Iron regulatory proteins and the molecular control of mammalian iron metabolism. Annu Rev Nutr 20, 627-662.

Elliott, M.J., Dong, Y.B., Yang, H., McMasters, K.M., **2001**. E2F-1 up-regulates c-Myc and p14(ARF) and induces apoptosis in colon cancer cells. Clin Cancer Res 7, 3590-3597.

Elsayed, Y.A., Sausville, E.A., **2001**. Selected novel anticancer treatments targeting cell signaling proteins. Oncologist 6, 517-537.

Enns, C.A., Sussman, H.H., **1981**. Physical characterization of the transferrin receptor in human placentae. J Biol Chem 256, 9820-9823.

Epstein, J.H., **1977**. Effects of beta-carotene on ultraviolet induced cancer formation in the hairless mouse skin. Photochem Photobiol 25, 211-213.

Epsztejn, S., Glickstein, H., Picard, V., Slotki, I.N., Breuer, W., Beaumont, C., Cabantchik, Z.I., **1999**. H-ferritin subunit overexpression in erythroid cells reduces the oxidative stress response and induces multidrug resistance properties. Blood 94, 3593-3603.

Epsztejn, S., Kakhlon, O., Glickstein, H., Breuer, W., Cabantchik, I., **1997**. Fluorescence analysis of the labile iron pool of mammalian cells. Anal Biochem 248, 31-40.

Estrov, Z., Tawa, A., Wang, X.H., Dube, I.D., Sulh, H., Cohen, A., Gelfand, E.W., Freedman, M.H., **1987**. In vitro and in vivo effects of deferoxamine in neonatal acute leukemia. Blood 69, 757-761.

Fadok, V.A., Voelker, D.R., Campbell, P.A., Cohen, J.J., Bratton, D.L., Henson, P.M., **1992**. Exposure of phosphatidylserine on the surface of apoptotic lymphocytes triggers specific recognition and removal by macrophages. J Immunol 148, 2207-2216.

Fan, L., Iyer, J., Zhu, S., Frick, K.K., Wada, R.K., Eskenazi, A.E., Berg, P.E., Ikegaki, N., Kennett, R.H., Frantz, C.N., **2001**. Inhibition of N-myc expression and induction of apoptosis by iron chelation in human neuroblastoma cells. Cancer Res 61, 1073-1079.

Fanzo, J.C., Reaves, S.K., Cui, L., Zhu, L., Wu, J.Y., Wang, Y.R., Lei, K.Y., **2001**. Zinc status affects p53, gadd45, and c-fos expression and caspase-3 activity in human bronchial epithelial cells. Am J Physiol Cell Physiol 281, C751-757.

Fargion, S., Fracanzani, A.L., Brando, B., Arosio, P., Levi, S., Fiorelli, G., **1991**. Specific binding sites for H-ferritin on human lymphocytes: modulation during cellular proliferation and potential implication in cell growth control. Blood 78, 1056-1061.

Ferris, C.D., Jaffrey, S.R., Sawa, A., Takahashi, M., Brady, S.D., Barrow, R.K., Tysoe, S.A., Wolosker, H., Baranano, D.E., Dore, S., Poss, K.D., Snyder, S.H., **1999**. Haem oxygenase-1 prevents cell death by regulating cellular iron. Nat Cell Biol 1, 152-157.

Feun, L., Modiano, M., Lee, K., Mao, J., Marini, A., Savaraj, N., Plezia, P., Almassian, B., Colacino, E., Fischer, J., MacDonald, S., **2002**. Phase I and pharmacokinetic study of 3-aminopyridine-2-carboxaldehyde thiosemicarbazone (3-AP) using a single intravenous dose schedule. Cancer Chemother Pharmacol 50, 223-229.

Finch, R.A., Liu, M., Grill, S.P., Rose, W.C., Loomis, R., Vasquez, K.M., Cheng, Y., Sartorelli, A.C., **2000**. Triapine (3-aminopyridine-2-carboxaldehyde- thiosemicarbazone): A potent inhibitor of ribonucleotide reductase activity with broad spectrum antitumor activity. Biochem Pharmacol 59, 983-991.

Fleming, M.D., Romano, M.A., Su, M.A., Garrick, L.M., Garrick, M.D., Andrews, N.C., **1998**. Nramp2 is mutated in the anemic Belgrade (b) rat: evidence of a role for Nramp2 in endosomal iron transport. Proc Natl Acad Sci U S A 95, 1148-1153.

Fleming, R.E., Migas, M.C., Holden, C.C., Waheed, A., Britton, R.S., Tomatsu, S., Bacon, B.R., Sly, W.S., **2000**. Transferrin receptor 2: continued expression in mouse liver in the face of iron overload and in hereditary hemochromatosis. Proc Natl Acad Sci U S A 97, 2214-2219.

Foltz, L.M., Dalal, B.I., Wadsworth, L.D., Broady, R., Chi, K., Eisenhauer, E., Kobayashi, K., Kollmannsburger, C., **2006**. Recognition and management of methemoglobinemia and hemolysis in a G6PD-deficient patient on experimental anticancer drug Triapine. Am J Hematol 81, 210-211.

Foote, C.S., Ching, T.Y., Geller, G.G., **1974**. Chemistry of singlet oxygen. XVIII. Rates of reaction and quenching of alpha-tocopherol and singlet oxygen. Photochem Photobiol 20, 511-513.

Frazer, D.M., Wilkins, S.J., Vulpe, C.D., Anderson, G.J., **2005**. The role of duodenal cytochrome b in intestinal iron absorption remains unclear. Blood 106, 4413; author reply 4414.

Frederick, J.E., Alberts, A.D., 1992. The natural UVA radiation environment. In: Urbach, F. (Ed.), Biological Responses to Ultraviolet A Radiation Vlademar Publishing Company Kansas, pp. 7-18.

Freeman, R.G., **1975**. Data on the action spectrum for ultraviolet carcinogenesis. J Natl Cancer Inst 55, 1119-1122.

Freeman, S.E., Hacham, H., Gange, R.W., Maytum, D.J., Sutherland, J.C., Sutherland, B.M., **1989**. Wavelength dependence of pyrimidine dimer formation in DNA of human skin irradiated in situ with ultraviolet light. Proc Natl Acad Sci U S A 86, 5605-5609.

Fridovich, I., **1978**. The biology of oxygen radicals. Science 201, 875-880.

Fryer, M.J., **1993**. Evidence for the photoprotective effects of vitamin E. Photochem Photobiol 58, 304-312.

Fu, D., Richardson, D.R., **2007**. Iron chelation and regulation of the cell cycle: 2 mechanisms of posttranscriptional regulation of the universal cyclin-dependent kinase inhibitor p21CIP1/WAF1 by iron depletion. Blood 110, 752-761.

Fuchs, O., Borova, J., Hradilek, A., Neuwirt, J., **1988**. Non-transferrin donors of iron for heme synthesis in immature erythroid cells. Biochim Biophys Acta 969, 158-165.

Fukuchi, K., Tomoyasu, S., Watanabe, H., Kaetsu, S., Tsuruoka, N., Gomi, K., **1995**. Iron deprivation results in an increase in p53 expression. Biol Chem Hoppe Seyler 376, 627-630.

Fukuya, Y., Higaki, M., Higaki, Y., Kawashima, M., **2002**. Effect of vitamin D3 on the increased expression of Bcl-xL in psoriasis. Arch Dermatol Res 293, 620-625.

Gaboriau, F., Demoulins-Giacco, N., Tirache, I., Morliere, P., **1995**. Involvement of singlet oxygen in ultraviolet A-induced lipid peroxidation in cultured human skin fibroblasts. Arch Dermatol Res 287, 338-340.

Gaeta, A., Hider, R.C., **2005**. The crucial role of metal ions in neurodegeneration: the basis for a promising therapeutic strategy. Br J Pharmacol 146, 1041-1059.

Gao, J., Richardson, D.R., **2001**. The potential of iron chelators of the pyridoxal isonicotinoyl hydrazone class as effective antiproliferative agents, IV: The mechanisms involved in inhibiting cell-cycle progression. Blood 98, 842-850.

Gardner, P.R., Raineri, I., Epstein, L.B., White, C.W., **1995**. Superoxide radical and iron modulate aconitase activity in mammalian cells. J Biol Chem 270, 13399-13405.

Garner, B., Roberg, K., Brunk, U.T., **1998**. Endogenous ferritin protects cells with iron-laden lysosomes against oxidative stress. Free Radic Res 29, 103-114.

Gasparro, F.P., Mitchnick, M., Nash, J.F., **1998**. A review of sunscreen safety and efficacy. Photochem Photobiol 68, 243-256.

Gilchrest, B.A., Soter, N.A., Hawk, J.L., Barr, R.M., Black, A.K., Hensby, C.N., Mallet, A.I., Greaves, M.W., Parrish, J.A., **1983**. Histologic changes associated with ultraviolet A--induced erythema in normal human skin. J Am Acad Dermatol 9, 213-219.

Giles, F.J., Fracasso, P.M., Kantarjian, H.M., Cortes, J.E., Brown, R.A., Verstovsek, S., Alvarado, Y., Thomas, D.A., Faderl, S., Garcia-Manero, G., Wright, L.P., Samson, T., Cahill, A., Lambert, P., Plunkett, W., Sznol, M., DiPersio, J.F., Gandhi, V., **2003**. Phase I and pharmacodynamic study of Triapine, a novel ribonucleotide reductase inhibitor, in patients with advanced leukemia. Leuk Res 27, 1077-1083.

Giordani, A., Morlière, P., Aubailly, M., Santus, R., **1997**. Photoinactivation of cellular catalase by UV radiation. Redox. Rep., 49-55.

Glickstein, H., El, R.B., Shvartsman, M., Cabantchik, Z.I., **2005**. Intracellular labile iron pools as direct targets of iron chelators: a fluorescence study of chelator action in living cells. Blood 106, 3242-3250.

Godar, D.E., Miller, S.A., Thomas, D.P., **1994**. Immediate and delayed apoptotic cell death mechanisms: UVA versus UVB and UVC radiation. Cell Death Differ 1, 59-66.

Gojo, I., Tidwell, M.L., Greer, J., Takebe, N., Seiter, K., Pochron, M.F., Johnson, B., Sznol, M., Karp, J.E., **2007**. Phase I and pharmacokinetic study of Triapine, a potent ribonucleotide reductase inhibitor, in adults with advanced hematologic malignancies. Leuk Res 31, 1165-1173.

Golias, C.H., Charalabopoulos, A., Charalabopoulos, K., **2004**. Cell proliferation and cell cycle control: a mini review. Int J Clin Pract 58, 1134-1141.

Gopinathan, V., Miller, N.J., Milner, A.D., Rice-Evans, C.A., **1994**. Bilirubin and ascorbate antioxidant activity in neonatal plasma. FEBS Lett 349, 197-200.

Grams, G.W., Eskins, K., **1972**. Dye-sensitized photooxidation of tocopherols. Correlation between singlet oxygen reactivity and vitamin E activity. Biochemistry 11, 606-608.

Grant, A.J., Jessup, W., Dean, R.T., **1992**. Accelerated endocytosis and incomplete catabolism of radical-damaged protein. Biochim Biophys Acta 1134, 203-209.

Green, D.A., Antholine, W.E., Wong, S.J., Richardson, D.R., Chitambar, C.R., **2001**. Inhibition of malignant cell growth by 311, a novel iron chelator of the pyridoxal isonicotinoyl hydrazone class: effect on the R2 subunit of ribonucleotide reductase. Clin Cancer Res 7, 3574-3579.

Greene, B.T., Thorburn, J., Willingham, M.C., Thorburn, A., Planalp, R.P., Brechbiel, M.W., Jennings-Gee, J., Wilkinson, J.t., Torti, F.M., Torti, S.V., **2002**. Activation of caspase pathways during iron chelator-mediated apoptosis. J Biol Chem 277, 25568-25575.

Greijer, A.E., van der Groep, P., Kemming, D., Shvarts, A., Semenza, G.L., Meijer, G.A., van de Wiel, M.A., Belien, J.A., van Diest, P.J., van der Wall, E., **2005**. Up-regulation of gene expression by hypoxia is mediated predominantly by hypoxia-inducible factor 1 (HIF-1). J Pathol 206, 291-304.

Guillen, C., McInnes, I.B., Kruger, H., Brock, J.H., **1998**. Iron, lactoferrin and iron regulatory protein activity in the synovium; relative importance of iron loading and the inflammatory response. Ann Rheum Dis 57, 309-314.

Guittet, O., Hakansson, P., Voevodskaya, N., Fridd, S., Graslund, A., Arakawa, H., Nakamura, Y., Thelander, L., **2001**. Mammalian p53R2 protein forms an active ribonucleotide reductase in vitro with the R1 protein, which is expressed both in resting cells in response to DNA damage and in proliferating cells. J Biol Chem 276, 40647-40651.

Gunshin, H., Mackenzie, B., Berger, U.V., Gunshin, Y., Romero, M.F., Boron, W.F., Nussberger, S., Gollan, J.L., Hediger, M.A., **1997**. Cloning and characterization of a mammalian proton-coupled metal-ion transporter. Nature 388, 482-488.

Gunshin, H., Starr, C.N., Direnzo, C., Fleming, M.D., Jin, J., Greer, E.L., Sellers, V.M., Galica, S.M., Andrews, N.C., **2005**. Cybrd1 (duodenal cytochrome b) is not necessary for dietary iron absorption in mice. Blood 106, 2879-2883.

Guo, B., Brown, F.M., Phillips, J.D., Yu, Y., Leibold, E.A., **1995**. Characterization and expression of iron regulatory protein 2 (IRP2). Presence of multiple IRP2 transcripts regulated by intracellular iron levels. J Biol Chem 270, 16529-16535.

Guo, K., Searfoss, G., Krolikowski, D., Pagnoni, M., Franks, C., Clark, K., Yu, K.T., Jaye, M., Ivashchenko, Y., **2001**. Hypoxia induces the expression of the pro-apoptotic gene BNIP3. Cell Death Differ 8, 367-376.

Gutierrez, J.A., Yu, J., Rivera, S., Wessling-Resnick, M., **1997**. Functional expression cloning and characterization of SFT, a stimulator of Fe transport. J Cell Biol 139, 895-905.

Gwilt, P.R., Tracewell, W.G., **1998**. Pharmacokinetics and pharmacodynamics of hydroxyurea. Clin Pharmacokinet 34, 347-358.

Habel, M.E., Jung, D., **2006**. c-Myc over-expression in Ramos Burkitt's lymphoma cell line predisposes to iron homeostasis disruption in vitro. Biochem Biophys Res Commun 341, 1309-1316.

Haile, D.J., Rouault, T.A., Harford, J.B., Kennedy, M.C., Blondin, G.A., Beinert, H., Klausner, R.D., **1992a**. Cellular regulation of the iron-responsive element binding protein: disassembly of the cubane iron-sulfur cluster results in high-affinity RNA binding. Proc Natl Acad Sci U S A 89, 11735-11739.

Haile, D.J., Rouault, T.A., Tang, C.K., Chin, J., Harford, J.B., Klausner, R.D., **1992b**. Reciprocal control of RNA-binding and aconitase activity in the regulation of the iron-responsive element binding protein: role of the iron-sulfur cluster. Proc Natl Acad Sci U S A 89, 7536-7540.

Halliwell, B., Gutteridge, J.M.C., 1999. Free radicals in biology and medicine. Oxford University Press, Oxford.

Han, O., Kim, E.Y., **2007**. Colocalization of ferroportin-1 with hephaestin on the basolateral membrane of human intestinal absorptive cells. J Cell Biochem 101, 1000-1010.

Hann, H.L., Stahlhut, M.W., Millman, I., **1984**. Human ferritins present in the sera of nude mice transplanted with human neuroblastoma or hepatocellular carcinoma. Cancer Res 44, 3898-3901.

Hann, H.W., Evans, A.E., Cohen, I.J., Leitmeyer, J.E., **1981**. Biologic differences between neuroblastoma stages IV-S and IV. Measurement of serum ferritin and E-rosette inhibition in 30 children. N Engl J Med 305, 425-429.

Hann, H.W., Evans, A.E., Siegel, S.E., Wong, K.Y., Sather, H., Dalton, A., Hammond, D., Seeger, R.C., **1985**. Prognostic importance of serum ferritin in patients with Stages III and IV neuroblastoma: the Childrens Cancer Study Group experience. Cancer Res 45, 2843-2848.

Hann, H.W., Levy, H.M., Evans, A.E., **1980**. Serum ferritin as a guide to therapy in neuroblastoma. Cancer Res 40, 1411-1413.

Hann, H.W., Stahlhut, M.W., Evans, A.E., **1988**. Basic and acidic isoferritins in the sera of patients with neuroblastoma. Cancer 62, 1179-1182.

Hann, H.W., Stahlhut, M.W., Hann, C.L., **1990**. Effect of iron and desferoxamine on cell growth and in vitro ferritin synthesis in human hepatoma cell lines. Hepatology 11, 566-569.

Hann, H.W., Stahlhut, M.W., Rubin, R., Maddrey, W.C., **1992**. Antitumor effect of deferoxamine on human hepatocellular carcinoma growing in athymic nude mice. Cancer 70, 2051-2056.

Hansen, C., Ablett, E., Green, A., Sturm, R.A., Dunn, I.S., Fairlie, D.P., West, M.L., Parsons, P.G., **1997**. Biphasic response of the metallothionein promoter to ultraviolet radiation in human melanoma cells. Photochem Photobiol 65, 550-555.

Hanson, K.M., Simon, J.D., **1998**. Epidermal trans-urocanic acid and the UV-A-induced photoaging of the skin. Proc Natl Acad Sci U S A 95, 10576-10578.

Hantschmann, P., Kurzl, R., **2000**. Regulation of apoptosis in squamous cell carcinoma of the vulva. J Reprod Med 45, 633-642.

Harrison, P.M., Arosio, P., **1996**. The ferritins: molecular properties, iron storage function and cellular regulation. Biochim Biophys Acta 1275, 161-203.

Hatakeyama, M., Weinberg, R.A., **1995**. The role of RB in cell cycle control. Prog Cell Cycle Res 1, 9-19.

Heeney, M.M., Andrews, N.C., **2004**. Iron homeostasis and inherited iron overload disorders: an overview. Hematol Oncol Clin North Am 18, 1379-1403, ix.

Heichman, K.A., Roberts, J.M., **1994**. Rules to replicate by. Cell 79, 557-562.

Helm, B.A., Gunn, J.M., **1986**. The effect of insulinomimetic agents on protein degradation in H35 hepatoma cells. Mol Cell Biochem 71, 159-166.

Hengartner, M.O., **2000**. The biochemistry of apoptosis. Nature 407, 770-776.

Hentze, M.W., Argos, P., **1991**. Homology between IRE-BP, a regulatory RNA-binding protein, aconitase, and isopropylmalate isomerase. Nucleic Acids Res 19, 1739-1740.

Hentze, M.W., Muckenthaler, M.U., Andrews, N.C., **2004**. Balancing acts: molecular control of mammalian iron metabolism. Cell 117, 285-297.

Hershko, C., Graham, G., Bates, G.W., Rachmilewitz, E.A., **1978**. Non-specific serum iron in thalassaemia: an abnormal serum iron fraction of potential toxicity. Br J Haematol 40, 255-263.

Hileti, D., Panayiotidis, P., Hoffbrand, A.V., **1995**. Iron chelators induce apoptosis in proliferating cells. Br J Haematol 89, 181-187.

Hino, Y., Asagami, H., Minakami, S., **1979**. Topological arrangement in microsomal membranes of hepatic haem oxygenase induced by cobalt chloride. Biochem J 178, 331-337.

Hintze, K.J., Theil, E.C., **2005**. DNA and mRNA elements with complementary responses to hemin, antioxidant inducers, and iron control ferritin-L expression. Proc Natl Acad Sci U S A 102, 15048-15052.

Hoffman, K.E., Yanelli, K., Bridges, K.R., **1991**. Ascorbic acid and iron metabolism: alterations in lysosomal function. Am J Clin Nutr 54, 1188S-1192S.

Hollander, M.C., Sheikh, M.S., Yu, K., Zhan, Q., Iglesias, M., Woodworth, C., Fornace, A.J., Jr., **2001**. Activation of Gadd34 by diverse apoptotic signals and suppression of its growth inhibitory effects by apoptotic inhibitors. Int J Cancer 96, 22-31.

Hollstein, M., Sidransky, D., Vogelstein, B., Harris, C.C., **1991**. p53 mutations in human cancers. Science 253, 49-53.

Holmgren, A., **1985**. Thioredoxin. Annu Rev Biochem 54, 237-271.

Honda, R., Tanaka, H., Yasuda, H., **1997**. Oncoprotein MDM2 is a ubiquitin ligase E3 for tumor suppressor p53. FEBS Lett 420, 25-27.

Horackova, M., Ponka, P., Byczko, Z., **2000**. The antioxidant effects of a novel iron chelator salicylaldehyde isonicotinoyl hydrazone in the prevention of H(2)O(2) injury in adult cardiomyocytes. Cardiovasc Res 47, 529-536.

Horton, J.J., Caffrey, E.A., Clark, K.G., MacDonald, D.M., Wells, R.S., Daker, M.G., **1984**. Leukaemia in psoriatic patients treated with razoxane. Br J Dermatol 110, 633-634.

Horton, J.J., MacDonald, D.M., Wells, R.S., **1983**. Epitheliomas in patients receiving razoxane therapy for psoriasis. Br J Dermatol 109, 675-678.

Huang, A.R., Ponka, P., **1983**. A study of the mechanism of action of pyridoxal isonicotinoyl hydrazone at the cellular level using reticulocytes loaded with non-heme 59Fe. Biochim Biophys Acta 757, 306-315.

Huebers, H., Huebers, E., Csiba, E., Finch, C.A., **1978**. Iron uptake from rat plasma transferrin by rat reticulocytes. J Clin Invest 62, 944-951.

Hugman, A., **2006**. Hepcidin: an important new regulator of iron homeostasis. Clin Lab Haematol 28, 75-83.

Iancu, T.C., **1989**. Iron and neoplasia: ferritin and hemosiderin in tumor cells. Ultrastruct Pathol 13, 573-584.

Iancu, T.C., Shiloh, H., Kedar, A., **1988**. Neuroblastomas contain iron-rich ferritin. Cancer 61, 2497-2502.

Imeryuz, N., Tahan, V., Sonsuz, A., Eren, F., Uraz, S., Yuksel, M., Akpulat, S., Ozcelik, D., Haklar, G., Celikel, C., Avsar, E., Tozun, N., **2007**. Iron preloading aggravates nutritional steatohepatitis in rats by increasing apoptotic cell death. J Hepatol 47, 851-859.

Ishikawa, K., Takeuchi, N., Takahashi, S., Matera, K.M., Sato, M., Shibahara, S., Rousseau, D.L., Ikeda-Saito, M., Yoshida, T., **1995**. Heme oxygenase-2. Properties of the heme complex of the purified tryptic fragment of recombinant human heme oxygenase-2. J Biol Chem 270, 6345-6350.

Ivan, M., Kondo, K., Yang, H., Kim, W., Valiando, J., Ohh, M., Salic, A., Asara, J.M., Lane, W.S., Kaelin, W.G., Jr., **2001**. HIFalpha targeted for VHL-mediated destruction by proline hydroxylation: implications for O2 sensing. Science 292, 464-468.

Jacobs, A., **1977**. Low molecular weight intracellular iron transport compounds. Blood 50, 433-439.

Jacobs, A., Worwood, M., **1975**. Ferritin in serum. Clinical and biochemical implications. N Engl J Med 292, 951-956.

Jessup, W., Mander, E.L., Dean, R.T., **1992**. The intracellular storage and turnover of apolipoprotein B of oxidized LDL in macrophages. Biochim Biophys Acta 1126, 167-177.

Johnson , M.T.B., Rose N.J., Goodwin W.H.and Pickart L. , **1982**. Cytotoxic chelators and chelates 1. Inhibition of DNA synthesis in cultured rodent and human cells by aroylhydrazones and by a copper(II) complex of salicylaldehyde benzoyl hydrazone. Inorg. Chim. Acta 67, 159-165.

Jones, D.P., Go, Y.M., Anderson, C.L., Ziegler, T.R., Kinkade, J.M., Jr., Kirlin, W.G., **2004**. Cysteine/cystine couple is a newly recognized node in the circuitry for biologic redox signaling and control. FASEB J 18, 1246-1248.

Jones, T., Spencer, R., Walsh, C., **1978**. Mechanism and kinetics of iron release from ferritin by dihydroflavins and dihydroflavin analogues. Biochemistry 17, 4011-4017.

Jordan, A., Pontis, E., Atta, M., Krook, M., Gibert, I., Barbe, J., Reichard, P., **1994**. A second class I ribonucleotide reductase in Enterobacteriaceae: characterization of the Salmonella typhimurium enzyme. Proc Natl Acad Sci U S A 91, 12892-12896.

Jordan, A., Reichard, P., **1998**. Ribonucleotide reductases. Annu Rev Biochem 67, 71-98.

Jornot, L., Junod, A.F., **1993**. Variable glutathione levels and expression of antioxidant enzymes in human endothelial cells. Am J Physiol 264, L482-489.

Joyce, D., Albanese, C., Steer, J., Fu, M., Bouzahzah, B., Pestell, R.G., **2001**. NF-kappaB and cell-cycle regulation: the cyclin connection. Cytokine Growth Factor Rev 12, 73-90.

Kaiser, B.K., Zimmerman, Z.A., Charbonneau, H., Jackson, P.K., **2002**. Disruption of centrosome structure, chromosome segregation, and cytokinesis by misexpression of human Cdc14A phosphatase. Mol Biol Cell 13, 2289-2300.

Kakhlon, O., Cabantchik, Z.I., **2002**. The labile iron pool: characterization, measurement, and participation in cellular processes(1). Free Radic Biol Med 33, 1037-1046.

Kakhlon, O., Gruenbaum, Y., Cabantchik, Z.I., **2001**. Repression of ferritin expression increases the labile iron pool, oxidative stress, and short-term growth of human erythroleukemia cells. Blood 97, 2863-2871.

Kaldis, P., Aleem, E., **2005**. Cell cycle sibling rivalry: Cdc2 vs. Cdk2. Cell Cycle 4, 1491-1494.

Kalinowski, D.S., Richardson, D.R., **2005**. The evolution of iron chelators for the treatment of iron overload disease and cancer. Pharmacol Rev 57, 547-583.

Kaplan, J., Jordan, I., Sturrock, A., **1991**. Regulation of the transferrin-independent iron transport system in cultured cells. J Biol Chem 266, 2997-3004.

Kaptain, S., Downey, W.E., Tang, C., Philpott, C., Haile, D., Orloff, D.G., Harford, J.B., Rouault, T.A., Klausner, R.D., **1991**. A regulated RNA binding protein also possesses aconitase activity. Proc Natl Acad Sci U S A 88, 10109-10113.

Kawabata, H., Germain, R.S., Vuong, P.T., Nakamaki, T., Said, J.W., Koeffler, H.P., **2000**. Transferrin receptor 2-alpha supports cell growth both in iron-chelated cultured cells and in vivo. J Biol Chem 275, 16618-16625.

Kawabata, H., Yang, R., Hirama, T., Vuong, P.T., Kawano, S., Gombart, A.F., Koeffler, H.P., **1999**. Molecular cloning of transferrin receptor 2. A new member of the transferrin receptor-like family. J Biol Chem 274, 20826-20832.

Ke, Q., Costa, M., **2006**. Hypoxia-inducible factor-1 (HIF-1). Mol Pharmacol 70, 1469-1480.

Kearsey, J.M., Coates, P.J., Prescott, A.R., Warbrick, E., Hall, P.A., **1995**. Gadd45 is a nuclear cell cycle regulated protein which interacts with p21Cip1. Oncogene 11, 1675-1683.

Kew, M.C., Torrance, J.D., Derman, D., Simon, M., Macnab, G.M., Charlton, R.W., Bothwell, T.H., **1978**. Serum and tumour ferritins in primary liver cancer. Gut 19, 294-299.

Keyomarsi, K., Herliczek, T.W., **1997**. The role of cyclin E in cell proliferation, development and cancer. Prog Cell Cycle Res 3, 171-191.

Keyse, S.M., Moss, S.H., Davies, D.J., **1983**. Action spectra for inactivation of normal and xeroderma pigmentosum human skin fibroblasts by ultraviolet radiations. Photochem Photobiol 37, 307-312.

Keyse, S.M., Tyrrell, R.M., **1989**. Heme oxygenase is the major 32-kDa stress protein induced in human skin fibroblasts by UVA radiation, hydrogen peroxide, and sodium arsenite. Proc Natl Acad Sci U S A 86, 99-103.

Keyse, S.M., Tyrrell, R.M., **1990**. Induction of the heme oxygenase gene in human skin fibroblasts by hydrogen peroxide and UVA (365 nm) radiation: evidence for the involvement of the hydroxyl radical. Carcinogenesis 11, 787-791.

Kielbassa, C., Roza, L., Epe, B., **1997**. Wavelength dependence of oxidative DNA damage induced by UV and visible light. Carcinogenesis 18, 811-816.

Kikyo, N., Hagiwara, K., Fujisawa, M., Yazaki, Y., Okabe, T., **1994a**. Purification of a cell growth factor from a human lung cancer cell line: its relationship with ferritin. J Cell Physiol 161, 106-110.

Kikyo, N., Suda, M., Hagiwara, K., Yasukawa, K., Fujisawa, M., Yazaki, Y., Okabe, T., **1994b**. Purification and characterization of a cell growth factor from a human leukemia cell line: immunological identity with ferritin. Cancer Res 54, 268-271.

Kim, H.J., Jung, W.H., Kim, D.Y., Lee, H.D., **2000**. Expression of cyclins in ductal hyperplasia, atypical ductal hyperplasia and ductal carcinoma in situ of the breast. Yonsei Med J 41, 345-353.

Klausner, R.D., Ashwell, G., van Renswoude, J., Harford, J.B., Bridges, K.R., **1983a**. Binding of apotransferrin to K562 cells: explanation of the transferrin cycle. Proc Natl Acad Sci U S A 80, 2263-2266.

Klausner, R.D., Rouault, T.A., Harford, J.B., **1993**. Regulating the fate of mRNA: the control of cellular iron metabolism. Cell 72, 19-28.

Klausner, R.D., Van Renswoude, J., Ashwell, G., Kempf, C., Schechter, A.N., Dean, A., Bridges, K.R., **1983b**. Receptor-mediated endocytosis of transferrin in K562 cells. J Biol Chem 258, 4715-4724.

Klotz, L.O., Briviba, K., Sies, H., **1997**. Singlet oxygen mediates the activation of JNK by UVA radiation in human skin fibroblasts. FEBS Lett 408, 289-291.

Knox, J.J., Hotte, S.J., Kollmannsberger, C., Winquist, E., Fisher, B., Eisenhauer, E.A., **2007**. Phase II study of Triapine in patients with metastatic renal cell carcinoma: a trial of the National Cancer Institute of Canada Clinical Trials Group (NCIC IND.161). Invest New Drugs 25, 471-477.

Kohen, R., **1999**. Skin antioxidants: their role in aging and in oxidative stress--new approaches for their evaluation. Biomed Pharmacother 53, 181-192.

Kohgo, Y., Ohtake, T., Ikuta, K., Suzuki, Y., Hosoki, Y., Saito, H., Kato, J., **2005**. Iron accumulation in alcoholic liver diseases. Alcohol Clin Exp Res 29, 189S-193S.

Kolberg, M., Strand, K.R., Graff, P., Andersson, K.K., **2004**. Structure, function, and mechanism of ribonucleotide reductases. Biochim Biophys Acta 1699, 1-34.

Konijn, A.M., Meyron-Holtz, E.G., Levy, R., Ben-Bassat, H., Matzner, Y., **1990**. Specific binding of placental acidic isoferritin to cells of the T-cell line HD-MAR. FEBS Lett 263, 229-232.

Kontou, M., Will, R.D., Adelfalk, C., Wittig, R., Poustka, A., Hirsch-Kauffmann, M., Schweiger, M., **2004**. Thioredoxin, a regulator of gene expression. Oncogene 23, 2146-2152.

Kountouras, J., Boura, P., Karolides, A., Zaharioudaki, E., Tsapas, G., **1995**. Recombinant a2 interferon (a-IFN) with chemo-hormonal therapy in patients with hepatocellular carcinoma (HCC). Hepatogastroenterology 42, 31-36.

Kovacevic, Z., Richardson, D.R., **2006**. The metastasis suppressor, Ndrg-1: a new ally in the fight against cancer. Carcinogenesis 27, 2355-2366.

Kowdley, K.V., **2004**. Iron, hemochromatosis, and hepatocellular carcinoma. Gastroenterology 127, S79-86.

Kralli, A., Moss, S.H., **1987**. The sensitivity of an actinic reticuloid cell strain to near-ultraviolet radiation and its modification by trolox-C, a vitamin E analogue. Br J Dermatol 116, 761-772.

Krinsky, N.I., Deneke, S.M., **1982**. Interaction of oxygen and oxy-radicals with carotenoids. J Natl Cancer Inst 69, 205-210.

Kruszewski, M., **2003**. Labile iron pool: the main determinant of cellular response to oxidative stress. Mutat Res 531, 81-92.

Kubli, D.A., Ycaza, J.E., Gustafsson, A.B., **2007**. Bnip3 mediates mitochondrial dysfunction and cell death through Bax and Bak. Biochem J 405, 407-415.

Kuhn, L.C., **1994**. Molecular regulation of iron proteins. Baillieres Clin Haematol 7, 763-785.

Kulp, K.S., Green, S.L., Vulliet, P.R., **1996**. Iron deprivation inhibits cyclin-dependent kinase activity and decreases cyclin D/CDK4 protein levels in asynchronous MDA-MB-453 human breast cancer cells. Exp Cell Res 229, 60-68.

Kurdistani, S.K., Arizti, P., Reimer, C.L., Sugrue, M.M., Aaronson, S.A., Lee, S.W., **1998**. Inhibition of tumor cell growth by RTP/rit42 and its responsiveness to p53 and DNA damage. Cancer Res 58, 4439-4444.

Kurz, T., Gustafsson, B., Brunk, U.T., **2006**. Intralysosomal iron chelation protects against oxidative stress-induced cellular damage. FEBS J 273, 3106-3117.

Kurz, T., Terman, A., Gustafsson, B., Brunk, U.T., **2008**. Lysosomes and oxidative stress in aging and apoptosis. Biochim Biophys Acta 1780, 1291-1303.

Kvam, E., Noel, A., Basu-Modak, S., Tyrrell, R.M., **1999**. Cyclooxygenase dependent release of heme from microsomal hemeproteins correlates with induction of heme oxygenase 1 transcription in human fibroblasts. Free Radic Biol Med 26, 511-517.

Kvam, E., Tyrrell, R.M., **1997**. Induction of oxidative DNA base damage in human skin cells by UV and near visible radiation. Carcinogenesis 18, 2379-2384.

Kwok, J.C., Richardson, D.R., **2002**. The iron metabolism of neoplastic cells: alterations that facilitate proliferation? Crit Rev Oncol Hematol 42, 65-78.

LaCasse, E.C., Baird, S., Korneluk, R.G., MacKenzie, A.E., **1998**. The inhibitors of apoptosis (IAPs) and their emerging role in cancer. Oncogene 17, 3247-3259.

Langlois d'Estaintot, B., Santambrogio, P., Granier, T., Gallois, B., Chevalier, J.M., Precigoux, G., Levi, S., Arosio, P., **2004**. Crystal structure and biochemical properties of the human mitochondrial ferritin and its mutant Ser144Ala. J Mol Biol 340, 277-293.

Laporte, M., Galand, P., Fokan, D., de Graef, C., Heenen, M., **2000**. Apoptosis in established and healing psoriasis. Dermatology 200, 314-316.

Latunde-Dada, G.O., Takeuchi, K., Simpson, R.J., McKie, A.T., **2006**. Haem carrier protein 1 (HCP1): Expression and functional studies in cultured cells. FEBS Lett 580, 6865-6870.

Lautier, D., Luscher, P., Tyrrell, R.M., **1992**. Endogenous glutathione levels modulate both constitutive and UVA radiation/hydrogen peroxide inducible expression of the human heme oxygenase gene. Carcinogenesis 13, 227-232.

Lavoie, J.N., L'Allemain, G., Brunet, A., Muller, R., Pouyssegur, J., **1996**. Cyclin D1 expression is regulated positively by the p42/p44MAPK and negatively by the p38/HOGMAPK pathway. J Biol Chem 271, 20608-20616.

Lawen, A., **2003**. Apoptosis-an introduction. Bioessays 25, 888-896.

Lawson, D.M., Treffry, A., Artymiuk, P.J., Harrison, P.M., Yewdall, S.J., Luzzago, A., Cesareni, G., Levi, S., Arosio, P., **1989**. Identification of the ferroxidase centre in ferritin. FEBS Lett 254, 207-210.

Lazo, J.S., Kondo, Y., Dellapiazza, D., Michalska, A.E., Choo, K.H., Pitt, B.R., **1995**. Enhanced sensitivity to oxidative stress in cultured embryonic cells from transgenic mice deficient in metallothionein I and II genes. J Biol Chem 270, 5506-5510.

Le, N.T., Richardson, D.R., **2002**. The role of iron in cell cycle progression and the proliferation of neoplastic cells. Biochim Biophys Acta 1603, 31-46.

Le, N.T., Richardson, D.R., **2003**. Potent iron chelators increase the mRNA levels of the universal cyclin-dependent kinase inhibitor p21(CIP1/WAF1), but paradoxically inhibit its translation: a potential mechanism of cell cycle dysregulation. Carcinogenesis 24, 1045-1058.

Le, N.T., Richardson, D.R., **2004**. Competing pathways of iron chelation: angiogenesis or anti-tumor activity: targeting different molecules to induce specific effects. Int J Cancer 110, 468-469.

Leccia, M.T., Richard, M.J., Beani, J.C., Faure, H., Monjo, A.M., Cadet, J., Amblard, P., Favier, A., **1993**. Protective effect of selenium and zinc on UV-A damage in human skin fibroblasts. Photochem Photobiol 58, 548-553.

Lee, R.J., Albanese, C., Stenger, R.J., Watanabe, G., Inghirami, G., Haines, G.K., 3rd, Webster, M., Muller, W.J., Brugge, J.S., Davis, R.J., Pestell, R.G., **1999**. pp60(v-src) induction of cyclin D1 requires collaborative interactions between the extracellular signal-regulated kinase, p38, and Jun kinase pathways. A role for cAMP response element-binding protein and activating transcription factor-2 in pp60(v-src) signaling in breast cancer cells. J Biol Chem 274, 7341-7350.

Lee, S.K., Jang, H.J., Lee, H.J., Lee, J., Jeon, B.H., Jun, C.D., Kim, E.C., **2006**. p38 and ERK MAP kinase mediates iron chelator-induced apoptosis and -suppressed differentiation of immortalized and malignant human oral keratinocytes. Life Sci 79, 1419-1427.

Leibold, E.A., Munro, H.N., **1988**. Cytoplasmic protein binds in vitro to a highly conserved sequence in the 5' untranslated region of ferritin heavy- and light-subunit mRNAs. Proc Natl Acad Sci U S A 85, 2171-2175.

Leveque, N., Robin, S., Muret, P., Mac-Mary, S., Makki, S., Berthelot, A., Kantelip, J.P., Humbert, P., **2004**. In vivo assessment of iron and ascorbic acid in psoriatic dermis. Acta Derm Venereol 84, 2-5.

Levi, S., Arosio, P., **2004**. Mitochondrial ferritin. Int J Biochem Cell Biol 36, 1887-1889.

Levi, S., Corsi, B., Bosisio, M., Invernizzi, R., Volz, A., Sanford, D., Arosio, P., Drysdale, J., **2001**. A human mitochondrial ferritin encoded by an intronless gene. J Biol Chem 276, 24437-24440.

Levi, S., Yewdall, S.J., Harrison, P.M., Santambrogio, P., Cozzi, A., Rovida, E., Albertini, A., Arosio, P., **1992**. Evidence of H- and L-chains have co-operative roles in the iron-uptake mechanism of human ferritin. Biochem J 288 (Pt 2), 591-596.

Levy, A.P., Levy, N.S., Wegner, S., Goldberg, M.A., **1995**. Transcriptional regulation of the rat vascular endothelial growth factor gene by hypoxia. J Biol Chem 270, 13333-13340.

Ley, R.D., Applegate, L.A., **1985**. Ultraviolet radiation-induced histopathologic changes in the skin of the marsupial Monodelphis domestica. II. Quantitative studies of the photoreactivation of induced hyperplasia and sunburn cell formation. J Invest Dermatol 85, 365-367.

Liang, S.X., Richardson, D.R., **2003**. The effect of potent iron chelators on the regulation of p53: examination of the expression, localization and DNA-binding activity of p53 and the transactivation of WAF1. Carcinogenesis 24, 1601-1614.

Lilenbaum, R.C., List, M., Desch, C., **1999**. Single-agent versus combination chemotherapy in advanced non-small cell lung cancer: a meta-analysis and the Cancer and Leukemia Group B randomized trial. Semin Oncol 26, 52-54.

Lin, A.W., Lowe, S.W., **2001**. Oncogenic ras activates the ARF-p53 pathway to suppress epithelial cell transformation. Proc Natl Acad Sci U S A 98, 5025-5030.

Lin, F., Girotti, A.W., **1997**. Elevated ferritin production, iron containment, and oxidant resistance in hemin-treated leukemia cells. Arch Biochem Biophys 346, 131-141.

Linder, M.C., Schaffer, K.J., Hazegh-Azam, M., Zhou, C.Y., Tran, T.N., Nagel, G.M., **1996**. Serum ferritin: does it differ from tissue ferritin? J Gastroenterol Hepatol 11, 1033-1036.

Linke, S.P., Clarkin, K.C., Di Leonardo, A., Tsou, A., Wahl, G.M., **1996**. A reversible, p53-dependent G0/G1 cell cycle arrest induced by ribonucleotide depletion in the absence of detectable DNA damage. Genes Dev 10, 934-947.

Lippens, M., Room, G., De Groote, G., Decuypere, E., **2000**. Early and temporary quantitative food restriction of broiler chickens. 1. Effects on performance characteristics, mortality and meat quality. Br Poult Sci 41, 343-354.

Lippens, S., Hoste, E., Vandenabeele, P., Agostinis, P., Declercq, W., **2009**. Cell death in the skin. Apoptosis 14, 549-569.

Lloyd, J.B., Cable, H., Rice-Evans, C., **1991**. Evidence that desferrioxamine cannot enter cells by passive diffusion. Biochem Pharmacol 41, 1361-1363.

Lo Muzio, L., Staibano, S., Pannone, G., Mignogna, M.D., Mariggio, A., Salvatore, G., Chieffi, P., Tramontano, D., De Rosa, G., Altieri, D.C., **2001**. Expression of the apoptosis inhibitor survivin in aggressive squamous cell carcinoma. Exp Mol Pathol 70, 249-254.

Lodish, H.F., 2008. Molecular cell biology. W. H. Freeman, New York ; Basingstoke.

Lovejoy, D.B., Richardson, D.R., **2002**. Novel "hybrid" iron chelators derived from aroylhydrazones and thiosemicarbazones demonstrate selective antiproliferative activity against tumor cells. Blood 100, 666-676.

Lucas, J.J., Szepesi, A., Domenico, J., Takase, K., Tordai, A., Terada, N., Gelfand, E.W., **1995**. Effects of iron-depletion on cell cycle progression in normal human T lymphocytes: selective inhibition of the appearance of the cyclin A-associated component of the p33cdk2 kinase. Blood 86, 2268-2280.

Lum, J.B., Infante, A.J., Makker, D.M., Yang, F., Bowman, B.H., **1986**. Transferrin synthesis by inducer T lymphocytes. J Clin Invest 77, 841-849.

MacGillivray, R.T., Mendez, E., Shewale, J.G., Sinha, S.K., Lineback-Zins, J., Brew, K., **1983**. The primary structure of human serum transferrin. The structures of seven cyanogen bromide fragments and the assembly of the complete structure. J Biol Chem 258, 3543-3553.

MacKenzie, E.L., Iwasaki, K., Tsuji, Y., **2008**. Intracellular iron transport and storage: from molecular mechanisms to health implications. Antioxid Redox Signal 10, 997-1030.

Mackenzie, M.J., Saltman, D., Hirte, H., Low, J., Johnson, C., Pond, G., Moore, M.J., **2007**. A Phase II study of 3-aminopyridine-2-carboxaldehyde thiosemicarbazone (3-AP) and gemcitabine in advanced pancreatic carcinoma. A trial of the Princess Margaret hospital Phase II consortium. Invest New Drugs 25, 553-558.

Madison, K.C., **2003**. Barrier function of the skin: "la raison d'etre" of the epidermis. J Invest Dermatol 121, 231-241.

Maines, M.D., Trakshel, G.M., Kutty, R.K., **1986**. Characterization of two constitutive forms of rat liver microsomal heme oxygenase. Only one molecular species of the enzyme is inducible. J Biol Chem 261, 411-419.

Marcus, D.M., Zinberg, N., **1975**. Measurement of serum ferritin by radioimmunoassay: results in normal individuals and patients with breast cancer. J Natl Cancer Inst 55, 791-795.

Marks, J., Miller, J., 2006. Lookingbill and Marks' Principles of Dermatology Elsevier Saunders.

Martinez-Cayuela, M., **1995**. Oxygen free radicals and human disease. Biochimie 77, 147-161.

Martinez, J.C., Otley, C.C., **2001**. The management of melanoma and nonmelanoma skin cancer: a review for the primary care physician. Mayo Clin Proc 76, 1253-1265.

Maruyama, Y., Ono, M., Kawahara, A., Yokoyama, T., Basaki, Y., Kage, M., Aoyagi, S., Kinoshita, H., Kuwano, M., **2006**. Tumor growth suppression in pancreatic cancer by a putative metastasis suppressor gene Cap43/NDRG1/Drg-1 through modulation of angiogenesis. Cancer Res 66, 6233-6242.

Mathews-Roth, M.M., Krinsky, N.I., **1987**. Carotenoids affect development of UV-B induced skin cancer. Photochem Photobiol 46, 507-509.

Matsumoto, M., Natsugoe, S., Nakashima, S., Okumura, H., Sakita, H., Baba, M., Takao, S., Aikou, T., **2001**. Clinical significance and prognostic value of apoptosis related proteins in superficial esophageal squamous cell carcinoma. Ann Surg Oncol 8, 598-604.

Maytin, E.V., Ubeda, M., Lin, J.C., Habener, J.F., **2001**. Stress-inducible transcription factor CHOP/gadd153 induces apoptosis in mammalian cells via p38 kinase-dependent and -independent mechanisms. Exp Cell Res 267, 193-204.

McAuliffe, D.J., Blank, I.H., **1991**. Effects of UVA (320-400 nm) on the barrier characteristics of the skin. J Invest Dermatol 96, 758-762.

McCann, J., **1997**. Texas center studies research alternative treatments. J Natl Cancer Inst 89, 1485-1486.

McClarty, G.A., Chan, A.K., Choy, B.K., Wright, J.A., **1990**. Increased ferritin gene expression is associated with increased ribonucleotide reductase gene expression and the establishment of hydroxyurea resistance in mammalian cells. J Biol Chem 265, 7539-7547.

McCoubrey, W.K., Jr., Huang, T.J., Maines, M.D., **1997**. Isolation and characterization of a cDNA from the rat brain that encodes hemoprotein heme oxygenase-3. Eur J Biochem 247, 725-732.

McGrath, J.A., Eady, R.A., Pope, F.M., 2004. Rook's Textbook of Dermatology. Blackwell Publishing.

McKie, A.T., Marciani, P., Rolfs, A., Brennan, K., Wehr, K., Barrow, D., Miret, S., Bomford, A., Peters, T.J., Farzaneh, F., Hediger, M.A., Hentze, M.W., Simpson, R.J., **2000**. A novel duodenal iron-regulated transporter, IREG1, implicated in the basolateral transfer of iron to the circulation. Mol Cell 5, 299-309.

Meewes, C., Brenneisen, P., Wenk, J., Kuhr, L., Ma, W., Alikoski, J., Poswig, A., Krieg, T., Scharffetter-Kochanek, K., **2001**. Adaptive antioxidant response protects dermal fibroblasts from UVA-induced phototoxicity. Free Radic Biol Med 30, 238-247.

Meister, A., Anderson, M.E., **1983**. Glutathione. Annu Rev Biochem 52, 711-760.

Menezes, S., Tyrrell, R.M., **1982**. Damage by solar radiation at defined wavelengths: involvement of inducible repair systems. Photochem Photobiol 36, 313-318.

Menter, A., **2009**. The status of biologic therapies in the treatment of moderate to severe psoriasis. Cutis 84, 14-24.

Michalides, R., van Veelen, N., Hart, A., Loftus, B., Wientjens, E., Balm, A., **1995**. Overexpression of cyclin D1 correlates with recurrence in a group of forty-seven operable squamous cell carcinomas of the head and neck. Cancer Res 55, 975-978.

Mims, M.P., Prchal, J.T., **2005**. Divalent metal transporter 1. Hematology 10, 339-345.

Mizutani, A., Furukawa, T., Adachi, Y., Ikehara, S., Taketani, S., **2002**. A zinc-finger protein, PLAGL2, induces the expression of a proapoptotic protein Nip3, leading to cellular apoptosis. J Biol Chem 277, 15851-15858.

Modjtahedi, N., Frebourg, T., Fossar, N., Lavialle, C., Cremisi, C., Brison, O., **1992**. Increased expression of cytokeratin and ferritin-H genes in tumorigenic clones of the SW 613-S human colon carcinoma cell line. Exp Cell Res 201, 74-82.

Molin, L., Wester, P.O., **1973**. Iron content in normal and psoriatic epidermis. Acta Derm Venereol 53, 473-476.

Molina-Holgado, F., Gaeta, A., Francis, P.T., Williams, R.J., Hider, R.C., **2008**. Neuroprotective actions of deferiprone in cultured cortical neurones and SHSY-5Y cells. J Neurochem 105, 2466-2476.

Morales-Ducret, C.R., van de Rijn, M., LeBrun, D.P., Smoller, B.R., **1995**. bcl-2 expression in primary malignancies of the skin. Arch Dermatol 131, 909-912.

Morel, Y., Barouki, R., **1999**. Repression of gene expression by oxidative stress. Biochem J 342 Pt 3, 481-496.

Morgan, E.H., **1983**. Effect of pH and iron content of transferrin on its binding to reticulocyte receptors. Biochim Biophys Acta 762, 498-502.

Morliere, P., Moysan, A., Santus, R., Huppe, G., Maziere, J.C., Dubertret, L., **1991**. UVA-induced lipid peroxidation in cultured human fibroblasts. Biochim Biophys Acta 1084, 261-268.

Morris, C.J., Earl, J.R., Trenam, C.W., Blake, D.R., **1995**. Reactive oxygen species and iron--a dangerous partnership in inflammation. Int J Biochem Cell Biol 27, 109-122.

Morrone, G., Corbo, L., Turco, M.C., Pizzano, R., De Felice, M., Bridges, S., Venuta, S., **1988**. Transferrin-like autocrine growth factor, derived from T-lymphoma cells, that inhibits normal T-cell proliferation. Cancer Res 48, 3425-3429.

Mosmann, T., **1983**. Rapid colorimetric assay for cellular growth and survival: application to proliferation and cytotoxicity assays. J Immunol Methods 65, 55-63.

Moysan, A., Marquis, I., Gaboriau, F., Santus, R., Dubertret, L., Morliere, P., **1993**. Ultraviolet A-induced lipid peroxidation and antioxidant defense systems in cultured human skin fibroblasts. J Invest Dermatol 100, 692-698.

Muakkassah-Kelly, S.F., Andresen, J.W., Shih, J.C., Hochstein, P., **1982**. Decreased [3H]serotonin and [3H]spiperone binding consequent to lipid peroxidation in rat cortical membranes. Biochem Biophys Res Commun 104, 1003-1010.

Mullner, E.W., Rothenberger, S., Muller, A.M., Kuhn, L.C., **1992**. In vivo and in vitro modulation of the mRNA-binding activity of iron-regulatory factor. Tissue distribution and effects of cell proliferation, iron levels and redox state. Eur J Biochem 208, 597-605.

Munro, H.N., Linder, M.C., **1978**. Ferritin: structure, biosynthesis, and role in iron metabolism. Physiol Rev 58, 317-396.

Murren, J., Modiano, M., Clairmont, C., Lambert, P., Savaraj, N., Doyle, T., Sznol, M., **2003**. Phase I and pharmacokinetic study of triapine, a potent ribonucleotide reductase inhibitor, administered daily for five days in patients with advanced solid tumors. Clin Cancer Res 9, 4092-4100.

Myers, W.A., Gottlieb, A.B., Mease, P., **2006**. Psoriasis and psoriatic arthritis: clinical features and disease mechanisms. Clin Dermatol 24, 438-447.

Nakamura, H., Matsuda, M., Furuke, K., Kitaoka, Y., Iwata, S., Toda, K., Inamoto, T., Yamaoka, Y., Ozawa, K., Yodoi, J., **1994**. Adult T cell leukemia-derived factor/human thioredoxin protects endothelial F-2 cell injury caused by activated neutrophils or hydrogen peroxide. Immunol Lett 42, 75-80.

Nakano, K., Balint, E., Ashcroft, M., Vousden, K.H., **2000**. A ribonucleotide reductase gene is a transcriptional target of p53 and p73. Oncogene 19, 4283-4289.

Napier, I., Ponka, P., Richardson, D.R., **2005**. Iron trafficking in the mitochondrion: novel pathways revealed by disease. Blood 105, 1867-1874.

Neuzil, J., Gebicki, J.M., Stocker, R., **1993**. Radical-induced chain oxidation of proteins and its inhibition by chain-breaking antioxidants. Biochem J 293 (Pt 3), 601-606.

Neville, J.A., Welch, E., Leffell, D.J., **2007**. Management of nonmelanoma skin cancer in 2007. Nat Clin Pract Oncol 4, 462-469.

Nie, G., Chen, G., Sheftel, A.D., Pantopoulos, K., Ponka, P., **2006**. In vivo tumor growth is inhibited by cytosolic iron deprivation caused by the expression of mitochondrial ferritin. Blood 108, 2428-2434.

Nie, G., Sheftel, A.D., Kim, S.F., Ponka, P., **2005**. Overexpression of mitochondrial ferritin causes cytosolic iron depletion and changes cellular iron homeostasis. Blood 105, 2161-2167.

Nurtjahja-Tjendraputra, E., Fu, D., Phang, J.M., Richardson, D.R., **2007**. Iron chelation regulates cyclin D1 expression via the proteasome: a link to iron deficiency-mediated growth suppression. Blood 109, 4045-4054.

Nyholm, S., Thelander, L., Graslund, A., **1993**. Reduction and loss of the iron center in the reaction of the small subunit of mouse ribonucleotide reductase with hydroxyurea. Biochemistry 32, 11569-11574.

O'Donnell, K.A., Yu, D., Zeller, K.I., Kim, J.W., Racke, F., Thomas-Tikhonenko, A., Dang, C.V., **2006**. Activation of transferrin receptor 1 by c-Myc enhances cellular proliferation and tumorigenesis. Mol Cell Biol 26, 2373-2386.

Oexle, H., Gnaiger, E., Weiss, G., **1999**. Iron-dependent changes in cellular energy metabolism: influence on citric acid cycle and oxidative phosphorylation. Biochim Biophys Acta 1413, 99-107.

Omoto, E., Tavassoli, M., **1990**. Purification and partial characterization of ceruloplasmin receptors from rat liver endothelium. Arch Biochem Biophys 282, 34-38.

Orino, K., Lehman, L., Tsuji, Y., Ayaki, H., Torti, S.V., Torti, F.M., **2001**. Ferritin and the response to oxidative stress. Biochem J 357, 241-247.

Pacifici, R.E., Davies, K.J., **1990**. Protein degradation as an index of oxidative stress. Methods Enzymol 186, 485-502.

Page, M.A., Baker, E., Morgan, E.H., **1984**. Transferrin and iron uptake by rat hepatocytes in culture. Am J Physiol 246, G26-33.

Pahl, P.M., Horwitz, L.D., **2005**. Cell permeable iron chelators as potential cancer chemotherapeutic agents. Cancer Invest 23, 683-691.

Parrish, J.A., Jaenicke, K.F., Anderson, R.R., **1982**. Erythema and melanogenesis action spectra of normal human skin. Photochem Photobiol 36, 187-191.

Pastila, R., **2006**. Effect of long-wave UV radiation on mouse melanoma: an *in vitro* and *in vivo* study Faculty of Biosciences. Department of Biological and Environmental Sciences. University of Helsinki, Helsinki.

Peak, J.G., Peak, M.J., **1990**. Ultraviolet light induces double-strand breaks in DNA of cultured human P3 cells as measured by neutral filter elution. Photochem Photobiol 52, 387-393.

Peak, J.G., Peak, M.J., **1995**. Induction of slowly developing alkali-labile sites in human P3 cell DNA by UVA and blue- and green-light photons: action spectrum. Photochem Photobiol 61, 484-487.

Peak, M.J., Peak, J.G., Carnes, B.A., **1987**. Induction of direct and indirect single-strand breaks in human cell DNA by far- and near-ultraviolet radiations: action spectrum and mechanisms. Photochem Photobiol 45, 381-387.

Pelle, E., Mammone, T., Maes, D., Frenkel, K., **2005**. Keratinocytes act as a source of reactive oxygen species by transferring hydrogen peroxide to melanocytes. J Invest Dermatol 124, 793-797.

Petersen, D.R., **2005**. Alcohol, iron-associated oxidative stress, and cancer. Alcohol 35, 243-249.

Petrat, F., de Groot, H., Rauen, U., **2000**. Determination of the chelatable iron pool of single intact cells by laser scanning microscopy. Arch Biochem Biophys 376, 74-81.

Petrat, F., de Groot, H., Rauen, U., **2001**. Subcellular distribution of chelatable iron: a laser scanning microscopic study in isolated hepatocytes and liver endothelial cells. Biochem J 356, 61-69.

Petrat, F., Rauen, U., de Groot, H., **1999**. Determination of the chelatable iron pool of isolated rat hepatocytes by digital fluorescence microscopy using the fluorescent probe, phen green SK. Hepatology 29, 1171-1179.

Piccinelli, P., Samuelsson, T., **2007**. Evolution of the iron-responsive element. RNA 13, 952-966.

Plowman, G.D., Brown, J.P., Enns, C.A., Schroder, J., Nikinmaa, B., Sussman, H.H., Hellstrom, K.E., Hellstrom, I., **1983**. Assignment of the gene for human melanoma-associated antigen p97 to chromosome 3. Nature 303, 70-72.

Ponka, P., Borova, J., Neuwirt, J., Fuchs, O., **1979a**. Mobilization of iron from reticulocytes. Identification of pyridoxal isonicotinoyl hydrazone as a new iron chelating agent. FEBS Lett 97, 317-321.

Ponka, P., Borova, J., Neuwirt, J., Fuchs, O., Necas, E., **1979b**. A study of intracellular iron metabolism using pyridoxal isonicotinoyl hydrazone and other synthetic chelating agents. Biochim Biophys Acta 586, 278-297.

Poola, I., **1997**. An estrogen inducible 104 kDa chaperone glycoprotein binds ferric iron containing proteins: a possible role in intracellular iron trafficking. FEBS Lett 416, 139-142.

Poola, I., Kiang, J.G., **1994**. The estrogen-inducible transferrin receptor-like membrane glycoprotein is related to stress-regulated proteins. J Biol Chem 269, 21762-21769.

Poola, I., Lucas, J.J., **1988**. Purification and characterization of an estrogen-inducible membrane glycoprotein. Evidence that it is a transferrin receptor. J Biol Chem 263, 19137-19146.

Poola, I., Mason, A.B., Lucas, J.J., **1990**. The chicken oviduct and embryonic red blood cell transferrin receptors are distinct molecules. Biochem Biophys Res Commun 171, 26-32.

Popp, S., Waltering, S., Holtgreve-Grez, H., Jauch, A., Proby, C., Leigh, I.M., Boukamp, P., **2000**. Genetic characterization of a human skin carcinoma progression model: from primary tumor to metastasis. J Invest Dermatol 115, 1095-1103.

Porter, J.B., Huehns, E.R., **1989**. The toxic effects of desferrioxamine. Baillieres Clin Haematol 2, 459-474.

Pourzand, C., Reelfs, O., Kvam, E., Tyrrell, R.M., **1999a**. The iron regulatory protein can determine the effectiveness of 5-aminolevulinic acid in inducing protoporphyrin IX in human primary skin fibroblasts. J Invest Dermatol 112, 419-425.

Pourzand, C., Reelfs, O., Tyrrell, R.M., **2000**. Approaches to define the involvement of reactive oxygen species and iron in ultraviolet-A inducible gene expression. Methods Mol Biol 99, 257-276.

Pourzand, C., Rossier, G., Reelfs, O., Borner, C., Tyrrell, R.M., **1997**. Overxpression of Bcl-2 inhibits UVA-mediated immediate apoptosiinrat 6 fibroblasts: evidence for the involvement of Bcl-2 as an antioxidant. Cancer Res 57, 1405-1411.

Pourzand, C., Tyrrell, R.M., **1999**. Apoptosis, the role of oxidative stress and the example of solar UV radiation. Photochem Photobiol 70, 380-390.

Pourzand, C., Watkin, R.D., Brown, J.E., Tyrrell, R.M., **1999b**. Ultraviolet A radiation induces immediate release of iron in human primary skin fibroblasts: the role of ferritin. Proc Natl Acad Sci U S A 96, 6751-6756.

Prather, R.S., Boquest, A.C., Day, B.N., **1999**. Cell cycle analysis of cultured porcine mammary cells. Cloning 1, 17-24.

Price, B.D., Calderwood, S.K., **1992**. Gadd45 and Gadd153 messenger RNA levels are increased during hypoxia and after exposure of cells to agents which elevate the levels of the glucose-regulated proteins. Cancer Res 52, 3814-3817.

Proby, C.M., Purdie, K.J., Sexton, C.J., Purkis, P., Navsaria, H.A., Stables, J.N., Leigh, I.M., **2000**. Spontaneous keratinocyte cell lines representing early and advanced stages of malignant transformation of the epidermis. Exp Dermatol 9, 104-117.

Proksch, E., Brandner, J.M., Jensen, J.M., **2008**. The skin: an indispensable barrier. Exp Dermatol 17, 1063-1072.

Punnonen, K., Puntala, A., Ahotupa, M., **1991**. Effects of ultraviolet A and B irradiation on lipid peroxidation and activity of the antioxidant enzymes in keratinocytes in culture. Photodermatol Photoimmunol Photomed 8, 3-6.

Qin, J.Z., Chaturvedi, V., Denning, M.F., Bacon, P., Panella, J., Choubey, D., Nickoloff, B.J., **2002**. Regulation of apoptosis by p53 in UV-irradiated human epidermis, psoriatic plaques and senescent keratinocytes. Oncogene 21, 2991-3002.

Qiu, A., Jansen, M., Sakaris, A., Min, S.H., Chattopadhyay, S., Tsai, E., Sandoval, C., Zhao, R., Akabas, M.H., Goldman, I.D., **2006**. Identification of an intestinal folate transporter and the molecular basis for hereditary folate malabsorption. Cell 127, 917-928.

Quiec, D., Maziere, C., Santus, R., Andre, P., Redziniak, G., Chevy, F., Wolf, C., Driss, F., Dubertret, L., Maziere, J.C., **1995**. Polyunsaturated fatty acid enrichment increases ultraviolet A-induced lipid peroxidation in NCTC 2544 human keratinocytes. J Invest Dermatol 104, 964-969.

Raha, S., Robinson, B.H., **2000**. Mitochondria, oxygen free radicals, disease and ageing. Trends Biochem Sci 25, 502-508.

Raj, D., Brash, D.E., Grossman, D., **2006**. Keratinocyte apoptosis in epidermal development and disease. J Invest Dermatol 126, 243-257.

Raja, K.B., Pippard, M.J., Simpson, R.J., Peters, T.J., **1986**. Relationship between erythropoiesis and the enhanced intestinal uptake of ferric iron in hypoxia in the mouse. Br J Haematol 64, 587-593.

Rakba, N., Aouad, F., Henry, C., Caris, C., Morel, I., Baret, P., Pierre, J.L., Brissot, P., Ward, R.J., Lescoat, G., Crichton, R.R., **1998**. Iron mobilisation and cellular protection by a new synthetic chelator O-Trensox. Biochem Pharmacol 55, 1797-1806.

Raval, C., **2008**. The role of Bach1 in ultraviolet-A mediated human Heme oxygenase-1 gene regulation. University of Bath,, Bath.

Recalcati, S., Minotti, G., Cairo, G., **2010**. Iron regulatory proteins: from molecular mechanisms to drug development. Antioxid Redox Signal 13, 1593-1616.

Record, I.R., Dreosti, I.E., Konstantinopoulos, M., Buckley, R.A., **1991**. The influence of topical and systemic vitamin E on ultraviolet light-induced skin damage in hairless mice. Nutr Cancer 16, 219-225.

Reed, S.I., **1997**. Control of the G1/S transition. Cancer Surv 29, 7-23.

Reelfs, O., Eggleston, I.M., Pourzand, C., **2010**. Skin protection against UVA-induced iron damage by multiantioxidants and iron chelating drugs/prodrugs. Curr Drug Metab 11, 242-249.

Reelfs, O., Tyrrell, R.M., Pourzand, C., **2004**. Ultraviolet a radiation-induced immediate iron release is a key modulator of the activation of NF-kappaB in human skin fibroblasts. J Invest Dermatol 122, 1440-1447.

Renton, F.J., Jeitner, T.M., **1996**. Cell cycle-dependent inhibition of the proliferation of human neural tumor cell lines by iron chelators. Biochem Pharmacol 51, 1553-1561.

Richardson, **1997**. Iron chelators as effective anti-proliferative agents. Can. J. Physiol. Pharmacol 75 1164–1180

Richardson, D., Baker, E., **1991a**. The uptake of inorganic iron complexes by human melanoma cells. Biochim Biophys Acta 1093, 20-28.

Richardson, D., Ponka, P., Baker, E., **1994**. The effect of the iron(III) chelator, desferrioxamine, on iron and transferrin uptake by the human malignant melanoma cell. Cancer Res 54, 685-689.

Richardson, D.R., **2002**. Iron chelators as therapeutic agents for the treatment of cancer. Crit Rev Oncol Hematol 42, 267-281.

Richardson, D.R., **2005**. Molecular mechanisms of iron uptake by cells and the use of iron chelators for the treatment of cancer. Curr Med Chem 12, 2711-2729.

Richardson, D.R., Baker, E., **1990**. The uptake of iron and transferrin by the human malignant melanoma cell. Biochim Biophys Acta 1053, 1-12.

Richardson, D.R., Baker, E., **1991b**. The release of iron and transferrin from the human melanoma cell. Biochim Biophys Acta 1091, 294-302.

Richardson, D.R., Baker, E., **1994**. Two saturable mechanisms of iron uptake from transferrin in human melanoma cells: the effect of transferrin concentration, chelators, and metabolic probes on transferrin and iron uptake. J Cell Physiol 161, 160-168.

Richardson, D.R., Bernhardt, P.V., **1999**. Crystal and molecular structure of 2-hydroxy-1-naphthaldehyde isonicotinoyl hydrazone (NIH) and its iron(III) complex: an iron chelator with anti-tumour activity. J Biol Inorg Chem 4, 266-273.

Richardson, D.R., Kalinowski, D.S., Lau, S., Jansson, P.J., Lovejoy, D.B., **2009**. Cancer cell iron metabolism and the development of potent iron chelators as anti-tumour agents. Biochim Biophys Acta 1790, 702-717.

Richardson, D.R., Milnes, K., **1997**. The potential of iron chelators of the pyridoxal isonicotinoyl hydrazone class as effective antiproliferative agents II: the mechanism of action of ligands derived from salicylaldehyde benzoyl hydrazone and 2-hydroxy-1-naphthylaldehyde benzoyl hydrazone. Blood 89, 3025-3038.

Richardson, D.R., Ponka, P., **1994**. The iron metabolism of the human neuroblastoma cell: lack of relationship between the efficacy of iron chelation and the inhibition of DNA synthesis. J Lab Clin Med 124, 660-671.

Richardson, D.R., Ponka, P., **1997**. The molecular mechanisms of the metabolism and transport of iron in normal and neoplastic cells. Biochim Biophys Acta 1331, 1-40.

Richardson, D.R., Sharpe, P.C., Lovejoy, D.B., Senaratne, D., Kalinowski, D.S., Islam, M., Bernhardt, P.V., **2006**. Dipyridyl thiosemicarbazone chelators with potent and selective antitumor activity form iron complexes with redox activity. J Med Chem 49, 6510-6521.

Richardson, D.R., Tran, E.H., Ponka, P., **1995**. The potential of iron chelators of the pyridoxal isonicotinoyl hydrazone class as effective antiproliferative agents. Blood 86, 4295-4306.

Rigel, D.S., **2008**. Cutaneous ultraviolet exposure and its relationship to the development of skin cancer. J Am Acad Dermatol 58, S129-132.

Rose, T.M., Plowman, G.D., Teplow, D.B., Dreyer, W.J., Hellstrom, K.E., Brown, J.P., **1986**. Primary structure of the human melanoma-associated antigen p97 (melanotransferrin) deduced from the mRNA sequence. Proc Natl Acad Sci U S A 83, 1261-1265.

Rotenberg, M.O., Maines, M.D., **1991**. Characterization of a cDNA-encoding rabbit brain heme oxygenase-2 and identification of a conserved domain among mammalian heme oxygenase isozymes: possible heme-binding site? Arch Biochem Biophys 290, 336-344.

Rothenberger, S., Mullner, E.W., Kuhn, L.C., **1990**. The mRNA-binding protein which controls ferritin and transferrin receptor expression is conserved during evolution. Nucleic Acids Res 18, 1175-1179.

Rothfuss, A., Radermacher, P., Speit, G., **2001**. Involvement of heme oxygenase-1 (HO-1) in the adaptive protection of human lymphocytes after hyperbaric oxygen (HBO) treatment. Carcinogenesis 22, 1979-1985.

Rouault, T.A., Haile, D.J., Downey, W.E., Philpott, C.C., Tang, C., Samaniego, F., Chin, J., Paul, I., Orloff, D., Harford, J.B., et al., **1992**. An iron-sulfur cluster plays a novel regulatory role in the iron-responsive element binding protein. Biometals 5, 131-140.

Rouault, T.A., Stout, C.D., Kaptain, S., Harford, J.B., Klausner, R.D., **1991**. Structural relationship between an iron-regulated RNA-binding protein (IRE-BP) and aconitase: functional implications. Cell 64, 881-883.

Ruas, M., Peters, G., **1998**. The p16INK4a/CDKN2A tumor suppressor and its relatives. Biochim Biophys Acta 1378, F115-177.

Rünger, T.M., 2009. Solar Ultraviolet Light. In: Schwab, M. (Ed.), Encyclopedia of Cancer. Springer Berlin Heidelberg, pp. 2774-2778.

Sah, P.P., Peoples, S.A., **1954**. Isonicotinyl hydrazones as antitubercular agents and derivatives for identification of aldehydes and ketones. J Am Pharm Assoc Am Pharm Assoc (Baltim) 43, 513-524.

Samokyszyn, V.M., Miller, D.M., Reif, D.W., Aust, S.D., **1989**. Inhibition of superoxide and ferritin-dependent lipid peroxidation by ceruloplasmin. J Biol Chem 264, 21-26.

Samuni, A.M., Krishna, M.C., DeGraff, W., Russo, A., Planalp, R.P., Brechbiel, M.W., Mitchell, J.B., **2002**. Mechanisms underlying the cytotoxic effects of Tachpyr--a novel metal chelator. Biochim Biophys Acta 1571, 211-218.

Sanchez, M., Galy, B., Dandekar, T., Bengert, P., Vainshtein, Y., Stolte, J., Muckenthaler, M.U., Hentze, M.W., **2006**. Iron regulation and the cell cycle: identification of an iron-responsive element in the 3'-untranslated region of human cell division cycle 14A mRNA by a refined microarray-based screening strategy. J Biol Chem 281, 22865-22874.

Santambrogio, P., Biasiotto, G., Sanvito, F., Olivieri, S., Arosio, P., Levi, S., **2007**. Mitochondrial ferritin expression in adult mouse tissues. J Histochem Cytochem 55, 1129-1137.

Sartorelli, A.C., Agrawal, K.C., Moore, E.C., **1971**. Mechanism of inhibition of ribonucleoside diphosphate reductase by a-(N)-heterocyclic aldehyde thiosemicarbazones. Biochem Pharmacol 20, 3119-3123.

Sartorelli, A.C., Booth, B.A., **1967**. Inhibition of the growth of sarcoma 180 ascites cells by combinations of inhibitors of nucleic acid biosynthesis and the cupric chelate of kethoxal bis-(thiosemicarbazone). Cancer Res 27, 1614-1619.

Sausville, E.A., Johnson, J., Alley, M., Zaharevitz, D., Senderowicz, A.M., **2000**. Inhibition of CDKs as a therapeutic modality. Ann N Y Acad Sci 910, 207-221; discussion 221-202.

Schaeffer, E., Lucero, M.A., Jeltsch, J.M., Py, M.C., Levin, M.J., Chambon, P., Cohen, G.N., Zakin, M.M., **1987**. Complete structure of the human transferrin gene. Comparison with analogous chicken gene and human pseudogene. Gene 56, 109-116.

Schallreuter, K.U., Pittelkow, M.R., Wood, J.M., **1986**. Free radical reduction by thioredoxin reductase at the surface of normal and vitiliginous human keratinocytes. J Invest Dermatol 87, 728-732.

Schallreuter, K.U., Wood, J.M., Mensing, H., Breitbart, E.W., **1991**. Local treatment of cutaneous and subcutaneous metastatic malignant melanoma with fotemustine. Cancer Chemother Pharmacol 29, 167-171.

Schenk, H., Klein, M., Erdbrugger, W., Droge, W., Schulze-Osthoff, K., **1994**. Distinct effects of thioredoxin and antioxidants on the activation of transcription factors NF-kappa B and AP-1. Proc Natl Acad Sci U S A 91, 1672-1676.

Secretan, B., 2009. UV Radiation. In: Schwab, M. (Ed.), Encyclopedia of Cancer. Springer Berlin Heidelberg, pp. 3129-3132.

Seite, S., Popovic, E., Verdier, M.P., **2004**. Iron chelation can modulate UVA-induced lipid peroxidation and ferritin expression in human reconstructed epidermis. Photodermatol Photoimmunol Photomed, 47–52

Sekyere, E.O., Dunn, L.L., Rahmanto, Y.S., Richardson, D.R., **2006**. Role of melanotransferrin in iron metabolism: studies using targeted gene disruption in vivo. Blood 107, 2599-2601.

Selig, R.A., Madafiglio, J., Haber, M., Norris, M.D., White, L., Stewart, B.W., **1993**. Ferritin production and desferrioxamine cytotoxicity in human neuroblastoma cell lines. Anticancer Res 13, 721-725.

Selig, R.A., White, L., Gramacho, C., Sterling-Levis, K., Fraser, I.W., Naidoo, D., **1998**. Failure of iron chelators to reduce tumor growth in human neuroblastoma xenografts. Cancer Res 58, 473-478.

Semenza, G.L., **1999**. Regulation of mammalian O2 homeostasis by hypoxia-inducible factor 1. Annu Rev Cell Dev Biol 15, 551-578.

Shao, J., Zhou, B., Di Bilio, A.J., Zhu, L., Wang, T., Qi, C., Shih, J., Yen, Y., **2006**. A Ferrous-Triapine complex mediates formation of reactive oxygen species that inactivate human ribonucleotide reductase. Mol Cancer Ther 5, 586-592.

Shao, J., Zhou, B., Zhu, L., Qiu, W., Yuan, Y.C., Xi, B., Yen, Y., **2004**. In vitro characterization of enzymatic properties and inhibition of the p53R2 subunit of human ribonucleotide reductase. Cancer Res 64, 1-6.

Shayeghi, M., Latunde-Dada, G.O., Oakhill, J.S., Laftah, A.H., Takeuchi, K., Halliday, N., Khan, Y., Warley, A., McCann, F.E., Hider, R.C., Frazer, D.M., Anderson, G.J., Vulpe, C.D., Simpson, R.J., McKie, A.T., **2005**. Identification of an intestinal heme transporter. Cell 122, 789-801.

Sherr, C.J., **1994**. G1 phase progression: cycling on cue. Cell 79, 551-555.

Sherr, C.J., **2000**. The Pezcoller lecture: cancer cell cycles revisited. Cancer Res 60, 3689-3695.

Sherr, C.J., Roberts, J.M., **1999**. CDK inhibitors: positive and negative regulators of G1-phase progression. Genes Dev 13, 1501-1512.

Sheth, S., Brittenham, G.M., **2000**. Genetic disorders affecting proteins of iron metabolism: clinical implications. Annu Rev Med 51, 443-464.

Shinar, E., Rachmilewitz, E.A., **1990**. Oxidative denaturation of red blood cells in thalassemia. Semin Hematol 27, 70-82.

Shindo, Y., Hashimoto, T., **1997**. Time course of changes in antioxidant enzymes in human skin fibroblasts after UVA irradiation. J Dermatol Sci 14, 225-232.

Shindo, Y., Witt, E., Packer, L., **1993**. Antioxidant defense mechanisms in murine epidermis and dermis and their responses to ultraviolet light. J Invest Dermatol 100, 260-265.

Simonart, T., Boelaert, J.R., Mosselmans, R., Andrei, G., Noel, J.C., De Clercq, E., Snoeck, R., **2002**. Antiproliferative and apoptotic effects of iron chelators on human cervical carcinoma cells. Gynecol Oncol 85, 95-102.

Simonart, T., Degraef, C., Andrei, G., Mosselmans, R., Hermans, P., Van Vooren, J.P., Noel, J.C., Boelaert, J.R., Snoeck, R., Heenen, M., **2000**. Iron chelators inhibit the growth and induce the apoptosis of Kaposi's sarcoma cells and of their putative endothelial precursors. J Invest Dermatol 115, 893-900.

Simunek, T., Boer, C., Bouwman, R.A., Vlasblom, R., Versteilen, A.M., Sterba, M., Gersl, V., Hrdina, R., Ponka, P., de Lange, J.J., Paulus, W.J., Musters, R.J., **2005**. SIH--a novel lipophilic iron chelator--protects H9c2 cardiomyoblasts from oxidative stress-induced mitochondrial injury and cell death. J Mol Cell Cardiol 39, 345-354.

Singh, S., Khodr, H., Taylor, M.I., Hider, R.C., **1995**. Therapeutic iron chelators and their potential side-effects. Biochem Soc Symp 61, 127-137.

Skinner, M.K., Griswold, M.D., **1980**. Sertoli cells synthesize and secrete transferrin-like protein. J Biol Chem 255, 9523-9525.

Soriani, M., Rice-Evans, C., Tyrrell, R.M., **1998**. Modulation of the UVA activation of haem oxygenase, collagenase and cyclooxygenase gene expression by epigallocatechin in human skin cells. FEBS Lett 439, 253-257.

Spector, A., Yan, G.Z., Huang, R.R., McDermott, M.J., Gascoyne, P.R., Pigiet, V., **1988**. The effect of H2O2 upon thioredoxin-enriched lens epithelial cells. J Biol Chem 263, 4984-4990.

St Pierre, T.G., Richardson, D.R., Baker, E., Webb, J., **1992**. A low-spin iron complex in human melanoma and rat hepatoma cells and a high-spin iron(II) complex in rat hepatoma cells. Biochim Biophys Acta 1135, 154-158.

Stadtman, E.R., **1992**. Protein oxidation and aging. Science 257, 1220-1224.

Stein, B., Rahmsdorf, H.J., Steffen, A., Litfin, M., Herrlich, P., **1989**. UV-induced DNA damage is an intermediate step in UV-induced expression of human immunodeficiency virus type 1, collagenase, c-fos, and metallothionein. Mol Cell Biol 9, 5169-5181.

Stein, S., Thomas, E.K., Herzog, B., Westfall, M.D., Rocheleau, J.V., Jackson, R.S., 2nd, Wang, M., Liang, P., **2004**. NDRG1 is necessary for p53-dependent apoptosis. J Biol Chem 279, 48930-48940.

Stevenson, O., Zaki, I., **2002**. Introduction to psoriasis. Hospital Pharmacist 9, 187-190.

Stockmann, C., Fandrey, J., **2006**. Hypoxia-induced erythropoietin production: a paradigm for oxygen-regulated gene expression. Clin Exp Pharmacol Physiol 33, 968-979.

Sturrock, A., Alexander, J., Lamb, J., Craven, C.M., Kaplan, J., **1990**. Characterization of a transferrin-independent uptake system for iron in HeLa cells. J Biol Chem 265, 3139-3145.

Sugiyama, M., Tsuzuki, K., Matsumoto, K., Ogura, R., **1992**. Effect of vitamin E on cytotoxicity, DNA single strand breaks, chromosomal aberrations, and mutation in Chinese hamster V-79 cells exposed to ultraviolet-B light. Photochem Photobiol 56, 31-34.

Sun, Y., Bian, J., Wang, Y., Jacobs, C., **1997**. Activation of p53 transcriptional activity by 1,10-phenanthroline, a metal chelator and redox sensitive compound. Oncogene 14, 385-393.

Suryo Rahmanto, Y., Dunn, L.L., Richardson, D.R., **2007**. The melanoma tumor antigen, melanotransferrin (p97): a 25-year hallmark--from iron metabolism to tumorigenesis. Oncogene 26, 6113-6124.

Sutherland, R., Delia, D., Schneider, C., Newman, R., Kemshead, J., Greaves, M., **1981**. Ubiquitous cell-surface glycoprotein on tumor cells is proliferation-associated receptor for transferrin. Proc Natl Acad Sci U S A 78, 4515-4519.

Swanson, C.A., **2003**. Iron intake and regulation: implications for iron deficiency and iron overload. Alcohol 30, 99-102.

Syed, B.A., Sargent, P.J., Farnaud, S., Evans, R.W., **2006**. An overview of molecular aspects of iron metabolism. Hemoglobin 30, 69-80.

Tacchini, L., Bianchi, L., Bernelli-Zazzera, A., Cairo, G., **1999**. Transferrin receptor induction by hypoxia. HIF-1-mediated transcriptional activation and cell-specific post-transcriptional regulation. J Biol Chem 274, 24142-24146.

Taetle, R., Honeysett, J.M., **1987**. Effects of monoclonal anti-transferrin receptor antibodies on in vitro growth of human solid tumor cells. Cancer Res 47, 2040-2044.

Takeda, E., Weber, G., **1981**. Role of ribonucleotide reductase in expression in the neoplastic program. Life Sci 28, 1007-1014.

Tenopoulou, M., Kurz, T., Doulias, P.T., Galaris, D., Brunk, U.T., **2007**. Does the calcein-AM method assay the total cellular 'labile iron pool' or only a fraction of it? Biochem J 403, 261-266.

Terada, N., Lucas, J.J., Gelfand, E.W., **1991**. Differential regulation of the tumor suppressor molecules, retinoblastoma susceptibility gene product (Rb) and p53, during cell cycle progression of normal human T cells. J Immunol 147, 698-704.

Theil, E.C., **1987**. Ferritin: structure, gene regulation, and cellular function in animals, plants, and microorganisms. Annu Rev Biochem 56, 289-315.

Thelander, L., Graslund, A., Thelander, M., **1983**. Continual presence of oxygen and iron required for mammalian ribonucleotide reduction: possible regulation mechanism. Biochem Biophys Res Commun 110, 859-865.

Thelander, L., Reichard, P., **1979**. Reduction of ribonucleotides. Annu Rev Biochem 48, 133-158.

Thiele, J.J., Traber, M.G., Polefka, T.G., Cross, C.E., Packer, L., **1997**. Ozone-exposure depletes vitamin E and induces lipid peroxidation in murine stratum corneum. J Invest Dermatol 108, 753-757.

Thomson, A.M., Rogers, J.T., Leedman, P.J., **1999**. Iron-regulatory proteins, iron-responsive elements and ferritin mRNA translation. Int J Biochem Cell Biol 31, 1139-1152.

Tibbetts, R.S., Brumbaugh, K.M., Williams, J.M., Sarkaria, J.N., Cliby, W.A., Shieh, S.Y., Taya, Y., Prives, C., Abraham, R.T., **1999**. A role for ATR in the DNA damage-induced phosphorylation of p53. Genes Dev 13, 152-157.

Toro, J.R., Hamouda, R.S., Bale, S., 2009. Basal Cell Carcinoma. In: Schwab, M. (Ed.), Encyclopedia of Cancer. Springer Berlin Heidelberg, pp. 297-299.

Torti, S.V., Ma, R., Venditto, V.J., Torti, F.M., Planalp, R.P., Brechbiel, M.W., **2005**. Preliminary evaluation of the cytotoxicity of a series of tris-2-aminoethylamine (Tren) based hexadentate heterocyclic donor agents. Bioorg Med Chem 13, 5961-5967.

Torti, S.V., Torti, F.M., Whitman, S.P., Brechbiel, M.W., Park, G., Planalp, R.P., **1998**. Tumor cell cytotoxicity of a novel metal chelator. Blood 92, 1384-1389.

Toyokuni, S., **1996**. Iron-induced carcinogenesis: the role of redox regulation. Free Radic Biol Med 20, 553-566.

Tran, T.N., Eubanks, S.K., Schaffer, K.J., Zhou, C.Y., Linder, M.C., **1997**. Secretion of ferritin by rat hepatoma cells and its regulation by inflammatory cytokines and iron. Blood 90, 4979-4986.

Trekli, M.C., Riss, G., Goralczyk, R., Tyrrell, R.M., **2003**. Beta-carotene suppresses UVA-induced HO-1 gene expression in cultured FEK4. Free Radic Biol Med 34, 456-464.

Trenam, C.W., Blake, D.R., Morris, C.J., **1992**. Skin inflammation: reactive oxygen species and the role of iron. J Invest Dermatol 99, 675-682.

Trevithick, J.R., Xiong, H., Lee, S., Shum, D.T., Sanford, S.E., Karlik, S.J., Norley, C., Dilworth, G.R., **1992**. Topical tocopherol acetate reduces post-UVB, sunburn-associated erythema, edema, and skin sensitivity in hairless mice. Arch Biochem Biophys 296, 575-582.

Trinder, D., Morgan, E., Baker, E., **1986**. The mechanisms of iron uptake by fetal rat hepatocytes in culture. Hepatology 6, 852-858.

Trowbridge, I.S., Lopez, F., **1982**. Monoclonal antibody to transferrin receptor blocks transferrin binding and inhibits human tumor cell growth in vitro. Proc Natl Acad Sci U S A 79, 1175-1179.

Tsihlias, J., Kapusta, L., Slingerland, J., **1999**. The prognostic significance of altered cyclin-dependent kinase inhibitors in human cancer. Annu Rev Med 50, 401-423.

Tsuji, Y., Kwak, E., Saika, T., Torti, S.V., Torti, F.M., **1993**. Preferential repression of the H subunit of ferritin by adenovirus E1A in NIH-3T3 mouse fibroblasts. J Biol Chem 268, 7270-7275.

Turner, J., Koumenis, C., Kute, T.E., Planalp, R.P., Brechbiel, M.W., Beardsley, D., Cody, B., Brown, K.D., Torti, F.M., Torti, S.V., **2005**. Tachpyridine, a metal chelator, induces G2 cell-cycle arrest, activates checkpoint kinases, and sensitizes cells to ionizing radiation. Blood 106, 3191-3199.

Tyrrell, R.M., 1991. UVA (320-380 nm) radiation as an oxidative stress. In: H., S. (Ed.), Oxidative Stress: Oxidants and Antioxidants. Academic Press, London pp. 57-83.

Tyrrell, R.M., **1994**. The molecular and cellular pathology of solar ultraviolet radiation. Mol Aspects Med 15, 1-77.

Tyrrell, R.M., **1996a**. Activation of mammalian gene expression by the UV component of sunlight--from models to reality. Bioessays 18, 139-148.

Tyrrell, R.M., **1996b**. UV activation of mammalian stress proteins. EXS 77, 255-271.

Tyrrell, R.M., Pidoux, M., **1986**. Endogenous glutathione protects human skin fibroblasts against the cytotoxic action of UVB, UVA and near-visible radiations. Photochem Photobiol 44, 561-564.

Tyrrell, R.M., Pidoux, M., **1987**. Action spectra for human skin cells: estimates of the relative cytotoxicity of the middle ultraviolet, near ultraviolet, and violet regions of sunlight on epidermal keratinocytes. Cancer Res 47, 1825-1829.

Tyrrell, R.M., Pidoux, M., **1988**. Correlation between endogenous glutathione content and sensitivity of cultured human skin cells to radiation at defined wavelengths in the solar ultraviolet range. Photochem Photobiol 47, 405-412.

Tyrrell, R.M., Pidoux, M., **1989**. Singlet oxygen involvement in the inactivation of cultured human fibroblasts by UVA (334 nm, 365 nm) and near-visible (405 nm) radiations. Photochem Photobiol 49, 407-412.

Ursini, F., Maiorino, M., Brigelius-Flohe, R., Aumann, K.D., Roveri, A., Schomburg, D., Flohe, L., **1995**. Diversity of glutathione peroxidases. Methods Enzymol 252, 38-53.

Ursini, F., Maiorino, M., Valente, M., Ferri, L., Gregolin, C., **1982**. Purification from pig liver of a protein which protects liposomes and biomembranes from peroxidative degradation and exhibits glutathione peroxidase activity on phosphatidylcholine hydroperoxides. Biochim Biophys Acta 710, 197-211.

Vaca, C.E., Wilhelm, J., Harms-Ringdahl, M., **1988**. Interaction of lipid peroxidation products with DNA. A review. Mutat Res 195, 137-149.

Vairapandi, M., Balliet, A.G., Hoffman, B., Liebermann, D.A., **2002**. GADD45b and GADD45g are cdc2/cyclinB1 kinase inhibitors with a role in S and G2/M cell cycle checkpoints induced by genotoxic stress. J Cell Physiol 192, 327-338.

Valko, M., Leibfritz, D., Moncol, J., Cronin, M.T., Mazur, M., Telser, J., **2007**. Free radicals and antioxidants in normal physiological functions and human disease. Int J Biochem Cell Biol 39, 44-84.

Valko, M., Rhodes, C.J., Moncol, J., Izakovic, M., Mazur, M., **2006**. Free radicals, metals and antioxidants in oxidative stress-induced cancer. Chem Biol Interact 160, 1-40.

van Reyk, D., Sarel, S., Hunt, N., **2000**. Inhibition of in vitro lymphoproliferation by three novel iron chelators of the pyridoxal and salicyl aldehyde hydrazone classes. Biochem Pharmacol 60, 581-587.

Vandewalle, B., Hornez, L., Revillion, F., Lefebvre, J., **1989**. Secretion of transferrin by human breast cancer cells. Biochem Biophys Res Commun 163, 149-154.

Vidal, A., Koff, A., **2000**. Cell-cycle inhibitors: three families united by a common cause. Gene 247, 1-15.

Vile, G.F., Basu-Modak, S., Waltner, C., Tyrrell, R.M., **1994**. Heme oxygenase 1 mediates an adaptive response to oxidative stress in human skin fibroblasts. Proc Natl Acad Sci U S A 91, 2607-2610.

Vile, G.F., Tyrrell, R.M., **1993**. Oxidative stress resulting from ultraviolet A irradiation of human skin fibroblasts leads to a heme oxygenase-dependent increase in ferritin. J Biol Chem 268, 14678-14681.

Vile, G.F., Tyrrell, R.M., **1995**. UVA radiation-induced oxidative damage to lipids and proteins in vitro and in human skin fibroblasts is dependent on iron and singlet oxygen. Free Radic Biol Med 18, 721-730.

Vince, G.S., Dean, R.T., **1987**. Is enhanced free radical flux associated with increased intracellular proteolysis? FEBS Lett 216, 253-256.

Vita, M., Henriksson, M., **2006**. The Myc oncoprotein as a therapeutic target for human cancer. Semin Cancer Biol 16, 318-330.

Voest, E.E., Neijt, J.P., Keunen, J.E., Dekker, A.W., van Asbeck, B.S., Nortier, J.W., Ros, F.E., Marx, J.J., **1993**. Phase I study using desferrioxamine and iron sorbitol citrate in an attempt to modulate the iron status of tumor cells to enhance doxorubicin activity. Cancer Chemother Pharmacol 31, 357-362.

Vogelstein, B., Lane, D., Levine, A.J., **2000**. Surfing the p53 network. Nature 408, 307-310.

Von Wangenheim, K.H., Peterson, H.P., **2001**. A mechanism of intracellular timing and its cooperation with extracellular signals in controlling cell proliferation and differentiation, an amended hypothesis. J Theor Biol 211, 239-251.

Vostrejs, M., Moran, P.L., Seligman, P.A., **1988**. Transferrin synthesis by small cell lung cancer cells acts as an autocrine regulator of cellular proliferation. J Clin Invest 82, 331-339.

Vousden, K.H., Woude, G.F., **2000**. The ins and outs of p53. Nat Cell Biol 2, E178-180.

Vulpe, C.D., Kuo, Y.M., Murphy, T.L., Cowley, L., Askwith, C., Libina, N., Gitschier, J., Anderson, G.J., **1999**. Hephaestin, a ceruloplasmin homologue implicated in intestinal iron transport, is defective in the sla mouse. Nat Genet 21, 195-199.

Wadler, S., Makower, D., Clairmont, C., Lambert, P., Fehn, K., Sznol, M., **2004**. Phase I and pharmacokinetic study of the ribonucleotide reductase inhibitor, 3-aminopyridine-2-carboxaldehyde thiosemicarbazone, administered by 96-hour intravenous continuous infusion. J Clin Oncol 22, 1553-1563.

Wagstaff, M., Worwood, M., Jacobs, A., **1978**. Properties of human tissue isoferritins. Biochem J 173, 969-977.

Walden, W.E., Patino, M.M., Gaffield, L., **1989**. Purification of a specific repressor of ferritin mRNA translation from rabbit liver. J Biol Chem 264, 13765-13769.

Wang, D., Liu, Y.F., Wang, Y.C., **2006**. [Deferoxamine induces apoptosis of HL-60 cells by activating caspase-3]. Zhongguo Shi Yan Xue Ye Xue Za Zhi 14, 485-487.

Wang, F., Elliott, R.L., Head, J.F., **1999**. Inhibitory effect of deferoxamine mesylate and low iron diet on the 13762NF rat mammary adenocarcinoma. Anticancer Res 19, 445-450.

Wang, G., Miskimins, R., Miskimins, W.K., **2000**. Mimosine arrests cells in G1 by enhancing the levels of p27(Kip1). Exp Cell Res 254, 64-71.

Wang, G., Miskimins, R., Miskimins, W.K., **2004**. Regulation of p27(Kip1) by intracellular iron levels. Biometals 17, 15-24.

Wang, G.L., Jiang, B.H., Rue, E.A., Semenza, G.L., **1995**. Hypoxia-inducible factor 1 is a basic-helix-loop-helix-PAS heterodimer regulated by cellular O2 tension. Proc Natl Acad Sci U S A 92, 5510-5514.

Wang, M.Y., Liehr, J.G., **1995a**. Induction by estrogens of lipid peroxidation and lipid peroxide-derived malonaldehyde-DNA adducts in male Syrian hamsters: role of lipid peroxidation in estrogen-induced kidney carcinogenesis. Carcinogenesis 16, 1941-1945.

Wang, M.Y., Liehr, J.G., **1995b**. Lipid hydroperoxide-induced endogenous DNA adducts in hamsters: possible mechanism of lipid hydroperoxide-mediated carcinogenesis. Arch Biochem Biophys 316, 38-46.

Wang, T.C., Cardiff, R.D., Zukerberg, L., Lees, E., Arnold, A., Schmidt, E.V., **1994**. Mammary hyperplasia and carcinoma in MMTV-cyclin D1 transgenic mice. Nature 369, 669-671.

Wang, W., Fang, H., Groom, L., Cheng, A., Zhang, W., Liu, J., Wang, X., Li, K., Han, P., Zheng, M., Yin, J., Mattson, M.P., Kao, J.P., Lakatta, E.G., Sheu, S.S., Ouyang, K., Chen, J., Dirksen, R.T., Cheng, H., **2008**. Superoxide flashes in single mitochondria. Cell 134, 279-290.

Webb, R.B., 1977. Lethal and mutagenic effects of near-ultraviolet radiation. In: Smith, K.C. (Ed.), Photochemical and Photobiological Reviews Plenum, New York, pp. 169–261

Weedon, D., Searle, J., Kerr, J.F., **1979**. Apoptosis. Its nature and implications for dermatopathology. Am J Dermatopathol 1, 133-144.

Weinberg, R.A., **1995**. The retinoblastoma protein and cell cycle control. Cell 81, 323-330.

Whitnall, M., Howard, J., Ponka, P., Richardson, D.R., **2006**. A class of iron chelators with a wide spectrum of potent antitumor activity that overcomes resistance to chemotherapeutics. Proc Natl Acad Sci U S A 103, 14901-14906.

Winrow, V.R., Winyard, P.G., Morris, C.J., Blake, D.R., **1993**. Free radicals in inflammation: second messengers and mediators of tissue

destruction

Br Med Bull 49, 506-522.

Witt, L., Yap, T., Blakley, R.L., **1978**. Regulation of ribonucleotide reductase activity and its possible exploitation in chemotherapy. Adv Enzyme Regul 17, 157-171.

Wlaschek, M., Wenk, J., Brenneisen, P., Briviba, K., Schwarz, A., Sies, H., Scharffetter-Kochanek, K., **1997**. Singlet oxygen is an early intermediate in cytokine-dependent ultraviolet-A induction of interstitial collagenase in human dermal fibroblasts in vitro. FEBS Lett 413, 239-242.

Wojas-Pelc, A., Marcinkiewicz, J., **2007**. What is a role of haeme oxygenase-1 in psoriasis? Current concepts of pathogenesis. Int J Exp Pathol 88, 95-102.

Wolff, S.P., Dean, R.T., **1986**. Fragmentation of proteins by free radicals and its effect on their susceptibility to enzymic hydrolysis. Biochem J 234, 399-403.

Wong, S.F., Halliwell, B., Richmond, R., Skowroneck, W.R., **1981**. The role of superoxide and hydroxyl radicals in the degradation of hyaluronic acid induced by metal ions and by ascorbic acid. J Inorg Biochem 14, 127-134.

Wong, S.S., Li, R.H., Stadlin, A., **1999**. Oxidative stress induced by MPTP and MPP(+): selective vulnerability of cultured mouse astrocytes. Brain Res 836, 237-244.

Wrone-Smith, T., Bergstrom, J., Quevedo, M.E., Reddy, V., Gutierrez-Steil, C., Nickoloff, B.J., **1999**. Differential expression of cell survival and cell cycle regulatory proteins in cutaneous squamoproliferative lesions. J Dermatol Sci 19, 53-67.

Wrone-Smith, T., Mitra, R.S., Thompson, C.B., Jasty, R., Castle, V.P., Nickoloff, B.J., **1997**. Keratinocytes derived from psoriatic plaques are resistant to apoptosis compared with normal skin. Am J Pathol 151, 1321-1329.

Wu, K.J., Polack, A., Dalla-Favera, R., **1999**. Coordinated regulation of iron-controlling genes, H-ferritin and IRP2, by c-MYC. Science 283, 676-679.

Wuarin, J., Nurse, P., **1996**. Regulating S phase: CDKs, licensing and proteolysis. Cell 85, 785-787.

Yang, F., Lum, J.B., McGill, J.R., Moore, C.M., Naylor, S.L., van Bragt, P.H., Baldwin, W.D., Bowman, B.H., **1984**. Human transferrin: cDNA characterization and chromosomal localization. Proc Natl Acad Sci U S A 81, 2752-2756.

Yiakouvaki, A., Savovic, J., Al-Qenaei, A., Dowden, J., Pourzand, C., **2006**. Caged-iron chelators a novel approach towards protecting skin cells against UVA-induced necrotic cell death. J Invest Dermatol 126, 2287-2295.

Yohn, J.J., Norris, D.A., Yrastorza, D.G., Buno, I.J., Leff, J.A., Hake, S.S., Repine, J.E., **1991**. Disparate antioxidant enzyme activities in cultured human cutaneous fibroblasts, keratinocytes, and melanocytes. J Invest Dermatol 97, 405-409.

Yoon, G., Kim, H.J., Yoon, Y.S., Cho, H., Lim, I.K., Lee, J.H., **2002**. Iron chelation-induced senescence-like growth arrest in hepatocyte cell lines: association of transforming growth factor beta1 (TGF-beta1)-mediated p27Kip1 expression. Biochem J 366, 613-621.

Young, A.R., **1987**. The sunburn cell. Photodermatol 4, 127-134.

Yu, B.P., **1994**. Cellular defenses against damage from reactive oxygen species. Physiol Rev 74, 139-162.

Yu, J., Wessling-Resnick, M., **1998**. Structural and functional analysis of SFT, a stimulator of Fe Transport. J Biol Chem 273, 21380-21385.

Yu, Y., Kovacevic, Z., Richardson, D.R., **2007**. Tuning cell cycle regulation with an iron key. Cell Cycle 6, 1982-1994.

Yu, Y., Wong, J., Lovejoy, D.B., Kalinowski, D.S., Richardson, D.R., **2006**. Chelators at the cancer coalface: desferrioxamine to Triapine and beyond. Clin Cancer Res 12, 6876-6883.

Yuan, J., Lovejoy, D.B., Richardson, D.R., **2004**. Novel di-2-pyridyl-derived iron chelators with marked and selective antitumor activity: in vitro and in vivo assessment. Blood 104, 1450-1458.

Zahringer, J., Baliga, B.S., Munro, H.N., **1976**. Novel mechanism for translational control in regulation of ferritin synthesis by iron. Proc Natl Acad Sci U S A 73, 857-861.

Zerbini, L.F., Libermann, T.A., **2005**. GADD45 deregulation in cancer: frequently methylated tumor suppressors and potential therapeutic targets. Clin Cancer Res 11, 6409-6413.

Zetterberg, A., Larsson, O., Wiman, K.G., **1995**. What is the restriction point? Curr Opin Cell Biol 7, 835-842.

Zhan, Q., Lord, K.A., Alamo, I., Jr., Hollander, M.C., Carrier, F., Ron, D., Kohn, K.W., Hoffman, B., Liebermann, D.A., Fornace, A.J., Jr., **1994**. The gadd and MyD genes define a novel set of mammalian genes encoding acidic proteins that synergistically suppress cell growth. Mol Cell Biol 14, 2361-2371.

Zhang, L., Yu, J., Park, B.H., Kinzler, K.W., Vogelstein, B., **2000**. Role of BAX in the apoptotic response to anticancer agents. Science 290, 989-992.

Zhang, X., Rosenstein, B.S., Wang, Y., Lebwohl, M., Mitchell, D.M., Wei, H., **1997**. Induction of 8-oxo-7,8-dihydro-2'-deoxyguanosine by ultraviolet radiation in calf thymus DNA and HeLa cells. Photochem Photobiol 65, 119-124.

Zhao, G., Arosio, P., Chasteen, N.D., **2006**. Iron(II) and hydrogen peroxide detoxification by human H-chain ferritin. An EPR spin-trapping study. Biochemistry 45, 3429-3436.

Zhao, R., Planalp, R.P., Ma, R., Greene, B.T., Jones, B.T., Brechbiel, M.W., Torti, F.M., Torti, S.V., **2004**. Role of zinc and iron chelation in apoptosis mediated by tachpyridine, an anti-cancer iron chelator. Biochem Pharmacol 67, 1677-1688.

Zhong, J.L., Yiakouvaki, A., Holley, P., Tyrrell, R.M., Pourzand, C., **2004**. Susceptibility of skin cells to UVA-induced necrotic cell death reflects the intracellular level of labile iron. J Invest Dermatol 123, 771-780.

Ziegler, A., Jonason, A.S., Leffell, D.J., Simon, J.A., Sharma, H.W., Kimmelman, J., Remington, L., Jacks, T., Brash, D.E., **1994**. Sunburn and p53 in the onset of skin cancer. Nature 372, 773-776.